DEVELOPPEMENT DE NANOVECTEURS POUR L'ADMINISTRATION D'ACIDES NUCLEIQUES PAR VOIE SYSTEMIQUE

Stephanie David

université angers

Année 2011
N° d'ordre 1198

DEVELOPPEMENT DE NANOVECTEURS POUR L'ADMINISTRATION D'ACIDES NUCLEIQUES PAR VOIE SYSTEMIQUE

THESE DE DOCTORAT

Spécialité : **Pharmacologie expérimentale et clinique**

Ecole doctorale : **Biologie Santé Angers - Nantes**

Présentée et soutenue publiquement

le 09 décembre 2011, à Angers

par Stephanie DAVID

Devant le jury ci-dessous :

Nathalie Mignet Chargée de recherches, CNRS, université Paris Descartes	**Rapporteur**
Véronique Mathieu Professeur à l'université Libre de Bruxelles	**Rapporteur**
Didier Betbeder Professeur à l'université Lille 2	**Examinateur**
Jean-Pierre Benoit Professeur à l'université d'Angers	**Examinateur**
Tristan Montier Maitre de conférences à l'université de Brest	**Membre invité**
Bruno Pitard Directeur de recherche, CNRS, université de Nantes	**Codirecteur de thèse**
Catherine Passirani Professeur à l'université d'Angers	**Codirecteur de thèse**

INSERM U915 – Institut du thorax
IRT-UN, 8 quai Moncousu, 44007 Nantes Cedex 1, France

INSERM U646 – Ingénierie de la vectorisation particulaire
IBS – CHU, 4 rue Larrey, 49933 Angers Cedex 9, France

ED 502

REMERCIEMENTS

Je tiens à remercier en premier lieu le Professeur Jean-Pierre Benoit de m'avoir accueillie au sein du laboratoire Inserm U646 à Angers et le Professeur Pierre Pacaud de m'avoir accueillie au sein du laboratoire Inserm U915 à Nantes, me permettant d'effectuer cette thèse en codirection.

Je tiens à exprimer mes plus sincères remerciements aux membres du jury pour avoir accepté et pris de leur temps pour juger ce travail.

Un merci particulier au Dr Nathalie Mignet et au Dr Véronique Mathieu de me faire l'honneur d'être rapporteurs de cette thèse et au Professeur Didier Betbeder d'avoir accepté de faire part du jury en tant qu'examinateur.

Je tiens également à remercier le Dr Tristan Montier pour son accueil à Brest, pour ses conseils concernant les différentes expériences *in vivo* et pour la correction de mes publications. Merci aussi de faire partie du jury en tant qu'examinateur invité.

J'exprime ma reconnaissance au Dr Bruno Pitard, codirecteur de cette thèse, pour les échanges scientifiques et la confiance qu'il m'a accordée pour gérer cette thèse entre Angers, Nantes et Brest. Ses conseils dans les expériences à mener ainsi que l'aide à la rédaction des articles m'ont été très utiles.

J'exprime enfin ma profonde reconnaissance au Professeur Catherine Passirani, également codirectrice de cette thèse, pour son encadrement de qualité me permettant entre autre d'acquérir les outils pour la rédaction scientifique et de

prendre mes marques dans le monde de la recherche, pour sa disponibilité malgré son emploi de temps déjà chargé, pour sa patience quand je n'étais pas dans les temps, ses conseils, sa motivation dans les moments difficiles et son soutien tout au long de cette thèse.

J'adresse également mes remerciements à la Région Pays de Loire (Projet CIMATH) pour les aides financières octroyées.

Un grand merci pour leur soutien aussi bien sur le plan scientifique que sur le plan personnel à :

- Odile Cruaud et Alexandra Giteau qui m'ont encadrée pendant mon stage de recherche ERASMUS et qui m'ont fait découvrir et donné envie de continuer dans le domaine de la recherche. Merci aussi, Odile, pour les excursions dans la région angevine.
- Emmanuel Belamie et les membres de l'EPHE pendant mon master qui m'ont permis d'approfondir mes connaissances en biologie qui m'ont été bien utiles pendant cette thèse.
- Bea Le Ray et Anne Clavreul qui m'ont formée à la culture cellulaire à Nantes et à Angers respectivement. Merci Anne aussi pour tes conseils pendant cette thèse.
- Marie Morille (Angers) et Clothilde Gourden (Nantes) qui m'ont aidée à faire mes premières formulations de nanovecteurs et qui m'ont montré un grand nombre de manipulations effectuées dans les deux laboratoires.
- Romain Labas, puis Mathieu Mevel, mes fournisseurs de F108-gal.
- Agnès Hivonnait et Fanny Beilvert (Nantes), Nathalie Carmoy et Caroline Denis (Brest), Pierre Legras et Pauline Resnier (Angers) qui m'ont aidée à réaliser les nombreuses expériences *in vivo* à Nantes, Brest ou Angers.

Merci Agnès pour l'apprentissage des injections en i.v. et merci à l'équipe de l'UTE-IRT (Nantes), l'équipe de l'animalerie à Brest et l'équipe du SCAHU (Angers) qui se sont bien occupés de mes souris.

- Marie-Claire Venier, Brigitte Pech Fréderic Lagarce et Catherine Passirani qui m'ont encadrée pendant mon monitorat et m'ont aidée à faire mes premiers pas dans l'enseignement. Merci aussi au CIES (Centre d'initiation à l'enseignement supérieur) dont les formations qui m'ont été et me seront utiles.

Merci également à Alexis Guillot et Pauline Resnier, les stagiaires que j'ai encadrés et qui ont initié avec moi le travail concernant les siRNA. Merci Pauline aussi pour ta bonne humeur et les bons moments passés ensemble. Bon courage pour ta thèse et la suite de ce sujet.

Un grand merci à mes collègues de bureau qui ont été nombreux durant ces années de thèse et avec qui j'ai partagé des bons moments :

- à Marie Claire et Catherine C., puis Trinh à l'IBT ; c'était vraiment très agréable de partager un bureau avec vous.
- à Raphael, Romain, Fanny Emilie LB et Benoit C. à la fac de médecine ; c'était un peu serré, mais l'ambiance était bonne. Merci pour votre accueil et soutien tout au long de cette thèse.
- à Emilie G., et Jennifer à l'IRT UN, puis toute l'équipe qui travaillait dans le labo où on ne s'ennuyait jamais.
- à JP, Nico, Elodie et Kien à l'IRIS, pas toujours facile de se concentrer avec tant de monde dans une si petite pièce, mais on s'est bien amusé. JP, tes commentaires, blagues et chansons vont me manquer à Tours, c'est sûr. Bon courage pour la dernière ligne droite. Nico également, toujours prêt à

faire une blague et de bonne humeur. Courage pour la suite de ta thèse. Kien plus calme, mais on a fait bonne équipe pendant les formations du CIES et le monitorat. Bon courage aussi pour ta dernière année. Elodie, ma collègue de sport, tu vas me manquer à Tours, pas seulement pour le sport, mais aussi pour les diverses pauses chocolat ou thé et les bons moments passés ensemble. Bon courage également pour la suite, les manips et l'enseignement.

Je tiens également à remercier les membres de l'équipe de Tristan Montier pour leur accueil chaleureux à Brest, le reste de l'équipe de Bruno Pitard et d'InCell Art que je n'ai pas encore nommés pour leur accueil et soutien tout au long de cette thèse et bien sûr les membres de l'U915 que j'ai côtoyés pendant cette thèse.

Je tiens aussi à remercier tous les membres de l'U646 actuels et anciens qui ont fait de cette thèse une période agréable malgré le stress et la quantité importante de travail.

- Un grand merci à Séverine et Leila pour les voyages que j'ai pu faire avec vous, à travers les nombreuses sorties restos et/ou cinémas et tous les bons moments passés ensemble. Vous étiez à l'écoute et toujours prêtes à me changer les idées. Bon courage pour la suite de ta thèse, Leila et même si c'est parfois difficile et que l'on n'obtient pas les résultats attendus, essaye de prendre un peu de recul et de voir les choses positivement. Séverine, également bonne chance pour la suite et que tu trouves le poste dont tu rêves.

- Merci beaucoup aux stagiaires (ERASMUS) allemands (Florian, Anne, Hallouma, Andrea, Miriam M., Miriam V., Julia, Katrin, Johanna und Caddie) qui sont passés au labo et qui m'ont apporté un peu d'Allemagne à Angers.
- Merci aussi aux « anciens » (thésards ou pas) Mathilde et Simon, Emilie R ., Emilie A. et Fabien, Archibald, Maud, Thanh, Erika et William, Claire et Nico, Gaëtan, Jérôme C., Elisa G., Marie et Julien, Sandy et Michael, Guillaume et Maud, Nolwenn et Gildas pour les nombreuses sorties et fêtes, mais aussi leurs conseils si besoin.
- Merci aussi à Jérôme B., Samuli, Brice, Thomas P., Florian, Anne-Laure, Audrey, Anne-Claire, Khaled, Camille pour les bons moments passés ensemble, bon courage pour la suite.
- Merci aussi à Edith, Olivier, Laurence, Laurent, Claudia, Emmanuel, Patrick pour leur aide et les réponses à mes questions.

Merci aussi à mes amis allemands (Jessi, Natalie, Doreen, Micha, Kerstin, Thomas, Nadja, Sonja) qui ont toujours pris du temps pour venir me voir quand j'étais de retour à Erlangen.

Je clos enfin ces remerciements en dédiant cette thèse à mes parents et frères et sœurs qui m'ont soutenue toutes ces années et sans qui tout cela n'aurait pas été possible. Merci beaucoup aussi à ma grand-mère, mes tantes et oncles ainsi qu'à Nicole et Grégoire qui ont toujours été là pour moi.

SOMMAIRE

LISTE DES FIGURES

LISTE DES TABLEAUX

ABREVIATIONS

A

ADN	acide désoxyribonucléique
AMM	autorisation de mise sur le marché
ARN	acide ribonucléique
ASPGR	récepteur aux asialoglycoprotéines
ATP	adénosine triphosphate

B

BET	bromure d'éthidium
BFI	imagerie par biofluorescence *in vivo*
BGTC	bis(guanidium)-tren-cholesterol
BLI	imagerie par bioluminescence *in vivo*
bp	voir pb

C

CR	rapport de charge positives/charges négatives
CpG	cytosine – phosphate - guanine

D

DiD	1,1'-dioctadécyl-3,3,3',3'-tétraméthylindodicarbocyanine perchlorate
DNA	voir ADN
DNA LNC	voir LNC ADN
DNA MMS	voir MMS ADN
DNA MMS BGTC	voir MMS ADN BGTC
DOSP	dioleylamine-A-succinyl-paromomycine
DOTAP	1,2-dioléyl-3-triméthylammonium-propane
DSPE-PEG_{2000}	1,2-distéaroyl-sn-glycéro-3-phosphoéthanolamine-N-[méthoxy(poly(éthylène glycol)-2000]

E

EPO	érythropoïétine

F

F108	pluronic F108 (PEO_{127}-PPO_{50}-PEO_{127})
F108-gal	F108 galactosylé (1-O-F108-β-D-galactopyranoside)

G

gal	galactose
GAL DNA MMS	voir MMS ADN GAL
GCV	ganciclovir
GDEPT	gene directed enzyme prodrug therapy

H

HSPEG	hydroxystéarate de PEG
HSV-tk	thymidine kinase du virus herpes simplex

L

LNC	nanocapsules lipidiques
LNC ADN	LNC encapsulant un ADN plasmidique
LNC ADN PEG	LNC ADN recouverte de longues chaînes de PEG

M

MDA	dégénérescence maculaire
MMS ADN	systèmes multimodulaires contenant un ADN plamidique
MMS ADN BGTC	MMS ADN contenant le lipide cationique BGTC
MMS ADN DOSP	MMS ADN contenant le lipide cationique DOSP
MMS ADN GAL	MMS ADN galactosylé, contenant du F108-gal
MW	poids moléculaire

N

NaCl	chlorure de sodium

O

O/W emulsion	émulsion huile dans eau

P

P	phosphate
pb	paire de bases
PBS	tampon phosphate saline
PDI	indice de polydispersité
PEG	poly(éthylène glycol)
PEO	poly(oxyde d'éthylène)
pgWIZ^{TM}-luc	plasmide codant pour le gène rapporteur de la luciférase
PIT	température d'inversion de phase
PNP	purine nucleoside phosphorylase
pORF-TK-ΔCpG	plasmide codant pour le gène de la thymidine kinase du virus herpès simplex
PPO	poly(oxyde de propylène)

R

RLB	reporter lysis buffer

S

siRNA	petit ARN interférents

T

TAE	tampon tris-acétate-EDTA
TBE	tampon tris borate EDTA

W

W/O emulsion	émulsion eau dans huile

Z

ZIP	zone d'inversion de phase

PREFACE

Du développement d'un médicament jusqu'à son autorisation de mise sur le marché (AMM), il se passe en général 10 à 15 ans et plusieurs centaines de millions d'euros sont dépensés. Cette période de développement peut être divisée en plusieurs phases, la phase préclinique, dans laquelle le médicament est développé et son efficacité testée sur des cellules (*in vitro*) et sur des animaux (*in vivo*), puis les phases cliniques I à IV chez l'homme. Dans la première phase clinique, la tolérance du médicament et l'absence d'effets secondaires sont évaluées, souvent sur des volontaires sains. En phase II, la dose optimale et ses effets secondaires sont déterminés sur un petit à moyen nombre de patients avant de montrer, en phase III, l'intérêt du nouveau médicament par rapport à un traitement existant ou un traitement placebo sur un grand nombre de patients. Une fois cette phase III terminée et le résultat satisfaisant, le médicament peut obtenir l'AMM, et la dernière phase de suivi à long terme (phase IV) est enclenchée. Malgré la multitude de médicaments développés au sein des différents laboratoires académiques, peu d'entre eux arriveront à franchir l'étape des essais cliniques et encore moins nombreux sont ceux qui obtiendront une AMM.

Ce travail de thèse se situe en phase préclinique ; l'un des vecteurs développés ici entrera-t-il un jour en phase clinique afin d'aboutir à de nouveaux traitements ?

Introduction Générale

1. La thérapie génique

Le principe de la thérapie génique consiste en l'introduction de matériel génétique dans une cellule cible afin d'obtenir un effet thérapeutique. Depuis le premier essai clinique de Rosenberg *et al*. en 1989 [1], le nombre d'essais cliniques dans le monde n'a cessé d'augmenter (Figure 1). D'après le site de « The Journal of Gene Medicine – Gene Therapy Clinical Trials Worldwide », 1714 essais cliniques de thérapie génique étaient approuvés, en cours ou complétés dans le monde en juin 2011.

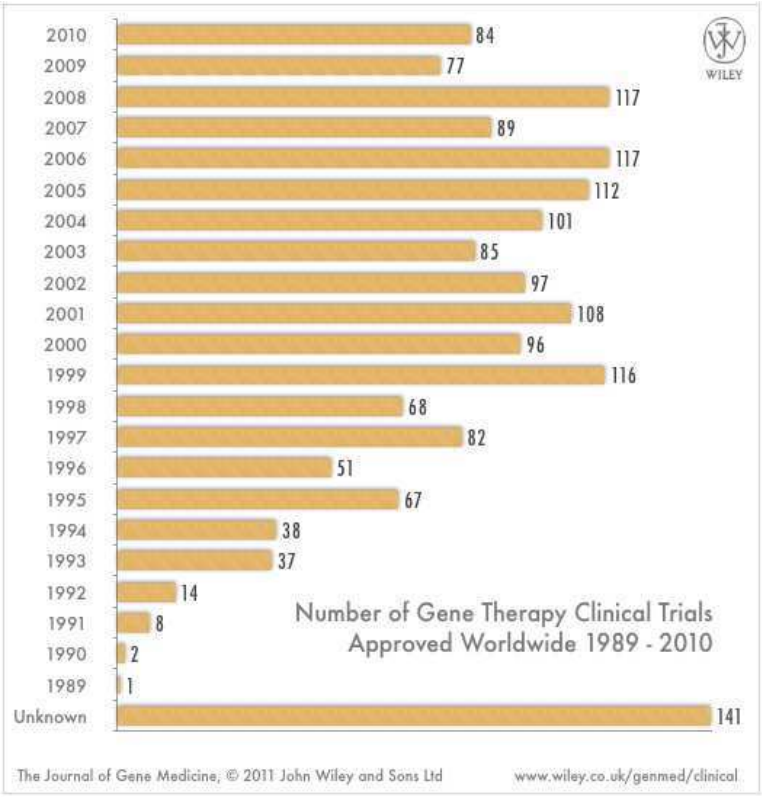

***Figure 1** : Nombre d'essais cliniques approuvés par an entre 1989 et 2010.*

Source : http://www.abedia.com/wiley/years.php 16/10/2011

Au départ, l'objectif premier était de corriger des gènes défectueux impliqués dans des maladies génétiques héréditaires et nécessitant la correction d'un gène à long-terme. Entre-temps, le nombre d'indications a augmenté et la plus répandue est maintenant le cancer avec presque 65% des essais cliniques concernés dans le monde [2]. Ces travaux de thèse se sont focalisés sur deux types de cancers, le mélanome et le gliome (voir §4).

Plusieurs approches ont été testées à travers les différents essais cliniques : antigènes, cytokines, facteurs de croissances, gènes suicides, suppresseurs de tumeurs, siRNA, ADN et d'autres encore. Nous nous sommes intéressés aux deux dernières, basées sur l'utilisation des siRNA et de l'ADN plasmidique.

1.1. La vectorisation

Pour introduire ces acides nucléiques dans la cellule cible, plusieurs techniques différentes ont été étudiées [3]. D'un côté, il existe des méthodes physiques qui provoquent des effets uniquement locaux. Ce sont par exemple, l'électroporation qui est basée sur l'utilisation de pulsations électriques ; la « gene gun » qui est une sorte de pistolet permettant d'introduire des particules de métaux lourds recouvertes de plasmide ADN sous forte pression ; ou encore la sonoration qui exploite les ultrasons afin de perméabiliser la membrane cellulaire.

En parallèle, des techniques de vectorisation se développent permettant idéalement une injection par voie systémique. Dans ce cadre, il existe deux grandes classes de vecteurs, les vecteurs viraux et les vecteurs non-viraux. Ces derniers peuvent encore être divisés en sous-classes selon leur nature : vecteurs lipidiques, vecteurs polymères ou vecteurs peptidiques/protéiques [4].

Dans les essais cliniques, la vectorisation utilisant des virus est majoritaire contrairement aux vecteurs non-viraux (http://www.abedia.com/wiley/vectors.php). L'avantage des vecteurs viraux est leur capacité naturelle à introduire le matériel génétique dans la cellule hôte. Par contre, l'usage de virus, pouvant induire des réponses immunitaires indésirées, et notamment des virus réplicatifs, nécessite des précautions importantes pour éviter un retour à la pathogénicité, ce qui augmente leur coût de production, mais aussi le coût des essais cliniques [5]. De plus, la taille des gènes qu'ils peuvent transporter est limitée [6].

En revanche, les vecteurs non-viraux ne présentent pas ces inconvénients et ont en plus l'avantage d'être facilement formulés, ce qui diminue les coûts de production [2, 7]. Par ailleurs, ils peuvent être aisément modifiés afin de cibler des cellules précises, en utilisant soit des ligands spécifiques pour un ciblage actif, soit un recouvrement de surface qui augmente la furtivité pour un meilleur ciblage passif [8, 9].

Une administration par voie systémique a l'avantage d'engendrer un effet thérapeutique rapide et de ne pas être limitée par la localisation des cellules cibles. De plus, dans le milieu hospitalier, cette voie d'administration est préférée car elle peut être facilement appliquée à

tous les patients. Pour ces raisons, cette voie d'administration a été privilégiée durant ce travail de thèse.

Par ailleurs, le vecteur doit posséder différentes propriétés pour permettre au gène de franchir les nombreuses barrières biologiques pouvant se présenter, avant d'atteindre la cellule cible et d'y effectuer son action (Figure 2). Les barrières à franchir entre le site d'administration et le site d'action, les outils pour développer un vecteur « idéal », tout comme des exemples de vecteurs non viraux pour administrer des siRNA par voie systémique ont été décrits dans la revue bibliographique réalisée en première partie de thèse [4] et ne seront donc pas re-détaillés ici. Nous rappellerons simplement brièvement quels sont les objectifs à atteindre pour un vecteur « idéal » :

1) protéger le gène d'une éventuelle dégradation par les nucléases présentes dans le flux sanguin,
2) être furtif afin d'éviter son élimination par le système immunitaire,
3) atteindre la cellule cible sélectionnée par un ciblage passif ou actif,
4) être internalisé dans la cellule,
5) délivrer l'acide nucléique intact dans la cellule afin de permettre une action thérapeutique.

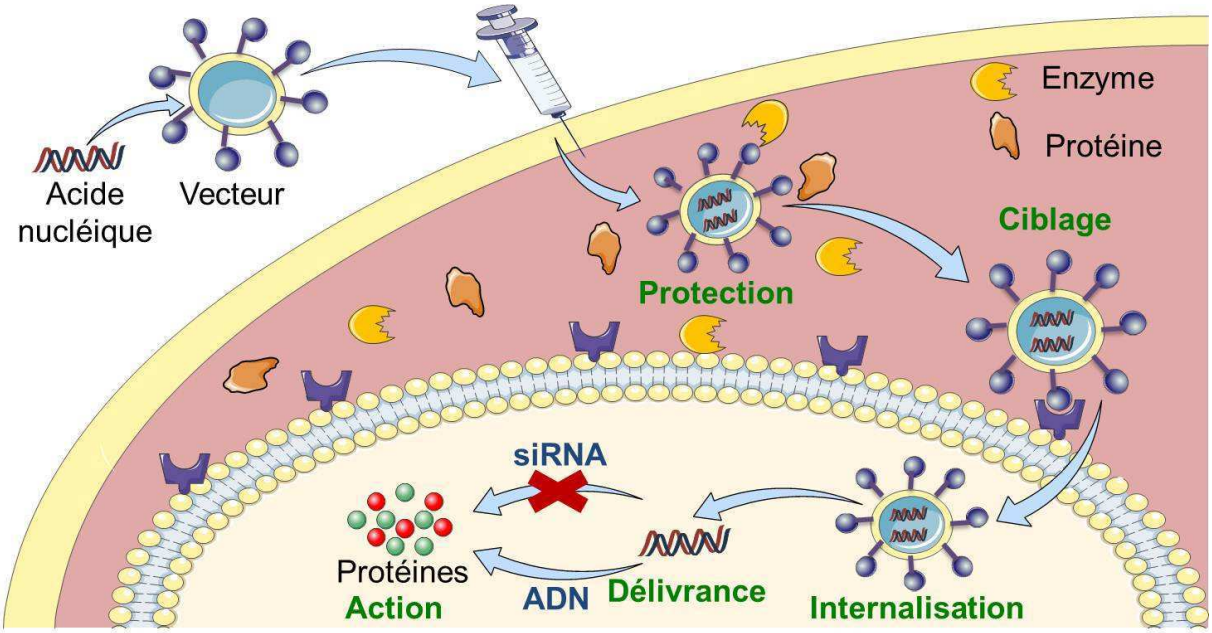

Figure 2 *: Barrières à franchir pour permettre l'action des acides nucléiques*

1.2. Les acides nucléiques

Deux types d'acides nucléiques ont été étudiés, les siRNA et l'ADN plasmidique, tous deux constitués de nucléotides ayant un poids moléculaire d'environ 330 g/mol et portant une charge négative due à un groupement phosphate.

Les siRNA

- Ce sont des petits ARN interférents double brin, composés de 21 à 25 paires de bases, capables de diminuer ou inhiber la synthèse de protéines une fois dans le cytoplasme de la cellule cible [10].
- Le mécanisme d'action et les limites du processus nommé « interférence d'ARN » sont décrits dans la revue bibliographique [4].
- La plupart des essais cliniques repose sur l'administration de siRNA non vectorisé pour applications locales comme dans le cas de la dégénérescence maculaire (MDA).

En complément de la revue bibliographique, le tableau 1 montre quels sont les quelques vecteurs de siRNA non-viraux administrés par infusion en intraveineuse qui sont actuellement en essai clinique. La description de ces vecteurs est détaillée dans la revue bibliographique [4].

No	nom	vecteur	maladie	phase clinique	periode d'essai	sponsor
1	PRO-040201	TKM-ApoB	Hypercholestérolémie	I	06/09 – 01/10	Tekmira Pharmaceuticals Corporation
2	Atu027	AtuPLEXes	Tumeurs solides avancées	I	06/09 – 12/11	Silence Therapeutics AG
3	CALAA-01	Stabilized nanoparticles	Tumeurs solides	I	05/08 – 03/12	Calando Pharmaceuticals
4	ALN-VSP02	SNALPs	Tumeurs solides	I	03/09 – 08/11 07/10 – 01/12	Alnylam Pharmaceuticals

***Tableau 1** : Essais cliniques utilisant des siRNA vectorisés administrés par voie systémique (infusion en iv)*
Source : clinicaltrials.gov 14/10/2011

L'ADN plasmidique

- Il est beaucoup plus grand et peut comporter entre une centaine et quelques milliers de paires de bases [11].
- Il doit, contrairement aux siRNA, atteindre le noyau cellulaire pour utiliser la machinerie cellulaire et exprimer la protéine codée par le plasmide [11].

- Ceux utilisés dans ces travaux de thèse sont le plasmide HSV-tk avec 4384 paires de bases et le plasmide gWIZ^{TM} luciférase qui comporte 6732 paires de bases.

Dans le cadre de cette thèse, le plasmide gWIZ^{TM} luciférase a été utilisé pour quantifier l'efficacité de transfection *in vivo* et comme plasmide modèle dans le développement et la caractérisation physico-chimique des nouveaux vecteurs ADN formulés. L'efficacité de transfection est déterminée en quantifiant la bioluminescence générée par l'oxydation du substrat luciférine ajouté au moment de la quantification. Cette oxydation se fait en présence d'ATP et de l'enzyme luciférase qui est exprimée après transfection du plasmide et qui catalyse cette réaction [12].

L'efficacité de traitement, en revanche, a été déterminée en utilisant le plasmide HSV-tk suivi d'un traitement au ganciclovir (GCV) dans le cadre d'une approche par gène suicide ou en anglais « gene directed enzyme prodrug therapy » (GDEPT) [13, 14]. Le GCV est une prodrogue non-active et non-toxique. L'enzyme HSV-tk, puis d'autres phosphorylases, sont nécessaires pour phosphoryler le GCV et l'activer. Le GCV-triphosphate actif est un analogue de nucléoside et inhibe l'action des polymérases ADN, ce qui conduit à la mort cellulaire (Figure 3).

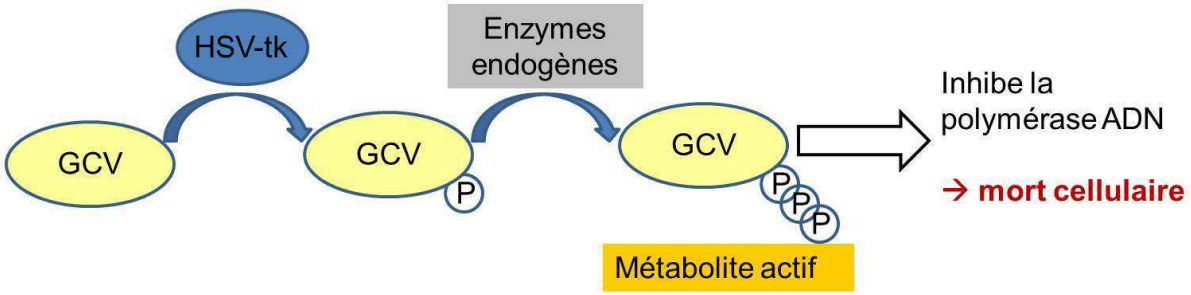

***Figure 3** : Mécanisme d'action de l'approche par gène suicide (HSV-tk/GCV)*

Cette approche utilisant des gènes codant pour des enzymes combinée avec des pro-drogues n'est pas restreinte au système HSV-tk/GCV, même si ce couple est utilisé majoritairement. Une multitude d'autres enzymes et de pro-drogues a également été étudiée dans la littérature et testée dans différents essais cliniques. Dans le tableau 2 sont présentés quelques essais cliniques en cours, utilisant soit le couple HSV-tk/GCV soit PNP/Fludarabine (PNP =

phosphorylase de nucléoside purine qui transforme le fludarabine en 2-fluoroadénine, son métabolite actif). Il est à noter que l'approche par gène suicide dans les essais cliniques se fait en général en utilisant des vecteurs viraux, soit en les injectant directement, le plus souvent en intratumoral, soit en modifiant des lymphocytes *ex vivo*.

No	nom	vecteur	couple enzyme/prodrogue	maladie	phase clinique	periode d'essai	sponsor
1	HSV-tk lymphocytes	Lymphocytes modifiés	HSV-tk/GCV	Hematological Malignancies	I et II	07/02 – 12/11	MolMed S.p.A.
2	Donor lymphocyte infusion	Lymphocytes modifiés	HSV-tk/GCV	Hematological Malignancies	I et II	02/10 – 12/12	Assistance Publique – Hôpitaux de Paris Université Paris 12 et 6
3	Donor lymphocyte infusion	Lymphocytes modifiés	HSV-tk/GCV	Haploidentical Stem Cell transplantation	I et II	01/11 – 09/15	Great Ormond Street Hospital for Children NHS Trus
4	Ad5.SSTR/TK.-RGD	Adénovirus	HSV-tk/GCV	Cancer des ovaires	I	08/09 – 12/11	University of Alabama at Birmingham + NCI
5	Ad5 – y CD/mutTKSR39rep-ADP	Adénovirus	HSV-tk/GCV	Cancer de la prostate	II et III	12/07 – 12/13	Henry Ford Health System
6	FP253	Ovine atadénovirus	PNP/Fludarabine	Cancer de la prostate	I	03/08 – 12/12	Biotech Equity Partners Pty Ltd
7	Ad/PNP	Adénovirus	PNP/Fludarabine	Cancer de la tête et du cou Tumeurs solides avancées	I	02/11– 08/12	PNP Therapeutics, Inc.

***Tableau 2** : Essais cliniques à base de plasmide ADN utilisant l'approche par gène suicide actuellement en cours ou récemment terminés*

Source : clinicaltrials.gov 14/10/2011

2. Les nanovecteurs étudiés

Au sein des laboratoires, Inserm U646 à Angers et Inserm U915 à Nantes, deux types de vecteurs prometteurs ont été développés respectivement, les nanocapsules lipidiques (LNC) et les systèmes multimodulaires (MMS). Les deux systèmes sont basés sur la formation de lipoplexes (complexes entre lipides cationiques et acides nucléiques) [15].

2.1. Les lipides cationiques

Un grand nombre de lipides cationiques a été développé à ce sujet et des stratégies de synthèse ainsi que des exemples de la littérature sont décrits dans la revue bibliographique présentée en annexe [16].

Les lipides cationiques ont une structure commune qui peut se diviser en trois domaines : une tête polaire, une queue lipophile et un bras espaceur qui relie les deux (Fig. 4). La partie lipophile peut être composée soit d'une ou de plusieurs chaînes aliphatiques soit de

cholestérol. La tête polaire peut porter une ou plusieurs charges positives, souvent sous forme de fonctions amines, qui permettent d'interagir avec les phosphates des acides nucléiques, chargés négativement, afin de former les lipoplexes. Le bras espaceur a une influence importante sur la stabilité et la biodégradabilité du lipide.

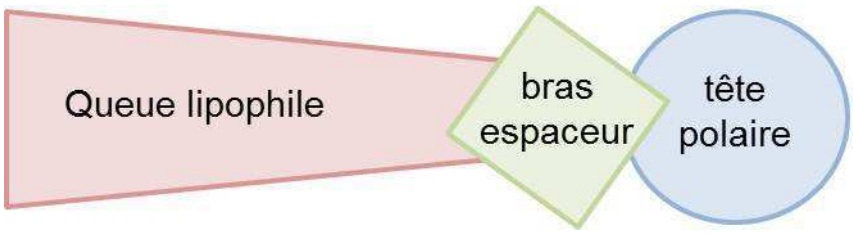

Figure 4 *: Structure schématique des lipides cationiques*

Les lipides cationiques peuvent être classés en plusieurs catégories, soit en fonction de leur tête polaire (monocationiques, polycationiques) soit en fonction de leur queue lipophile (dérivés du cholestérol ou possédant des chaînes grasses aliphatiques). Pour ce travail de thèse, trois lipides cationiques DOTAP (1,2-dioleyl-3-trimethylammoniumpropane), BGTC (bis(guanidinium)-tris(2-aminoethyl)amine-cholesterol) et DOSP (dioleylamine-succinyl-paromomycine) (Fig. 5) ont été utilisés en présence ou absence d'un lipide neutre, le DOPE (1,2-dioleyl-sn-glycero-3-phosphoethanolamine) (Fig. 6). Le lipide DOTAP est composé d'un groupement amine quaternaire en tête, portant une charge positive, et deux chaînes aliphatiques insaturées constituant la partie lipophile. Ce lipide cationique a déjà été largement étudié pour la transfection *in vitro* et *in vivo* [17, 18]. Le lipide BGTC comporte deux charges positives sur des groupements de guanidium et une queue hydrophobe de cholestérol. Le BGTC s'est avéré efficace pour la transfection d'ADN plasmidique [16, 19]. La tête polaire du lipide DOSP est un dérivé d'aminoglycoside portant quatre charges positives. Son segment lipophile est constitué de deux chaînes aliphatiques. Pour ce lipide, les interactions avec l'ADN sont moins importantes que celles entre siRNA et lipide cationique et il s'est avéré plus efficace pour la transfection de siRNA. Cela est lié au fait que les aminoglycosides sont utilisés comme antibiotiques grâce à leur interaction avec l'ARN ribosomal bactérien [16, 20, 21]. Le lipide DOPE, est un lipide neutre, parfois aussi appelé « helper lipid » car il facilite l'échappement endosomal grâce à ses propriétés fusogéniques [22, 23].

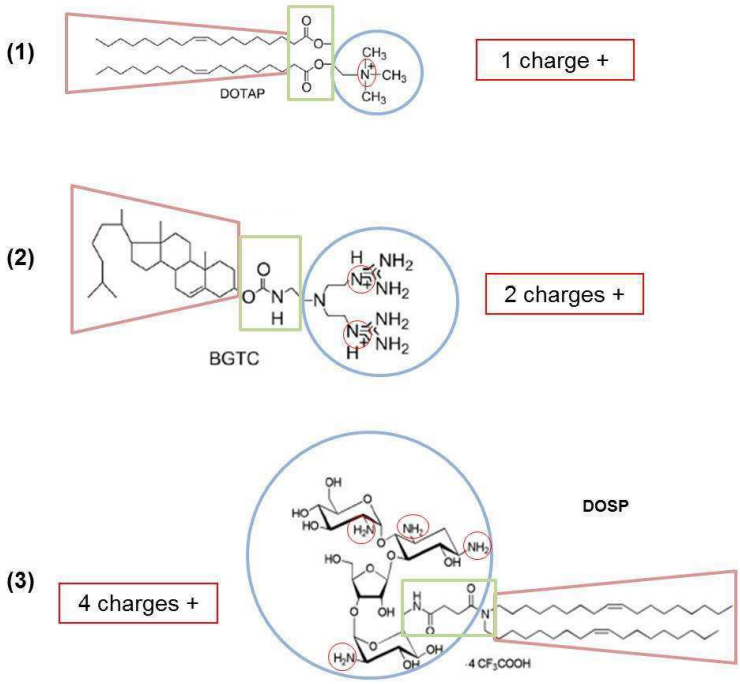

***Figure 5** : Structure et nombre de charges positives par molécule des lipides cationiques étudiés*

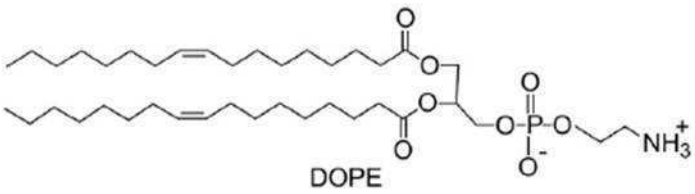

***Figure 6** : Structure du lipide neutre DOPE*

2.2. Les lipoplexes

Pour la formation des lipoplexes, les lipides cationiques en présence de DOPE ont été préparés sous forme de liposomes, le lipide DOSP en absence de DOPE sous forme de micelles. Les liposomes ou micelles préparés ont été mélangés aux acides nucléiques ADN ou siRNA, en présence de NaCl, pour former les lipoplexes. Le rapport de charge (CR), défini comme le rapport des charges positives apportées par les lipides sur les charges négatives portées par l'acide nucléique [+/-], a une grande influence sur la stabilité colloïdale des lipoplexes. Celle-ci peut être mise en évidence par des mesures de taille, de fluorescence et en effectuant des électrophorèses à différents rapports de charge [24]. Le bromure d'éthidium (BET) utilisé pour faire les mesures de fluorescence et les électrophorèses est un intercalant d'ADN. La fluorescence émise peut seulement être détectée si le BET arrive à s'intercaler,

cependant si l'ADN plasmidique est entièrement complexé par les lipides cationiques, le BET n'arrive plus à l'atteindre et, en conséquence, aucune fluorescence ne peut plus être détectée. En général, trois zones distinctes peuvent être déterminées (Fig. 7). Dans la zone A, l'acide nucléique n'est pas encore entièrement complexé par manque de lipide cationique. Cela se manifeste par une petite taille, une fluorescence élevée et une charge de surface négative. Ensuite, en zone B, la quantité de lipide cationique et d'acide nucléique est équivalente, ce qui conduit à une charge de surface neutre et provoque une agrégation des complexes menant à une taille élevée. La fluorescence en revanche est basse car l'acide nucléique est entièrement complexé. Dans la zone C, la quantité de lipide cationique est supérieure à la quantité d'acides nucléiques provoquant une charge de surface positive, une répulsion des complexes et donc une petite taille. La fluorescence est également basse puisque l'acide nucléique est toujours entièrement complexé.

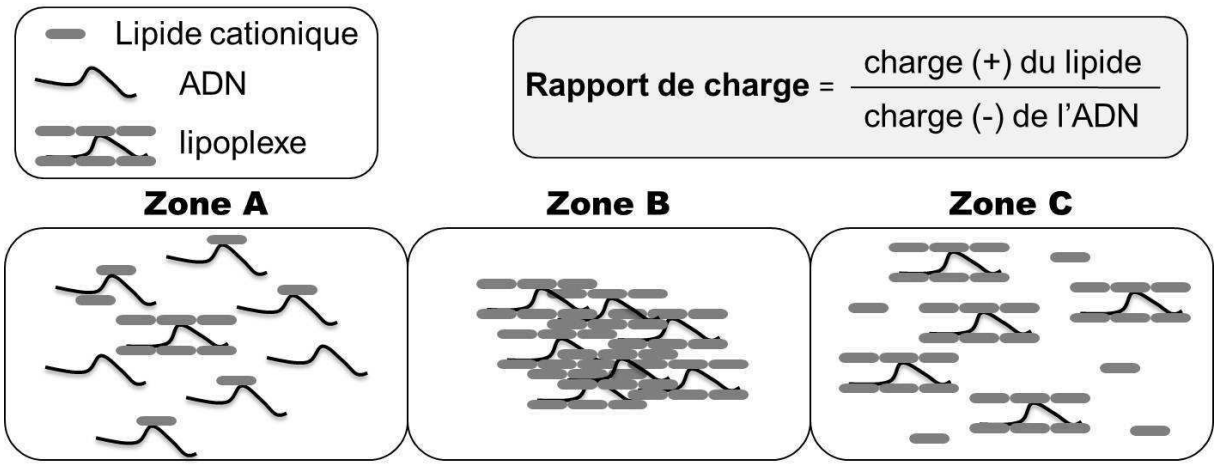

Zone	A	B	C
Rapport de charge	faible	intermédiaire	élevé
Stabilité colloïdale	stable	instable	stable
taille	petite	grande	petite
Charge de surface	negative	(proche de la) neutralité	positive
Complexation de l'ADN	incomplète	complète	complète

Figure 7: *Propriétés des lipoplexes en fonction de leur rapport de charge*

2.3. Les nanocapsules lipidiques classiques

Les nanocapsules lipidiques (LNC) classiques sont constituées d'un cœur liquide de triglycérides et d'une coque rigide composée de lécithine et de chaînes de polyéthylène glycol (PEG). Le procédé de formulation est simple et basé sur l'inversion de phase d'une émulsion [25] (figure 8). Après avoir mélangé toutes les constituants, trois cycles de température autour de la température d'inversion de phase (PIT) sont effectués, tout en agitant la formulation. Une grande quantité d'eau froide est ensuite ajoutée rapidement, ce qui provoque un refroidissement et une dilution de la formulation pour aboutir à la formation de LNC. La taille des LNC peut être modulée en ajustant la quantité des différents constituants pour obtenir au choix des LNC de 20, 50 ou 100nm.

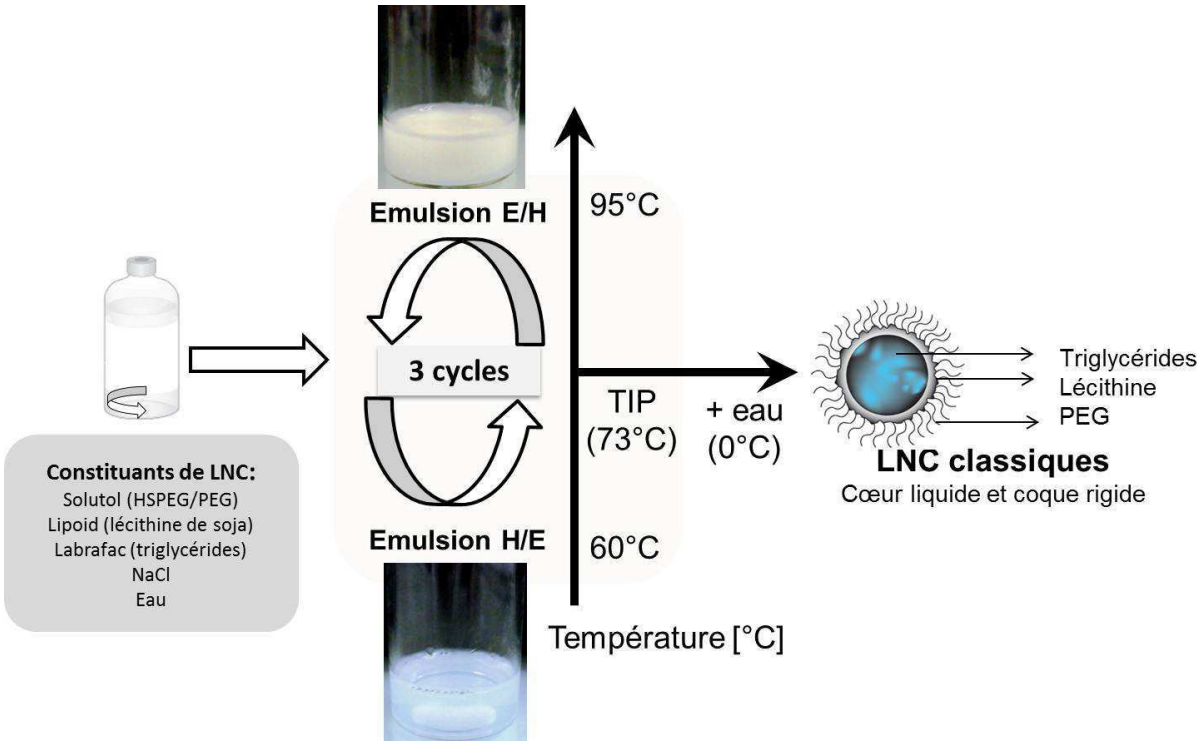

***Figure 8** : Procédé de formulation des nanocapsules lipidiques*

2.4. Les nanocapsules lipidiques ADN

Précédemment, cette formulation de LNC classiques a été modifiée pour encapsuler de l'ADN [26] en remplaçant la lécithine par un autre lipide, le Plurol, constitué de polyglycéryl-6-dioléate (figure 9). La présence de ce nouveau lipide s'est avérée indispensable pour l'encapsulation de l'ADN et a entraîné une nette diminution de la température d'inversion de

phase de 73°C à 28°C. L'ADN a été complexé avec des liposomes DOTAP/DOPE au rapport de charge de 5 avant de les ajouter aux autres constituants et de poursuivre le procédé de formulation classique. En utilisant les quantités de constituants menant à une formulation classique de 50 nm, cette nouvelle formulation présente, après encapsulation des lipoplexes d'ADN une taille d'environ 120 nm et un potentiel zêta positif d'environ 30mV. Un recouvrement de la surface avec des longues chaînes de PEG (DSPE-PEG2000) augmente le temps de circulation dans le sang et mène à des objets de taille similaire, mais avec un potentiel zêta négatif (-17mV) dû aux dipôles négatifs qui se forment au sein des chaînes de PEG [27]. Ces LNC ADN se sont avérées efficaces pour une transfection *in vitro* et *in vivo* [28-30].

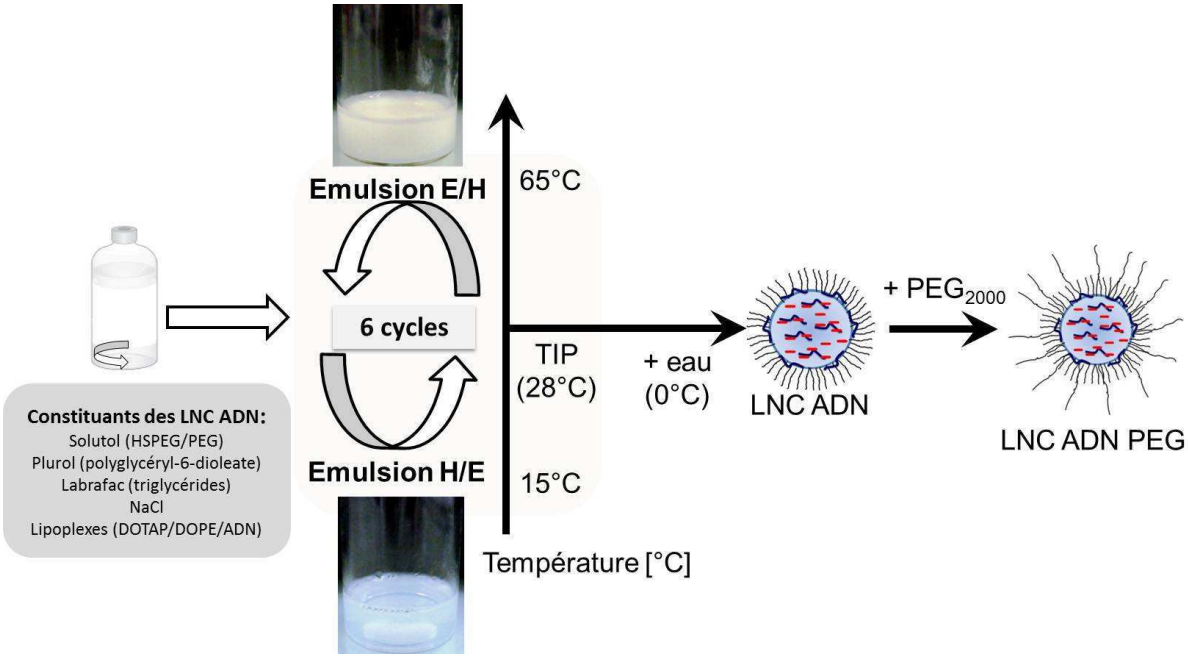

***Figure 9** : Procédé de formulation des LNC ADN (PEG)*

2.5. Les systèmes multimodulaires ADN

Les systèmes multimodulaires (MMS) ADN sont également constitués d'une structure double, avec un cœur de lipoplexes et une couronne composée de stabilisateurs stériques. Pour la formulation de ces MMS ADN, un rapport de charge dans la zone B a été choisi, afin d'obtenir des objets neutres. Comme une charge de surface neutre mène à l'agrégation des complexes, l'ajout d'un stabilisateur stérique est indispensable pour obtenir une petite taille et une stabilité colloïdale des systèmes permettant de les injecter ensuite par voie systémique. Les MMS ADN « classiques » sont constitués d'un plasmide luciférase et de liposomes

BGTC/DOPE à un rapport de charge de 2 et d'un copolymère à blocs, le F108, constitué d'unités de polyéthylène et de polypropylène, au rapport polymère/ADN de 300 [31]. Pour la formulation, les constituants sont simplement mélangés les uns avec les autres et laissés 20 mn à température ambiante, permettant aux MMS ADN de se former (figure 10). Un ligand galactose peut être rajouté au stabilisateur stérique F108 pour cibler les hépatocytes, formant ainsi des GAL ADN MMS. Ces vecteurs se sont avérés efficaces *in vitro* [31]

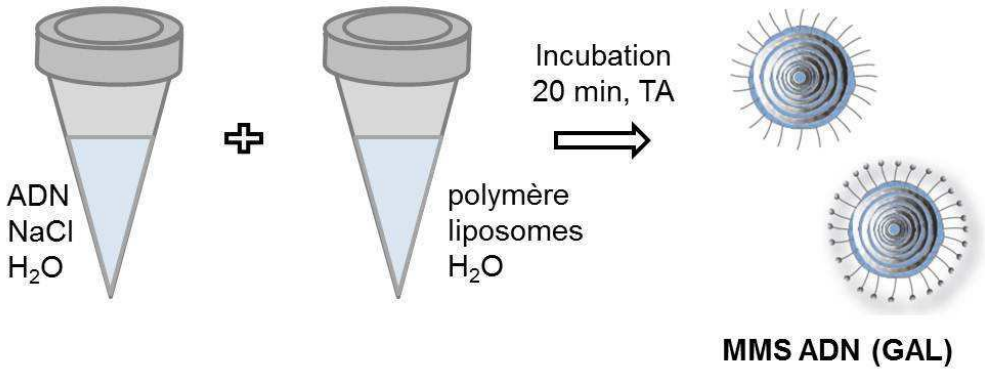

***Figure 10** : Formulation des MMS ADN (GAL)*

3. L'imagerie sur l'animal entier

Afin d'analyser la distribution des vecteurs développés après injection systémique chez la souris (injection intraveineuse dans la veine caudale), une sonde fluorescente émettant dans le proche infrarouge, le DiD (1,1'-dioctadecyl-3,3,3',3'-tetraméthylindodicarbocyanine perchlorate), a été encapsulée dans les différents vecteurs avant leur administration. Le DiD n'étant pas soluble dans l'eau, il est encapsulé dans la phase huileuse ou lipophile des vecteurs (le labrafac pour les LNC et le film lipidique pour les MMS), ce qui renforce ses propriétés optiques [32]. A noter est que la quantité de DiD et la quantité de lipide n'était pas la même pour les différents systèmes et en conséquence la fluorescence n'est pas comparable dans l'absolu pour les différents systèmes (0.01 g/l de DiD/injection avec un rapport DiD/lipide de 1/100 pour les MMS et 0.04 g/l de DiD/injection avec un rapport DiD/lipide de 4/10 000 pour les LNC).

Ces vecteurs fluorescents ont été ensuite suivis en imagerie par biofluorescence *in vivo* (BFI). Cette technique rapide, simple et relativement peu coûteuse est un processus non-invasif, ce qui permet de réduire le nombre d'animaux utilisés [33]. De plus, les différents vecteurs peuvent être suivis en fonction du temps sur le même animal, ce qui permet d'obtenir des

informations plus détaillées. Pour cela, les souris sont anesthésiées par de l'isoflurane et introduites dans l'imageur qui est équipé d'une caméra [34] qui détecte la fluorescence. Pour avoir une vue plus générale et pour mieux identifier les différents organes, les images sont prises en vue latérale et en vue décubitus dorsale. Par contre, l'imagerie par fluorescence n'est pas une méthode réellement quantitative et dépend aussi du tissu étudié et de sa localisation [35].

Le même appareil peut servir également pour suivre l'expression de la luciférase dans l'animal entier en utilisant l'imagerie par bioluminescence *in vivo* (BLI). L'animal reçoit une injection de luciférine (en intrapéritonéal) environ cinq minutes avant l'acquisition, puis il est anesthésié et placé ensuite dans l'imageur. Le principe de la réaction chimique a déjà été décrit dans le paragraphe 1.1.2. au niveau de la présentation du plasmide gWIZ^{TM} luciférase. Au cours de la thèse, cette imagerie BLI a été surtout utilisée pour suivre la croissance tumorale de cellules de mélanome exprimant constitutivement la luciférase.

4. Les types de cancer étudiés

Deux types de cancer ont été étudiés pendant cette thèse utilisant des modèles sous cutanés chez la souris, le mélanome et le gliome.

4.1. Le mélanome

Les mélanocytes qui se situent dans la peau ou dans les yeux produisent de la mélanine et sont à l'origine de leur pigmentation. Le paradoxe de ces cellules est que, d'une part, ils jouent un rôle important dans la prévention des cancers de la peau en protégeant l'épiderme des radiations UV, mais d'autre part, ils sont également les précurseurs du mélanome, la forme la plus agressive du cancer de la peau [36, 37]. Le pronostic de mélanome dépend de l'avancement de la maladie et de la présence ou non de métastases. Après un diagnostic précoce, le mélanome est le plus souvent traité en pratiquant la chirurgie (dans 80% des cas), et le pronostic vital se situe alors entre 75 et 85% de survie à 10 ans ; mais, si le diagnostic est trop tardif et qu'il y a présence de métastases, le pronostic devient assez sombre (entre 20 et 70% de survie en fonction du stade du mélanome) et de nouveaux traitements efficaces ont besoin d'être développés [38, 39].

Pour analyser la distribution des différents vecteurs dans une situation qui ressemble le plus possible à la situation chez l'homme, un modèle orthotopique (dans le même tissu, c'est-à-dire la peau) de mélanome humain sur des souris nude a été développé dans le laboratoire Inserm U613 à Brest. Pour cela, des cellules humaines de mélanome (SK-Mel28) exprimant constitutivement la luciférase ont été cultivées et implantées en transdermique dans le flanc droit des souris nude. Ces souris sont athymiques et diminuent donc le rejet des cellules tumorales implantées. Puis, la croissance tumorale a été suivie en utilisant l'imagerie par bioluminescence *in vivo*.

4.2. Le gliome

Les gliomes incluant les astrocytomes et les glioblastomes sont des tumeurs du cerveau qui, malheureusement, ont un diagnostic très peu favorable [40]. Les gliomes de grade I et II sont en règle générale des astrocytomes bénins qui peuvent être éliminés chirurgicalement. Pour les tumeurs de grade II, la médiane de temps de survie est de 6 à 8 ans. Mais, si l'agressivité atteint les grades III (astrocytomes anaplasiques) ou IV (glioblastomes), ce temps se réduit à seulement 2 à 3 ans (grade III) voire moins [41]. La chirurgie devient de plus en plus difficile car l'infiltration dans les tissus sains est trop avancée pour éliminer l'intégralité du tissu tumoral sans abimer les parties saines du cerveau. Pour ces gliomes de haut grade, le traitement standard consiste à éliminer le plus de tissu tumoral possible puis d'effectuer une radiothérapie et une chimiothérapie avec du témozolomide [42, 43].

Afin d'étudier l'efficacité de nos traitements sans avoir besoin de chirurgie, un modèle de gliome sous-cutané a été développé au laboratoire Inserm U646 à Angers. Des cellules humaines de gliome U87MG cultivées au laboratoire sont implantées en transdermique dans le flanc droit de souris Swiss nudes. Ces souris athymiques ont été choisies pour éviter le rejet de la tumeur. Pour déterminer l'efficacité du traitement, le volume tumoral a été déterminé en mesurant régulièrement la longueur et la largeur de la tumeur, et par le calcul selon la formule $V = \pi/6 * \text{longueur}^2 * \text{largeur}$.

5. Les objectifs de thèse

- ***Développer de nouveaux vecteurs pour administrer des siRNA par voie systémique***

En premier lieu, l'objectif de cette thèse était de développer de nouveaux vecteurs de siRNA, en s'inspirant des vecteurs ADN existants. Dans ce but, une **revue bibliographique**, constituant la première partie de ce manuscrit, présente les vecteurs non-viraux de la littérature permettant d'administrer des siRNA par voie systémique. La deuxième partie (**Conception et caractérisation**) débute par la description de LNC de siRNA obtenues à partir de différents lipides cationiques (**Publication No 1**).

- ***Poursuivre la caractérisation des vecteurs ADN existants***

Dans un deuxième temps, nous avons mis au point un dosage ADN permettant de mieux caractériser nos vecteurs ADN, et développé de nouveaux systèmes multimodulaires ADN à l'aide du lipide cationique DOSP. L'analyse de la distribution de ces vecteurs sur des souris saines a été réalisée en imagerie par biofluorescence afin de compléter leur caractérisation (**Publication No 2**).

- ***Etudier l'efficacité de ces vecteurs ADN sur des modèles tumoraux de mélanome et de gliome***

Dans ce troisième objectif, les LNC ADN ont été testées sur un modèle orthotopique de mélanome, en étudiant leur distribution et leur efficacité dans une approche par gène suicide (**Publication No 3**). Les DNA MMS, n'ayant encore jamais été testés in vivo, ont d'abord été étudiés sur un modèle de gliome en comparaison avec les LNC ADN (préalablement décrites dans le modèle gliome par Morille *et al.* [29]. Puis, un traitement basé également sur l'approche par gène suicide, a été appliqué sur ce même modèle à partir des vecteurs les plus prometteurs (**Publication No 4**).

Liste des Publications issues de cette thèse

1. Revue bibliographique

Non-viral nanosystems for systemic siRNA delivery

David S., Pitard B., Benoit JP. and Passirani C.

Pharmacological Research 2010 Aug; 62 (2): 100-14

2. Conception et caractérisation

SiRNA LNCs – a novel platform of lipid nanocapsules for systemic siRNA administration

David S., Resnier P., Guillot A., Pitard B., Benoit JP. and Passirani C.

European Journal of Pharmaceutics and Biopharmaceutics – soumis

DNA nanocarriers for systemic administration – characterization and in vivo bioimaging in healthy mice

David S., Passirani C., Carmoy N., Morille M., Benoit JP., Montier T. and Pitard B.

Molecular Therapy - soumis

3. Efficacité des nanovecteurs

***In vivo* imaging of DNA lipid nanocapsules after systemic administration in a melanoma mouse model**

David S., Carmoy N., Resnier P., Denis C., Misery L., Pitard B., Benoit JP, Passirani C. and Montier T

International Journal of Pharmaceutics, 2011, in press

Treatment efficacy of DNA lipid nanocapsules and DNA multimodular systems after systemic administration in a human glioma model

David S., Montier T., Carmoy N., Clavreul A., Pitard B., Benoit JP. and Passirani C.

Gene Therapy – soumis

4. Annexes

Nature as a source of inspiration for cationic lipid synthesis

Labas R., Beilvert F., Barteau B., David S., Chèvre R. and Pitard B.

Genetica 2010 Feb ; 138 (2) : 153 - 68

RÉFÉRENCES

1. **Rosenberg, S.A., et al., Gene transfer into humans--immunotherapy of patients with advanced melanoma, using tumor-infiltrating lymphocytes modified by retroviral gene transduction. N Engl J Med, 1990. 323(9): p. 570-8.**

2. **Morille, M., et al., Progress in developing cationic vectors for non-viral systemic gene therapy against cancer. Biomaterials, 2008. 29(24-25): p. 3477-96.**

3. **Kawakami, S., Y. Higuchi, and M. Hashida, Nonviral approaches for targeted delivery of plasmid DNA and oligonucleotide. J Pharm Sci, 2008. 97(2): p. 726-45.**

4. **David, S., et al., Non-viral nanosystems for systemic siRNA delivery. Pharmacol Res, 2010. 62(2): p. 100-14.**

5. **Cross, D. and J.K. Burmester, Gene therapy for cancer treatment: past, present and future. Clin Med Res, 2006. 4(3): p. 218-27.**

6. **Collins, S.A., et al., Viral vectors in cancer immunotherapy: which vector for which strategy? Curr Gene Ther, 2008. 8(2): p. 66-78.**

7. **Jin, S. and K. Ye, Nanoparticle-mediated drug delivery and gene therapy. Biotechnol Prog, 2007. 23(1): p. 32-41.**

8. **Huynh, N.T., et al., The rise and rise of stealth nanocarriers for cancer therapy: passive versus active targeting. Nanomedicine (Lond), 2010. 5(9): p. 1415-33.**

9. **Kang, J.H., R. Toita, and Y. Katayama, Bio and nanotechnological strategies for tumor-targeted gene therapy. Biotechnol Adv, 2010. 28(6): p. 757-63.**

10. **De Paula, D., M.V. Bentley, and R.I. Mahato, Hydrophobization and bioconjugation for enhanced siRNA delivery and targeting. Rna, 2007. 13(4): p. 431-56.**

11. **Elsabahy, M., A. Nazarali, and M. Foldvari, Non-viral nucleic acid delivery: key challenges and future directions. Curr Drug Deliv, 2011. 8(3): p. 235-44.**

12. **Roda, A., et al., Bioluminescence in analytical chemistry and in vivo imaging. TrAC Trends in Analytical Chemistry, 2009. 28(3): p. 307-322.**

13. **Altaner, C., Prodrug cancer gene therapy. Cancer Lett, 2008. 270(2): p. 191-201.**

14. **Portsmouth, D., J. Hlavaty, and M. Renner, Suicide genes for cancer therapy. Mol Aspects Med, 2007. 28(1): p. 4-41.**

15. **Felgner, P.L., et al., Nomenclature for synthetic gene delivery systems. Hum Gene Ther, 1997. 8(5): p. 511-2.**

16. **Labas, R., et al., Nature as a source of inspiration for cationic lipid synthesis. Genetica, 2010. 138(2): p. 153-68.**

17. **Caracciolo, G., et al., Factors Determining the Superior Performance of Lipid/DNA/Protammine Nanoparticles over Lipoplexes. J Med Chem, 2011. 54(12): p. 4160-4171.**

18. **Simberg, D., et al., DOTAP (and other cationic lipids): chemistry, biophysics, and transfection. Crit Rev Ther Drug Carrier Syst, 2004. 21(4): p. 257-317.**

19. **Vigneron, J.P., et al., Guanidinium-cholesterol cationic lipids: efficient vectors for the transfection of eukaryotic cells. Proc Natl Acad Sci U S A, 1996. 93(18): p. 9682-6.**

20. **Sainlos, M., et al., Kanamycin A-derived cationic lipids as vectors for gene transfection. Chembiochem, 2005. 6(6): p. 1023-33.**

21. **Desigaux, L., et al., Self-assembled lamellar complexes of siRNA with lipidic aminoglycoside derivatives promote efficient siRNA delivery and interference. Proc Natl Acad Sci U S A, 2007. 104(42): p. 16534-9.**

22. **Zuhorn, I.S., et al., Nonbilayer phase of lipoplex-membrane mixture determines endosomal escape of genetic cargo and transfection efficiency. Mol Ther, 2005. 11(5): p. 801-10.**

23. **Hirsch-Lerner, D., et al., Effect of "helper lipid" on lipoplex electrostatics. Biochim Biophys Acta, 2005. 1714(2): p. 71-84.**

24. **Pitard, B., Supramolecular assemblies of DNA delivery systems. Somat Cell Mol Genet, 2002. 27(1-6): p. 5-15.**

25. **Heurtault, B., et al., A novel phase inversion-based process for the preparation of lipid nanocarriers. Pharm Res, 2002. 19(6): p. 875-80.**

26. **Vonarbourg, A., et al., The encapsulation of DNA molecules within biomimetic lipid nanocapsules. Biomaterials, 2009. 30(18): p. 3197-204.**

27. **Vonarbourg, A., et al., Electrokinetic properties of noncharged lipid nanocapsules: influence of the dipolar distribution at the interface. Electrophoresis, 2005. 26(11): p. 2066-75.**

28. **Morille, M., et al., Galactosylated DNA lipid nanocapsules for efficient hepatocyte targeting. Int J Pharm, 2009. 379(2): p. 293-300.**

29. **Morille, M., et al., Long-circulating DNA lipid nanocapsules as new vector for passive tumor targeting. Biomaterials, 2009. 31(2): p. 321-9.**

30. **Morille, M., et al., Tumor transfection after systemic injection of DNA lipid nanocapsules. Biomaterials, 2010.**

31. **Letrou-Bonneval, E., et al., Galactosylated multimodular lipoplexes for specific gene transfer into primary hepatocytes. J Gene Med, 2008. 10(11): p. 1198-209.**

32. **Texier, I., et al., Cyanine-loaded lipid nanoparticles for improved in vivo fluorescence imaging. Journal of Biomedical Optics, 2009. 14(5): p. 054005.**

33. **Goutayer, M., et al., Tumor targeting of functionalized lipid nanoparticles: assessment by in vivo fluorescence imaging. Eur J Pharm Biopharm, 2010. 75(2): p. 137-47.**

34. **Hardy, J., et al., Bioluminescence imaging of lymphocyte trafficking in vivo. Exp Hematol, 2001. 29(12): p. 1353-60.**

35. **Dufort, S., et al., Optical small animal imaging in the drug discovery process. Biochim Biophys Acta, 2010. 1798(12): p. 2266-73.**

36. **Lin, J.Y. and D.E. Fisher, Melanocyte biology and skin pigmentation. Nature, 2007. 445(7130): p. 843-50.**

37. **Gray-Schopfer, V., C. Wellbrock, and R. Marais, Melanoma biology and new targeted therapy. Nature, 2007. 445(7130): p. 851-7.**

38. **Garbe, C., et al., Diagnosis and treatment of melanoma: European consensus-based interdisciplinary guideline. Eur J Cancer, 2010. 46(2): p. 270-83.**

39. **Tawbi, H. and N. Nimmagadda, Targeted therapy in melanoma. Biologics, 2009. 3: p. 475-84.**

40. **Westphal, M. and K. Lamszus, The neurobiology of gliomas: from cell biology to the development of therapeutic approaches. Nat Rev Neurosci, 2011. 12(9): p. 495-508.**

41. **Louis, D.N., et al., The 2007 WHO classification of tumours of the central nervous system. Acta Neuropathol, 2007. 114(2): p. 97-109.**

42. **Stupp, R., et al., Radiotherapy plus concomitant and adjuvant temozolomide for glioblastoma. N Engl J Med, 2005. 352(10): p. 987-96.**

43. **Arko, L., et al., Experimental approaches for the treatment of malignant gliomas. Pharmacol Ther, 2010. 128(1): p. 1-36.**

Revue bibliographique

Pharmacological Research 62 (2010) 100–114

Contents lists available at ScienceDirect

Pharmacological Research

journal homepage: www.elsevier.com/locate/yphrs

Review

Non-viral nanosystems for systemic siRNA delivery

Stephanie David[a,b], Bruno Pitard[b,**], Jean-Pierre Benoît[a], Catherine Passirani[a,*]

[a] INSERM U646, Université d'Angers, 10 rue André Boquel, 49100 Angers, France
[b] Institut du Thorax, INSERM UMR 915, IRT-UN, 8 quai Moncousu, BP 7072, 44007 Nantes, France

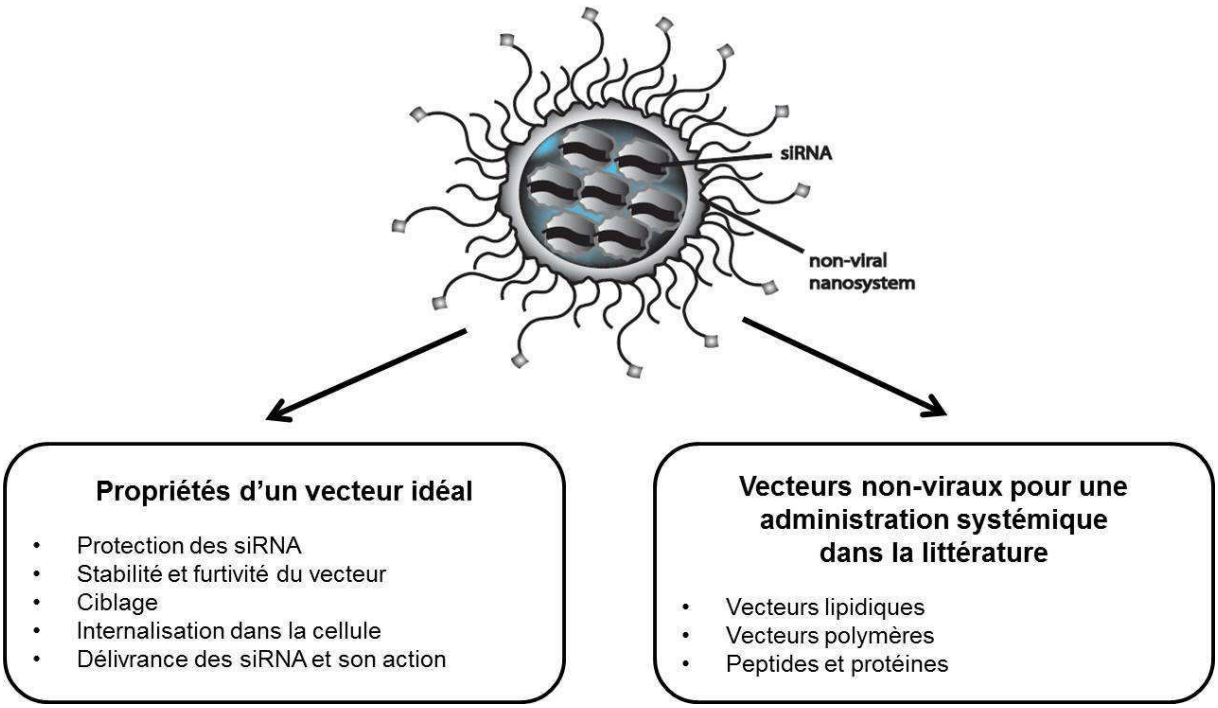

Une recherche bibliographique approfondie sur le sujet de la délivrance de petits ARN à interférence (siRNA) par voie systémique a été menée. En première partie, le mécanisme d'action des siRNA et se limites sont décrits, ainsi que les propriétés du vecteur idéal. En deuxième partie, différents vecteurs non-viraux utilisés pour administrer des siRNA par voie systémique *in vivo*, décrits dans la littérature, sont présentés.

Non-viral nanosystems for systemic siRNA delivery

Stephanie David[a,b], Bruno Pitard[b]*, Jean-Pierre Benoît[a], Catherine Passirani[a]*

[a] INSERM U646, Université d'Angers, 10 rue André Boquel, 49100 Angers, France

[b] Institut du Thorax, INSERM UMR 915, IRT-UN, 8 quai Moncousu, BP 7072, 44007 Nantes, France

* Corresponding author:

Catherine Passirani, Tel. : +33 241 735850 ; fax : + 33 241 735853 ;

E-mail address: catherine.passirani@univ-angers.fr

Bruno Pitard, Tel.: +33 228 080128 ; fax: +33 228 080130 ;

E-mail address: Bruno.pitard@univ-nantes.fr

ABSTRACT

To use siRNA (small interfering ribonucleic acids) for systemic administration, a delivery system is often necessary to overcome barriers between administration and the target sites. These delivery systems require different properties to be efficient. On the one hand, they have to protect siRNA from degradation and/or inactivation and, on the other hand, they have themselves to be stable in blood and possess stealth properties to avoid elimination and degradation. Active and/or passive targeting should help the delivery system to reach the desired cell type or tissue, to be internalised, and to deliver siRNA to the cytoplasm so that siRNA can act by RNA interference and inhibit protein synthesis.

This review presents an overview of different non-viral delivery systems, which have been evaluated in vivo or entered in clinical trials, with a focus on their physicochemical properties in order to help the development of new and efficient siRNA delivery systems, as the therapeutic solutions of tomorrow.

Keywords: siRNA, delivery system, physicochemical properties, gene silencing

CONTENTS

1. INTRODUCTION

SiRNA (small interfering ribonucleic acids) can inhibit the gene expression of specific proteins by a mechanism which is called RNA interference (RNAi). This technology presents a promising new approach and is on the rise since its discovery in 1998. Delivery systems, of various origins, can help siRNA to overcome barriers after systemic administration to enhance their efficacy.

Nanotechnology is a research field which has gained a lot of interest over the last few years. As nanosystems were developed to target drugs, different research teams have combined these technologies to create nanosystems for siRNA delivery. This area of research started about ten years ago, and progress in this field is very rapid, but only few systems have yet been evaluated *in vivo* or undergone clinical trials.

In this review different nanosystems will be presented with a focus on their physicochemical properties. To develop a new therapy, the action mechanism of the drug and the properties of the system have to be examined. With this aim in mind, we will first present the RNAi mechanism with its advantages and limits and will then describe the different delivery systems and their required properties to deliver siRNA in an efficient manner to the cytoplasm, the action site of siRNA. Later, promising, non-viral delivery systems have been selected from the literature, and are presented along with comparisons of their physicochemical properties.

2. RNA INTERFERENCE

RNA interference (RNAi) is a natural mechanism of gene silencing conserved in plant and mammalian cells. This process, related to normal defence to protect the genome, inhibits protein synthesis by targeting a specific messenger RNA (mRNA) for degradation [1]. This mechanism was first described in Petunia flowers in 1990 and later named post-transcriptional gene silencing. In 1998 Fire *et al.* discovered RNAi in the nematode *C. Elegans* [2] and received the Nobel Prize in physiology or medicine in 2006 for their discovery. This technology represents a promising new strategy for drug target validation and the study of functional genomics, but since its discovery, it has also rapidly emerged as having promising therapeutic potential for human diseases.

2.1. The RNAi pathway

The RNAi pathway is located in the cytoplasm of the cell and can be divided into 2 phases: the initiation phase (generation of effector molecules) and the subsequent effector phase (the actual RNAi mechanism). There are two groups of effector molecules: small interfering RNA (siRNA), which are generally composed of 21 – 23 nucleotides (nt) double-stranded RNA (dsRNA) segments with two nucleotide 3'-overhangs, and micro RNA (miRNA), which generally consists of 22 nt dsRNA segments. The generation of siRNA, on the one hand, begins in the cytoplasm with the cleavage of long dsRNA by Dicer (a multidomain enzyme of the RNase III family). The generation of miRNA, on the other hand, begins in the nucleus where endogenously-encoded primary miRNA transcripts (pri-miRNA) are processed into precursor miRNA (pre-miRNA). Then pre-miRNA (with an imperfect stem-loop structure) is transported in the cytoplasm where it is cleaved by Dicer. In the effector phase, siRNA and miRNA are unwound and then assembled into RNA-induced silencing complexes (RISC). Activated RISC contain only single-stranded (antisense) siRNA or miRNA, guiding RISC to its complementary target mRNA. SiRNA generally has perfect sequence complementarity with its target messenger RNA (mRNA) and induces site-specific cleavage of the mRNA (Fig. 1), contrary to miRNA which has typically imperfect sequence complementarity which leads to translational repression without mRNA degradation. The result of both pathways is the inhibition of protein synthesis [3-8].

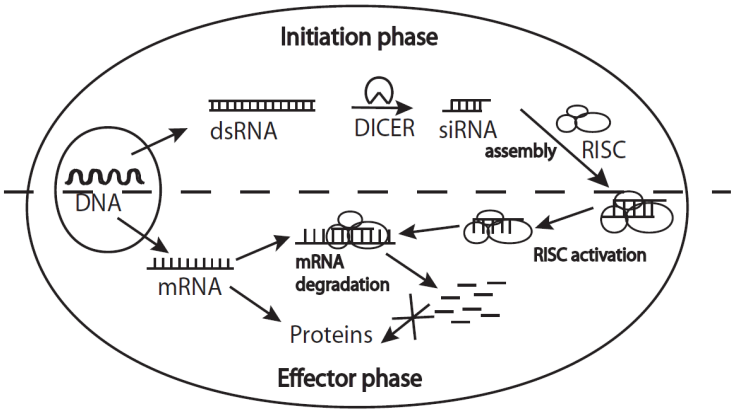

Figure 1: Mechanism of RNA interference by siRNA

This mechanism can be divided in 2 phases, the initiation phase (siRNA production) and the effector phase (siRNA acts to induce gene silencing). SiRNA are produced from long dsRNA by cleavage of Dicer and then assembled to RISC. The antisense siRNA strand guides the complex to the target mRNA where mRNA degradation is initiated to inhibit protein synthesis.

2.2. Strategies to trigger RNA interference

It is possible to exploit this native gene silencing pathway for regulating genes of interest. There are three basic strategies to trigger RNAi: 1. Introduction of a DNA plasmid in the nucleus of the target cell, 2. delivering precursor molecules (dsRNA to generate siRNA, or shRNA to generate miRNA) or 3. delivering synthetic siRNA to the cytoplasm of the target cells. The third strategy is a simple way to induce potent gene silencing with a transient effect, whereas the two first strategies have the potential of being stably introduced, for example by a single treatment of viral vector-delivered shRNA genes [9].

In this review, we will limit ourselves to the third strategy, the delivery of synthetic siRNA. Advantages of this strategy include the relatively easy chemical synthesis of small RNA molecules, the lower probability of nonspecific side effects, and the safety due to the fact that siRNA delivery is based on non-viral transfer strategies and siRNA cannot integrate into the genome [3]. Furthermore, siRNA only needs to reach the cytoplasm of the cell, contrary to DNA-based strategies which start in the nucleus, and they do not require the action of Dicer.

Limits of this strategy are their short half life (unmodified, naked siRNA are rapidly degraded by nucleases) and their difficulty to cross cellular membranes due to their large molecular weight (around 13kDa) and their negative phosphate charges (around 40) [10]. These limits can be reduced using a vector which can protect siRNA, augment their half-life time and help to cross cellular membranes.

Another limit is the induction of non-specific side effects and the activation of an innate immune response. RIG-I like receptors (RLR) as RIG-I (retinoic acid-inducible gene I) or MDA5 (melanoma differentiation-associated antigen 5) and Toll-like Receptors (TLR) as TLR3, TLR7, TLR8 and TLR9 are involved in viral nucleic acid recognition. RIG-I and MDA5 are cytosolic helicases and essential for controlling viral infection whereas TLR3, TLR7, TLR8 and TLR9 are located in the endosomal membrane and largely dispensable for effective antiviral defence. These receptors seem also able to recognize synthetic siRNA. Different studies showed, that a well-defined molecular structure, like 5’ triphosphate, rather than a specific sequence motif could be the activator of these receptors and induce an interferon (IFN) response [11]. Marques *et al*. showed also in their study [12], that the structure of siRNA (siRNA with blunt ends or with 2-nt 3’ overhang) but also the length of the siRNA (23 – 27 nt) had an influence on the activation of an IFN response. SiRNA with 2-nt 3’ overhang and short sequences (23 nt) had less influence and should be favoured when using synthetic siRNA to minimize these non-specific side effects.

3. SIRNA ADMINISTRATION AND DELIVERY SYSTEMS

The first point to think of when developing a drug delivery system for siRNA is whether systemic or local administration is needed. This decision depends on the disease and the target tissue or cell localisation. The advantages of local administration are firstly, that only a simple formulation is needed which leads to an easier production and administration, and secondly, that lower doses are required, which limits intracellular (concentration-dependent) immune responses. But this technique is limited to tissues that are sufficiently accessible, such as skin, lung or muscle [3,4]. In parallel, the principle advantage for systemic administration is the rapid action and biodistribution but also the wide range of application. Moreover in the clinic many diseases require intravenous (i.v.) or intraperitoneal (i.p.) injection treatment regiments. For this reason, we chose to focus on systemic administration by i.v. injection.

The biggest challenge in the use of siRNA-based therapies by systemic administration is the difficulty of siRNA delivery. To help siRNA reach the cytoplasm of the target cell, where they can become effective and induce gene silencing, different delivery systems have been developed. They can be classified into two main groups: viral and non-viral delivery systems. Viral delivery systems are mostly used to deliver DNA plasmids or precursor molecules to induce RNAi, whereas synthetic siRNA-delivery more commonly occurs by non-viral delivery systems. Both groups of delivery systems have their advantages and disadvantages. Actually, there are five groups of viral delivery systems used for RNAi (Retrovirus, Lentivirus, Adenovirus, Adeno-Associated-Virus (AAV), and Baculovirus) (reviewed in Li et *al.* [13]). High transduction efficacy, due to the inherent ability of viruses to transport genetic material into cells, is one of their advantageous properties [14]. But the potential of mutagenicity or oncogenesis, several host immune responses, and the high cost of production limit their application [10]. For these reasons, different kinds of non-viral siRNA delivery systems have been tested to avoid viral vectors (for example, the injection of chemically-stabilised or modified RNA, encapsulating siRNA in microparticles, nanoparticles or liposomes, binding siRNA to cationic or other particulate carriers).

This review will focus on the delivery of synthetic siRNA with non-viral delivery systems, in particular, on nanosystems. Nanoparticles used as drug delivery vehicles are generally < 100nm in at least one dimension, and consist of different biodegradable materials such as natural or synthetic polymers, lipids, or metals [15].

4. NON-VIRAL NANOSYSTEM PROPERTIES

To deliver siRNA into the cytoplasm after systemic administration, the chosen delivery system has to possess different properties to be efficient; this is the subject of this section.

4.1. SiRNA protection

After systemic administration, naked siRNA (administrated without vectors) are rapidly degraded by serum and tissue nucleases, excreted via the kidney, or taken up by macrophages of the mononuclear phagocyte system (MPS). The consequence is that they do not have enough time to reach the target and/or to perform their function and so, gene silencing is ineffective. There are different possibilities to prolong their circulation time in the bloodstream and to protect siRNA from elimination and inactivation (by enzymatic or chemical degradation). SiRNA can be chemically modified (for example by phosphodiester modification [16,17] or 2'-sugar modification [18,19]) or bioconjugated (for example with lipids at one or both strands of siRNA [20]) (reviewed in De Paula *et al.* [5]). These modifications can protect siRNA from elimination and inactivation but do not necessarily augment the efficacy of gene silencing *in vivo*. Another possibility is to use a synthetic vector that should be inert (for example complexation with cationic lipids or polymers, or encapsulation into lipid particles (see below)). Additional properties like stealth or targeting properties allow the enhancement of gene silencing efficacy and will also be described.

4.2. Stability and stealth properties

Effective gene silencing requires vector stability (against degradation or disassembly in blood [21]) and stealth properties (to be undetectable by macrophages) for the vector; the surface charge of the vector is an important parameter for its stability. *In vitro*, a positive surface charge is advantageous for effective siRNA delivery because it facilitates binding to negatively-charged cell membranes and induces cell uptake [22]. For *in vivo* applications, a positive surface charge is rather a handicap because interactions with negatively charged serum proteins such as serum albumin, lipoproteins or IgG proteins, can inhibit cell uptake. Indeed Zelphati *et al.* [23] showed that non-specific interactions between cationic lipids and serum proteins lead to neutralisation of the positive charges and/or an increase in size, and cause aggregation of the neutralised complexes. The charge neutralisation diminishes interaction with cell membranes, size increase reduces the internalisation efficacy, and the aggregates can cause lung embolism [24]. Additionally, serum albumin may act as a steric

barrier and inhibit endosomal destabilisation and/or siRNA release. Another important point is that cationic complexes can activate the complement system, which lead to opsonisation and sequestration in Kupffer cells in the liver [23]. When organs of the mononuclear phagocyte system (MPS) (spleen, liver …) are targeted, vectors can be used without surface modification. In contrast, if the target is outside the MPS, "stealth" nanocarriers are needed [25]. To limit these interactions with charged serum proteins, the surface charge can be masked by covering the vector with hydrophilic polymers (such as (poly)ethylene glycol (PEG), (poly)hydroxylpropyl methacrylamide (pHPMA) or (poly)vinyl pyrrolidine (PVP)) [26] which form a dense, hydrophilic network around the vector and limit hydrophobic or electrostatic interaction with the extracellular medium. The result is a longer circulation time by avoiding MPS-uptake [27] and a vector with stability and stealth properties. Another possibility is to use vectors with a near-neutral surface charge [24,28].

Vector size is another important parameter to consider to avoid MPS-uptake. To avoid embolism, particles should be less than 1µm when they are administered by intravenous injection, but to escape MPS-uptake, the particle-diameters should be less than 100nm [29].

4.3. Targeting

Once the delivery system is in the bloodstream, it must reach the target cell or tissue. When the targeted cell or tissue is a tumour and/or located in the MPS, in general, targeting ligands are unnecessary. For cells located in the MPS, macrophages and complement system activation will lead to an accumulation of the delivery system in the MPS. For tumour cells outside the MPS, passive targeting can be achieved by the enhanced permeability and retention effect (EPR). This effect is based on the characteristics of tumour vasculation which is usually not found in normal vascular tissue. These characteristics include having high vascular density due to extensive angiogenesis, extensive permeability induced by various vascular mediators, a defective vascular architecture, and impaired lymphatic clearance from the interstitial spaces of tumour tissues [30]. To observe this EPR effect, delivery systems have to be larger than 40kDa with a long plasma half life because smaller molecules usually return to blood circulation without retention [31], and it takes at least six hours for drugs in circulation to exert the EPR effect [30].

For targets other than tumours or MPS, different types of ligands can be used (glyosylated molecules, peptides, proteins or antibodies) depending on the location and/or cell/tissue properties in an active-targeting strategy. Asialoglycoprotein receptors (ASGPR) are tissue-

specific receptors which are specific for hepatocytes and are expressed on their surface. To target these receptors the vector has to be covered by galactose- or lactose-terminated ligands [32]. Mannose receptors and mannose-related receptors are tissue specific for macrophages or dendritic cells and recognise mannose as ligands. Transferrin receptors or folate receptors are tissue-unspecific receptors because they are localised on different cell types, but they are over-expressed on many tumour cells. So, if the aim is to reach tumour cells, transferrin or folate can be the best ligands [33]. Other ligands for tumour cells are peptides with an arginine-glycine-aspartic acid (RGD) motif. These ligands bind to integrins which are heterodimeric cell adhesion receptors and are expressed on activated endothelial cells in tumour vasculature [34]. Antibodies or antibody fragments can also be used as ligands [35-37]. The major problems with antibodies are the high cost and the need of mammalian cells for their production. Antibody fragments (Fab, Fv, scFv), in contrast, can be prepared in bacteria or by the proteolytic digestion of intact antibodies. The advantages of these fragments are that interactions with non-targeted cells are reduced (no Fc domains which bind to Fc receptors in normal tissues), the potential for tissue penetration is enhanced and, economical production without mammalian cells is possible [38]. These ligands are often fixed on PEG chains which facilitate the binding between the delivery system and the receptor, situated at the target cell surface, and can help to internalise the vector with the siRNA.

4.4. Cellular uptake

When the delivery system has reached the target cell, siRNA has to be internalised into the cell to reach the cytoplasm. Not all the internalisation mechanisms are well understood but there is evidence that endocytosis plays a major role. The term endocytosis includes different pathways as the “classic” clathrin-coated pit pathway, the caveolar pathway, one or more non-caveolar, clathrin-independent pathways (CLIC pathway), phagocytosis or macropinocytosis (reviewed in Khalil *et al.* [39] and Juliano *et al.* [40]). Rejman *et al*. showed that the size and nature of the delivery system influence the internalisation mechanism. In their first study [41], they used fluorescent latex particles of well-defined sizes, instead of DNA lipoplexes that are impossible to obtain in a homogenous way, and non-phagocytic B16 cells. An immediately internalisation at 37°C for approx. 3h with about 50% accumulation after 30 minutes were observed for particles up to 200nm in the perinuclear region, whereas particles of 500nm in diameter showed a significant accumulation after 2 – 3 h in the periphery of the cells. There was no uptake of 1,000nm particles. They also showed that particles up to 200nm in diameter

were internalised by clathrin-mediated endocytosis whereas particles with a diameter larger than 200nm entered by a caveola-dependent pathway. These results demonstrated that the particle size had an influence on the duration of the internalisation process, the internalisation mechanism, and the target location in the cell. In contrast, Spagnou *et al*. [42] did not observe a difference in gene silencing when they used different sizes of siRNA-lipoplexes (50 – 100nm or 200 – 600nm) *in vitro*. In their second study, Rejman *et al*. [43] demonstrated that DOTAP lipoplexes were internalised by clathrin-mediated endocytosis, wheras PEI polyplexes were internalised by clathrin- and caveola-mediated endocytosis, but only the caveola-mediated pathway was effective for transfection with the polyplexes. Rather than a size effect, these differences in transfection efficiency could be explained by the difference in releasing nucleic acid from the different systems.

4.5. SiRNA delivery and action

After initial uptake, the delivery system is often transported in a variety of low pH endomembrane compartments (early endosome, late endosome, lysosome) to be degraded [44]. To reach the cytoplasm, the delivery system (or at least the siRNA) has to escape from the endosome. In the literature, different hypothesises are described for DNA-lipo- or polyplexes but how this escape take course in detail, still remains unclear. The first escape mechanism concerns lipoplexes and occurs by membrane destabilisation [45-46]. In this hypothesis the complex is internalised via an endosome, whose membrane is then destabilised. The result is a flip-flop of anionic lipids, from the endosomal membrane, which move from the cytoplasmic side to the cationic lipids in the complexes, and release the DNA into the cytoplasm. Another mechanism concerns polyplexes (with ionisable amine groups) and is named the “proton sponge effect” [47]. These polymers can buffer the acidic pH in endosomes, which causes the ATPase (a pH-regulating enzyme in the endosomal membrane) to transport more protons in the endosome to reach the desired pH. The consequence is an influx of counterions (Cl-), osmotic swelling and finally rupture of endosomal membranes; this facilitates the release of polyplexes (or nucleic acid) into the cytoplasm. The polymers that possess an intrinsic endosomolytic activity can either be the main component of the vector (for example, PEI or lipopolyamines) or can be added to the vector as an endosomolytic agent (for example, DOPE, chloroquine or fusogenic peptides). These polymers are also called “helper lipids” and they can improve transfection efficiency of lipoplexes. The most used are cholesterol and DOPE but they have both advantages and

drawbacks. DOPE for example decreases the positive electrical surface potential and destabilises the liposomes but this can result in aggregation and lose of transfection efficiency, whereas cholesterol slightly increases (or does not affect) the electrical surface potential [48].

In summary (also see Figure 2), the "ideal" vector has to protect the siRNA, be stable in the blood, and possess stealth and targeting properties, to reach the target cell or tissue. The delivery system then has to be internalised into the cell, the siRNA has to be released in a reversible manner to conserve its activity in the cytosol, and the gene silencing pathway has to be activated. Compromises have to be found to develop the best-acting vector as we will see in the following section discussing different existing vectors.

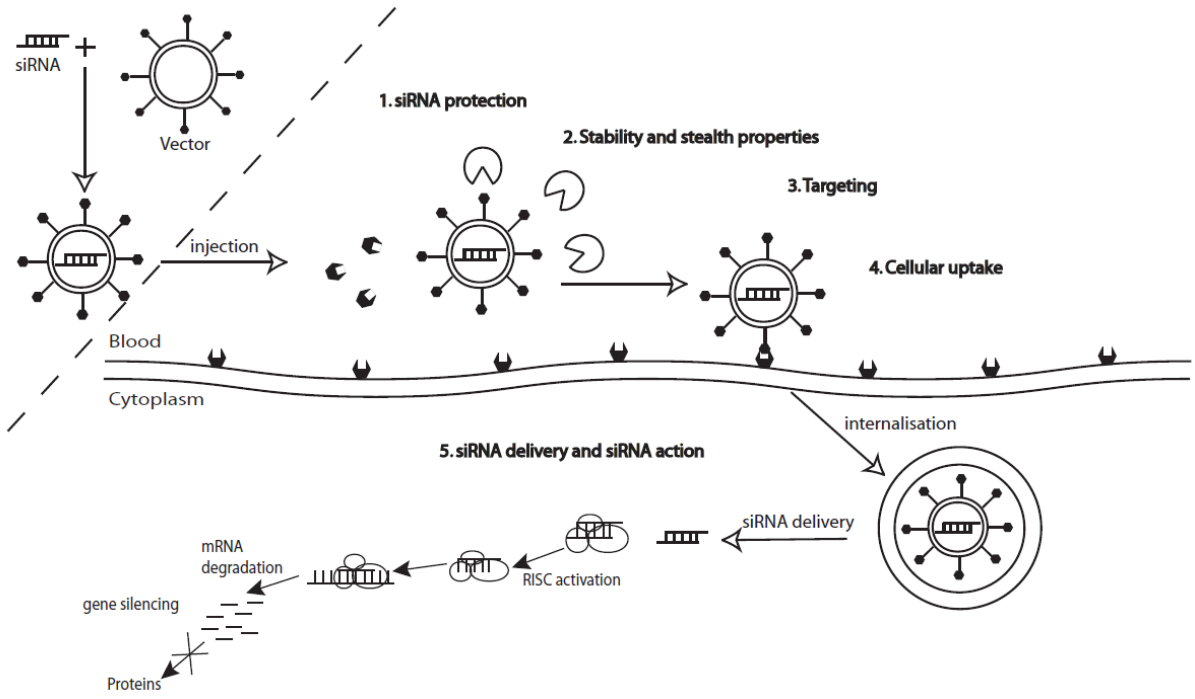

Figure 2: Required properties to form an efficient siRNA delivery system.

An efficient delivery system protects siRNA against degradation, elimination, non-specific distribution and tissue barricades. Stability and stealth properties of the delivery system can be achieved by surface modification (for example recovering the surface with PEG). To deliver siRNA to a specific cell type or tissue, the delivery system can be recovered by ligands as galactose, transferrin, antibodies or peptides. The size of the delivery systems should be as small as possible (between 20 and 100nm) and the system should contain an endosomolytical agent (such as DOPE) or constituents with endosomolytical activity (such as PEI) for efficient cell uptake and siRNA delivery. Once the siRNA is free in the cytoplasm, it can act by the RNAi pathway (described in Figure 1).

5. DELIVERY SYSTEMS FOR SYSTEMIC ADMINISTRATION

Several types of synthetic vectors have been investigated for gene silencing application. This review will focus on non-viral delivery systems for systemic administration by intravenous injection described in the literature. The different delivery systems can be divided into lipid systems, polymer systems, and peptides or proteins, and are summarised in Table 1.

5.1. Lipid systems

Lipid systems typically contain a cationic or fusogenic lipid, a PEG-lipid and a neutral co-lipid. They can be cationic or neutral liposomes or contain natural lipids and are generally called lipoplexes. Complexes and nanoparticles are generally less than 100nm to avoid renal excretion and being taken up by cells. Once inside cells, the inclusion of fusogenic lipids and/or pH-sensitive peptides in siRNA delivery systems is thought to help destabilising endosomal membranes to facilitate their release into the cytosol.

5.1.1. Neutral liposomes

Neutral liposomes, for example based on dioleyl-glycero-phosphatidylcholine (DOPC), have been successfully used to deliver siRNA *in vivo*. Landen *et al.* mixed DOPC and siRNA (siRNA/DOPC = 1:10 (w/w)) in the presence of excess tertiary butanol and then added Tween 20 (Tween 20: siRNA/DOPC = 1:19) [49]. The incorporated amount of siRNA was estimated to be around 65% and the stability of these liposomes was at least 4 weeks (stored at -20°C). These DOPC liposomes were effective delivery agents compared to cationic DOTAP (1,2-Dioleoyl-3-trimethylammonium-propane) liposomes, with a 10-fold improvement in siRNA-delivery, or to naked siRNA (delivery without a vector) with a 30-fold improvement. Landen *et al.* worked in this study with an orthotopic *in vivo* model of advanced ovarian cancer (female athymic nude mice + HeyA8 or SKOV3ip1 cells). The over-expression of EphA2, a tyrosine kinase receptor which can also function as an oncoprotein, in ovarian cancer is associated with poor clinical outcome [50] and pre-clinical studies showed that down-regulation reduces tumourigenicity [51]. For this reason Landen *et al.* chose treatments with formulated anti-EphA2-siRNA, paclitaxel (an approved chemotherapeutic for ovarian cancer) plus formulated control siRNA, and paclitaxel plus formulated anti-EphA2-siRNA (as combination therapy) twice weekly for 4 weeks. These treatments were all effective in reducing tumour size but combination therapy had the best results with 86% to 91% reduction compared to a treatment with formulated control siRNA alone or 67% to 82% reduction

compared with non-specific siRNA-DOPC and paclitaxel. Treatment with formulated anti-EphA2-siRNA alone diminished also tumour growth compared with the control siRNA-DOPC alone in both cell lines (HeyA8 cells 35%, SKOV3ip1 cells 50%). Additionally, both groups tested with EphA2-targeting siRNA-DOPC showed about 50% reduction of EphA2 expression compared with control siRNA-DOPC or control siRNA-DOPC plus paclitaxel and significant reduction of microvessel density in the tumour (52% with EphA2-targeting siRNA alone and 74% with combination therapy). No toxicities were observed during the study. The problem of this formulation is that it is not tissue-specific. As a consequence, the right choice of the target gene, down-regulated by siRNA, is very important, and the target gene should not be crucial for the function of normal cells.

A more complex formulation was successfully used on cynomolgus monkeys, targeting apolipoprotein B (apoB). The liposomes were composed of distearoyl-glycero-phosphatidylcholine (DSPC), dilinoleyloxy-dimethyl-aminopropane (DLinDMA), methoxy-polyethyleneglycol-carbamoyl-dimyristyloxy-propylamine (PEG-c-DMA), and cholesterol. These liposomes complexed with siRNA are called stable nucleic acid lipid particles (SNALP). Different studies have been carried out with these complexes [52-54].

Zimmermann *et al*. [52] used these particles on cynomolgus monkeys after preliminary tests on mice. They chose apoB as an endogenous gene target and potential therapeutic target for hypercholesterolemia. Their SNALP had a size between 77 and 83nm, a polydispersity range of 0.09 – 0.15, and encapsulation efficiencies between 92 and 97%. The results showed that the silencing effect of SNALP-formulated siRNA represented more than a 100-fold improvement in potency compared with systemic administration of cholesterol-conjugated siApoB. In their study, Zimmermann *et al*. treated cynomolgus monkeys with two different doses (1 and 2.5mg/kg SNALP-formulated siApoB) in a single injection and observed a clear and statistically significant dose-dependent gene-silencing effect on cynomolgus liver ApoB mRNA. The mRNA levels were reduced by 68±12% for the lower dose and about 90±12% for the higher dose consistent across the liver for 11 days (reduction of 91±15% for the higher dose at Day 11). A significant reduction of Plasma ApoB, serum cholesterol, and LDL levels (low density lipoprotein particle containing ApoB) was also observed in this period, with a maximal reduction of 62±5.5% for cholesterol and 82±7% for LDL at Day 11 for the higher dose. In contrast, HDL levels (high density lipoprotein particles without ApoB) showed no significant changes during this period. No toxicity or off-target effects were noted on animals during this study. This study demonstrated a specific, rapid and lasting gene silencing effect

on mRNA and protein levels in the liver of non-human primates (no ApoB silencing expressed in the jejunum) for 11 days but the recovery-time (time required to return to pre-dose levels) was not determined.

Morrissey *et al.* used these SNALP to target the hepatitis B virus (HBV) and used stabilised siRNA targeted to the HBV RNA [54]. They prepared SNALP with a mean particle size of 140±12nm, a polydispersity of 0.11±0.02, and an encapsulation efficiency of 93%±3%. The modifications on siRNA increased siRNA *in vivo* stability, formulated modified siRNA had a plasma half-life of 6.5h, and avoided undesirable immuno-stimulatory properties and toxicity of unmodified siRNA. Morissey *et al.* used a model of HBV replication to evaluate the *in vivo* efficacy of modified siRNA-SNALP complexes at a dose of 3 mg/kg/day for 3 consecutive days and then weekly for 5 weeks. They showed that the HBV serum titers were reduced by an average of 0.85 $\log_{10}$ (statistically equivalent over 6 weeks), and observed reduced toxic and immuno-stimulatory side effects likely due to lower doses and reduced dosing frequency as used in previous reports [20,55].

Judge *et al.* [53] also chose apoB and used SNALPs in their experiments as the delivery vehicle. Firstly, they showed that only minimal 2'O-Methyl (2'OMe) modifications within one strand of the duplex were sufficient to avoid the immuno-stimulatory activity of siRNA. Then they administered encapsulated (2'OMe-modified) apoB siRNA intravenously to BALB/c mice at a concentration of 5mg/kg/day for 3 days to deliver the siRNA to the liver as Morissey *et al*. had shown previously [54]. The results showed an effective delivery of the siRNA payload to the target organ, in this case the liver. Comparison of 2'OMe siRNA and unmodified siRNA resulted in equivalent *in vivo* potency with about 82% reduction of apoB mRNA in the liver, 75% reduction of serum apoB and 50% reduction of serum cholesterol, but 2'OMe siRNA avoided the immuno-toxicity (IFNα production) and other off-target effects (body weight loss, mild deterioration in general body condition) associated with the systemic administration of unmodified siRNA.

Other neutral liposomes were prepared with dioleyl-phosphatidylethanolamine (DOPE) and galactosyl-C4-cholesterol (Gal-C4-Chol). These structures permitted an improvement of siRNA plasma-circulation-time and limited renal excretion, in comparison to naked siRNA. A characteristic of these liposomes is to target liver parenchymal cells. This effect was confirmed in mice, even following intravenous administration. Sato *et al.* [32] mixed Galactose-C4-Cholesterol with DOPE at a molar ratio of 3:2 in 5% dextrose solution before complexing these liposomes with siRNA at a charge ratio (-/+) of 1:2.3 for cell-selective

delivery. They obtained siRNA complexes with a diameter of 75.3±5.8nm and a zeta potential of 35.8±1.8mV and suggested that the complexes were formed by electrostatic interactions. Sato et al. used siRNA against Ubc13, an ubiquitously expressed endogenous gene, and administered galactosylated liposomes/siRNA complexes by intravenous injection in male ICR mice. They observed an efficacy delivery to parenchymal liver cells compared to cationic liposomes (DC-Chol/DOPE) and a reduction of Ubc13 gene in liver by over 60%. Their galactosylated liposome/siRNA complexes provided a dose-dependent effect from 0.18 to 0.36nmol/g with the most liver-selctive effects at 0.18nmol/g without inducing hepatitis or interferon (IFN) responses.

Peer *et al.*, developed liposome-based β_7 integrin-targeted, stabilised nanoparticles (β_7I-tsNP) to deliver siRNA by systemic administration [56]. These nanoparticles had a liposomal core of phosphatidylcholine (PC), dipalmitoylphosphatidylethanolamine (DPPE) and cholesterol (Chol) at molar ratios of 3:1:1 (PC:DPPE:Chol) and had a size of about 80nm. These liposomes were first recovered by high-weight hyaluronan (HA) which was covalently linked to DPPE to form stabilised nanoparticles (sNP) before a monoclonal antibody (mAb FIB504) against β_7 integrins was coupled to HA by an amine-coupling method to obtain β_7I-tsNP. To load these particles with siRNA, the particles were lyophilised and rehydrated with a siRNA-protamine solution, developed before [37] (see below), which was pre-incubated for 30 min. at RT to form a complex and had a 1:5 siRNA:protein ratio. In their study [56], Peer *et al.* chose to target Cyclin D1 (CyD1) in an experimental model of intestinal inflammation to explore the role of leukocyte-expressed CyD1 in the pathogenesis of inflammation and the ability to use CyD1 as a target. Cyclin D1 is a key regulating molecule which is implicated in cell proliferation and is upregulated in colon epithelial and immune cells in inflammatory bowel diseases. They showed that these nanocarriers, with high cargo capacity, protected siRNA from degradation, allowed highly efficient intracellular delivery (due to the antibodies on their surface), and thus silence genes efficient *in vivo* at low doses (2.5mg/kg) with low off-target effects and toxicity.

Lipid systems	siRNA target	Dose and administration intervall	Animal model	Results (Gene silencing)	Ref.
DOPC liposomes	EphA2	150µg/kg siRNAs in liposomes 1 week after tumourinjection, twice weekly for 4 weeks	orthotopic model of advanced ovarian cancer in female athymic nude mice	86 – 91% Reduction of tumour growth with combination therapy (siRNA-liposomes and paclitaxel). 35 – 50% Reduction of tumour growth with siRNA-liposomes alone.	Landen *et al.*
SNALP	apoB	1 or 2.5mg/kg SNALP siApoB	cynomolgus monkeys	Dose-dependend silencing of ApoB mRNA (about 90% for the 2.5mg/kg dose). Significant reduction in ApoB protein, serum cholesterol (62%) and LDL (82%) (24h - 11 days).	Zimmermann *et al.*
SNALP	HBV (modified)	bolus 3mg/kg formulated HBV263M loading doses: days 1, 2, 3 of week 1 maintenance doses: day 1 of weeks 2, 3,4 and 5	female CD-1 mice	Specific dose-dependend reduction in HBV-mRNA.	Morissey *et al.*
SNALP	apoB (modified)	5 mg/kg lipid-encapsulated siRNA once a day for 3 consecutive days	Balb/C mice	Potent silencing of ApoB mRNA (82%). Significant reduction in serum apoB (74%) and cholesterol (52%).	Judge *et al.*
Gal-C4-Chol/DOPE liposomes	Ubc-13	0.18nmol siRNA/18µl/g	male ICR mice	Over 60% inhibition of endogenous Ubc13 gene expression in liver.	Sato *et al.*
β7-I-tsNP	CyD1 (protamine conjugate)	2,5mg/kg siRNA at days 0, 2, 4, and 6	C57BL/6 mice with DSS-induced colitis	High efficient intracellular delivery at low doses with low off target effects and toxicity.	Peer *et al.*
DOTAP liposomes	TLR-4	50µg/mouse daily for 2 or 3 days	female C57BL/6 mice	Potent induction of both type I and II interferon response and activation of STAT1.	Ma *et al.*
scL-HoKC	HER-2 (modified)	3mg/kg complexed or modified hybrid siRNA 3 times over 24h or 3 times weekly 3mg/kg (days 0-15), 2mg/kg (days 15-21), and 1.5mg/kg (days 21-33) scL-HoKC complexed modified hybrid siRNA	tumour xenografts in female athymic nude mice	Silencing of target gene (virtually elimination of HER-2), downstream components and significant tumor growth inhibition.	Pirollo *et al.*
CCLA-based cationic liposomes	c-raf	7.5mg/kg/day of siRNA, twice per day for 5 days	human breast tumour xenograft model in SCID mice	73% tumour growth inhibition.	Chien *et al.*
RPR209120/DOPE liposomes	TNF-α	10µg siRNA ± 10µg cDNA when clinical signs of arthritis appeared 3 times weekly for 3 weeks	DBA/1 mice with CIA	Complete cure of CIA (with carrier DNA). Inhibition (50-70%) of articular and systemic TNFα secretion, decrease in the levels of IL6 and MCP-1.	Khoury *et al.*
DDAB/cholesterol liposomes	caveolin-1	0.4 – 1.3mg/kg siRNA	male CD1 mice	Selective reduction of caveolin-1 expression by about 90% within 96h.	Miyawaki *et al.*
LIC-101	bcl-2 (human)	siRNA/LIC-101 (10mg/kg) 2x 5 day cycles of daily injections (day 6-10 and day 13-17)	model of liver metastasis in male BALB/c mice	75% tumour growth reduction.	Yano *et al.*
AtuPLEX	PTEN, CD31, Tie2	4 consecutive daily i.v. injections of 1.88mg/kg Cy3-siRNA and 14.5mg/kg lipid	immune-deficient male Hsd:NMRI-nu/nu mice	Target-specific gene silencing on mRNA and protein level (CD31 and Tie2).	Santel *et al.*

LNP01	Factor VII	bolus injection (5mg/kg)	C57BL/6 mice	Accumulation in liver (over 90%). Reversible, long-duration gene silencing without loss of activity following repeated administration.	Akinc *et al.*
Polymer systems	**siRNA target**	**Dose and administration intervall**	**Animal model**	**Results (Gene silencing)**	**Ref.**
Atelocollagen complexes	EZH2, p110α	50µg siRNA on days 3, 6 and 9 postinoculation	bone metastatic tumour model in male athymic nude mice	Efficient inhibition of metastatic tumour growth in bone tissues (no increase in luminescence).	Takeshita *et al.*
Atelocollagen complexes	PLK-1	25µg siRNA for 10 consecutive days from day 1 of transplantation	liver metastatic mouse model in specific pathogen-free BALB/c *nu/nu* mice	Long-lasting inhibition of tumour growth.	Kawata *et al.*
CDP complexes	EWS-FLI1	2.5mg/kg single injection on 2or 3 consecutive days	murine model of metastatic Ewing's sarcoma	Reduced EWS-FLI1 expression and tumour growth inhibition. Prevention of tumour cell engraftment and slowed tumour growth.	Hu-Lieskovan *et al.*
RGD-PEG-PEI complexes	VEGF R2	40µg siRNA per mouse in RPP-nanoplexes every 3 days	female nude mice with N2A neuroblastoma xenografts	Selective tumour uptake, siRNA sequence-specific inhibition of protein expression within the tumor and inhibition of both tumour angiogenesis and growth rate.	Schiffelers *et al.*
PEC	VEGF (siRNA-PEG)	1.5nmol of formulated siRNA on day 0, 4, 10, 18, and 28	xenograft tumour model of prostate cancer cells in female BALB/c mice	Reduction of VEGF expression (about 86%) Inhibition of intratoumoral neovascularisation and tumour growth in a drastic manner.	Kim *et al.*
Peptides and proteins	**siRNA target**	**Dose and administration intervall**	**Animal model**	**Results (Gene silencing)**	**Ref.**
RVG-9R	JEV (envelope gene)	50µg siRNA daily injection for 4 days	Balb/c mice NOD/SCID mice	Specific gene silencing within the brain and robust protection against fatal viral encephalitis (80% survival).	Kumar *et al.*
F105-P	c-myc, VEGF, MDM2	80µg siRNA on days 0, 1 and 3 after tumor implantation	xenograft tumour model in female C57/BL6 mice	Significant tumour growth reduction of envelope-expressing subcutaneous B16 tumours.	Song *et al.*
AL-57-PF	luciferase	6nmol Cy3-siRNA 5 days after tumour injection	SCID mice on a CB17 background	In vivo proof of principle for the effective systemic siRNA delivery.	Peer *et al.*

Table 1: Gene silencing experiments with different siRNA delivery nanosystems administrated by tail vein injection

5.1.2. Cationic liposomes

Although these results are promising, cationic liposomes are more commonly used *in vitro* for siRNA delivery. Cationic liposomes have in common their net positive charge which facilitates both complex formation with the polyanionic nucleic acid and interaction with the negatively-charged cell membrane.

DOTAP (1,2-Dioleoyl-3-trimethylammonium-propane) is a cationic lipid which is widely used for liposome formulation. This cationic lipid is either used alone to condense siRNA or with a neutral lipid, such as cholesterol or DOPE, to form liposomes.

Ma *et al*. used DOTAP liposomes which are composed of DOTAP and cholesterol in a 55:45 molar ratio [57]. In their study they showed that cationic lipid/siRNA complexes induced both type I and type II Interferon (IFN) responses and that these complexes activated STAT1 (signal transducer and activator of transcription 1). They administered TLR4-siRNA (specific to mouse toll-like receptor 4, which plays a role in pathogen recognition and activates innate immunity) complexed with the liposomes with a charge ratio (+/-) of 4:1 in 5% dextrose into mice by tail-vein injection. They observed a potent immune response with drastic increases of serum IFN-α and IFN-γ whereas after injection of DOTAP liposomes alone or naked siRNA (without liposomes), only low levels of serum IFN were measured. But they showed also that the activation of the IFN response was not associated with the choice of siRNA because administration of three other siRNA (ET-1, IRAK-M or Bcl-2) or single-stranded RNA (sense or anti-sense strand of ET-1-siRNA) complexed with DOTAP liposomes, also induced a potent IFN response. DOTAP/siRNA complexes also showed a drastic activation of STAT1 (which is involved in IFN signalling) compared to siRNA alone or DOTAP liposomes alone. No TNF-α response was observed with the DOTAP/siRNA complexes, siRNA alone or DOTAP liposomes alone. This study showed the potential toxicity of these carriers and suggests caution in data interpretation, but this delivery system could serve as immuno-stimulatory agent for immunotherapy.

Another way to prepare liposomes containing DOTAP is to form DOTAP/DOPE liposomes in a 1:1 ratio, recover the surface with an anti-TfR single-chain antibody fragment (TfRscFv) and encapsulate siRNA. Pirollo *et al*. named these liposomes nanoimmunoliposome complexes (scL complex). In their study [35], they prepared the cationic liposomes using the ethanol injection method and included MPB-DOPE (*N*-maleimido-phenylbutyrate-DOPE) at 5 molar percent of total lipids to allow conjugation of the TfRscFv and the peptide HoKC (a

synthetic pH-sensitive histidylated oligolysine, designed to aid endosomal escape) when scL-HoKC complexes were formed. Both particles scL and scL-HoKC were quite uniform and had an average size of about 100nm. The experiments were made with a 19-mer blunt-ended siRNA sense DNA/antisense RNA hybrid analogue (hybrid siRNA) and a modified hybrid siRNA where O-methyl constituents were incorporated in the central region of the sense strand with DNA flanks of the hybrid siRNA against HER-2 (modified hybrid siRNA). In a previous study [58], the size of TfRscFv-liposome siRNA (scL-siRNA) complexes (with a control modified hybrid siRNA) was 211 ± 18nm and they showed enhanced tumour delivery and specificity for both primary and metastatic cancers of various types including prostate, pancreatic and breast. In the later study [35], tumours were induced in female athymic nude mice by s.c. inoculation with different cell types (human pancreatic (PANC-1) and breast (MDA-MB-435) cancer cells, human lung (H157) and colon carcinoma (H630) cells). They concluded, that the systemic delivery of modified hybrid siRNA by the nanoimmunoliposome complex could efficiently silence the HER-2 gene (virtually elimination) and affect components in multiple signal-transduction pathways (for example phosphatidylinositol 3-kinase/AKT and RAS/mitogen-activated protein kinase (MAPK) pathways) leading to apoptosis in the tumour and even at low doses (the initial siRNA dose was 3mg/kg, which was decreased on Day 15 to 2mg/kg and on Day 21 to 1.5mg/kg), the efficient and targeted delivery of siRNA to the tumour via the nanoimmunoliposome resulted in an increased response to conventional chemotherapy with dramatic tumour-growth inhibition.

Over time, the cationic lipid DOTAP has been replaced by other cationic lipids to increase transfection efficiency. Chien *et al.*, for example, developed cationic cardiolipin-analogue (CCLA)-based cationic liposomes, which are composed of CCLA:DOPE at a molar ratio of 1:2 [59]. These liposomes were efficient to transfect siRNA *in vitro* and *in vivo* and had a lower toxicity rate than the DOTAP-based *in vivo* GeneSHUTTLE® (commercially available liposomes). The authors used c-raf siRNA and showed that the treatment of c-raf siRNA/CCLA-based liposome complex exhibited 73% tumour growth inhibition as compared to free c-raf siRNA group, 8 days after the initial treatment.

Khoury *et al.* prepared cationic liposomes containing the cationic lipid RPR209120 (2-(3-[Bis-(3-amino-propyl)-amino]-propylamino)-N-ditetradecylcarbamoylmethyl-acetamide) and DOPE in a molar ratio of 1:1 which they complexed either with siRNA alone or with a mix of siRNA and plasmid DNA (carrier DNA) to stabilise the lipoplexes at a charge ratio (+/-) of 6:1 [60]. The complexes formed small compacted particles and had a positive charge density

(about 30mV). Intravenous administration of fluorescent non-targeting control siRNA alone, complexed with the liposomes (siRNA-liposomes) or complexed with carrier DNA and liposomes (siRNA/carrier DNA-liposomes), showed that most of the fluorescence was detected in blood regardless of the formulation but the uptake and the distribution in the different organs varied with the formulation. The fluorescence uptake by organs for siRNA/carrier DNA-liposomes showed a 10-fold increase compared with siRNA alone and a 2-fold increase compared with siRNA-liposomes. The distribution analysis showed for siRNA/carrier DNA-liposomes that nearly one third of the siRNA were in liver, lungs, and spleen, respectively and only very low siRNA were found in the brain (5%). For siRNA-liposomes, almost the half of the siRNA dosis was found in the liver, the rest in lung, spleen and brain in almost equal parts whereas for siRNA alone, about half of the dosis was found both in the lungs and in the brain, respectively and only 3% in the liver. To investigate the therapeutic potential of their system, the authors used siRNA against TNFα (Tumour necrosis factor α, a cytokine involved in rheumatoid arthritis (RA)) and a model of mice with collagen-induced arthritis (CIA). The experiments showed that systemic treatment with RPR209120-targeted siRNA against TNFα induced a significant reduction in disease incidence and clinical scores by reduction of TNFα secretion in blood and knee tissue. Addition of carrier DNA to the formulation increased the effect further, for example knee tissue TNFα secretion was inhibited by 50-60% for siRNA alone or for siRNA-liposomes, versus 75% for siRNA/carrier DNA-liposomes.

Other cationic liposome-siRNA complexes were used by Miyawaki *et al*. in their experiments [61]. These liposomes were composed of 50% DDAB (dimethyl-dioctadecyl-ammonium bromide) and 50% cholesterol (mol/mol) with a ratio of siRNA to liposome of 1:5 (wt/vol). To explore the role of caveoline-1 (a scaffold and regulatory protein) in regulating lung vascular permeability mouse caveoline-1 siRNA was administered by tail-vein injection in male CD1 mice. The cationic liposome-siRNA complexes downregulated caveoline-1 expression in a concentration- (0.4 – 1.3 mg/kg) and time-dependent manner (maximal suppression between 72h and 144h post-injection and full recovery at 168h after siRNA administration). Contrary to caveolin-1 knock-out mice with constant caveoline-1 down-regulation, this system had the advantage that vascular barrier function could be studied during both down-regulation and recovery phases. The presence of caveolin-1 is a sign for caveolae whose primary function in vascular endothelial cells is to mediate the active process of endocytosis and transcytosis. Miyawaki *et al.* showed that caveolin-1 is an essential

requirement for caveolar biogenesis and that caveolin-1 plays a key role as a negative regulator of interendothelial junction (IEJ) permeability *in vivo*.

Yano *et al.* used 2-O-(2-dimethylaminoethyl)-carbamoyl-1,3-O-dioleylglycerol and egg phosphatidylcholine to form their liposomes named LIC-101 [62]. They charged these liposomes with synthetic siRNA (specific for the human bcl-2 oncogene) in a ratio of oligonucleotide to LIC-101 of 1:16 (w/w). 10mg/kg of these complexes were administered by i.v. bolus injection to mice bearing A549 (human lung cancer) liver metastasis in two, 5-day cycles of daily injections (Day 6-17). 21 days after the end of the treatment, the average liver weight of siRNA-treated mice was 1.77±0.12g compared to 2.35±0.28g for control mice which correspond to a strong antitumour activity (about 75%) in the liver metastasis model.

Santel *et al.* used AtuFECT01 (β-*L*-arginyl-2,3-*L*-diaminopropionic acid-*N*-palmityl-*N*-oleyl-amide trihydrochloride, a cationic lipid with a highly-charged head group), DPhyPE (1,2-diphytanoyl-*sn*-glycero-3-phosphoethanolamine, a neutral helper phospholipid) and DSPE-PEG (*N*-(carbonyl-methoxypolyethyleneglycol-2000)-1,2-distearoyl-*sn*-glycero-3-phospho-ethanolamine sodium salt) at a molar ratio of 50/49/1 which they mixed with AtuRNAi (blunt, 19-mer, double-stranded RNA oligonucleotides stabilised by alternating 2'OMe modifications on both strands) to form siRNA-lipoplexes [63]. Their siRNA-lipoplexes had a size of 117.8nm and a zeta potential of 46.4mV. 1 mol% of DSPE-PEG 2,000 in the siRNA lipoplex formulation was sufficient to reduce unspecific toxic side effects *in vivo* without a severe loss in RNAi efficacy *in vitro*. To perform a biodistribution analysis, a single dose of Cy3 fluorescently-labeled siRNA, either formulated as siRNA-lipoplexes or unformulated (siRNA alone), was injected into immune-competent mice by i.v. injection. This analysis revealed a predominant uptake of siRNA into endothelial cells, throughout the body, after the systemic administration of these siRNA-lipoplexes. In contrast, naked siRNA were not targeted to any cell type of analysed tissue, most likely due to instant renal excretion. To correlate siRNA uptake and distribution with the efficacy of RNAi, nude mice were treated with four, consecutive daily i.v. injections with three target-specific siRNA-lipoplexes (against CD31, Tie2, both only expressed in endothelial cells, or PTEN, ubiquitously expressed in all cell types). This experiment showed target-specific (for $siRNA^{Tie2}$- and $siRNA^{CD31}$-lipoplexes) gene silencing on mRNA and protein levels in the vascular endothelium (of lung, heart and liver) of the mouse.

Akinc *et al*. developed lipidoid-siRNA formulations [64]. Lipidoids are lipid-like molecules, synthesised by a one-step synthetic scheme (conjugate addition of alkyl-acrylates or alkyl-

acrylamides to primary or secondary amines). They created a large library of lipidoids (over 1,200 structurally diverse lipidoids) to find a new effective delivery system [65]. Their optimised delivery system (LNP01) contains the lipidoid $98N_{12}$-5(1), cholesterol, PEG-lipid ($mPEG_{2000}$-C14) in a molar ratio of 42:48:10 and siRNA in a total lipid:siRNA ratio of 7.5:1 (wt:wt). These particles had a size of roughly 50 to 60nm and a nearly neutral surface charge of about 3 mV. This formulation was stable for at least 5 months at 4, 25 and 37°C, and increased the siRNA $t_{1/2}$ in serum from about 15 minutes (unformulated, minimally chemically-modified siRNA) to over 24 hours (LNP01) *in vitro*. Biodistribution analysis showed that LNP01 (3 mg/kg siRNA) rapidly distributes primarily to the liver (over 90% at 1h) and the spleen (95% of the administered dose was accumulated in the liver and spleen) but only 0.5% of LNP01 was found in the lungs at 1h. This study also demonstrated that LNP01 can be administrated repeatedly with equal *in vivo* efficacy over extended time periods because three cycles of bolus injection of 5mg/kg siRNA against Factor VII, formulated with LNP01, in C57BL/6 mice showed no significant changes in silencing profiles compared to one bolus injection. Furthermore, repeated administration showed no observable negative effects on mice.

5.2. Polymer systems

Different cationic polymers can also be used. They can be divided into two groups: natural polymers (such as chitosan or atelocollagen), and synthetic polymers (such as polyethyleneimine (PEI), poly(L-lysine) (PLL) or dendrimers). For siRNA vectorisation, only a few polymers have been used compared to DNA vectorisation.

5.2.1. Natural polymers

Atelocollagen is one of these natural polymers. It derives from collagen-type I and is purified by pepsin-treatment. For this reason, it is less immunogenic but conserves its biodegradability and its biocompatibility.

Takeshita *et al*. prepared their siRNA/atelocollagen complexes by mixing equal volumes of atelocollagen and siRNA solution [66]. To evaluate these complexes *in vivo,* they used a model of bone metastatic mice. Systemic injection of these complexes delivered siRNA in an efficient manner into tumours, retained them for a longer period than siRNA alone in these sites, and inhibited gene expression in a specific manner (80-90% inhibition of bioluminescene in the whole body). They identified EZH2 and p110α as possible targets for

growth inhibition of bone metastasis and showed that it was possible to administer these siRNA/atelocollagen complexes without inducing an immune response (as IFN-α or IL-12).

Kawata *et al*. also used these siRNA/atelocollagen complexes, but with PLK-1 siRNA in a murine liver metastasis model of lung cancer [67]. PLK-1 is a polo-like kinase, belonging to the family of serine/threonine kinases and is crucial for cell division. The over-expression of PLK-1 is often found in cancerous tissues and a positive correlation with the survival of cancer patients has been reported [68]. In their study, Kawata *et al*. showed a significant tumour growth inhibition in the liver, without enhancing the innate immunity, even 70 days after the beginning of the 10 day-treatment which indicates a long-lasting inhibition of tumour growth.

Another natural polymer is cyclodextrin, a cyclic oligosaccharide composed of glucose monomers which exists in different forms. Hu-Lieskovan *et al.* used a delivery system, based on β-cyclodextrin containing polycations (CDP) [33]. This imidazole-modified CDP was first mixed with an adamantane-PEG_{5000} (AD-PEG) conjugate at a molar ratio of 1:1 AD:β-CD and then added to a transferrin-modified AD-PEG (AD-PEG-transferrin), at a 1:1,000 AD-PEG-transferrin:AD-PEG (w/w) ratio to target transferrin receptors. Afterwards the mixture was added to an equal volume of siRNA at a charge ratio of 3:1 (+/-) and an aqueous glucose solution to obtain a final polyplex formulation in 5% (w/v) glucose (D5W). For their study, they utilized TC71 cells, which express high levels of transferrin receptors, in a metastatic murine model for the Ewing's family of tumours (EFT). They demonstrated on the one hand, that their targeted multicomponent systems delivered siRNA (siEFBP2 against EWS-FLI1, which plays a significant role in tumourigenesis of EFT) to the established tumours, reduced EWS-FLI1 expression and inhibited tumour growth for 2 to 3 days after three consecutive daily injections. On the other hand, when these complexes were given twice weekly, starting on the same day as tumour cell injection, the tumour cell engraftment was prevented. Only 20% of the mice showed tumour growth compared to 90 to 100% in control mice and tumour growth slowed when tumours did develop. Nontargeted complexes only delayed tumour cell engraftment but did not influence tumour growth rate. These CDP-containing delivery systems were safe and induced low immunogenicity because no interferon response was observed, even when siRNA with known immuno-stimulatory motifs was used.

5.2.2. Synthetic polymers

Polyethyleneimine (PEI) is the synthetic polymer most studied for nucleic acid delivery and is considered as the most effective for gene transfection. The efficiency depends on its structure and molecular weight, the amine/phosphate (N/P) ratio of the complexes, and the quantity of complexed nucleic acids.

Schiffelers *et al.* prepared pegylated PEI-based polymers with or without RGD (Arg-Gly-Asp) peptides coupled at the distal PEG extremities [34]. To form complexes, equal volumes of aqueous solutions of cationic polymer (RGD-PEG-PEI (RPP) or PEG-PEI (PP) with PEI (P) in a 1:1 molar ratio) and nucleic acids were mixed in a N/P ratio of 2:1. They showed that PEI-nanoplexes without ligands had a size between 120 and 170nm and aggregated in less than 24h. After coupling with a ligand (PEG alone or with RGD-peptide), the size of the nanoplexes diminished (between 70 and 100nm) and the stability increased as particles remained unchanged for 9 days. The zeta potential also changed when ligands were added from 35±4mV without ligands to 5 or 6mV with ligands. These vectors complexed with siRNA were administered by intravenous injection on established neuroblastoma N2A tumours in nude mice. These complexes permitted on the one hand, to target the tumour by interaction between the RGD-peptide and the integrins on neo-vascular endothelial cells. FITC-siRNA alone was rapidly cleared and FITC-siRNA in P-nanoplexes accumulated in the liver and lung but not in tumour tissue, whereas RPP-nanoplexes accumulated in the tumour and only to a poor extend in the liver and lungs. On the other hand, RPP nanoplexes permitted a modification of protein expression by the tumour in a specific way and inhibited tumour growth and tumour angiogenesis when using siRNA against VEGF R2 (Vascular endothelial growth factor receptor-2).

Kim *et al*. developed polyelectrolyte complex (PEC) micelles which contained synthetic siRNA-PEG conjugates and PEI in a N/P ratio of 16 [69]. These spherical PEC micelles with a core-shell structure had a size of 50 – 80nm and a hydrodynamic diameter of 98.7±5.1nm. Kim *et al*. used siRNA against VEGF (a critical regulator of tumour-induced angiogenesis) to compare the efficacy of their PEC micelles with naked siRNA and siRNA/PEI complexes. Intravenous injections through the tail vein in a xenograft tumour model of prostate cancer in female nude mice were realized. The siRNA-PEG/PEI PEC micelles reduced the VEGF expression in a more effective manner than siRNA/PEI complexes (86.4±3.6% against 43.0±14.6%, compared to no-treatment control) or naked siRNA which had no effect on VEGF expression. The treatment inhibited intratumoural neovascularisation and tumour

growth in a drastic manner without apparent critical cytotoxicity during the experimental period.

5.3. Peptides and proteins

The third category of delivery systems concerns peptides and proteins which are also able to deliver siRNA *in vivo*.

Kumar *et al*. used a short peptide derived from rabies virus glycoprotein (RVG) to enable the transvascular delivery of siRNA to the brain [70]. RVG enables viral entry into neuronal cells via specific interactions with the nicotinic acetylcholine receptor (AchR). The RGV peptide was synthesised, purified and biotinylated at the carboxy terminus to add nine arginine residues. This peptide (RVG-9R) was then mixed with siRNA in 5% glucose (in a molar ratio peptide:siRNA of 10:1) to form RVG-9R/siRNA complexes. Kumar *et al*. showed that the intravenous injection of these RVG-9R/siRNA complexes allowed specific gene silencing of exogenous genes like GFP (green fluorescent protein) in GFP transgenic mice and endogenous genes like SOD1 (Cu-Zn superoxide dismutase 1) in wild-type Balb/c mice. GFP silencing and SOD1 siRNA were only detected in the brain and not in the liver or spleen, which demonstrated specific targeting to the brain, and neither inflammatory cytokines nor an anti-peptide antibody response were induced after repeated administration. A possible use of these complexes is the treatment of viral encephalitis because after intravenous administration of RVG-9R/siFvE^{j} complexes (siRNA targeting Japanese encephalitis virus (JEV)), about 80% of the infected mice survived whereas untreated mice, mice treated with control siRNA, or mice treated with control peptide/siFvE^{J} all died within 10 days.

Song *et al*. developed a protamine-antibody fusion protein to deliver siRNA [36]. The fusion protein (F105-P) consisted of a Fab antibody fragment directed against the HIV-1 envelope (*env*) (F105) and protamine and was mixed with siRNA against c-myc, MDM2 or VEGF, (oncogenes which enhance proliferation) alone or in combination at a molar ratio of 6:1 (siRNA:F105-P). These complexes were injected intravenously in syngeneic C57/BL6 mice with subcutaneously injected gp160-B16 cells. This tumour model with *env*-expressing cells was utilized due to the non-existence of a good mouse model for HIV. I.v. injection of FITC-labeled siRNA complexed with F105-P resulted in specific delivery, 30% uptake in gp160 B16 cells but no uptake in gp160^{-} B16 cells, and significantly reduction in tumour growth compared to naked siRNA.

Peer *et al*. developed other antibody-protamine fusion proteins (AL-57-PF) [37]. Their goal was to deliver siRNA specifically to activated leukocytes in order to minimise potential immunosuppressive effects on bystander lymphocytes. All leukocytes express integrin lymphocyte function-associated antigen-1 (LFA-1), which mediates adhesion to other immune cells on their surface. LFA-1 exists in two different conformations, one low-affinity non-adhesive form, which is found on non-activated leukocytes, and one high-affinity (HA) adhesive form, which is found on activated leukocytes. AL-57-PF is composed of AL-57 single-chain variable region fragments (scFv) and protamine fragments and binds selectively to the HA-LFA-1 whereas TS1/22-PF, a control antibody-protamine fusion protein, binds equally well to the HA and low-affinity forms of LFA-1. SCID mice were engrafted with K562 cells to stably express human wild-type LFA-1 (WT) or HA-LFA-1, because the antibodies did not recognise the murine form of LFA-1. Then Cy3-SiRNA was mixed in a 5:1 molar ratio with the fusion protein and injected intravenously in the tail vein of these mice. This experiment provided *in vivo* proof of the principle and showed that TS1/22-PF delivered siRNA selectively to LFA-1 expressing cells (WT or HA-LFA-1) and that AL-57-PF delivered siRNA only to the HA-LFA-1, without inducing an IFN response or activating lymphocytes.

6. CONCLUSION

In this section the properties of the different nanosystems, summarised in Table 2 are discussed.

Lipid systems	Components	siRNA protection	Stability and stealth properties		Targeting		Cellular uptake		Ref.
			Charge (mV)	Surface modification	Ligand	Target	Size (nm)	Helper lipid	
DOPC liposomes	DOPC, Tween 20	30-fold improvement over naked siRNA	not measured	-	-	tumour	not measured	-	Landen *et al.*
SNALP	Cholesterol, DSPC, PEG-cDMA, DLinDMA	38min in mice, 72min in cynomolus monkeys	not measured	PEG(2000)-cDMA	-	liver	77 - 83	cholesterol	Zimmermann *et al.*
SNALP	Cholesterol, DSPC, PEG-cDMA, DLinDMA	in vivo: naked siRNA: 2 min chemically modified siRNA: 0.8h stabilized siRNA + SNALP: 6.5h	not measured	PEG(2000)-cDMA	-	liver	141 ± 14	cholesterol	Morrissey *et al.*
SNALP	Cholesterol, DSPC, PEG-cDMA, DLinDMA	in vitro (37°C): naked siRNA: < 4h unmodified siRNA + SNALP: > 24h	not measured	PEG(2000)-cDMA	-	liver	100 - 130	cholesterol	Judge *et al.*
Gal-C4-Chol/DOPE	Gal-C4-Cholesterol, DOPE	in vitro: naked siRNA < 4h formulated siRNA > 30h in vivo: naked siRNA: 5min formulated siRNA: 60min	35.8 ± 1.8	-	galactose	liver	75.3 ± 5.8	DOPE	Sato *et al.*
β7-I-tsNP	PC, DPPE, Chol, HA, mAb FIB504	β7-I-tsNP protected siRNA from degradation	not measured	-	mAb FIB504	colon	80	cholesterol	Peer *et al.*
DOTAP liposomes	DOTAP + cholesterol	not tested	not measured	-	-	lung and spleen	-	cholesterol	Ma *et al.*
scL-HoKC	DOTAP, DOPE, TfRscFv, HoKC	not tested	not measured	-	TfR scFV	tumour	about 100 211 ± 18	DOPE, HoKC	Pirollo *et al.*
CCLA-based cationic liposomes	cationic cardiolipin analogue (CCLA), DOPE	not tested	not measured	-	-	tumour	110 - 120	DOPE	Chien *et al.*
RPR209120/DOPE	RPR209120 + DOPE	not tested	30	-	-	knee	not measured	DOPE	Khoury *et al.*
DDAB/cholesterol	DDAB + cholesterol	not tested	not measured	-	-	lung	not measured	cholesterol	Miyawaki-Shimizu *et al.*
LIC-101	2-O-(2-diethylaminoethyl)-carbamoyl-1,3-O-dioleylglycerol, egg phosphatidylcholine	not tested	not measured	-	-	liver metastasis	not measured	-	Yano *et al.*
AtuPLEX	AtuFECT01, DPhyPE, DSPE-PEG	no gene silencing with naked siRNA	46.4	DSPE-PEG(2000)	-	vascular endothelium	117.8	DPhyPE	Santel *et al.*
LNP01	lipioid 98N12-5(1), Chol, mPEG-C14	increased serum half-life from 15min to over 24h *in vitro*	2 - 4	mPEG(2000)-C14	-	liver	50 - 60	cholesterol	Akinc *et al.*

Polymer systems	Components	siRNA protection	Stability and stealth properties		Targeting		Cellular uptake		Ref.
			Charge (mV)	Surface modification	Ligand	Target	Size (nm)	Endosomolytic agent	
Atelocollagen complexes	atelocollagen	more efficient delivery into tumours than siRNAs alone	not measured	-	-	tumour	not measured	-	Takeshita *et al.*
Atelocollagen complexes	atelocollagen	-	not measured	-	-	tumour	not measured	-	Kawata *et al.*
CDP	CDP + AD-PEG + AD-PEG-Tf	protection for at least 72h	not measured	AD-PEG(5000)	AD-PEG-Tf	tumour	not measured	-	Hu-Lieskovan *et al.*
RGD-PEG-PEI	RGD-PEG-PEI	in vitro: formulated siRNA > 12h	6	PEG	RGD	tumour vasculature	90	PEI	Schiffelers *et al.*
PEC	PEI	over 48h in serum conditioned medium	not measured	PEG(5000)	-	tumour	50 - 80	PEI	Kim *et al.*
Peptides and proteins	**Components**	**siRNA protection**	**Stability and stealth properties**		**Targeting**		**Cellular uptake**		**Ref.**
			Charge (mV)	**Surface modification**	**Ligand**	**Target**	**Size (nm)**	**Endosomolytic agent**	
RVG-9R	RVG-9R peptide	in vitro: formulated siRNA at least partly stable for up to 8h	not measured	-	RVG-9R	brain (CNS)	not measured	-	Kumar *et al.*
F105-P	F105, protamine	not tested	not measured	-	F105	tumour	not measured	-	Song *et al.*
AL-57-PF	AL-57-scFv, protamine fragment	not tested	not measured	-	AL-57-scFv	lung leukocytes	not measured	-	Peer *et al.*

Table 2: Components and delivery properties of the reviewed siRNA delivery nanosystems

Abreviations (Components):

DOPC: dioleyl-glycero-phosphatidylcholine, *DSPC*: distearoyl-glycero-phosphatidylcholine, *PEG-c-DMA*: methoxy-polyethyleneglycol-carbamoyl-dimyristyloxy-propylamine, *DLinDMA*: dilinoleyloxy-dimethyl-aminopropane, *Gal-C4-Chol*: galactosyl-C4-cholesterol, *DOPE*: dioleyl-phosphatidylethanolamine, *PC*: phosphatidylcholine, *DPPE*: dipalmitoylphosphatidylethanolamine, *Chol*: cholesterol, *HA*: hyaluronan, *mAb FIB504*: monoclonal antibody against β_7 integrins, *DOTAP*: 1,2-Dioleoyl-3-trimethylammonium-propane, TfRscFv: anti-transferrin receptor single-chain antibody fragment, *HoKC*: pH-sensitive histidylated oligolysine, *CCLA*: cationic cardiolipin-analogue, *RPR209120*: 2-(3-[Bis-(3-amino-propyl)-amino]-propylamino)-N-ditetradecylcarbamoylmethyl-acetamide, *DDAB*: dimethyldioctadecylammonium bromide, *AtuFECT01*: β-*L*-arginyl-2,3-*L*-diaminopropionic acid-*N*-palmityl-*N*-oleyl-amide trihydrochloride, *DphyPE*: 1,2-diphytanoyl-*sn*-glycero-3-phosphoethanolamine, *DSPE-PEG*: *N*-(carbonyl-methoxypolyethyleneglycol-2000)-1,2-distearoyl-*sn*-glycero-3-phospho-ethanolamine sodium salt, *CDP*: β-cyclodextrin containing polycations, *AD-PEG*: adamantane-PEG_{5000}, *AD-PEG-Tf*: transferrin-modified AD-PEG, *PEI*: polyethyleneimine, *RVG-9R*: rabies virus glycoprotein with nine arginine residues, *F105*: Fab antibody fragment directed against HIV-1 envelope (*env*), *AL-57-PF*: leukocyte-targeted antibody-protamine conjugate

The first point of comparison is siRNA protection. As seen above, siRNA have to be protected from degradation and/or inactivation by serum and tissue nucleases, phagocytes of the MPS or the kidneys. SiRNA inclusion in a delivery system can improve their elimination half-life. This point is well documented for the delivery system SNALP. For example Morissey *et al*. showed that naked siRNA had an elimination half-life of about 2 min.; Chemical modifications of siRNA can prolong this half-life (0.8h or 49 minutes), but stabilised siRNA formulated with their delivery system SNALP achieved an elimination half-life of 6.5 hours in mice [54]. Zimmerman *et al*. also worked with SNALPs, but formulated them with unmodified siRNA. They measured an elimination half-life in mice of 38 min. and in cynomolgus monkeys of 72 min. [52]. Other delivery systems like RGD-PEG-PEI or RVG-9R were only tested *in vitro* and exposed a prolonged stability of siRNA. For other nanosystems, the stability of siRNA with or without delivery system was not tested or not documented in the literature cited here.

The second point is stability and stealth properties of the vector. The criteria for these properties are the surface modification and the charge of the delivery system. As described previously, the charge density of the different vectors plays an important role in siRNA delivery to avoid aggregation, complement activation or cytotoxic effects. The different systems are either neutral (neutral liposomes with DOPC, SNALPs …) or positive charged systems (liposomes with cationic lipids, atelocollagen, cyclodextrins …). To describe the charge density, the zeta potential of the different systems is measured, but very few information was given. LNP01 and RGD-PEG-PEI had a near neutral zeta potential which certainly limited the interactions with serum proteins, improved their stability in the blood and prolonged their circulation half-lives. Gal-C4-Chol/DOPE and AtuPLEX have greater positive potentials (35.8 and 46.6mV) which can augment the interactions with serum proteins, but can also facilitate the binding to negative charged cell membranes. For the other delivery systems, no comparison can be made about this point due to the lack of information.

Surface modifications of the vectors, for example by covering with PEG, also have an influence on siRNA delivery. Only some systems are covered by PEG (SNALPs, AtuPLEX, LNP01, RGD-PEG-PEI, PEC and CDP). These surface modifications increase the stealth properties of the delivery systems and can thereby prolong circulation time in blood. But having PEG on the surface can also interfere with the endosomolytical activity of the vector and inhibit the disruption of the endosomal membrane, dependent on the acyl chain length of

the lipid anchor and the molecular weight of the PEG moiety (2000 and 5000 are used in the reviewed systems) [71].

Another surface modification is the covery with specific ligands which allow specific tissues or organs to be targeted. The different ligands used in the reviewed systems are galactose (Gal-C4-Chol/DOPE liposomes), transferrin (CDP), and RGD peptide (PEI-based liposomes). Another way to target is to use one of the components as an antibody, an antibody fragment or peptide (β7-I-tsNP, scl-HoKC, RVG-9R, F105-P, AL-57-PF). The ligand is chosen in function of the target cell to deliver the siRNA in a specific manner. For example galactose is chosen to target the liver parenchymal cells, transferrin to target tumour cells and RGD targets the tumour vasculature. Antibodies or antibody fragments can be designed to target cells which express one specific antigen as for AL-57-PF which targeted only activated leukocytes. This can be a way to augment the selectivity of gene silencing, to reduce off-target effects and to reduce toxicity [37]. Most of the nanosystems without ligands target the liver or tumour tissue which is easier accessible by systemic administration than other tissues due to passive targeting and the EPR effect.

On the one hand, the cellular uptake is dependant on the size of the delivery system. As mentioned before, the delivery system should not be greater than 200nm to obtain a rapid internalisation, but to avoid uptake by the MPS, the nanosystems should have a size smaller than 100nm. The size of the discussed delivery systems is on a nanoscale level and varies from about 50 to 200nm. As for the surface charge, not all authors measured or published the size of their delivery systems, but most of the systems, for which we have this information, had a size around 100nm and met the mentioned criteria. Compromises have to be done between a small size and including components to augment the specificity and efficacy of the delivery. For example, Pirollo *et al.* [58] had particles with a size of about 200nm probably due to the ligand (TfR scFV) and the endosomolytical peptide HoKC.

On the other hand, escape from the endosome is also very important for delivering siRNA into the cell. Almost all the reviewed lipid delivery systems used a helper lipid like DOPE or cholesterol to help siRNA to escape from the endosome. For polymer systems, PEI is used as a main component in the formulation when an endosomolytic agent is used. As described before, DOPE acts by destabilising the endosomal membranes, whereas PEI uses the “proton-sponge” effect.

The last point is siRNA action which is characterised as a result of gene silencing. All the reviewed delivery systems delivered their siRNA in the target cell and gene silencing occured

in all cases but to a different extent. The aim is to silence the target gene without inducing an immune response (except for immunotherapy) and without (or as low as possible) off-target effects. For this, the delivery systems alone should be as inert as possible, but other parameters, such as the siRNA used, the dose, and the times of administration, can also have an influence to achieve this aim. In the reviewed studies, siRNA was used in different forms, such as unmodified siRNA (for example Landen *et al.* [49], Zimmermann *et al.* [52], …), modified siRNA (Morissey *et al.* [54], Judge *et al*. [53] Kim et *al*. [69] Peer *et al*. [56]), hybrid siRNA (Pirollo *et al.* [35,58]) or siRNA combined with carrier DNA (Khoury *et al*. [60]). Depending on the delivery system used, such modifications can be useful to reduce unwanted side effects and/or enhance gene silencing. The siRNA dose should be as low as possible and in the reviewed cases, the dose of siRNA varied between 0.1 and 7.5 mg/kg/day. In the presented studies, different administration modes were used. Some studies were realized with a single injection, others applied the siRNA once a day but on different days (consecutive or not), but there were also studies with two or three injections per day which could permit to diminish the doses per injection.

Other points of comparison are the siRNA target and the animal models. Luciferase and GFP-siRNA are often used to proof the principle or to show transfection efficiency. In function of the aim of the study, different siRNA and disease models were used but will not be discussed as they do not concern physicochemical properties.

7. PERSPECTIVES

The aim of developing non-viral nanosystems for systemic siRNA delivery is to use this system for human therapy in the future. The proof that the system is efficient *in vivo* is one condition to enter in clinical trials. Many of the current clinical trials for siRNA therapies are for local administration and/or for the use of naked or modified siRNA, but only few delivery systems for systemic administration of siRNA have entered clinical trials. The only ones are at the beginning (Phase I) to evaluate their safety, a safe dose range, and to identify side effects. Among the delivery systems for systemic administration in clinical trials are the cyclodextrin-based transferrin-receptor targeted nanoparticles CALAA-01 from Calando Pharmaceuticals and Atu027 from Silence Therapeutics AG, which are AtuPLEXes. Both are actually in Phase I clinical trials for solid tumours. Alnylam Pharmaceuticals has developed ALN-VSP which contains SNALPs as a delivery system (Tekmira’s lipid-based nanoparticle technology) and has also entered Phase I clinical trials.

The reason of the limited number of siRNA delivery systems in clinical trials is certainly the complexity of the approach. It is easier to administer naked or modified siRNA than to develop an efficient, reproducible and safe delivery system which has to undergo the same regulatory guidelines as the drug itself.

REFERENCES

[1] **Akhtar S and Benter I F. Nonviral delivery of synthetic siRNAs in vivo. J Clin Invest 2007;117:3623-32**

[2] **Fire A, Xu S, Montgomery M K, Kostas S A, Driver S E and Mello C C. Potent and specific genetic interference by double-stranded RNA in Caenorhabditis elegans. Nature 1998;391:806-11**

[3] **Aigner A. Applications of RNA interference: current state and prospects for siRNA-based strategies in vivo. Appl Microbiol Biotechnol 2007;76:9-21**

[4] **Lu P Y and Woodle M C. Delivering small interfering RNA for novel therapeutics. Methods Mol Biol 2008;437:93-107**

[5] **De Paula D, Bentley M V and Mahato R I. Hydrophobization and bioconjugation for enhanced siRNA delivery and targeting. Rna 2007;13:431-56**

[6] **Bartel D P. MicroRNAs: genomics, biogenesis, mechanism, and function. Cell 2004;116:281-97**

[7] **Tang G. siRNA and miRNA: an insight into RISCs. Trends Biochem Sci 2005;30:106-14**

[8] **Meister G and Tuschl T. Mechanisms of gene silencing by double-stranded RNA. Nature 2004;431:343-9**

[9] **Aagaard L and Rossi J J. RNAi therapeutics: principles, prospects and challenges. Adv Drug Deliv Rev 2007;59:75-86**

[10] **Kim W J and Kim S W. Efficient siRNA delivery with non-viral polymeric vehicles. Pharm Res 2009;26:657-66**

[11] **Hornung V, Ellegast J, Kim S, Brzozka K, Jung A, Kato H, Poeck H, Akira S, Conzelmann K K, Schlee M, Endres S and Hartmann G. 5'-Triphosphate RNA is the ligand for RIG-I. Science 2006;314:994-7**

[12] **Marques J T, Devosse T, Wang D, Zamanian-Daryoush M, Serbinowski P, Hartmann R, Fujita T, Behlke M A and Williams B R. A structural basis for discriminating between self and nonself double-stranded RNAs in mammalian cells. Nat Biotechnol 2006;24:559-65**

[13] **Li C X, Parker A, Menocal E, Xiang S, Borodyansky L and Fruehauf J H. Delivery of RNA interference. Cell Cycle 2006;5:2103-9**

[14] **Aigner A. Delivery Systems for the Direct Application of siRNAs to Induce RNA Interference (RNAi) In Vivo. J Biomed Biotechnol 2006;2006:71659**

[15] **Suri S S, Fenniri H and Singh B. Nanotechnology-based drug delivery systems. J Occup Med Toxicol 2007;2:16**

[16] **Braasch D A, Paroo Z, Constantinescu A, Ren G, Oz O K, Mason R P and Corey D R. Biodistribution of phosphodiester and phosphorothioate siRNA. Bioorg Med Chem Lett 2004;14:1139-43**

[17] **Hall A H, Wan J, Shaughnessy E E, Ramsay Shaw B and Alexander K A. RNA interference using boranophosphate siRNAs: structure-activity relationships. Nucleic Acids Res 2004;32:5991-6000**

[18] **Chiu Y L and Rana T M. siRNA function in RNAi: a chemical modification analysis. Rna 2003;9:1034-48**

[19] **Layzer J M, McCaffrey A P, Tanner A K, Huang Z, Kay M A and Sullenger B A. In vivo activity of nuclease-resistant siRNAs. Rna 2004;10:766-71**

[20] **Soutschek J, Akinc A, Bramlage B, Charisse K, Constien R, Donoghue M, Elbashir S, Geick A, Hadwiger P, Harborth J, John M, Kesavan V, Lavine G, Pandey R K, Racie T, Rajeev K G, Rohl I, Toudjarska I, Wang G, Wuschko S, Bumcrot D, Koteliansky V, Limmer S, Manoharan M and Vornlocher H P. Therapeutic silencing of an endogenous gene by systemic administration of modified siRNAs. Nature 2004;432:173-8**

[21] **Buyens K, Lucas B, Raemdonck K, Braeckmans K, Vercammen J, Hendrix J, Engelborghs Y, De Smedt S C and Sanders N N. A fast and sensitive method for measuring the integrity of siRNA-carrier complexes in full human serum. J Control Release 2008;126:67-76**

[22] **Tong A W, Jay C M, Senzer N, Maples P B and Nemunaitis J. Systemic therapeutic gene delivery for cancer: crafting Paris' arrow. Curr Gene Ther 2009;9:45-60**

[23] **Zelphati O, Uyechi L S, Barron L G and Szoka F C, Jr. Effect of serum components on the physico-chemical properties of cationic lipid/oligonucleotide complexes and on their interactions with cells. Biochim Biophys Acta 1998;1390:119-33**

[24] **Kircheis R, Schuller S, Brunner S, Ogris M, Heider K H, Zauner W and Wagner E. Polycation-based DNA complexes for tumor-targeted gene delivery in vivo. J Gene Med 1999;1:111-20**

[25] **de Martimprey H, Vauthier C, Malvy C and Couvreur P. Polymer nanocarriers for the delivery of small fragments of nucleic acids: oligonucleotides and siRNA. Eur J Pharm Biopharm 2009;71:490-504**

[26] **Ogris M and Wagner E. Targeting tumors with non-viral gene delivery systems. Drug Discov Today 2002;7:479-85**

[27] **Gref R, Minamitake Y, Peracchia M T, Trubetskoy V, Torchilin V and Langer R. Biodegradable long-circulating polymeric nanospheres. Science 1994;263:1600-3**

[28] **Pitard B, Oudrhiri N, Lambert O, Vivien E, Masson C, Wetzer B, Hauchecorne M, Scherman D, Rigaud J L, Vigneron J P, Lehn J M and Lehn P. Sterically stabilized BGTC-based lipoplexes: structural features and gene transfection into the mouse airways in vivo. J Gene Med 2001;3:478-87**

[29] **Li W and Szoka F C, Jr. Lipid-based nanoparticles for nucleic acid delivery. Pharm Res 2007;24:438-49**

[30] **Maeda H. The enhanced permeability and retention (EPR) effect in tumor vasculature: the key role of tumor-selective macromolecular drug targeting. Adv Enzyme Regul 2001;41:189-207**

[31] **Maeda H, Wu J, Sawa T, Matsumura Y and Hori K. Tumor vascular permeability and the EPR effect in macromolecular therapeutics: a review. J Control Release 2000;65:271-84**

[32] **Sato A, Takagi M, Shimamoto A, Kawakami S and Hashida M. Small interfering RNA delivery to the liver by intravenous administration of galactosylated cationic liposomes in mice. Biomaterials 2007;28:1434-42**

[33] **Hu-Lieskovan S, Heidel J D, Bartlett D W, Davis M E and Triche T J. Sequence-specific knockdown of EWS-FLI1 by targeted, nonviral delivery of small interfering RNA inhibits tumor growth in a murine model of metastatic Ewing's sarcoma. Cancer Res 2005;65:8984-92**

[34] **Schiffelers R M, Ansari A, Xu J, Zhou Q, Tang Q, Storm G, Molema G, Lu P Y, Scaria P V and Woodle M C. Cancer siRNA therapy by tumor selective delivery with ligand-targeted sterically stabilized nanoparticle. Nucleic Acids Res 2004;32:e149**

[35] **Pirollo K F, Rait A, Zhou Q, Hwang S H, Dagata J A, Zon G, Hogrefe R I, Palchik G and Chang E H. Materializing the potential of small interfering RNA via a tumor-targeting nanodelivery system. Cancer Res 2007;67:2938-43**

[36] **Song E, Zhu P, Lee S K, Chowdhury D, Kussman S, Dykxhoorn D M, Feng Y, Palliser D, Weiner D B, Shankar P, Marasco W A and Lieberman J. Antibody mediated in vivo delivery of small interfering RNAs via cell-surface receptors. Nat Biotechnol 2005;23:709-17**

[37] **Peer D, Zhu P, Carman C V, Lieberman J and Shimaoka M. Selective gene silencing in activated leukocytes by targeting siRNAs to the integrin lymphocyte function-associated antigen-1. Proc Natl Acad Sci U S A 2007;104:4095-100**

[38] **Ikeda Y and Taira K. Ligand-targeted delivery of therapeutic siRNA. Pharm Res 2006;23:1631-40**

[39] **Khalil I A, Kogure K, Akita H and Harashima H. Uptake pathways and subsequent intracellular trafficking in nonviral gene delivery. Pharmacol Rev 2006;58:32-45**

[40] **Juliano R, Alam M R, Dixit V and Kang H. Mechanisms and strategies for effective delivery of antisense and siRNA oligonucleotides. Nucleic Acids Res 2008;36:4158-71**

[41] **Rejman J, Oberle V, Zuhorn I S and Hoekstra D. Size-dependent internalization of particles via the pathways of clathrin- and caveolae-mediated endocytosis. Biochem J 2004;377:159-69**

[42] **Spagnou S, Miller A D and Keller M. Lipidic carriers of siRNA: differences in the formulation, cellular uptake, and delivery with plasmid DNA. Biochemistry 2004;43:13348-56**

[43] **Rejman J, Bragonzi A and Conese M. Role of clathrin- and caveolae-mediated endocytosis in gene transfer mediated by lipo- and polyplexes. Mol Ther 2005;12:468-74**

[44] **Juliano R, Bauman J, Kang H and Ming X. Biological barriers to therapy with antisense and siRNA oligonucleotides. Mol Pharm 2009;6:686-95**

[45] **Xu Y and Szoka F C, Jr. Mechanism of DNA release from cationic liposome/DNA complexes used in cell transfection. Biochemistry 1996;35:5616-23**

[46] **Zelphati O and Szoka F C, Jr. Mechanism of oligonucleotide release from cationic liposomes. Proc Natl Acad Sci U S A 1996;93:11493-8**

[47] **Boussif O, Lezoualc'h F, Zanta M A, Mergny M D, Scherman D, Demeneix B and Behr J P. A versatile vector for gene and oligonucleotide transfer into cells in culture and in vivo: polyethylenimine. Proc Natl Acad Sci U S A 1995;92:7297-301**

[48] **Hirsch-Lerner D, Zhang M, Eliyahu H, Ferrari M E, Wheeler C J and Barenholz Y. Effect of "helper lipid" on lipoplex electrostatics. Biochim Biophys Acta 2005;1714:71-84**

[49] **Landen C N, Jr., Chavez-Reyes A, Bucana C, Schmandt R, Deavers M T, Lopez-Berestein G and Sood A K. Therapeutic EphA2 gene targeting in vivo using neutral liposomal small interfering RNA delivery. Cancer Res 2005;65:6910-8**

[50] **Thaker P H, Deavers M, Celestino J, Thornton A, Fletcher M S, Landen C N, Kinch M S, Kiener P A and Sood A K. EphA2 expression is associated with aggressive features in ovarian carcinoma. Clin Cancer Res 2004;10:5145-50**

[51] **Noblitt L W, Bangari D S, Shukla S, Knapp D W, Mohammed S, Kinch M S and Mittal S K. Decreased tumorigenic potential of EphA2-overexpressing breast cancer cells following treatment with adenoviral vectors that express EphrinA1. Cancer Gene Ther 2004;11:757-66**

[52] **Zimmermann T S, Lee A C, Akinc A, Bramlage B, Bumcrot D, Fedoruk M N, Harborth J, Heyes J A, Jeffs L B, John M, Judge A D, Lam K, McClintock K, Nechev L V, Palmer L R, Racie T, Rohl I, Seiffert S, Shanmugam S, Sood V, Soutschek J, Toudjarska I, Wheat A J, Yaworski E, Zedalis W, Koteliansky V, Manoharan M, Vornlocher H P and MacLachlan I. RNAi-mediated gene silencing in non-human primates. Nature 2006;441:111-4**

[53] **Judge A D, Bola G, Lee A C and MacLachlan I. Design of noninflammatory synthetic siRNA mediating potent gene silencing in vivo. Mol Ther 2006;13:494-505**

[54] **Morrissey D V, Lockridge J A, Shaw L, Blanchard K, Jensen K, Breen W, Hartsough K, Machemer L, Radka S, Jadhav V, Vaish N, Zinnen S, Vargeese C, Bowman K, Shaffer C S, Jeffs L B, Judge A, MacLachlan I and Polisky B. Potent and persistent in vivo anti-HBV activity of chemically modified siRNAs. Nat Biotechnol 2005;23:1002-7**

[55] **Morrissey D V, Blanchard K, Shaw L, Jensen K, Lockridge J A, Dickinson B, McSwiggen J A, Vargeese C, Bowman K, Shaffer C S, Polisky B A and Zinnen S. Activity of stabilized short interfering RNA in a mouse model of hepatitis B virus replication. Hepatology 2005;41:1349-56**

[56] **Peer D, Park E J, Morishita Y, Carman C V and Shimaoka M. Systemic leukocyte-directed siRNA delivery revealing cyclin D1 as an anti-inflammatory target. Science 2008;319:627-30**

[57] **Ma Z, Li J, He F, Wilson A, Pitt B and Li S. Cationic lipids enhance siRNA-mediated interferon response in mice. Biochem Biophys Res Commun 2005;330:755-9**

[58] **Pirollo K F, Zon G, Rait A, Zhou Q, Yu W, Hogrefe R and Chang E H. Tumor-targeting nanoimmunoliposome complex for short interfering RNA delivery. Hum Gene Ther 2006;17:117-24**

[59] **Chien P Y, Wang J, Carbonaro D, Lei S, Miller B, Sheikh S, Ali S M, Ahmad M U and Ahmad I. Novel cationic cardiolipin analogue-based liposome for efficient DNA and small interfering RNA delivery in vitro and in vivo. Cancer Gene Ther 2005;12:321-8**

[60] **Khoury M, Louis-Plence P, Escriou V, Noel D, Largeau C, Cantos C, Scherman D, Jorgensen C and Apparailly F. Efficient new cationic liposome formulation for systemic delivery of small interfering RNA silencing tumor necrosis factor alpha in experimental arthritis. Arthritis Rheum 2006;54:1867-77**

[61] **Miyawaki-Shimizu K, Predescu D, Shimizu J, Broman M, Predescu S and Malik A B. siRNA-induced caveolin-1 knockdown in mice increases lung vascular permeability via the junctional pathway. Am J Physiol Lung Cell Mol Physiol 2006;290:L405-13**

[62] **Yano J, Hirabayashi K, Nakagawa S, Yamaguchi T, Nogawa M, Kashimori I, Naito H, Kitagawa H, Ishiyama K, Ohgi T and Irimura T. Antitumor activity of small interfering RNA/cationic liposome complex in mouse models of cancer. Clin Cancer Res 2004;10:7721-6**

[63] **Santel A, Aleku M, Keil O, Endruschat J, Esche V, Fisch G, Dames S, Loffler K, Fechtner M, Arnold W, Giese K, Klippel A and Kaufmann J. A novel siRNA-lipoplex technology for RNA interference in the mouse vascular endothelium. Gene Ther 2006;13:1222-34**

[64] **Akinc A, Goldberg M, Qin J, Dorkin J R, Gamba-Vitalo C, Maier M, Jayaprakash K N, Jayaraman M, Rajeev K G, Manoharan M, Koteliansky V, Rohl I, Leshchiner E S, Langer R and Anderson D G. Development of lipidoid-siRNA formulations for systemic delivery to the liver. Mol Ther 2009;17:872-9**

[65] **Akinc A, Zumbuehl A, Goldberg M, Leshchiner E S, Busini V, Hossain N, Bacallado S A, Nguyen D N, Fuller J, Alvarez R, Borodovsky A, Borland T, Constien R, de Fougerolles A, Dorkin J R, Narayanannair Jayaprakash K, Jayaraman M, John M, Koteliansky V, Manoharan M, Nechev L, Qin J, Racie T, Raitcheva D, Rajeev K G, Sah D W, Soutschek J, Toudjarska I, Vornlocher H P, Zimmermann T S, Langer R and Anderson D G. A combinatorial library of lipid-like materials for delivery of RNAi therapeutics. Nat Biotechnol 2008;26:561-9**

[66] **Takeshita F, Minakuchi Y, Nagahara S, Honma K, Sasaki H, Hirai K, Teratani T, Namatame N, Yamamoto Y, Hanai K, Kato T, Sano A and Ochiya T. Efficient delivery of small interfering RNA to bone-metastatic tumors by using atelocollagen in vivo. Proc Natl Acad Sci U S A 2005;102:12177-82**

[67] **Kawata E, Ashihara E, Kimura S, Takenaka K, Sato K, Tanaka R, Yokota A, Kamitsuji Y, Takeuchi M, Kuroda J, Tanaka F, Yoshikawa T and Maekawa T. Administration of PLK-1 small interfering RNA with atelocollagen prevents the growth of liver metastases of lung cancer. Mol Cancer Ther 2008;7:2904-12**

[68] **Strebhardt K and Ullrich A. Targeting polo-like kinase 1 for cancer therapy. Nat Rev Cancer 2006;6:321-30**

[69] **Kim S H, Jeong J H, Lee S H, Kim S W and Park T G. Local and systemic delivery of VEGF siRNA using polyelectrolyte complex micelles for effective treatment of cancer. J Control Release 2008;129:107-16**

[70] **Kumar P, Wu H, McBride J L, Jung K E, Kim M H, Davidson B L, Lee S K, Shankar P and Manjunath N. Transvascular delivery of small interfering RNA to the central nervous system. Nature 2007;448:39-43**

[71] Song L Y, Ahkong Q F, Rong Q, Wang Z, Ansell S, Hope M J and Mui B. Characterization of the inhibitory effect of PEG-lipid conjugates on the intracellular delivery of plasmid and antisense DNA mediated by cationic lipid liposomes. Biochim Biophys Acta 2002;1558:1-13

Travail expérimental

Conception et caractérisation

Publication No 1

SiRNA LNCs – a novel platform of lipid nanocapsules for systemic siRNA administration

David S., Resnier P., Guillot A., Pitard B., Benoit JP. and Passirani C.

European Journal of Pharmaceutics and Biopharmaceutics – soumis

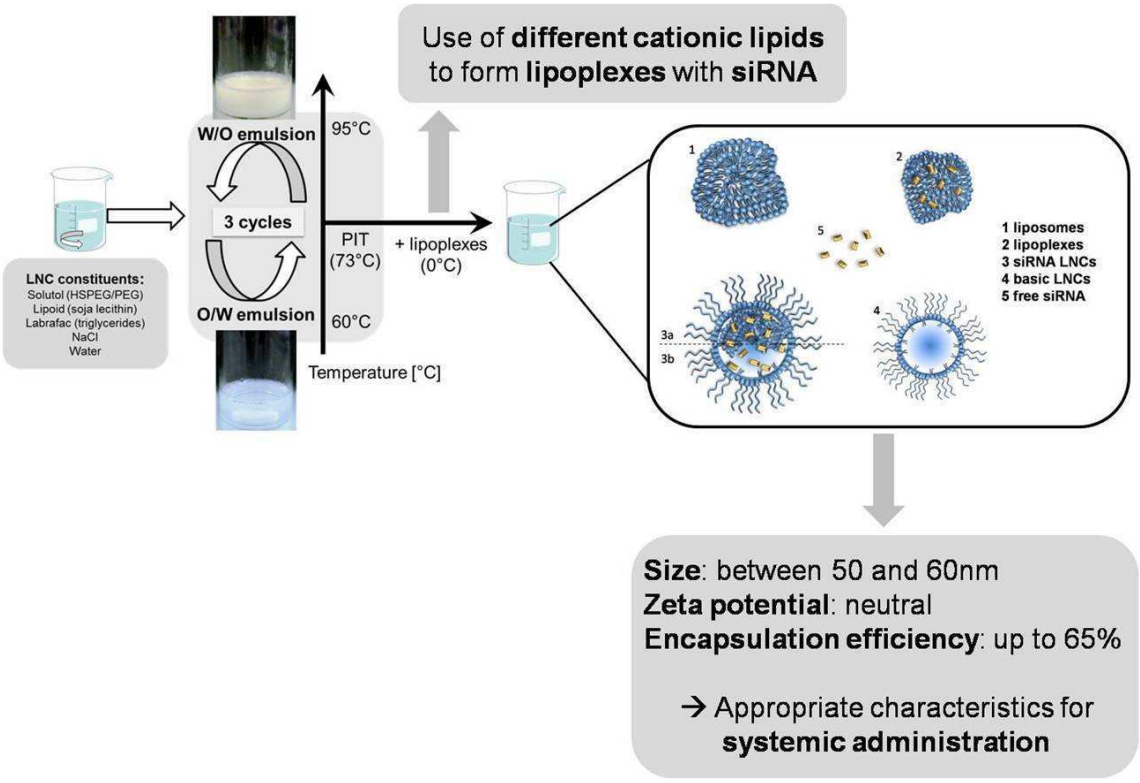

En s'inspirant des vecteurs déjà existants au laboratoire à Angers et en appliquant les connaissances acquises par la recherche bibliographique, des nouveaux vecteurs siRNA ont été développés et sont présentés dans cette première publication de résultats. Ces siRNA LNCs sont constituées de différents lipides cationiques et présentent des propriétés permettant de les utiliser pour une administration par voie systémique. Une analyse approfondie de ces formulations a mise en évidence différents compartiments pouvant contenir les siRNA. Pour une meilleure caractérisation, une méthode de quantification a été mise en place afin de localiser et déterminer la quantité de siRNA dans chaque compartiment.

SIRNA LNCS – A NOVEL PLATFORM OF LIPID NANOCAPSULES FOR SYSTEMIC SIRNA ADMINISTRATION

Stephanie David[a,b,c], Pauline Resnier[a,b], Alexis Guillot[a,b], Bruno Pitard[c], Jean-Pierre Benoit[a,b], Catherine Passirani[a,b*]

[a]*LUNAM Université – Ingénierie de la Vectorisation Particulaire, F-49933 Angers, France*
[b]*INSERM U646 – Université d'Angers, 4 rue Larrey, F-49933 Angers, France*
[c]*INSERM UMR915 – Université de Nantes, 8 quai Moncousu, F-44000 Nantes, France*

*Corresponding author:
C. Passirani:
Inserm U646, IBS-CHU, 4 rue Larrey, 49933 Angers Cedex 9, France
Tel.: +33 244 688534, Fax: +33 244 688546, E-mail: catherine.passirani@univ-angers.fr;

ABSTRACT

Several siRNA therapeutics are undergoing clinical trials for cancer, respiratory diseases or macular degeneration, but most are administrated locally. In order to overcome the different barriers to attain an efficient siRNA action after systemic administration, nanocarriers able to carry and protect siRNA are expected. In this aim, we developed a new platform of siRNA LNCs using different cationic lipids, combining the properties of lipid nanocapsules (siRNA protection and targeting) and lipoplexes (efficient siRNA delivery into the cell). The formulation revealed to contain different compartments. A siRNA quantification method based on UV spectroscopy was developed to localise and quantify siRNA in each compartment. All in all, these novel siRNA LNCs presented sizes about 55 nm with a neutral surface charge and siRNA encapsulation efficiencies up to 65% representing appropriate characteristics for systemic administration.

Keywords: nanocarrier, lipoplexes, formulation, siRNA quantification, cationic lipids

INTRODUCTION

SiRNA, are rapidly degraded by nucleases and other blood components after intravenous administration. Moreover, between administration and action site, different barriers have to be overcome. Therefore, different siRNA modifications and siRNA vectors have been already described in the literature, in the aim to find the "ideal" vector [1].

Lipid nanocapsules (LNCs) were developed in our laboratory, consisting of a lipid liquid core of triglycerides and a rigid shell of lecithin and polyethylene glycol [2]. The simple formulation process is based on phase inversions of an emulsion. These LNCs were recently modified to encapsulate DNA, complexed with cationic lipids, forming lipoplexes. These DNA LNCs were efficient for *in vitro* and *in vivo* transfection [3-5] in contrast to lipoplexes which were only efficient *in vitro*.

The association of LNCs and lipoplexes should combine LNC properties (nucleic acid protection, prolonged circulation time, possibility of active or passive targeting) with lipoplex properties (internalisation in cells, permitting nucleic acid action). This in mind, the objective of this work was to develop siRNA LNCs allowing efficient systemic siRNA administration. In this study, various ratios of different cationic lipids were used to formulate siRNA LNCs and the size, charge and payload characteristics of these novel promising nanocarriers were assessed.

MATERIALS AND METHODS

SiRNA LNC formulation

Basic lipid Nanocapsules (LNC) were formulated, as described before [2], by mixing 20% w/w Labrafac WL 1349 (caprylic-capric acid triglycerides, Gatefossé S.A. Saint-Priest, France), 1.5% w/w Lipoid S75-3 (Lipoid GmbH, Ludwigshafen, Germany), 17% w/w Solutol HS 15 (BASF, Ludwigshafen, Germany), 1.8% w/w NaCl (Prolabo, Fontenay-sous-Bois, France) and 59.8% w/w water (obtained from a Milli-Q system, Millipore, Paris, France) together under magnetic stirring. Three temperature cycles between 60 and 95°C were performed to obtain phase inversions of the emulsion obtained after mixing all the components. Then a rapid cooling and dilution with ice cooled water (1:1.4) at the phase inversion temperature (PIT) led to LNC formation.

To obtain siRNA LNCs, the water in the last step was replaced by lipoplexes which were prepared by adding equal volumes of siRNA (here a model siRNA targeted against PCSK9, (sense sequence: GGAAGAUCAUAAUGGACAGdTdT) Eurogenetec, Seraing, Belgium) and liposomes in a defined charge ratio of cationic lipid charge versus anionic siRNA charge. NaCl was added during preparation, to obtain a final concentration of 0,15M.

For liposome preparation, a cationic lipid DOSP (dioleylamin-succinyl paromomycin) (synthesis previously described in [6]), BGTC (bis(guanidinium)-tris(2-aminoethyl)amine-cholesterol) (synthesis previously described in [7]) or DOTAP (1.2-dioleyl-3-trimethylammoniumpropane) (Avanti® Polar Lipids Inc., Alabaster, AL, USA), solubilised in chloroform, was weighted in the ratio 1/1 (M/M), 3/2 (M/M) or 1/1 (M/M) respectively with the neutral lipid DOPE (1.2-dioleyl-sn-glycero-3-phosphoethanolamine) (Avanti® Polar Lipids Inc., Alabaster, AL, USA) to obtain a final concentration of 20 mM of cationic lipid charge, considering the number of lipid charges per molecule (4 for DOSP, 2 for BGTC and 1 for DOTAP). After chloroform evaporation under vacuum, deionised water was added to hydrate the lipid film over night at 4°C which was sonicated the next day.

DOSP micelles were prepared in the same way without the addition of DOPE.

Characterisation

Size and zeta potential measurements

Size and zeta potential of siRNA LNCs were measured using a Malvern Zetasizer® (Nano Series ZS, Malvern Instruments S.A., Worcestershire, UK) at 25°C, in triplicate, after dilution in a ratio of 1:100 with deionised water.

Agarose gel electrophoresis

To verify siRNA encapsulation in LNC, Triton® X100 (Sigma, Saint-Quentin Fallavier, France) was added to destroy LNCs. Samples were mixed with OrangeBlue loading dye (Promega, Madison, WI, USA) before deposition on 1% agarose gel containing ethidium bromide (Sigma, Saint-Quentin Fallavier, France) and migration at 100 V for 30 minutes.

SiRNA LNC purification

500µl of SiRNA LNC Formulation were deposited on a 1.5 x 40 cm Sepharose CL-4B column and were eluted with HEPES buffer (pH 7.4). Fractions of 500µl or 1ml were collected in glass tubes for further analysis. 100µl of each fraction was used for turbidity measurements and analysed at 580 nm. PEG was quantified using 20µl of each fraction which was mixed with 5µl KI/I_2 and 180µl H_2O milli-Q before analysing at 492 nm using a Multiskan Ascent microplate reader (Thermo Fisher Scientific Cergy-Pontoise, France). Size and zeta potential measurements were performed as described above and siRNA were evidenced using gel electrophoresis experiments.

SiRNA quantification

One volume of the formulation was mixed with three volumes water (obtained from a Milli-Q-plus® system, Millipore, Paris, France), six volumes 1M NaOH and two volumes chloroform, vortexed and immediately centrifuged for 15 min at 20000 g and 4°C. The aqueous phase, containing free siRNA and siRNA liberated from lipoplexes outside LNCs, was removed and analysed with a UV spectrophotometer (UVIKON 922, Kontron Instruments, Munich, Germany) at 260 nm. The volume removed for free siRNA quantification was replaced by ethanol, and two volumes water and 10 volumes NaOH 1M were added before vortexing and centrifuged a second time for 15 min at 20000 g and 4°C. The aqueous phase, containing the liberated siRNA from lipoplexes inside siRNA LNCs, was removed and analysed as previously at 260 nm. To analyse free and encapsulated siRNA quantity in siRNA LNCs, the same procedure was used, using two volumes of formulation and replacing water by 1M NaOH. The first aqueous phase contained free siRNA; the second aqueous phase contained siRNA encapsulated in siRNA LNCs. The siRNA quantity was calculated using a calibrating curve with different siRNA concentrations and compared to the total siRNA amount encapsulated in theory in siRNA LNCs. All samples were prepared in duplicate.

RESULTS AND DISCUSSION

Lipoplex characterisation

The colloidal stability of lipoplexes was determined at different charge ratios (CR = cationic lipid charge/siRNA charge (+/-)) for various cationic lipids (DOSP, DOSP/DOPE, BGTC/DOPE and DOTAP/DOPE) using size, fluorescence and electrophoresis analysis (table 1). Similar to DNA lipoplexes, three different zones of colloidal stability A, B and C could be determined with specific properties in each zone [8]. In summary, in zone A the quantity of cationic lipid is not sufficient to complex all nucleic acids, so they are still detectable. In this zone, lipoplexes possess a small size and a negative surface charge. In zone B, all nucleic acids are complexed and are no longer detectable. The surface charge is neutral, which leads to aggregation and an augmented size. This was the case for all lipoplexes tested at CR 2 and 2.5, for DOSP/siRNA lipoplexes at CR 3 and 4, and for BGTC/DOPE/siRNA lipoplexes at CR 3. They presented a size over the arbitrary value of 700 nm and only a slight fluorescence in electrophoresis experiments. In zone C, the quantity of cationic lipids is predominant and thus the surface charge is positive leading to repulsion and smaller lipoplexes which was observed for all lipoplexes tested at the CR 5 and for BGTC/DOPE/siRNA lipoplexes at CR 4. To encapsulate lipoplexes in the liquid lipid core of LNCs, lipoplexes of zone B and C were chosen as in zone B the neutral surface charge and the aggregation of lipoplexes suggest rather a lipophilic affinity, and DNA lipoplexes of zone C were already encapsulated efficiently in LNCs.

Electrophoresis experiments	Lipid	CR	Mean diameter [nm]	Zone
	DOSP	2 2,5 3 4 5	1818 1423 1858 1122 605	B B B B C
	DOSP/DOPE	2 2,5 5	2229 2026 234	B B C
	BGTC/DOPE	2,5 3 4	1314 770 344	B B C
	DOTAP/DOPE	2,5 5	1110 680	B C

Table 1: Characteristics of siRNA lipopolexes used for siRNA LNC formulations

SiRNA LNC formulation and characterisation

Basic LNCs were developed by Heurtault *et al*. [2]. Their easy formulation process and their good characterisation make these nanocarriers attractive. To formulate them, the components were mixed together and temperature cycles around the phase inversion temperature (PIT) were performed. In the last step, an important quantity of water was added at the PIT of the last cycle, resulting in the rapid cooling and dilution of the emulsion and the formation of LNCs. The addition of lipoplexes in the cooling water, at the end of the formulation process, contributed to siRNA LNC formulations and brought the advantage to avoid their exposition to high temperature during the formulation.

SiRNA encapsulation in LNCs was checked using electrophoresis experiments. As sometimes a low fluorescence band was visible, indicating an incomplete complexation or encapsulation, and to determine whether siRNA were encapsulated in LNCs or simply complexed in lipoplexes, a purification of siRNA LNCs DOTAP/DOPE CR 2.5 was performed on sepharose columns. The collected fractions were then analysed performing size and zeta potential measurements, PEG quantification, turbidity measurements and gel electrophoresis. The final result of these analyses (figure 1) suggested the presence of 5 different compartments in the formulation: (1) empty liposomes, (2) lipoplexes, (3) siRNA LNCs, (4) empty LNCs and (5) free siRNA. In the first compartment, empty liposomes were suspected as no PEG and no siRNA were found and a size of about 800 nm was measured. In the second

compartment the size diminished, siRNA were detected, the turbidity augmented and a slightly positive zeta potential was measured indicating the presence of DOTAP/DOPE lipoplexes (CR 2.5). In the third compartment PEG and siRNA were detected with a size about 100 nm and a near neutral zeta potential were measured, suggesting the presence of siRNA LNCs. In the fourth compartment PEG but no siRNA were detected and sizes about 50 nm and a slightly negative zeta potential were measured, indicating empty LNCs and/or free HS-PEG. In the last compartment, no PEG was detected, but siRNA were found, indicating free siRNA.

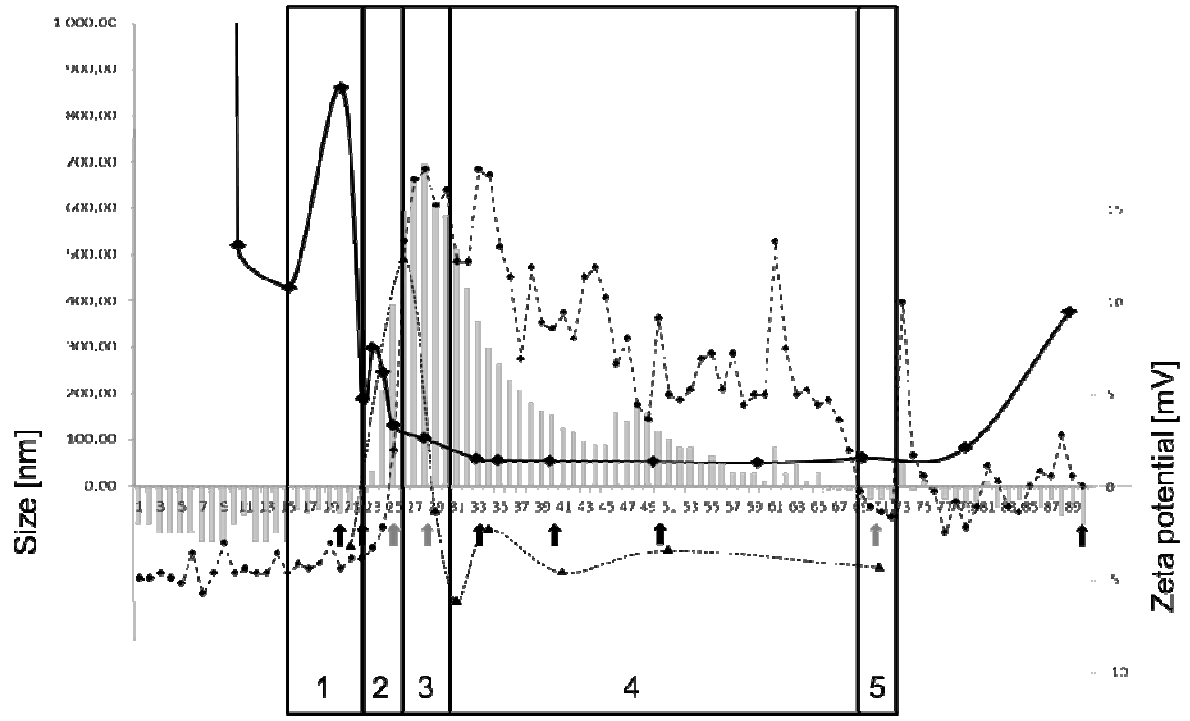

	1 lipo	2 lpx	3 siLNC	4 LNC/PEG	5 siRNA
Size ——	800 nm	200 - 300 nm	100 nm	50 nm	50 nm
Zeta potential - - -	-	5 – 10 mV	-5 – 5 mV	-5 mV	-5 mV
Turbidity ||| -	+	+	+	-
PEG – –	-	-	+	+	-
siRNA ⇧	-	+	+	-	+
Conclusion	empty liposomes	Lipoplexes	siRNA LNCs	empty LNCs/ free (HS)PEG	free siRNA

Figure 1: Purification of DOTAP/DOPE/siRNA LNC formulation (CR 2.5) on sepharose columns

According to the previous results, our hypothesis is that siRNA can be situated in 4 different compartments: in the second compartment in lipoplexes outside LNCs; in the third

compartment either (3a) complexed with cationic lipids in LNCs or (3b) associated to other components of the LNC formulation but dissociated from cationic lipids; or in the fifth compartment as free siRNA. To quantify and localize siRNA in the formulation, a quantification method using UV spectrometry analysis at 260 nm was developed (Figure 2). Free siRNA was quantified using a simple chloroform extraction to separate other constituents of the formulation which interfered at UV spectroscopy analysis. SiRNA in lipoplexes outside LNCs were quantified in the same way but NaOH was added to dissociate lipoplexes. SiRNA in LNCs were quantified using the "separated" formulations (without free siRNA and/or without lipoplexes) by addition of ethanol, to dissociate LNCs, and NaOH, to dissociate siRNAs from cationic lipids. To determine the siRNA quantity, calibrating curves for the different treatments were performed using siRNA quantities between 0µg and the maximal theoretical charge in one volume siRNA LNC formulation (c = 0.25 g/l) .

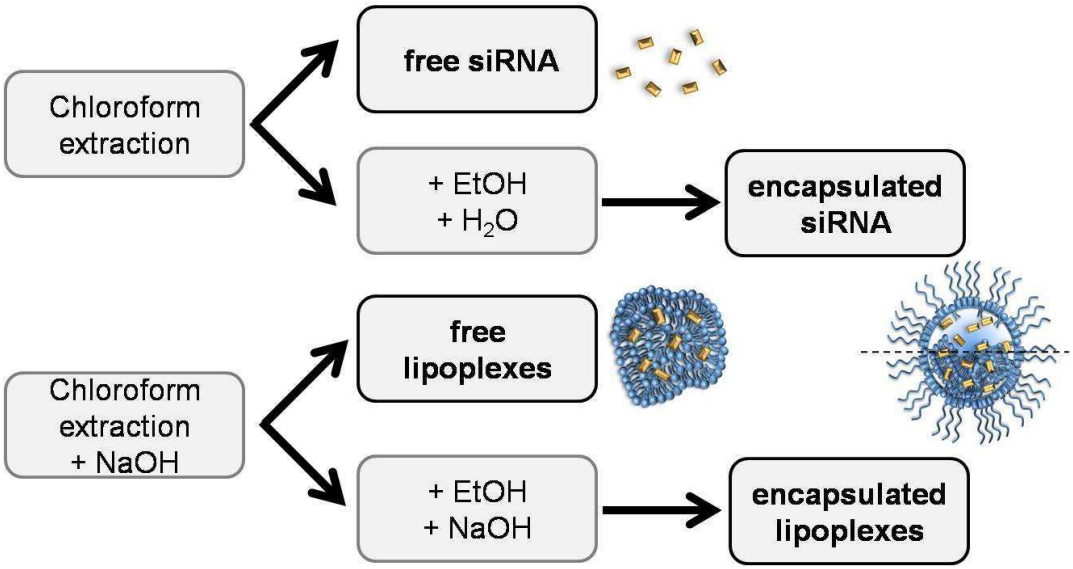

Figure 2: Schematic representation of siRNA quantification

Afterwards, siRNA LNCs were formulated with different cationic lipids and their size, zeta potential and encapsulation efficiency were determined (table 2). The basic LNC formulation presented a size of 55 nm with a small distribution indicated by a very low polydispersity index (PDI) of 0.04 and a slightly negative zeta potential of about -5 mV. The zeta potential of formulations prepared by the novel process was comprised between -25 and +25 mV and the encapsulation efficiencies in LNCs were situated between 4 and 65%. Both varied in function of the cationic lipids used for lipoplex formation and the CR. The sizes were around

55 nm with a very low PDI with exception of siRNA LNCs using DOTAP/DOPE/siRNA lipoplexes. Indeed, at CR 2.5, they showed 2 distinct populations of about 55 and 185 nm and at CR 5, a size of 125 nm with the highest siRNA encapsulation efficiency of 65%. These lipids and CR were also previously used for DNA encapsulation in DNA LNCs forming efficient nanocarriers for *in vitro* [3] and *in vivo* [4] transfection. The size of DOTAP/DOPE siRNA LNCs (CR 5) was similar to other promising siRNA vector one (100 – 170 nm), with efficient transfection *in vivo* after systemic administration [9]. However, the first siRNA nanocarriers for systemic administration which are in phase I clinical trials (CALAA-01 [10]) have sizes about 70 nm. This corresponds to siRNA LNC formulations containing the other lipids but, in contrast, they present only half or lower encapsulation efficiencies.

LNC formulation		Size [nm]	PDI	Zeta potential [mV]	Encapsulation efficiency [%]					Total siRNA found [%]
basic LNC formulation		55.5 +/- 0.5	0.04 +/- 0.01	-5.2 +/- 0.5						
LNC siRNA		Size [nm]	PDI	Zeta potential [mV]	Compartment				siLNC (3a+3b)	
Cationic lipids	CR [+/-]				5 siRNA	2 lpx	3a[1] siLNC	3b[2] siLNC		
BGTC/DOPE	2.5	55.3 +/- 0.1	0.13 +/- 0.03	1.5 +/- 0.7	20 +/- 0	66 +/- 3	3 +/- 1	10 +/- 4	13 +/- 3	108 +/- 4
DOSP	2	51.6 +/- 0.2	0.07 +/- 0,00	-2.4 +/- 0,7	2 +/- 1	94 +/- 5	0	4 +/- 6	4 +/- 6	107 +/- 7
	2.5	60.4 +/- 1.0	0.10 +/- 0.02	-1,1 +/- 0.1	8 +/- 9	75 +/- 18	13 +/- 9	4 +/- 1	17 +/-10	117 +/- 14
	5	52.8 +/- 0.0	0.08 +/- 0.00	24.1 +/- 1.7 10.1 +/- 3.2 -3.7 +/- 4.3	20 +/- 12	65 +/- 13	11 +/- 1	3 +/- 0	14 +/- 1	126 +/- 8
DOSP/DOPE	2	53.3 +/- 0.2	0,03 +/- 0.01	-25.7 +/- 1.9	4 +/- 1	80 +/- 8	8 +/- 12	7 +/- 2	15 +/- 10	75 +/- 9
	2.5	59.7 +/- 0.5	0.09 +/- 0.01	-1.5 +/- 0.4	2 +/- 2	91 +/- 0	2 +/- 2	5 +/- 0	7 +/- 2	88 +/- 2
	5	61.4 +/- 0.3	0.15 +/- 0.03	7.8 +/- 0.9	12 +/- 4	73 +/- 1	11 +/- 4	3 +/- 0	15 +/- 5	105 +/- 6
DOTAP/DOPE	2.5	53.5 +/- 6.8 184.1 +/- 28.4	0.29 +/- 0.03	-0.3 +/- 0.5	0	73 +/- 19	11 +/- 16	16 +/- 3	27 +/- 19	100 +/- 5
	5	124.8 +/- 0.6	0.24 +/- 0.00	1.6 +/- 0.3	0	34 +/- 1	20 +/- 4	45 +/- 5	65 +/- 2	79 +/- 7

[1] siRNA encapsulated in LNCs complexed with cationic lipids [2] siRNA encapsulated in LNCs dissociated from cationic lipids

Table 2: Size, zeta potential measurements and encapsulation efficiency of siRNA LNC formulations

In summary, we developed a new platform of siRNA LNCs showing appropriate characteristics for systemic administration with good encapsulation efficiencies and/or small sizes and neutral surface charges. However, further investigations need now to be carried out to test their transfection efficiency *in vitro* and *in vivo* and to find a compromise between a small size and a high siRNA payload.

REFERENCES

1. David, S., et al., Non-viral nanosystems for systemic siRNA delivery. Pharmacol Res. 62(2): p. 100-14.
2. Heurtault, B., et al., A novel phase inversion-based process for the preparation of lipid nanocarriers. Pharm Res, 2002. 19(6): p. 875-80.
3. Morille, M., et al., Galactosylated DNA lipid nanocapsules for efficient hepatocyte targeting. Int J Pharm, 2009. 379(2): p. 293-300.
4. Morille, M., et al., Tumor transfection after systemic injection of DNA lipid nanocapsules. Biomaterials, 2010.
5. Vonarbourg, A., et al., The encapsulation of DNA molecules within biomimetic lipid nanocapsules. Biomaterials, 2009. 30(18): p. 3197-204.
6. Desigaux, L., et al., Self-assembled lamellar complexes of siRNA with lipidic aminoglycoside derivatives promote efficient siRNA delivery and interference. Proc Natl Acad Sci U S A, 2007. 104(42): p. 16534-9.
7. Vigneron, J.P., et al., Guanidinium-cholesterol cationic lipids: efficient vectors for the transfection of eukaryotic cells. Proc Natl Acad Sci U S A, 1996. 93(18): p. 9682-6.
8. Pitard, B., Supramolecular assemblies of DNA delivery systems. Somat Cell Mol Genet, 2002. 27(1-6): p. 5-15.
9. Mahon, K.P., et al., Combinatorial approach to determine functional group effects on lipidoid-mediated siRNA delivery. Bioconjug Chem, 2010. 21(8): p. 1448-54.
10. Davis, M.E., et al., Evidence of RNAi in humans from systemically administered siRNA via targeted nanoparticles. Nature, 2010. 464(7291): p. 1067-1070.

Publication No 2

DNA nanocarriers for systemic administration – characterization and in vivo bioimaging in healthy mice

David S., Passirani C., Carmoy N., Morille M., Benoit JP., Montier T. and Pitard B.

Molecular Therapy – soumis

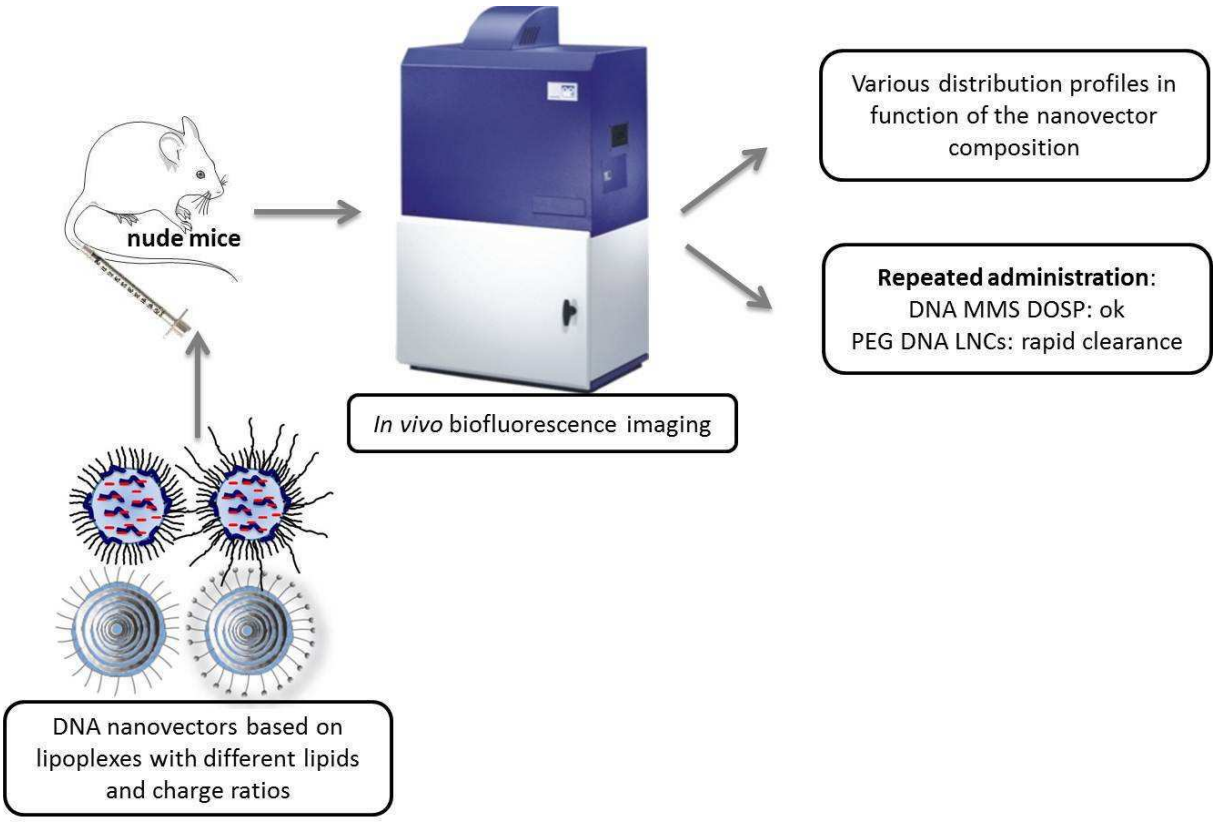

En parallèle, la caractérisation des vecteurs ADN a été approfondie. Des nouveaux MMS ADN utilisant le lipide cationique DOSP ont été caractérisés et le taux d'encapsulation d'ADN dans les LNC ADN quantifié pour la première fois en se basant sur le dosage de siRNA, développé dans la publication précédente. Les nanovecteurs ADN ont été ensuite injectés dans des souris saines par voie systémique et leur profil de biodistribution analysé en utilisant l'imagerie par fluorescence *in vivo*. De plus, les effets d'une injection répétée des deux systèmes les plus furtifs, les LNC ADN PEG et les MMS ADN DOSP ont été étudiés.

DNA NANOCARRIERS FOR SYSTEMIC ADMINISTRATION - CHARACTERISATION AND *IN VIVO* BIOIMAGING IN HEALTHY MICE

Stephanie David[1,2,3], Catherine Passirani[1,2,*], Nathalie Carmoy[4], Marie Morille[1,2], Jean-Pierre Benoit[1,2], Tristan Montier[4], Bruno Pitard[3,*]

[1]*LUNAM Université – Ingénierie de la Vectorisation Particulaire, F-49933 Angers, France*

[2]*INSERM – U646, F-49933 Angers, France*

[3]*INSERM UMR915 – Université de Nantes, 8 quai Moncousu, F-44000 Nantes, France*

[4]*DUMG – CHRU de Brest, 5 avenue du Maréchal Foch, F-29200 Brest, France*

*Correspondence should be addressed to C.P. (catherine.passirani@univ-angers.fr) or B.P. (bruno.pitard@nantes.inserm.fr)

C. Passirani: Inserm U646, IBS-CHU, 4 rue Larrey, 49933 Angers Cedex 9, France, Tel.: +33 244 688534, Fax: +33 244 688546

B. Pitard: Inserm U915, Institut du Thorax, IRT-UN Université de Nantes, 8 quai Moncousu, F-44000 Nantes, France, Tel: +33 228 080128, Fax: +33 228 080130

ABSTRACT

Nucleic acids such as DNA molecules often need a delivery vehicle for efficient action after systemic administration. In this aim, we present here different DNA nanocarriers consisting of new multimodular systems (MMS), containing the cationic lipid dioleylamine succinyl paromomycin (DNA MMS DOSP), or bis (guanidinium)-tren-cholesterol (DNA MMS BGTC), and DNA lipid nanocapsules (DNA LNCs). Active targeting of hepatocytes using galactose as ligand for DNA MMS (GAL DNA MMS) and passive targeting using PEG coating for DNA LNCs (PEG DNA LNCs) should improve the properties of these DNA nanocarriers. All systems were characterized via physico-chemical methods and the DNA payload of DNA LNCs was quantified for the first time. Afterwards, their biodistribution in healthy mice was analysed after encapsulation of a fluorescent dye via *in vivo* biofluorescence imaging, revealing various distribution profiles depending on the cationic lipid used and their surface characteristics. The lipid BGTC and the ligand galactose provided an accumulation in the liver, DNA LNCs showed a brought distribution profile but a rapid elimination and the lipid DOSP and the coating with PEG exposed a prolonged circulation in the bloodstream. Furthermore, the two vectors with the best prolonged circulation profile were administered twice in healthy mice revealing that the new vectors DNA MMS DOSP showed no toxicity and the same distribution profile for both injections, contrary to PEG DNA LNCs which showed a rapid clearance after the second injection certainly due to the accelerated blood clearance (ABC) phenomenon.

Keywords:

Lipid nanocapsules, multimodular systems, repeated administration, targeting, ABC phenomenon

INTRODUCTION

Gene therapy is an emerging technology that aims for permanent or transient correction of a gene defect by intracellular delivery of nucleic acids [1]. Gene defects can either arise during the cell division processes or be due to external agents (such as UV or other radiations, chemical substances …). The introduction of a plasmid DNA encoding the native form of the gene can be a way to conquer these gene defects. As naked plasmid DNA is quickly degraded by blood nucleases and expose in general no relevant therapeutic effects when administered systemically [1], vectors are necessary to carry out plasmid DNA into the cell nucleus. In general, as any drug, gene transfer complexes must reach its intended site of action to induce therapeutic effects but this can be compromised through unspecific interactions, especially if they are frequently re-administrated. Consequently, one basic challenge for non-viral gene therapy is to develop an approach that deliver a therapeutic gene into selected cells. In this aim, two different types of promising nanocarriers were developed in our laboratories, lipid nanocapsules (DNA LNCs) and multimodular systems (DNA MMS). DNA LNCs consist of a lipophilic lipid core, containing a mixture of triglycerides and polyglyceryl-6 dioleate surrounded by a shell composed of free polyethylene glycol (PEG) and hydroxystearate-PEG (HS-PEG) [2]. To encapsulate hydrophilic DNA in the lipophilic lipid core, the first step consists of complexing the anionic DNA with cationic lipids, to form lipoplexes which are then introduced in the formulation process of DNA LNCs, based on phase-inversions of an emulsion [3]. DNA LNCs encapsulating a luciferase coding plasmid DNA proved their transfection efficacy *in vitro* [4] and, after surface-coating with DSPE-PEG_{2000} chains forming PEG DNA LNCs, prolonged circulation in the blood and transfection efficacy *in vivo* in a tumour model [5, 6]. DNA MMS also exhibit a dual structure, a core composed of lipoplexes and an external corona of steric stabilizers capable to carry ligands for active targeting. The first developed DNA MMS consisted of the cholesterol derivate BGTC (bis-guanidinium-tren-cholesterol) as cationic lipid, the plasmid pCMV luciferase and the steric stabilizer F108 (a block copolymer of PEO and PPO), with or without galactose as ligand. They were already tested *in vitro* on primary hepatocytes [7] and demonstrated a specific transfection for galactosylated DNA MMS due to the recognition of the galactose ligands by asialoglycoprotein receptors, present on hepatocytes.

With the aim to develop new efficient non-viral DNA nanocarriers, new MMS containing the aminoglycoside derivate DOSP (dioleyl succinyl paromomycin) were developed and compared to the already *in vitro* tested DNA MMS BGTC. In parallel, the DNA payload in DNA LNCs was for the first time quantified and localised. Afterwards, both DNA MMs, in presence and absence of galactose, as well as DNA LNCs and PEG DNA LNCs were injected for the first time via intravenous injection in healthy mice and their different biodistribution and kinetic were explored, via non-invasive *in vivo* biofluorescence imaging (BFI) [8]. Finally, PEG DNA LNCs and DNA MMS DOSP, the DNA nanocarriers with the longest circulation time, were tested for a repeated administration as, in a future therapeutic application multiple injections can be envisaged to improve the effect of the plasmid DNA.

RESULTS

DNA nanocarrier characterisation

DNA MMS DOSP – new multimodular systems for systemic administration

Similar to DNA MMS BGTC, new DNA MMS containing the cationic lipid DOSP were developed. They could be recovered by galactose in order to target the asialoglycoprotein receptors in a future application directed to the liver. To determine their colloidal stability [9], electrophoresis experiments (figure 1a), size measurements (figure 1b) and fluorescence measurements (data not shown) of lipoplexes DOSP/DOPE/DNA were performed at different charge ratios (CR), defined as ratio of cationic lipid charge to anionic nucleic acid charge (+/-) [10]. Three zones of colloidal stability A (CR < 2), B (CR 2 – 5) and C (CR > 5) were determined with a complete complexation of the nucleic acids at CR ≥ 2 indicated by low fluorescence intensities in electrophoresis experiments and fluorescence measurements (data not shown). As consequence, the CR 2 was chosen, but lipoplexes at this CR had an increased size and were colloidal instable. To prevent their aggregation due to their neutral surface charge, the polymer F108 was added to reduce efficiently their size (final size about 100 - 130 nm, figure 1c). Additionally, for all F108/DNA ratios tested, no fluorescence signal was detected in electrophoresis experiments indicating no dissociation of the lipoplexes (figure 1d). In view of these results and in accordance to DNA MMS BGTC, the F108/DNA and F108-gal/DNA ratio of 300 (w/w) was chosen.

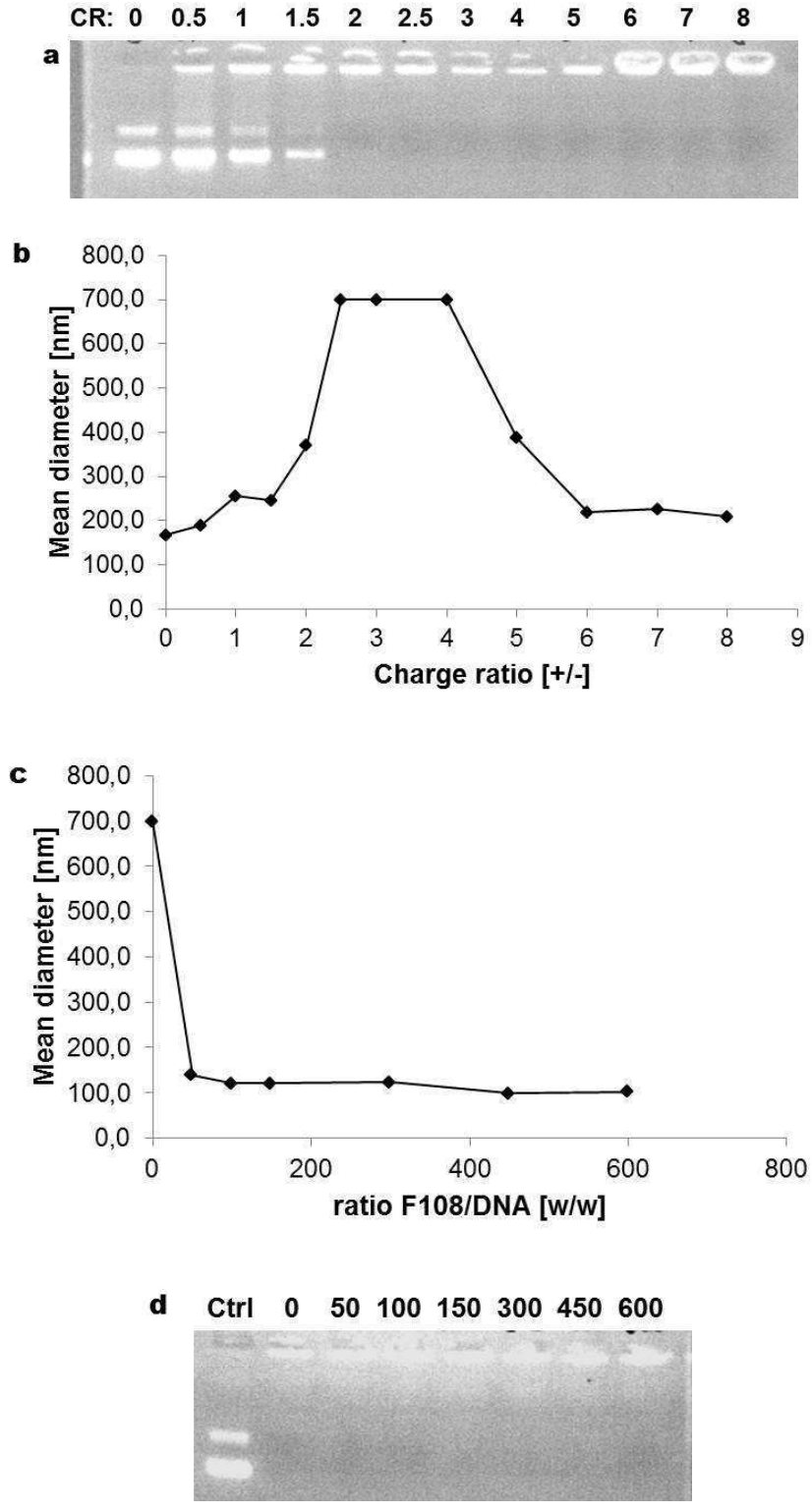

Figure 1: Development of DNA MMS DOSP

Electrophoresis experiments (1a) and size measurements (1b) were performed at different charge ratios of DOSP/DOPE/ADN lipoplexes to determine their colloidal stability. Size measurements (1c) and electrophoresis experiments (1d) of DOSP/DOPE/ADN lipoplexes at CR 2 with different polymer/DNA ratios were performed to determine the quantity of polymer used for DNA MMS DOSP.

DNA LNCs – quantification of the DNA payload

To check DNA complexation (lipoplexes) or encapsulation (DNA LNCs) and to confirm that the purification and post-insertion process did not modify the DNA encapsulation in PEG DNA LNCs, gel electrophoresis experiments were performed. When LNCs were intact, only very low fluorescence signals were detected for both types of LNCs, indicating neither a loss of DNA nor liberation of DNA from DNA LNCs (fig. 2a). In contrast, after LNC destruction with Triton, an intense fluorescence signal was observed in both cases. Afterwards, the DNA localisation (lipoplexes versus LNCs) was determined using a newly developed quantitative method based on chloroform extraction and subsequent UV spectroscopy analysis at 260nm. Our hypothesis is that DNA could be potentially localised in four different compartments of the formulation (fig. 2b): (1) free DNA molecules, (2) DNA molecules in lipoplexes outside LNCs, (3) lipoplexes encapsulated in LNCs, and (4) DNA molecules encapsulated in LNCs dissociated from cationic lipids. The DNA quantification, before purification or postinsertion (table 1), revealed about 16% free DNA molecules, corresponding to a small line of fluorescence at gel electrophoresis experiments, about 65% in lipoplexes outside DNA LNCs and up to 21% of DNA encapsulated in LNCs, whereas the major part was dissociated from cationic lipids (21% versus 1%). The experimentally determined encapsulation efficiency in LNCs, when the formulation weight was also considered, was about 23% and the experimental DNA payload about 0.07% compared to the theoretical DNA payload of 0.29%. To eliminate free DNA, DNA LNCs were purified by gel chromatography before coating with PEG and use for *in vivo* experiments.

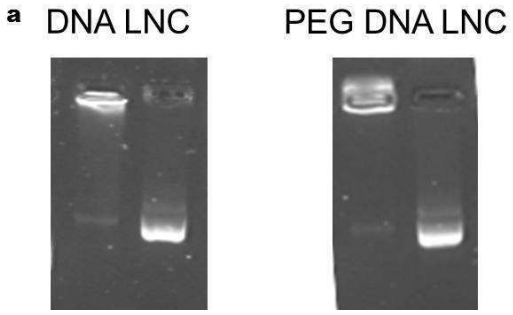

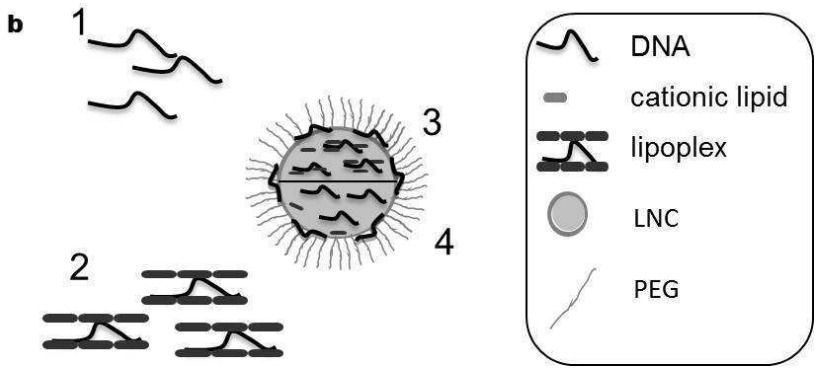

Figure 2: DNA Quantification in DNA LNCs

2a) Electrophoresis experiments were performed to check DNA encapsulation in DNA LNCs and PEG DNA LNCs. 2b) Schematic representation of the DNA localization in the DNA LNC formulation (1) as free DNA, (2) in lipoplexes outside LNCs, (3) in lipoplexes inside LNCs or (4) in LNCs dissociated from cationic lipids.

Table 1 :

	1 Free DNA [%]	2 Free lipoplexes [%]	3 Encapsulated lipoplexes [%]	4 Encapsulated DNA [%]	DNA in LNCs [%] (3 + 4)	DNA payload[a] [%]	Entrapment efficiency[b] [%]
Formulation 1	0	85 +/- 4	1 +/- 1	15 +/- 6	16 +/- 4	0.05 +/- 0.01	16 +/- 5
Formulation 2	21 +/- 20	56 +/- 34	6 +/- 8	21 +/- 21	26 +/- 14	0.09 +/- 0.06	31 +/- 20
Formulation 3	27 +/- 5	53 +/- 1	0	21 +/- 4	21 +/- 4	0.07 +/- 0.02	23 +/- 5
Mean	**16 +/- 14**	**65 +/- 18**	**1 +/- 2**	**21 +/- 5**	**21 +/- 5**	**0.07 +/- 0.02**	**23 +/- 7**

[a]Experimental DNA payload [%] calculated as w (DNA in LNCs)/ w (DNA LNCs) * 100

[b]Entrapment efficiency calculated as experimental DNA payload/ theoretical DNA payload

Table 1: *DNA quantification in three different formulations before purification and postinsertion with DSPE-PEG*

Physico-chemical characterisation of the different DNA nanocarriers

The lipoplex composition used for DNA LNCs, PEG DNA LNCs, DNA MMS BGTC, GAL DNA MMS BGTC and the new developed DNA MMS DOSP and GAL DNA MMS DOSP, as well as the polymer/DNA ratios used for *in vivo* experiments were listed in Table 2. The plasmid luciferase was chosen in a first time as model because it can be quantified quite easily. Before using these DNA nanocarriers for *in vivo* experiments, they were characterized by size and zeta potential measurements (table 2). DNA LNCs had a size of 114 nm with a PDI of 0.3 and a positive zeta potential of +27 mV. Coating the surface with DSPE-PEG_{2000}

resulted in a size of 132 nm and a negative zeta potential of -17 mV due to dipolar interactions of PEG with water as previously described [11]. DNA MMS showed sizes of 150 nm (BGTC) and 200 nm (DOSP) with a polydispersity index (PDI) of 0.4. The addition of galactose resulted in sizes of 300 nm (BGTC), which is in good accordance to previous results [7], and 150 nm (DOSP) with a PDI of 0.5 and unchanged neutral zeta potentials.

DNA nanocarrier specifications						
	DNA LNC	**PEG DNA LNC**	**DNA MMS BGTC**	**GAL DNA MMS BGTC**	**DNA MMS DOSP**	**GAL DNA MMS DOSP**
	Lipoplex composition					
Plasmid:	pgWIZ-luciférase					
Lipids for lipoplexes:	DOTAP/DOPE		BGTC/DOPE		DOSP/DOPE	
Charge ratio	5		2			
	Polymer composition					
Polymer:	-	DSPE-PEG_{2000}	F108	F108-gal	F108	F108-gal
Ratio polymer/DNA	-	70 (w/w)	300 (w/w)			
	Physico-chemical characteristics					
Size [nm]	114 +/- 25	132 +/- 3	150 +/- 32	298 +/- 171	198 +/- 57	152 +/- 58
PDI	0.3	0.3	0.4	0.5	0.4	0.5
Zeta potential [mV]	27 +/- 12	-17 +/- 4	-3 +/- 2	-2 +/- 1	0	-2 +/- 0

Table 2: Characteristics of the different DNA nanocarriers

In vivo biofluorescence imaging in healthy animals

Biodistribution after one systemic administration

For *in vivo* experiments, nude mice were chosen to avoid hair autofluorescence, facilitate observations by *in vivo* biofluorescence imaging (BFI) [12] and to compare the results with previously obtained ones on different tumour models [5, 6, 13]. To follow the DNA nanocarriers via BFI, the fluorescent dye DiD (a near infrared fluorophore used to avoid the autofluorescence wave length emitted by animals) was encapsulated and images taken 1, 3, 5 and 24h after systemic administration (Fig 3) in lateral and decubitus dorsal views. The DNA MMS BGTC and GAL DNA MMS BGTC were rapidly accumulated in the liver. This accumulation persisted during the whole observation period whereas the addition of the ligand

showed a more specific accumulation in the liver region, starting at 1h after intravenous administration. DNA MMS DOSP showed an accumulation in the urinary system and in the lungs during the whole observation period. These DNA nanocarriers showed also an accumulation in the liver, but in a lesser extent than for DNA MMS BGTC and an augmentation at 24h. The addition of galactose ligands to these systems also provides an accentuated accumulation in the liver with less accumulation in the urinary system and the lungs than for DNA MMS DOSP. However, DNA MMS DOSP had an increased circulation time compared to the other DNA MMS tested, as fluorescence in the whole body could still be observed 24h after administration. DNA LNCs showed a large distribution 1h after intravenous administration, but were rapidly eliminated by the urinary system. The addition of long DSPE-PEG chains augmented the circulation time until 5h after administration with a large distribution in the whole body. However, 24h after their administration no fluorescence was detected indicating the elimination of these systems.

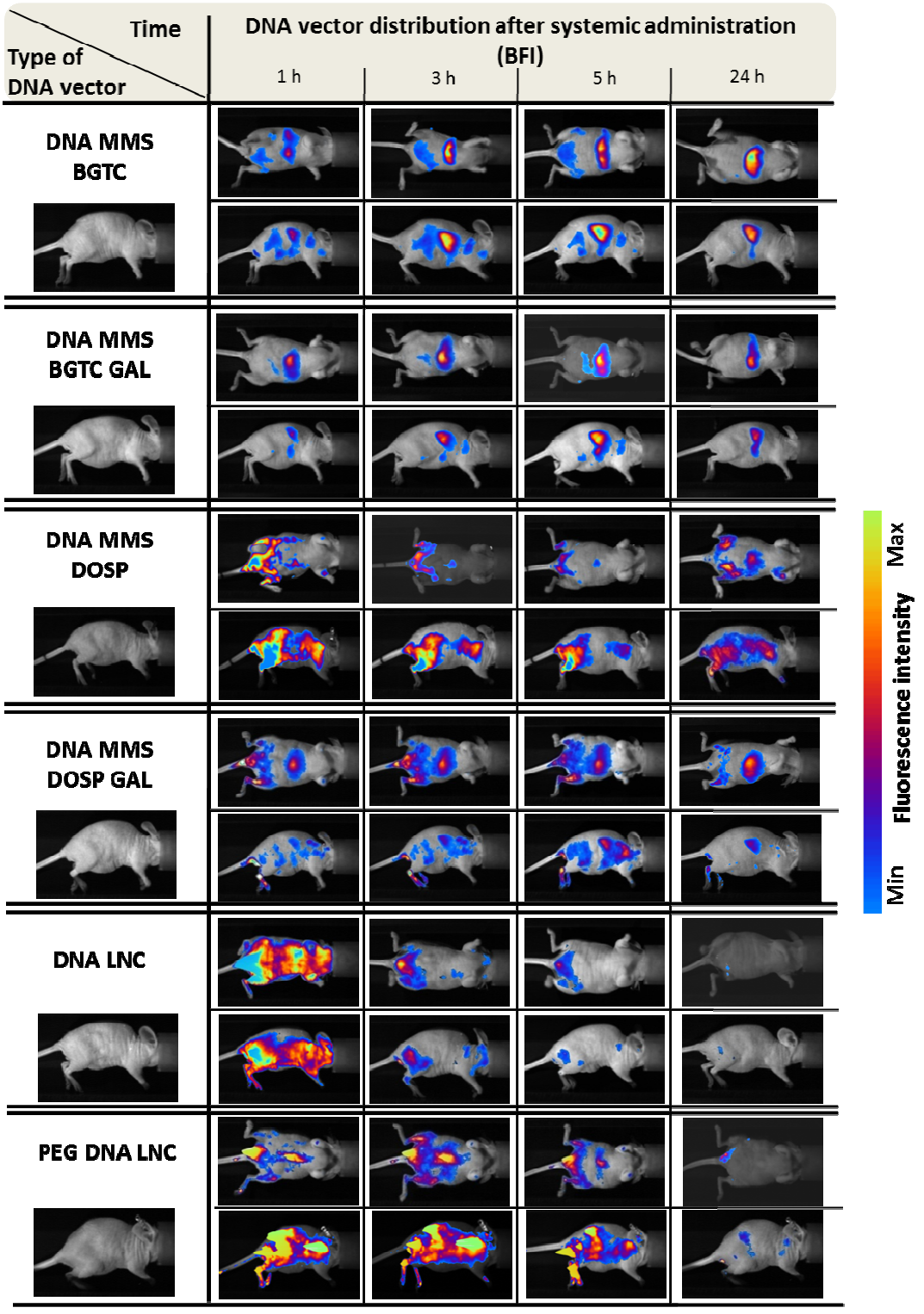

Figure 3: BFI of the different DNA nanocarriers administered via i.v. injection in healthy animals at different times

DNA MMS BGTC, GAL DNA MMS BGTC, DNA MMS DOSP, GAL DNA MMS DOSP, DNA LNCs and PEG DNA LNCs encapsulating a fluorescent tracer, DiD, were injected i.v. in healthy mice and BFI images were taken at different times (1h, 3h, 5h and 24h after injection) from decubitus dorsal (first line) and lateral (second line) views to follow their biodistribution.

Biodistribution after repeated administration

As the repeated administration of these systems could be envisaged in a treatment context (chronic disease), the two systems with the longest circulation profile (PEG DNA LNCs and DNA MMS DOSP) were followed via BFI after two intravenous injections administered in the time interval of one week (Fig. 4). Images of the first injection were already described in the previous section. After the second injection of DNA MMS DOSP, the biodistribution profile was similar to the first one, represented by a prolonged circulation time and an accumulation in the urinary system and in the lungs. The accumulation in the liver seemed more important after the second injection, but augmented also with time and was maximal at 24h after the second injection. The biodistribution profile for the PEG DNA LNCs after the second injection showed a reduced circulation time and a profile similar to DNA LNCs with a large distribution in the whole body one hour after administration. In contrast, an augmented accumulation in the lungs after the second injection and an important intolerance of PEG DNA LNCs after the second injection were observed.

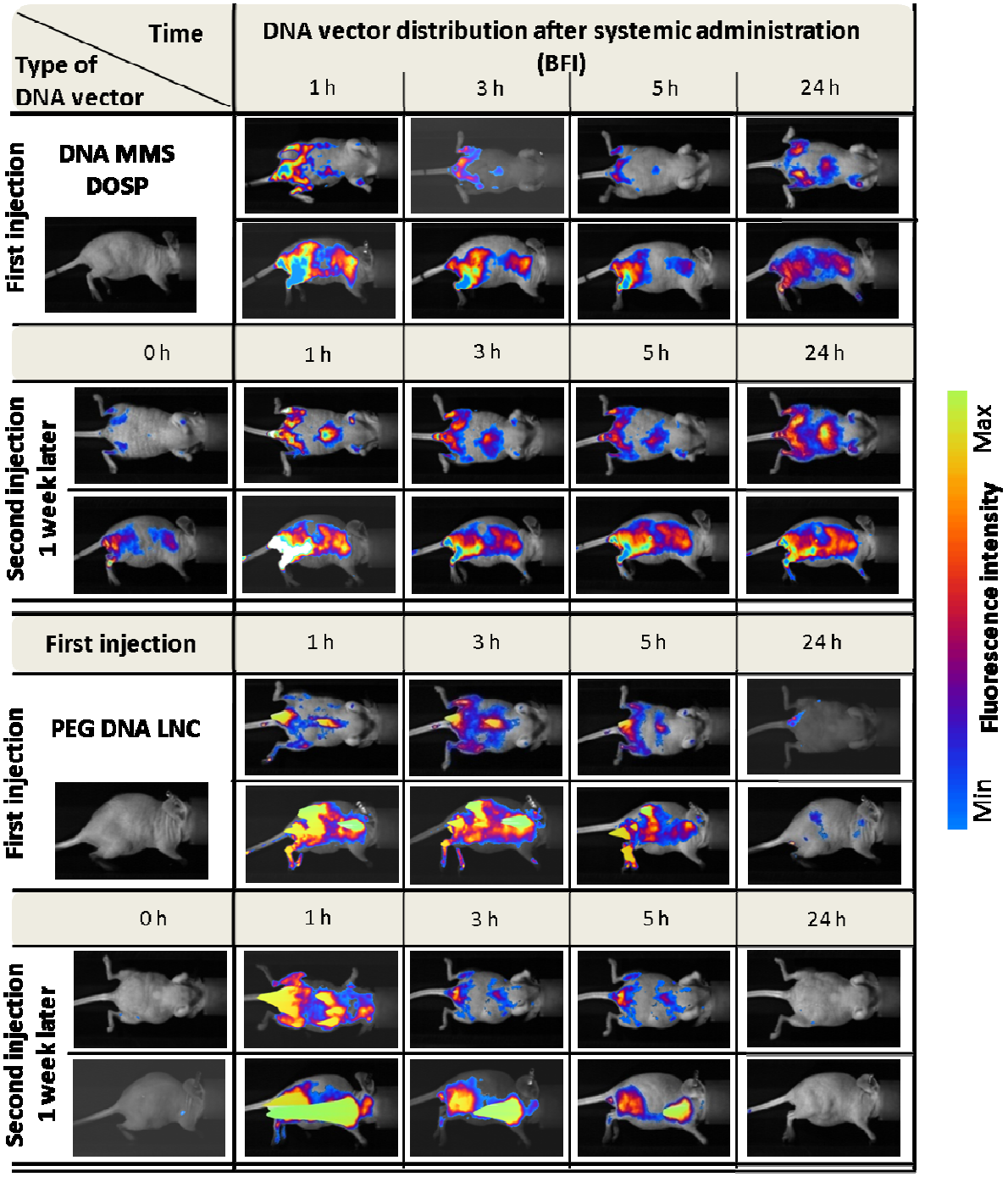

Figure 4: BFI of DNA nanocarriers in healthy animals after repeated systemic administration

PEG DNA LNCs and DNA MMS DOSP encapsulating the fluorescent dye DiD were injected twice intravenously in healthy animals with a time interval of 1 week between administrations and BFI images were taken at different times (1h, 3h, 5h and 24h after each injection and one day before the second injection (0h)) from decubitus dorsal (first line) and lateral (second line) views to follow their biodistribution.

Hepatotoxicity of PEG DNA LNCs and DNA MMS DOSP

To determine the hepatotoxicity of PEG DNA LNCs and DNA MMS DOSP, blood samples were collected regularly during the observation period and the enzyme activity of ALAT (alanine aminotransferase) and ASAT (aspartate aminotransferase) were quantified (Fig. 5) indicating a hepato-toxicity when both ALAT values, specific to the liver, and ASAT values, also found in other organs and tissues, were augmented. For the group receiving PEG DNA LNCs, ASAT and ALAT values showed a slight augmentation 24h after the first injection. These values augmented another time, but in lesser intent, 24h after the second injection. However, these values are near to the values obtained for the control group (without nanocarrier injection). ASAT and ALAT values for the mice receiving DNA MMS DOSP, showed nearly the same profile as the ASAT and ALAT values for the control group indicating no hepato-toxicity of these DNA MMS.

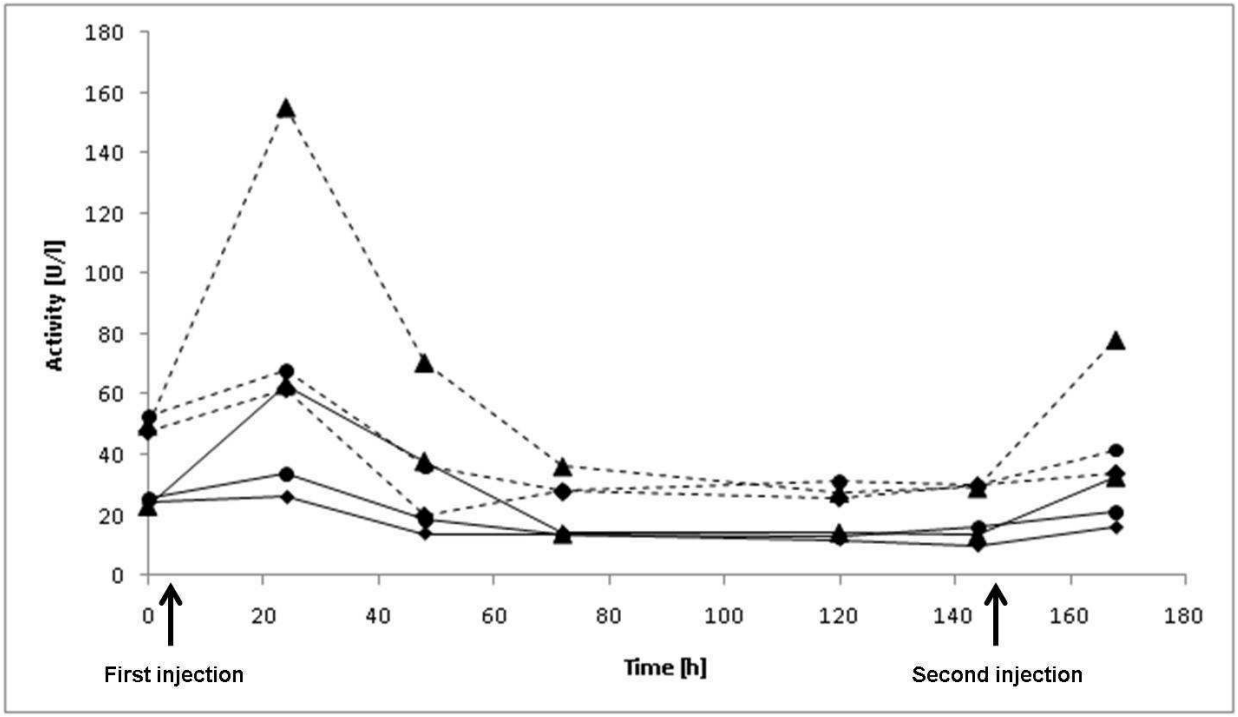

Figure 5: ALAT and ASAT quantification to determine hepatotoxicity of PEG DNA LNCs and DNA MMS DOSP

Blood samples of animals receiving no injection (control, diamonds), PEG DNA LNCs (triangles) or DNA MMS DOSP (circles) were collected once a day during the observation period, starting 1h before the injection of the DNA nanocarriers, to analyse hepatotoxicity of these DNA nanocarriers, represented by ALAT (continuous lines) and ASAT values (dashed lines).

Fluorescence accumulation and luciferase quantification in different organs 24h after i.v. injection

Twenty four hours after the last administration of DNA nanocarriers (two administrations for PEG DNA LNCs and DNA MMS DOSP, one administration for DNA LNCs, DNA MMS BGTC, GAL DNA MMS BGTC and GAL DNA MMS DOSP, and no injection for the control group), animals were sacrificed and the fluorescence localisation was determined in different organs (liver, lungs, kidneys, spleen and heart) to confirm BF images as BFI is affected by tissue depth [8] (figure 6). For all DNA nanocarriers, the major intensity was observed in the liver, followed by some fluorescence in the lungs and almost no fluorescence intensity in the heart, the spleen and the kidneys. In mice receiving the two injections, the luciferase expression was also quantified but revealed few luciferase expression (less than 2 RLU/mg proteins) (data not shown).

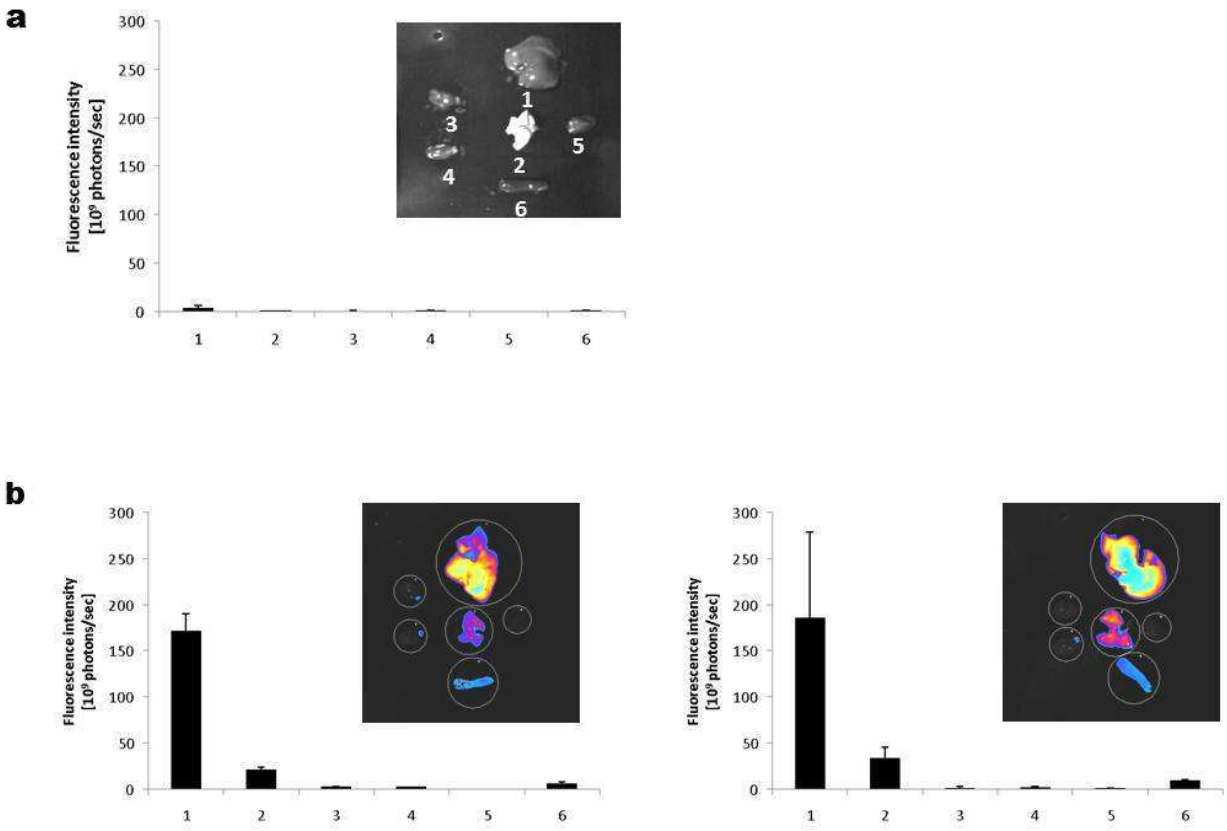

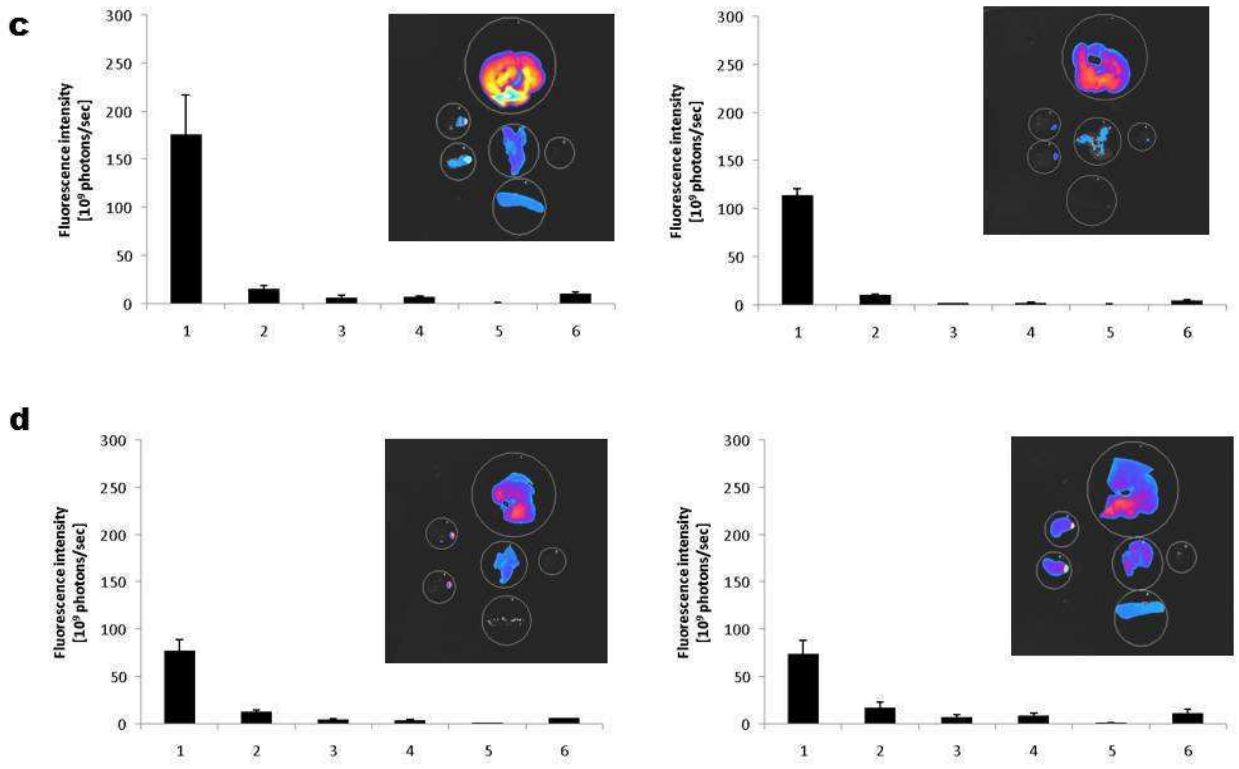

Figure 6: BFI of DNA nanocarriers in different organs 24h after the last systemic administration

Animals were sacrificed 24h after the last injection of DNA nanocarriers and the fluorescence intensity in (1) liver, (2) lungs, (3 and 4) kidneys, (5) heart and (6) spleen measured via BFI. All images were taken with the same settings. (a) control animals receiving no injection, (b) animals receiving one DNA MMS BGTC injection (left) or one GAL DNA MMS BGT injection (right), (c) animals receiving two DNA MMS DOSP injections (left) or one GAL DNA MMS DOSP injection (right), (d) animals receiving one DNA LNC injection (left) or two PEG DNA LNC injections (right)

DISCUSSION

New MMS containing the lipids DOSP/DOPE were developed showing comparable physico-chemical characteristics as the previously described DNA MMS BGTC. In parallel, the DNA encapsulation efficiency in LNCs of about 23% was quantified and localised for the first time using a method based on chloroform extraction and spectroscopy analysis. The major part of DNA encapsulated in LNCs was dissociated from cationic lipids, certainly due to a rearrangement of the different lipids around the nucleic acids during the formulation process, as lipoplexes with an initial size of about 400nm were encapsulated in DNA LNCs presenting a size about 100nm [2]. However, a big part of DNA was still complexed in lipoplexes outside DNA LNCs which remained in the formulation even after the purification step, realized to eliminate the excess of free components, as they both present similar sizes. This

was also confirmed by electrophoresis analysis, showed similar fluorescence intensities for DNA LNCs (before the purification step) and PEG DNA LNCs (after purification step) (Figure 2A). Most of these (PEG) DNA LNCs and DNA MMS, developed in our laboratories, presented appropriated characteristics for systemic administration.

In vivo biofluorescence imaging (BFI), a fast, simple and relatively low-cost technique [14] was used to determine the biodistribution profiles of the DNA nanocarriers in healthy mice. In this aim, the fluorescent tracer, DiD, which is not soluble in water and is known to be prone to aggregation and auto-quenching in aqueous buffer [15], was encapsulated in DNA nanocarriers, which mimicked an "organic like" medium, and thus improved its optical properties. However, the fluorescence intensity is not an absolutely quantitative method and depends on the tissue and its localisation [16]. Furthermore, the quantity of DiD was not equal in all systems, but quantities in DNA MMS with the different lipids and ligands were equal, so they could be compared on the one side, and quantities in DNA LNCs and PEG DNA LNCs on the other side, were also equal and could thus also be compared with each other. Each DNA nanocarrier showed a specific biodistribution profile in function of its composition. DNA MMS composed of the cationic lipid BGTC had a short circulation time and accumulated preferentially in the liver while DNA MMS composed of the cationic lipid DOSP favoured prolonged circulation time. The addition of the ligand galactose to both systems accentuated their accumulation in the liver. This phenomenon is certainly due to the asialoglycoprotein receptor (ASGP-R) situated on hepatocytes which recognizes terminal galactose-bearing asialoglycoproteins and favours the specific internalisation of galactose containing systems [7, 17, 18]. DNA LNCs had a large distribution but a short circulation time which could be increased by coating with DSPE-PEG chains, as was also seen previously on different tumour models [5, 6, 13].

Afterwards, the systems DNA MMS DOSP and PEG DNA LNCs which had the longest circulation times were chosen for a repeated administration on healthy animals. DNA MMS DOSP showed no hepatotoxicity and similar biodistribution profiles for both injections, contrary to PEG DNA LNCs which were rapidly eliminated and showed an augmented intolerance on healthy mice after the second injection. Mice presented signs of paralysis of the extremities and difficulty to breath, typical of a shock response, to the point of rapid mortality within 10 to 30 minutes after injection of some animals. This could be due to the accelerated

blood clearance (ABC) phenomenon of the PEGylated carriers in combination of their immunogenic payload (plasmid DNA) and the use of athymic (nude) mice. This phenomenon has already been reported in the literature [19-21] but is still not fully elucidated. Two distinct phases can be determined in this phenomenon [22, 23]. (1) The induction phase following the first injection, where liposomes or in our case PEG DNA LNCs bind and crosslink surface immunoglobulin on PEG-reactive B-cells [24], inducing the production of anti-PEG IgM and (2) the effectuation phase following the second injection, where on the one hand, the DNA payload is internalised followed by B-cell stimulatory pathway activation, such as TLR 9 [25] and on the other hand accessory cells are induced to produce cytokines, independent of T cell help [25-27] followed by the rapid clearance of the PEGylated carriers from the bloodstream, mainly by Kupffer cells in the liver. The severe reactions observed here, including the death of some mice, could be due to the non-regulation of the immune response due to the use of nude (athymic) mice [21, 28, 29], but the regulation is complex and need further investigations to be fully understood.

For the long circulating systems, PEG DNA LNCs and DNA MMS DOSP, no luciferase expression could be detected 24h after the last injection in any organ although fluorescence was observed in the liver. This could suggest that an active or passive targeting is necessary as no specific accumulation was observed in healthy animals contrary to the tumour model studies with PEG DNA LNCs [5, 6, 13]. For PEG DNA LNCs, an important point for the absence of luciferase expression is certainly the rapid clearance of these DNA nanocarriers after the second injection due to the ABC phenomenon. For the future, there are different possibilities to diminish this immunogenic response by considering the time interval between the different injections [20, 30], the lipid composition of the PEG component [20, 31], the sequence of the pDNA [21] and/or the animals [19] used.

In summary, we presented here various DNA nanocarriers for systemic administration with appropriate physico-chemical properties and different biodistribution profiles depending on their lipid and surface composition. These DNA nanocarriers represent a promising tool for various applications as tumour targeting or hepatocyte targeting. Furthermore, this platform can easily be complemented using other lipids and/or ligands.

MATERIALS AND METHODS

DNA nanocarrier preparations

All DNA nanocarriers used were based on lipoplexes formation prepared by adding equal volumes of DNA plasmid (pgWIZ^{TM}-luciferase (Gene Therapy systems, Inc., San Diego, CA USA)) and liposomes in a defined charge ratio of cationic lipid charge and anionic DNA charge to obtain a final DNA concentration of 0.25 g/l for DNA MMS or 0.825 g/l for DNA LNCs. NaCl was added during preparation, to obtain a final concentration of 0.15M. Lipoplexes were incubated for 20min at room temperature before use. For liposome preparation a cationic lipid DOSP (dioleylamin-succinyl paromomycin) (synthesis previously described in [32]), BGTC (bis(guanidinium)-tris(2-aminoethyl)amine-cholesterol) (synthesis previously described in [33]) or DOTAP (1.2-dioleyl-3-trimethylammoniumpropane) (Avanti® Polar Lipids Inc., Alabaster, AL, USA) was weighted with the neutral lipid DOPE (1.2-dioleyl-sn-glycero-3-phosphoethanolamine) (Avanti® Polar Lipids Inc., Alabaster, AL, USA) in the ratio 1/1, 3/2 or 1/1 (M/M) respectively to obtain a final concentration of 20 mM of cationic lipid charge (considering the number of positive charges per molecule: 4 for DOSP, 2 for BGTC and 1 for DOTAP), and solubilised in chloroform. Then chloroform was evaporated under vacuum to obtain a homogen lipid film which was hydrated with deionised water over night at 4°C. The next day, liposomes were sonicated and size measurement was performed before use. To prepare DNA MMS for BFI, 1,1'-dioctadecyl-3,3,3',3'-tetramethylindodicarbocyanine perchlorate (DiD, em. = 644 nm; exc. = 665 nm) (Invitrogen, Cergy-Pontoise, France) was added to the lipids prior lipid film preparation and the steric stabilizers F108 (80% poly(ethylene oxide), MW 14600, generously provided by BASF) or F108-gal (synthesis previously described in [7]) were added to DOSP/DOPE or BGTC/DOPE liposomes prior lipoplex preparation. To obtain fluorescent DNA LNCs for BFI, DOTAP/DOPE/DNA lipoplexes (CR = 5), corresponding to 78.9 % (w/w) were added to 9.9 % (w/w) lipophilic Labrafac® WL 1349 (Gatefossé S.A., Saint-Priest, France) mixed with DiD as described in [34], 3.9 % (w/w) oleic Plurol® (Polyglyceryl-6 dioleate) which was kindly provided by Gatefossé S.A. (Saint-Priest, France), 1.4 % (w/w) NaCl (Prolabo, Fontenay-sous-Bois, France), and 5.9 % (w/w) Solutol® HS-15 (BASF, Ludwigshafen, Germany) [3]. Briefly, after mixing all the components, temperature-cycles around the phase-inversion-temperature (PIT) were performed under magnetic stirring. Afterwards, ice cooled water (obtained from a Milli-Q-plus® system, Millipore, Paris, France) was added (in a ratio

1:1.96) to dilute the obtained microemulsion and form LNCs. To eliminate free components, DNA LNCs were purified, using PD10 Sephadex columns (Amersham Biosciences Europe, Orsay, France), ultrafiltrated with MilliporeAmicon® Ultra-15 centrifugal filter devices (Millipore, St Quentin-Yvelines, France) and the salt- and LNC-concentration were readjusted afterwards to obtain a physiologic concentration of NaCl (150mM) and the initial concentration of LNCs (152 g/l) [2]. PEG DNA LNCs with a final polymer concentration of 10mM were obtained by a post-insertion process which consisted of mixing purified DNA LNCs with DSPE-mPEG$_{2000}$ (1,2-DiStearoyl-sn-glycero-3-PhosphoEthanolamine-N-[methoxy (polyethylene glycol)-2000], Mean Molecular Weight (MMW) = 2,805 g/mol, Avanti Polar Lipids, Inc, Alabaster, USA), and an incubation for 4 h at 30 °C by vortexing every 15 minutes [5].

DNA nanocarrier characterisation

Size and zeta potential measurements

Size measurements for DNA MMS DOSP development described in the first section of the results were performed using a Malvern Zetasizer 300HSA (Malvern Instruments S.A., Worcestershire, UK) with a dilution of 4:100 in 0.15M NaCl. Size and zeta potential measurements for DNA nanocarrier characterisation were performed using a Malvern Zetasizer® (Nano Series ZS, Malvern Instruments S.A., Worcestershire, UK) at 25 °C, in triplicate after dilution in a ratio of 1:100 with deionised water for DNA LNCs or in a ratio of 4:100 with 0.15M NaCl for DNA MMS DOSP.

Agarose gel electrophoresis

Sample preparation for electrophoresis experiments in the aim of DNA MMS DOSP development, described in the first section of the results, was performed by mixing complexes with Orange Blue loading dye (Promega, Madison, WI, USA). In contrast, sample preparation for electrophoresis experiments with (PEG) DNA LNCs formulations was performed as previously described [2]. Briefly, a treatment with Triton® X100 (Sigma, Saint-Quentin Fallavier, France) was performed to destroy a volume of LNCs equivalent to 0.2 µg of DNA and samples with or without treatment were mixed with gel-loading solution (Sigma, Saint-Quentin Fallavier, France). The prepared samples were then in both cases deposited on 1% agarose gel containing ethidium bromide (Sigma, Saint-Quentin Fallavier, France) to migrate about 30 min, at 100 V.

DNA quantification in DNA LNCs

To analyse the free and encapsulated DNA quantity in DNA LNCs, a volume of DNA LNCs was mixed with four volumes water (obtained from a Milli-Q-plus® system, Millipore, Paris, France) and one volume chloroform, vortexed and immediately centrifuged for 15 min at 12600 rpm at 4°C. The aqueous phase, containing free DNA, was removed and analysed with a UV spectrophotometer (UVIKON 922, Kontron Instruments, Munic, Germany) at 260 nm. The volume removed for quantifying the free DNA was replaced by ethanol (absolut), to liberate the DNA encapsulated in DNA LNCs, and 6 volumes water were added before vortexing and immediately centrifuging a second time for 15 min at 12600 rpm at 4°C. The aqueous phase, containing the liberated DNA from DNA LNCs, was removed and analysed as previously with a UV spectrophotometer (UVIKON 922, Kontron Instruments, Munic, Germany) at 260 nm. To analyse the DNA quantity complexed with cationic lipids inside or outside the DNA LNCs, the same procedure was used, but water was replaced by 1M NaOH to dissociate lipoplexes. The first aqueous phase contained the DNA liberated from lipoplexes outside of DNA LNCs; the second aqueous phase contained the DNA liberated from lipoplexes inside DNA LNCs. The DNA quantity was calculated using a calibrating curve with different DNA concentrations and compared to the total DNA amount encapsulated in theory in DNA LNCs.

***In vivo* experiments**

DNA nanocarrier administration

Six- to nine-week-old female, nude SWISS mice (Charles River, France) were housed and maintained at the University animal facility; they were processed in accordance with the Laboratory Animal Care Guidelines (NIH Publication 85-23, revised 1985) and with the agreement of the regional veterinary services (authorisation FR; 29-024). The different nanocarriers were injected at volumes of 150µl for DNA LNCs and PEG DNA LNCs, and 200µl for DNA MMS, by intravenous injection into the tail vein of mice. Animals receiving PEG DNA LNCs and DNA MMS DOSP were injected twice with a time interval of 1 week between the two injections. Animals were sacrificed 24h after the last intravenous injection.

In vivo biofluorescence imaging

To follow the biodistribution of the different nanocarriers, non-invasive fluorescent imaging (BFI) was performed 1, 3, 5, and 24 h post-injection as described before [David, melanoma]. Briefly, the BFI system of the NightOWL II (Berthold Technologies, Germany) equipped with cooled, slow-scan CCD camera and driven with the WinLight 32 software (Berthold Technology, Germany) was used and the 590 nm excitation and 655 nm emission filters selected. Each mouse was anaesthetised with isofluran during the acquisition time (3 seconds for one fluorescent acquisition). The fluorescent signal was then overlaid on a picture of each mouse.

Fluorescence and luciferase quantification in different organs

24h after the last DNA nanocarrier injection animals were sacrificed and the organs heart, lungs, spleen, liver and kidneys dissected. Organs from animals receiving no or one DNA nanocarrier injection and organs from half of the animals receiving two DNA nanocarrier injections were immediately placed in the BFI-system and biofluorescence images were taken using the same settings as with the whole animals. Organs from the other half of the animals receiving two injections were placed in tubes with PLB 1x (Passive Lysis Buffer, Promega) and shred with the gentleMACS Dissociator for luciferase quantification. Tubes were centrifuged for 10min at 1150g at 4°C and the upper phase transferred in Eppendorf tubes. After another centrifugation of 10 min at 20000g at 4°C, 25µl of the upper phase was placed, in triplicate, in a white 96 well plate and the quantification with the luciferin reagent (Promega) was performed with the MLX luminometer plate reader (Dynex, Guyancourt, France).

ALAT – ASAT determination

Blood samples were collected from the lateral saphenous vein as described in [35] from animals receiving no injections, PEG DNA LNCs and DNA MMS DOSP. Blood was collected once a day during the analysing period on different animals to prevent too important blood loss and collected in Microvette® collection tubes (Sarstedt, Numbrecht, Germany). Afterwards the samples were centrifuged for 2 min at 10000g at 4°C and the plasma removed for further analysis. ALAT- and ASAT- values were determined using a Selectra-E (Elitech, Signes, France).

ACKNOWLEDGEMENTS

The authors would like to thank Mathieu Mevel (Inserm U915, Nantes, France) for synthesis of the polymer F108-galactose and Caroline Denis (Inserm U613, Brest, France) for their help with *in vivo* experiments as well as the platform SynNanoVect. This work was supported by grants from Région Pays de la Loire (CIMATH), Biogenouest, Région Bretagne, Ligue contre le cancer 29 and Canceropole Grand Ouest.

REFERENCES

1. **Viola, J.R., et al., Non-viral nanovectors for gene delivery: factors that govern successful therapeutics. Expert Opin Drug Deliv, 2010. 7(6): p. 721-35.**
2. **Vonarbourg, A., et al., The encapsulation of DNA molecules within biomimetic lipid nanocapsules. Biomaterials, 2009. 30(18): p. 3197-204.**
3. **Heurtault, B., et al., A novel phase inversion-based process for the preparation of lipid nanocarriers. Pharm Res, 2002. 19(6): p. 875-80.**
4. **Morille, M., et al., Galactosylated DNA lipid nanocapsules for efficient hepatocyte targeting. Int J Pharm, 2009. 379(2): p. 293-300.**
5. **Morille, M., et al., Long-circulating DNA lipid nanocapsules as new vector for passive tumor targeting. Biomaterials, 2009. 31(2): p. 321-9.**
6. **Morille, M., et al., Tumor transfection after systemic injection of DNA lipid nanocapsules. Biomaterials, 2010.**
7. **Letrou-Bonneval, E., et al., Galactosylated multimodular lipoplexes for specific gene transfer into primary hepatocytes. J Gene Med, 2008. 10(11): p. 1198-209.**
8. **Waerzeggers, Y., et al., Methods to monitor gene therapy with molecular imaging. Methods, 2009. 48(2): p. 146-60.**
9. **Pitard, B., Supramolecular assemblies of DNA delivery systems. Somat Cell Mol Genet, 2002. 27(1-6): p. 5-15.**
10. **Felgner, P.L., et al., Nomenclature for synthetic gene delivery systems. Hum Gene Ther, 1997. 8(5): p. 511-2.**
11. **Vonarbourg, A., et al., Electrokinetic properties of noncharged lipid nanocapsules: influence of the dipolar distribution at the interface. Electrophoresis, 2005. 26(11): p. 2066-75.**
12. **Hilderbrand, S.A. and R. Weissleder, Near-infrared fluorescence: application to in vivo molecular imaging. Curr Opin Chem Biol, 2010. 14(1): p. 71-9.**
13. **David, S., et al., In vivo imaging of DNA lipid nanocapsules after systemic administration in a melanoma mouse model. Int J Pharm, 2011.**
14. **Goutayer, M., et al., Tumor targeting of functionalized lipid nanoparticles: assessment by in vivo fluorescence imaging. Eur J Pharm Biopharm, 2010. 75(2): p. 137-47.**
15. **Texier, I., et al., Cyanine-loaded lipid nanoparticles for improved in vivo fluorescence imaging. Journal of Biomedical Optics, 2009. 14(5): p. 054005.**
16. **Dufort, S., et al., Optical small animal imaging in the drug discovery process. Biochim Biophys Acta, 2010. 1798(12): p. 2266-73.**
17. **Schwartz, A.L., The hepatic asialoglycoprotein receptor. CRC Crit Rev Biochem, 1984. 16(3): p. 207-33.**

18. Steirer, L.M., et al., The asialoglycoprotein receptor regulates levels of plasma glycoproteins terminating with sialic acid alpha2,6-galactose. J Biol Chem, 2009. 284(6): p. 3777-83.

19. Semple, S.C., et al., Immunogenicity and rapid blood clearance of liposomes containing polyethylene glycol-lipid conjugates and nucleic Acid. J Pharmacol Exp Ther, 2005. 312(3): p. 1020-6.

20. Judge, A., et al., Hypersensitivity and loss of disease site targeting caused by antibody responses to PEGylated liposomes. Mol Ther, 2006. 13(2): p. 328-37.

21. Tagami, T., et al., CpG motifs in pDNA-sequences increase anti-PEG IgM production induced by PEG-coated pDNA-lipoplexes. J Control Release, 2010. 142(2): p. 160-6.

22. Laverman, P., et al., Factors affecting the accelerated blood clearance of polyethylene glycol-liposomes upon repeated injection. J Pharmacol Exp Ther, 2001. 298(2): p. 607-12.

23. Ishida, T., et al., Spleen plays an important role in the induction of accelerated blood clearance of PEGylated liposomes. J Control Release, 2006. 115(3): p. 243-50.

24. Mosier, D.E. and B. Subbarao, Thymus-independent antigens: complexity of B-lymphocyte activation revealed. Immunology Today, 1982. 3(8): p. 217-222.

25. Peng, S.L., Signaling in B cells via Toll-like receptors. Curr Opin Immunol, 2005. 17(3): p. 230-6.

26. Jego, G., et al., Plasmacytoid dendritic cells induce plasma cell differentiation through type I interferon and interleukin 6. Immunity, 2003. 19(2): p. 225-34.

27. Poeck, H., et al., Plasmacytoid dendritic cells, antigen, and CpG-C license human B cells for plasma cell differentiation and immunoglobulin production in the absence of T-cell help. Blood, 2004. 103(8): p. 3058-64.

28. Aschenbrenner, K., et al., Selection of Foxp3+ regulatory T cells specific for self antigen expressed and presented by Aire+ medullary thymic epithelial cells. Nat Immunol, 2007. 8(4): p. 351-8.

29. Pecanha, L.M., et al., IL-10 inhibits T cell-independent but not T cell-dependent responses in vitro. J Immunol, 1993. 150(8 Pt 1): p. 3215-23.

30. Ishida, T., et al., Accelerated clearance of a second injection of PEGylated liposomes in mice. Int J Pharm, 2003. 255(1-2): p. 167-74.

31. Ishihara, T., et al., Evasion of the accelerated blood clearance phenomenon by coating of nanoparticles with various hydrophilic polymers. Biomacromolecules, 2010. 11(10): p. 2700-6.

32. Sainlos, M., et al., Kanamycin A-derived cationic lipids as vectors for gene transfection. Chembiochem, 2005. 6(6): p. 1023-33.

33. Vigneron, J.P., et al., Guanidinium-cholesterol cationic lipids: efficient vectors for the transfection of eukaryotic cells. Proc Natl Acad Sci U S A, 1996. 93(18): p. 9682-6.

34. Garcion, E., et al., A new generation of anticancer, drug-loaded, colloidal vectors reverses multidrug resistance in glioma and reduces tumor progression in rats. Mol Cancer Ther, 2006. 5(7): p. 1710-22.

35. Hem, A., A.J. Smith, and P. Solberg, Saphenous vein puncture for blood sampling of the mouse, rat, hamster, gerbil, guinea pig, ferret and mink. Lab Anim, 1998. 32(4): p. 364-8.

Efficacité des nanovecteurs

Publication No 3

G Model
IJP-11999; No. of Pages 8
ARTICLE IN PRESS
International Journal of Pharmaceutics xxx (2011) xxx–xxx
Contents lists available at ScienceDirect
International Journal of Pharmaceutics
journal homepage: www.elsevier.com/locate/ijpharm

In vivo imaging of DNA lipid nanocapsules after systemic administration in a melanoma mouse model

Stephanie David[a,b,c], Nathalie Carmoy[d], Pauline Resnier[a,b], Caroline Denis[d], Laurent Misery[e], Bruno Pitard[c], Jean-Pierre Benoit[a,b], Catherine Passirani[a,b,*], Tristan Montier[d,**]

[a] LUNAM Université – Ingénierie de la Vectorisation Particulaire, F-49933 Angers, France
[b] INSERM U646, F-49933 Angers, France
[c] INSERM UMR915 – Université de Nantes, 8 quai Moncousu, F-44000 Nantes, France
[d] INSERM U613 – Université de Brest, 5 avenue du Maréchal Foch, F-29200 Brest, France
[e] Laboratoire de Neurobiologie de la Peau, Service de Dermatologie, CHU de Brest, F-29609 Brest, France

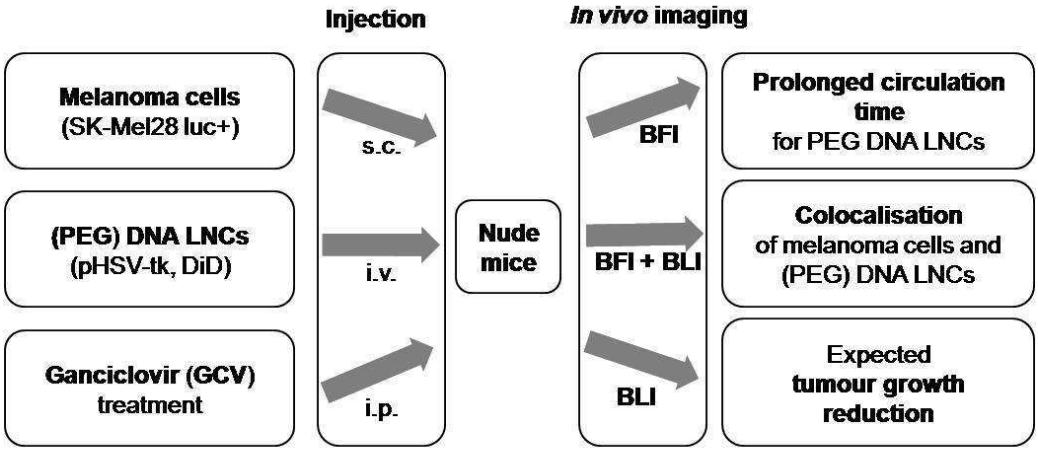

BFI: biofluorescence imaging, BLI: bioluminescence imaging

Une fois les vecteurs ADN caractérisés, les LNC ADN et les LNC ADN PEG, ont été injectés par voie systémique sur un modèle orthotopique de mélanome. L'imagerie par fluorescence *in vivo* a été utilisée pour suivre les nanovecteurs ADN et l'imagerie par bioluminescence *in vivo* pour suivre la croissance tumorale des cellules mélanome exprimant la luciférase. Après avoir étudié la biodistribution de nos vecteurs sur ce modèle, un premier traitement utilisant une approche par gène suicide a été effectué.

In vivo imaging of DNA lipid nanocapsules after systemic administration in a melanoma mouse model

Stephanie David[a,b,c], Nathalie Carmoy[d], Pauline Resnier[a,b], Caroline Denis[d], Laurent Misery[e], Bruno Pitard[c], Jean-Pierre Benoit[a,b], Catherine Passirani[a,b,*] and Tristan Montier[d,*]

[a]LUNAM Université – Ingénierie de la Vectorisation Particulaire, F-49933 Angers, France
[b]INSERM – U646, F-49933 Angers, France
[c]INSERM UMR915 – Université de Nantes, 8 quai Moncousu, F-44000 Nantes, France
[d]INSERM U613 – Université de Brest, 5 avenue du Maréchal Foch, F-29200 Brest, France
[e]Laboratoire de Neurobiologie de la Peau, Service de Dermatologie, CHU de Brest, F-29609 Brest, France

*Corresponding authors:
C. Passirani: Inserm U646, IBS-CHU, 4 rue Larrey, 49933 Angers Cedex 9, France, Tel.: +33 244 688534, Fax: +33 244 688546, E-mail: catherine.passirani@univ-angers.fr;
T. Montier: Inserm U613, Hopital Morvan – CHU Brest, 5 avenue du Maréchal Foch, 29200 Brest, France, Tel: +33 298 018080, Fax: +33 298 467910, E-mail: Tristan.Montier@univ-brest.fr

ABSTRACT

The biodistribution of intravenously injected DNA lipid nanocapsules (DNA LNCs), encapsulating pHSV-tk, was analysed by *in vivo* imaging on an orthotopic melanoma mouse model and by a subsequent treatment with ganciclovir (GCV), using the gene-directed enzyme prodrug therapy (GDEPT) approach. Luminescent melanoma cells, implanted subcutaneously in the right flank of the mice, allowed us to follow tumour growth and tumour localisation with *in vivo* bioluminescence imaging (BLI). In parallel, DNA LNCs or PEG DNA LNCs (DNA LNCs recovered with PEG_{2000}) encapsulating a fluorescent probe, DiD, allowed us to follow their biodistribution with *in vivo* biofluorescence imaging (BFI). The BF-images confirmed a prolonged circulation-time for PEG DNA LNCs as was previously observed on an ectotopic model of glioma; comparison with BL-images evidenced the colocalisation of PEG DNA LNCs and melanoma cells. After these promising results, treatment with PEG DNA LNCs and GCV on a few animals was performed and the treatment efficacy measured by BLI. The first results showed tumour growth reduction tendency and, once optimised, this therapy strategy could become a new option for melanoma treatment.

Key words:
skin cancer, DNA LNCs, real-time imaging, pHSV-tk, ganciclovir, intravenous injection

INTRODUCTION

In homeostatic conditions, melanocytes produce melanin and thus contribute to the pigmentation of skin and hair, protect the skin from damage by ultraviolet radiation, and prevent skin cancer (Lin and Fisher, 2007). But they are also precursors of melanoma, the most deadly form of skin cancer, following mutations of critical growth regulatory genes, the production of autocrine growth factors, and/or a loss of adhesion receptors (Gray-Schopfer *et al.*, 2007). The primary site of melanoma is the skin, but other pigmented tissues, such as the eyes or the intestine, can also be at the origin of melanoma. The tumour-specific, 10-year survival for melanoma is 75-85% when diagnosed as primary tumours without any evidence of metastasis, but melanoma metastasis dramatically reduces this percentage to 20 – 70%, this being dependent on the metastasis type (Garbe *et al.*, 2010). If diagnosed early, local surgical resection can cure melanoma in 80% of cases, contrary to metastatic melanoma which is largely refractory to existing therapies (Tawbi and Nimmagadda, 2009).

For these reasons, new therapies need to be developed, and gene therapy, which is an emerging field in cancer treatment, represents a promising option. Gene therapy can be used with the aim of treating the tumour (destructive approach) or with the aim of reverting its malignant phenotype (corrective approach). One tumour-treatment possibility is the 'gene suicide' approach, also called gene-directed enzyme prodrug therapy (GDEPT). This approach is based on the delivery of a gene which codes for an enzyme, and is able to convert a nontoxic prodrug into a cytotoxic metabolite (Gutzmer and Guerry, 1998, Portsmouth *et al.*, 2007). The first proof-of principle of GDEPT was made with the enzyme HSV-tk (Herpes simplex thymidine kinase) and the prodrug ganciclovir (GCV) (Moolten, 1986), which is still widely used in clinical and experimental applications in different tumour models (Portsmouth *et al.*, 2007). The efficacy of this concept was for example shown in 2004 in a randomised controlled study on patients with operable primary or recurrent malignant glioma and allowed a significant increase in patient survival time (71 weeks in the treated group compared to 39 weeks in the control group) (Immonen *et al.*, 2004). To transfer a gene effectively, different parameters, such as the administration route, the length of gene expression time, the animal model and/or the need of a delivery vehicle, have to be fixed. Local administration does not necessarily need a delivery vehicle and low doses are usually required; however, the targeted tissue has to be accessible to use this administration route. Systemic administration allows accessibility to the different tissues and has the advantage of rapid action and of allowing

repeated administration but it needs a delivery vehicle in order to be effective. Moreover, in clinical applications, many diseases require intravenous (i.v.) or intraperitoneal (i.p.) injection treatment regimens. Delivery vehicles for systemic administration can be classified into two main groups: viral and non-viral delivery systems. Although viral vectors are very effective in terms of gene delivery and expression, the major drawbacks are their potential risk associated with replication-competent viruses, immunogenicity and high cost (Chowdhury, 2009, Collins *et al.*, 2008, Jin and Ye, 2007). Non-viral vectors do not show these drawbacks; they present the advantages of being able to carry large inserts and to be easily formulated (Jin and Ye, 2007, Kreiss *et al.*, 1999, Morille *et al.*, 2008); they can also be adapted to passive or active tumour targeting (Huynh *et al.*, 2010, Kang *et al.*, 2010, Wagner *et al.*, 2004).

In recent literature, nanocarriers (lipid or polymer) used in various treatment strategies, carrying different agents such as plasmids, siRNA, ODN or pharmacological inhibitors, and applied by several different administration routes (intravenous, intratumoural, topical…), have been shown to increase melanoma cell delivery and treatment efficacy (De Campos *et al.*, 2010, Stone *et al.*, 2009, Weiss and Aplin, 2010, Zheng *et al.*, 2009).

Lipid nanocapsules (LNCs) developed in our laboratory (Heurtault *et al.*, 2002) have already been shown to be efficient for *in vitro* and *in vivo* transfection (Morille, Montier *et al.*, 2009), (Morille *et al.*, 2010). The formulation process of LNCs requires neither organic solvents nor high energy, and is based on the phase-inversion temperature (PIT) method. It consists of using non-ionic polyethoxylated surfactants to allow the phase inversion of an emulsion (Shinoda K. and Saito, 1968, Shinoda Kozo and Saito, 1969) and the application of a temperature-cycle treatment around the PIT to obtain small sizes with a low polydispersity index (PDI) (Anton *et al.*, 2007). A sudden cooling and dilution of the micro-emulsion at the PIT leads to the obtention of LNCs, which consist of a lipid, liquid core of triglycerides, and a rigid shell of lecithin and short chains of poly(ethylene glycol) (PEG_{660}) (Heurtault *et al.*, 2002). This formulation process allows fragile molecules such as nucleic acids to be encapsulated. To encapsulate hydrophilic DNA in the lipid core, DNA was complexed with cationic lipids prior to encapsulation (Vonarbourg *et al.*, 2009). As already observed (Morille, Montier *et al.*, 2009, Vonarbourg *et al.*, 2009), the encapsulation of these lipoplexes should provide an efficient loss of toxicity allowing higher doses to be injected *in vivo*. Furthermore, in order to enhance stealth properties of DNA LNCs, PEG was used (see the review of Huynh et al. (Huynh *et al.*, 2010) describing the advantages and drawbacks of this polymer). The coating of the DNA-LNC surface with longer PEG chains (PEG_{2000}) improved nanocapsule *in*

vivo circulation time on a mouse model of subcutaneously-injected glioma cells (Morille, Montier *et al.*, 2009)

In this study, non-viral LNCs were used to deliver pHSV-tk in melanoma tumour cells after IV injection into mice. Considering the melanoma mice model, some *luc+* human melanoma cells were engrafted on nude mice. Thus, the localisation and the growth of the tumours could be followed by luminescence. Once the tumours were established, the biodistribution and localisation of intravenously-injected DNA LNCs in this orthotopic melanoma mouse model were traced via *in vivo* fluorescence imaging. Bioluminescence and fluorescence images were then compared in order to localise DNA LNCs versus PEG DNA LNCs, and a treatment with ganciclovir (GCV) was carried out in order to evaluate the efficiency of the gene suicide approach.

MATERIALS AND METHODS

Preparation of nanocarriers

Liposomes and lipoplexes

Solutions of DOTAP (1.2-DiOleoyl-3-TrimethylAmmonium-Propane) and DOPE (1.2-DiOleyl-sn-glycero-3-PhosphoEthanolamine) in chloroform (20mg/ml) (Avanti Polar Lipids, Inc, Alabaster, USA) were first dried by an evaporation process under vacuum and the formed lipid film was then hydrated with deionized water over night at 4 °C. The next day, liposomes were sonicated for 20 minutes and lipoplexes were prepared. For their preparation, DOTAP/DOPE (1/1, M/M) liposomes were mixed with 660 µg of HSV-tk encoding plasmid (pORF-TK-ΔCpG ; InvivoGen ; 4.35kb) at a charge ratio of 5 (+/-) in 150 mM NaCl.

DNA-loaded lipid nanocapsules (DNA LNCs)

LNCs were composed of lipophilic Labrafac® WL 1349 (Gatefossé S.A., Saint-Priest, France), a mixture of caprylic and capric acid triglycerides, oleic Plurol® (Polyglyceryl-6 dioleate) which was kindly provided by Gatefossé S.A. (Saint-Priest, France), NaCl (Prolabo, Fontenay-sous-Bois, France), water (obtained from a Milli-Q-plus® system, Millipore, Paris, France) and Solutol® HS-15 (30 % of free polyethylene glycol 660 and 70 % of polyethylene glycol 660 hydroxystearate (HS-PEG)) (BASF, Ludwigshafen, Germany). The formulation process is based on phase-inversions of a microemulsion described by Heurtault *et al.* (Heurtault *et al.*, 2002). Briefly, all the components, in a well defined ratio (3.9 % of oleic Plurol® (w/w), 5.9 % of Solutol® (w/w), 9.9 % of Labrafac® (w/w), 78.9 % of water (w/w)

and 1.4 % of NaCl), were mixed together under magnetic stirring and temperature cycles around the phase-inversion-temperature (PIT) were performed. In the last step, cold water was added (in a ratio 1:1.96) to dilute the emulsion and to form the LNCs. To formulate fluorescent DNA LNCs, lipoplexes were added instead of the formulation water (Vonarbourg *et al.*, 2009), and a mixture of 1,1'-dioctadecyl-3,3,3',3'-tetramethylindodicarbocyanine perchlorate (DiD, em. = 644 nm; exc. = 665 nm) (Invitrogen, Cergy-Pontoise, France) and Labrafac® replaced Labrafac® alone. To obtain the Labrafac® - DiD mixture, a solution of DiD in acetone at 0.6% (w/w) was prepared, incorporated in Labrafac® in a ratio of 1:10 (w/w) and acetone was evaporated before use (Garcion *et al.*, 2006).

Preparation of coated nanocapsules by post-insertion

Coated nanocapsules were prepared as previously described (Morille, Montier *et al.*, 2009). Briefly, fluorescent DNA LNCs were purified after their formulation, using PD10 Sephadex columns (Amersham Biosciences Europe, Orsay, France). To compensate for the dilution of our formulation and the desalting effect caused by this purification step, an ultrafiltration step was performed with MilliporeAmicon® Ultra-15 centrifugal filter devices (Millipore, St Quentin-Yvelines, France) and the salt- and LNC-concentration were readjusted afterwards to obtain a physiologic concentration of NaCl (150mM) and the initial concentration of LNCs (152 g/l). These purified fluorescent DNA LNCs were then mixed with 1,2-DiStearoyl-sn-glycero-3-PhosphoEthanolamine-N-[methoxy(polyethyleneglycol)-2000] (DSPE-mPEG$_{2000}$) (Mean Molecular Weight (MMW) = 2,805 g/mol) (Avanti Polar Lipids, Inc, Alabaster, USA) to obtain a final polymer concentration of 10mM. The mixture was incubated for 4 h at 30 °C and vortexed every 15 minutes.

Characterisation of nanocarriers

Physicochemical characteristics of DNA LNCs

Coated and non-coated fluorescent DNA LNCs were characterised using a Malvern Zetasizer® (Nano Series ZS, Malvern Instruments S.A., Worcestershire, UK). The formulation was diluted in a 1:100 ratio with deionised water and size and zeta potential measurements were performed with the same sample at 25 °C. All measurements were performed in triplicate and with similar conductivity values.

Agarose gel electrophoresis

The encapsulation and integrity of the DNA molecules after the process of nanocapsule formulation and post-insertion, were evaluated by agarose gel electrophoresis as described previously (Vonarbourg *et al.*, 2009). Briefly, a treatment with Triton® X100 (Sigma, Saint-Quentin Fallavier, France) was performed to destroy the LNCs. A volume of LNCs equivalent to 0.2 µg of DNA before and after this treatment was mixed with gel-loading solution (Sigma, Saint-Quentin Fallavier, France) and deposited in each well of 1% agarose gel containing ethidium bromide (Sigma, Saint-Quentin Fallavier, France). The migration time was about 30 min, at 100 V.

In vivo fluorescence and bioluminescence imaging

Orthotopic mouse model of melanoma

Six- to nine-week-old female, nude NMRI mice (Elevage Janvier, France) were housed and maintained at the University animal facility; they were processed in accordance with the Laboratory Animal Care Guidelines (NIH Publication 85-23, revised 1985) and with the agreement of the regional veterinary services (authorisation FR; 29-024).

Tumour bearing mice were prepared by injecting subcutaneously a suspension of $3x10^6$ SK-Mel28 *Luc*+ melanoma cells (n°HTB-72-ATCC) in 100 µl of PBS 1X into the right flank of athymic nude NMRI mice (6-week-old females, 20-24 g). The SK-Mel28 cell line had previously been transfected with a plasmid encoding the luciferase, and bearing the resistance gene to the neomycine (pTG11033; Transgene; 9.6kb). Under neomycine pressure, one clone was selected due to its high and stable expression of luciferase and its proliferative capacities. Thus, the stable luminescence of these cells allowed the localisation and growth of the tumours to be measured. Concerning immunohistological analyses, tumours were PS100+, Ag HMB45+ and Ag melan-A+. All these criteria indicated the malignity and the melanomic nature of the tumours.

Three weeks after tumour implantation, 150µl of DNA LNCs or PEG DNA LNCs were administered by intravenous injection into the tail vein of the mice.

In vivo bioluminescence imaging

In order to follow the tumour cell growth of the luciferase-expressing melanoma cells, non-invasive bioluminescence imaging (BLI) was performed after 19 days, immediately before injection of the nanoparticles, and 24 h and 48 h post-injection.

Mice to be imaged first received an intraperitoneal injection of highly-purified synthetic D-luciferin (4 mg in 200 µL of water; Interchim, France). Five minutes later, the animals were anaesthetised with a 4% air-isofluorane blend and maintained with a 2% air-isofluran mixture through a nose cone. Ten minutes after luciferin injection, luminescence images were acquired using an *in vivo* imaging system (NightOWL II; Berthold Technologies, Germany) and associated software (WinLight 32; Berthold, Germany) with a binning of 8*8 and exposure time of 4 minutes. Luminescence images were then superimposed onto still images of each mouse. The signals were quantified within the regions of interest in units of photons per second.

In vivo biofluorescence imaging

Non-invasive fluorescent imaging (BFI) was performed 1 h, 3 h, 5 h, 24 h and 48 h post-injection, using the BFI system of the NightOWL II (Berthold Technologies, Germany) equipped with cooled, slow-scan CCD camera and driven with the WinLight 32 software (Berthold Technology , Germany). Considering the fluorescent characteristics of the DiD fluorescent tag used to localise the nanoparticles, the 590 nm excitation and 655 nm emission filters were selected. In parallel, the light beam was kept constant for each fluorescent measurement, which was ideal with the ringlight, epi-illumination. As the ringlight was always set at the same height, the excitation energy on the sample would always be the same.
Each mouse was anaesthetised with a 4 % air-isofluran blend. Once placed in the acquisition chamber, the anaesthesia of the mice was maintained with a 2 % air-isofluran mixture throughout the experiment as described above. With the BFI system, the fluorescent acquisition time was 3 seconds and the fluorescent signal was then overlaid on a picture of each mouse.

Treatment with ganciclovir (GCV)

To evaluate the treatment efficacy, nude NMRI mice (n=10) bearing subcutaneous melanomas were prepared as described above. Five weeks after tumour implantation, 150µl PEG DNA LNCs were administrated by intravenous injection and the mice were treated twice a day with 150µl ganciclovir [Concentration 50 mg/ml ; Invivogen] for 4 days. Bioluminescence imaging was performed once a day to follow and quantify tumour growth as described above. The control group (n=5) was prepared in the same way for tumour establishment, but received no treatment.

RESULTS AND DISCUSSION

Preparation and characterization of DNA LNCs

DNA LNCs encapsulating the fluorescent probe DiD and the plasmid HSV-tk were prepared, purified and then half of the formulation was covered with DSPE-PEG_{2000} chains by post-insertion. Afterwards, agarose gel electrophoresis experiments were performed and demonstrated the encapsulation of the HSV-tk plasmid (Table 1). The first lane shows LNCs without treatment. As very low fluorescence is visible, we consider that the major part of the plasmid is encapsulated. The second lane shows LNCs with a treatment of Triton to destabilise the LNCs and hence liberate the encapsulated plasmid. Here, the fluorescence indicates that the plasmid is intact since only one distinct line is visible and corresponds to that of the plasmid alone (data not shown). The comparison of both electrophoresis gels shows no influence of the post-insertion process on the DNA encapsulation, since the plasmid is well encapsulated before and after post-insertion. These results also evidence that our original encapsulation method of lipoplexes in LNCs is valid for different kinds of plasmids. Indeed, this HSV-tk coding plasmid has been encapsulated for the first time in LNCs and shows similar characteristics to DNA LNCs encapsulating a luciferase-coding plasmid (Vonarbourg *et al.*, 2009).

Both types of LNCs were then characterised by size and zeta potential measurements (Table 1). DNA LNCs are small particles with a size of 90 nm, and a low polydispersity index of 0.18. This result of PDI, inferior to 0.3 indicates a narrow size distribution of the system. The plasmid HSV-tk is complexed with cationic lipids prior to encapsulation which results in positively-charged DNA LNCs with a zeta potential of + 31 mV. After post-insertion with DSPE-PEG_{2000}, size measurements of PEG DNA LNCs showed a slight increase in size of about 6 nm. An almost doubling of the polydispersity index (0.34) was observed, proving the real insertion of some long chains of PEG at the surface of the nanocapsules. In contrast, the zeta potential diminished by 37 mV from positive to near-neutral particles, as previously observed (Morille, Montier *et al.*, 2009). These results can be explained by the fact that DSPE-PEG_{2000} chains carry negative, dipolar charges (Vonarbourg *et al.*, 2005) and are thereby able to mask the positive surface charges due to the encapsulation of the positively-charged lipoplexes. The positive surface charge of DNA-LNCs before post-insertion could help to interact with negatively-charged cell membranes and lead to better internalisation and transfection effects *in vitro* as shown, for example, on Hela, H1299 or HEK293β3 cells

(Morille, Passirani *et al.*, 2009, Morille *et al.*, 2010). However, positive surface charge can also interact with negatively-charged proteins in the blood and dramatically reduce the circulation time in blood in comparison to PEG DNA LNCs (Morille, Montier *et al.*, 2009). In conclusion, the coating by longer PEG chains yielded small pegylated neutral particles and thus optimised the characteristics of the PEG DNA LNCs required for intravenous administration (Viola *et al.*, 2010, Vonarbourg *et al.*, 2006).

HSV-tk DiD LNCs	DNA LNCs		PEG DNA LNCs	
Size	90 nm	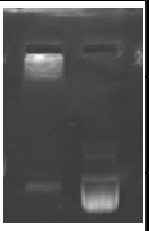	96 nm	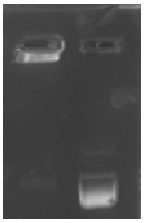
Polydispersity index	0.18		0.34	
Zeta potential	31 mV		-6 mV	

Table 1: Size and zeta potential of DNA LNCs and PEG DNA LNCs encapsulating the plasmid HSV-tk and the fluorescent probe DiD. Agarose gel electrophoresis shows the fluorescence of DNA LNCs or PEG DNA LNCs before (first lane) and after (second lane) destruction with Triton.

The melanoma mouse model

Luciferase-expressing melanoma cells were injected subcutaneously into the right flank of nude mice and, as the tumour growth was quite heterogeneous, the groups were drawn by chance. After tumour establishment, the tumours were dissected and histological analysis was carried out on fresh tumours in the anatomopathological service of the academical hospital (CHU) of Brest. There, the tumours were soaked in buffered formalin solution before their inclusion in paraffin. For standard examination, 3 µm slices were prepared and coloured with hematoxyline-eosin-safran (HES). For immunohistochemical analysis, 5 µm slices were prepared and deposited on glass slides. After rehydration of the probes, they were tagged with anti-PS100 antibodies (a marker of various cell types: melanocytes, nerve cells, sweat cells, etc), anti-HMB45 antibodies, anti-Melan-A antibodies (marker of melanocytes) and Ki67 (cell proliferation marker). These analyses were carried out on several tumours.

In standard histology, a tumoural infiltration, constituted of cells presenting various atypical characteristics such as nuclei with voluminous nucleoli, and infiltrating the muscles in certain areas, was observed (see Fig.1). In immunohistochemical analysis, positive labelling, to a

greater or lesser extent, of the protein S100, but also of the antigen HMB45 and Melan-A, was observed (see Fig. 1). All these criteria were compatible with the diagnosis of malignant tumours of melanocytic origin.

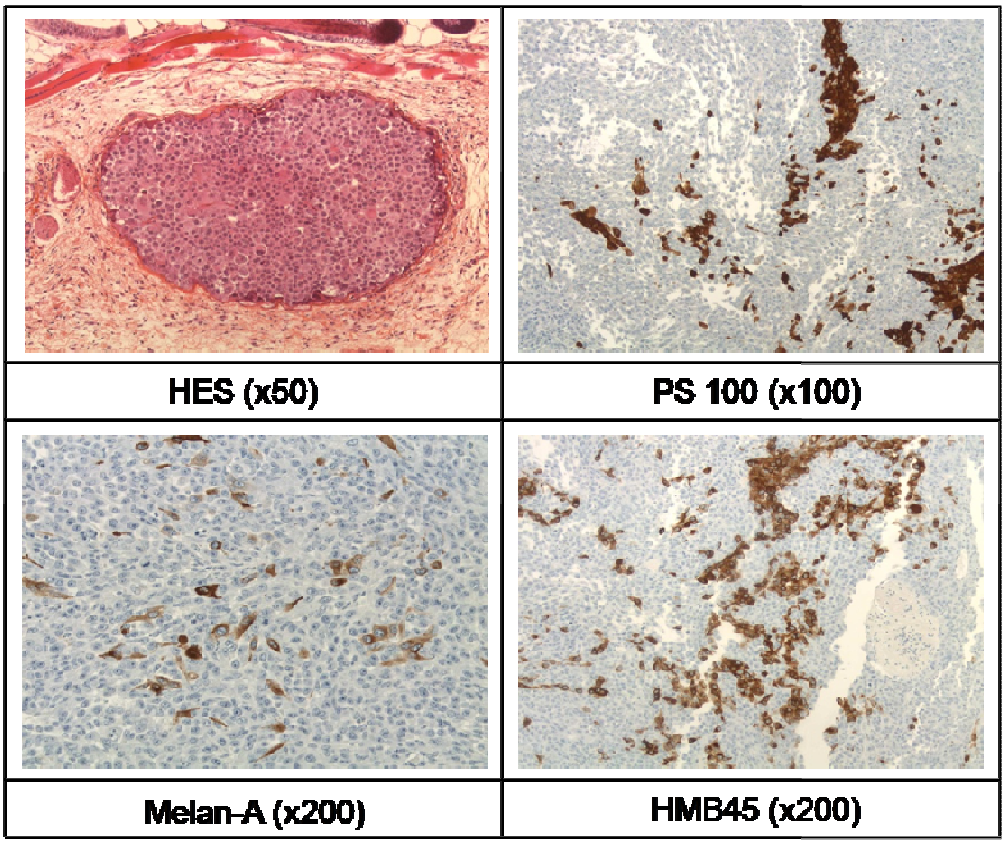

Fig. 1: Immunohistochemical analysis of melanoma. Standard treatment with hematoxyline-eosin-safran (HES) allows differentiating the tumour cells from other cells. Treatment with PS100 antibody (PS100), Melan-A antibody or HMB45 antibody, evidences the malignity of the melanoma tumours.

Following the biodistribution of DNA LNCs by in vivo fluorescence imaging

The formulated DNA LNCs and PEG DNA LNCs were injected three weeks after cell injection by intravenous injection in the tail vein of the mice. Biofluorescence imaging (BFI) was performed at different times after LNC administration (1 h, 3 h, 5 h, 24 h, and 48 h) to follow the tissue distribution of LNCs thanks to the encapsulated NIR fluorescent probe DiD (see Figure 2). BFI is a fast, simple and low-cost method, and allows the number of sacrificed animals to be reduced, since it can be carried out on living animals at different times, but it is not an absolutely quantitative method as the absorption and diffusion of the visible light depends on the tissues (Goutayer *et al.*, 2010). The NIR dye DiD has usually been used to

follow the biodistribution of labelled molecules or nanocapsules, since the dye is not fluorescent in aqueous media, and the fluorescent signal cannot come from free DiD (Texier *et al.*, 2009). Images were taken from lateral and decubitus dorsal views to obtain a general view of the biodistribution, and to better identify the organs and subjacent tissues which are more or less visible by BFI, depending on the position.

Images of mice which received DNA LNCs showed an intense fluorescence signal in the right flank, where the tumour cells had been grafted. A lower fluorescent signal was observed in the liver and uterus/ovaries, and persisted for only a few hours. Indeed, it was hardly visible 5 h after LNC injection, whereas an intense fluorescent signal persisted in the right flank and, was still visible 48 h after LNC administration. Images of mice that received PEG DNA LNCs revealed an intense fluorescent signal in the liver, the right flank, and the uterus/ovaries which was still visible 48 h after LNC injection. This is in concordance with the fact, that these tissues are highly vascular, have a high degree of microcirculation, and are sufficiently present at the body surface. However, contrary to the fluorescent signal of DNA LNCs, which presented a maximum at 1h after LNC administration and diminished with time, the fluorescent signal of PEG DNA LNCs was relatively low at 1h after LNC administration and then increased with a maximum at 3h and 5h after LNC administration. The fluorescent signal seems to be more important for PEG DNA LNCs than for DNA LNCs. In conclusion, the circulation time of PEG DNA LNCs is prolonged compared to that of DNA LNCs since intense fluorescence signals are obtained up to 48 h post-PEG DNA-LNC-injection. Even if the tumour was different (glioma versus melanoma), a similar phenomenon has already been observed as a direct consequence of pegylation (Maeda *et al.*, 2000, Morille, Montier *et al.*, 2009).

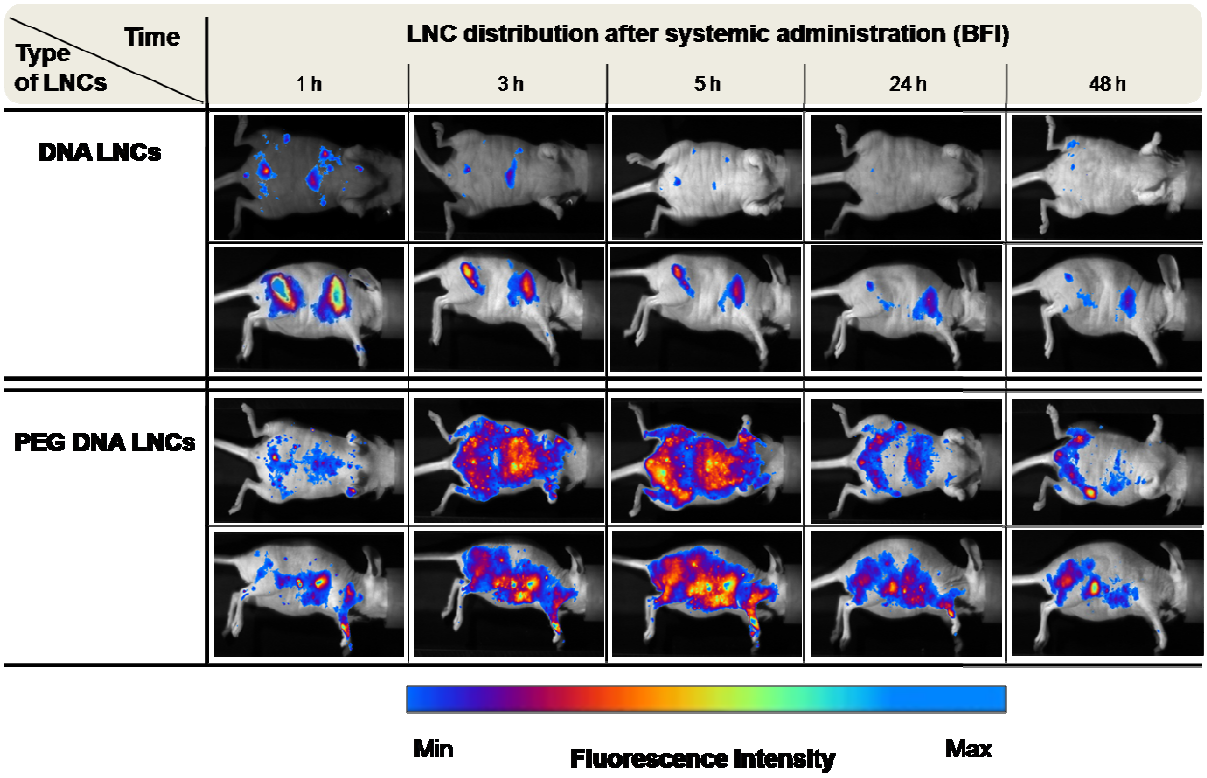

Fig. 2 Biofluorescence images (BFI) at different times after injection of DNA LNCs and PEG DNA LNCs in a mouse model of melanoma following the biodistribution of the injected vectors. Images represent one mouse after injection of DNA LNCs and PEG DNA LNCs (first and second two lines of images respectively) (lateral and decubitus dorsal views of the mice) at 1 h, 3 h, 5 h, 24 h and 48 h.

Following the tumour cells by in vivo bioluminescence imaging and comparison of BLI and BFI images

In parallel, tumour establishment and growth were followed by *in vivo* bioluminescence imaging (BLI) and BL- and BF-images were compared as shown in Figure 3, to look more closely at the localisation of the LNCs versus the luciferase-expressing melanoma cells. BLI is based on the production of light from living luciferase cells due to a chemical reaction between the substrate luciferin, injected intraperitoneally before imaging, and ATP. This light is then captured externally by a cooled, charge-coupled device (CDD) camera (Hardy *et al.*, 2001). The advantages of BLI are, as BFI, the sensitivity of the technology, the cost-effective instrumentation, the simple procedure and the significant reduction in the number of sacrificed animals (Roda *et al.*, 2009). The location and growth of luciferase expressing melanoma cells can be monitored in real-time and, in contrast to BFI, quantified as photons per second. BL-images clearly show the location of luciferase-expressing melanoma cells in the right flank of the mice and quantification of the luciferase expression showed a mean

luciferase expression of $3,3x10^6 \pm 4,0x10^6$ photons/second before LNC injection for the group of mice that received DNA LNCs (n=4) and $5,1x10^6 \pm 8,2x10^6$ photons/second for the mice receiving the PEG DNA LNCs (n=4).

As seen in the previous section, PEG DNA LNCs had a prolonged circulation time compared to DNA LNCs, and provoked an intense fluorescent signal in the whole body at 5 h, and a more specific localisation in the tumours at 24 h. A comparison of the BF-images and BL-images showed a clear colocalisation of luciferase-expressing melanoma cells and fluorescent LNCs at 24 h after LNC administration. These observations confirm that DNA LNCs and PEG DNA LNCs attain the tumour site after intravenous administration via passive targeting, probably due to the enhanced permeability and retention (EPR) effect, which is known to be due to the combination of the leaky tumour vasculature and the low lymphatic drainage observed in the tumours in comparison to the healthy tissues (Maeda *et al.*, 2000, Maeda, 2001).

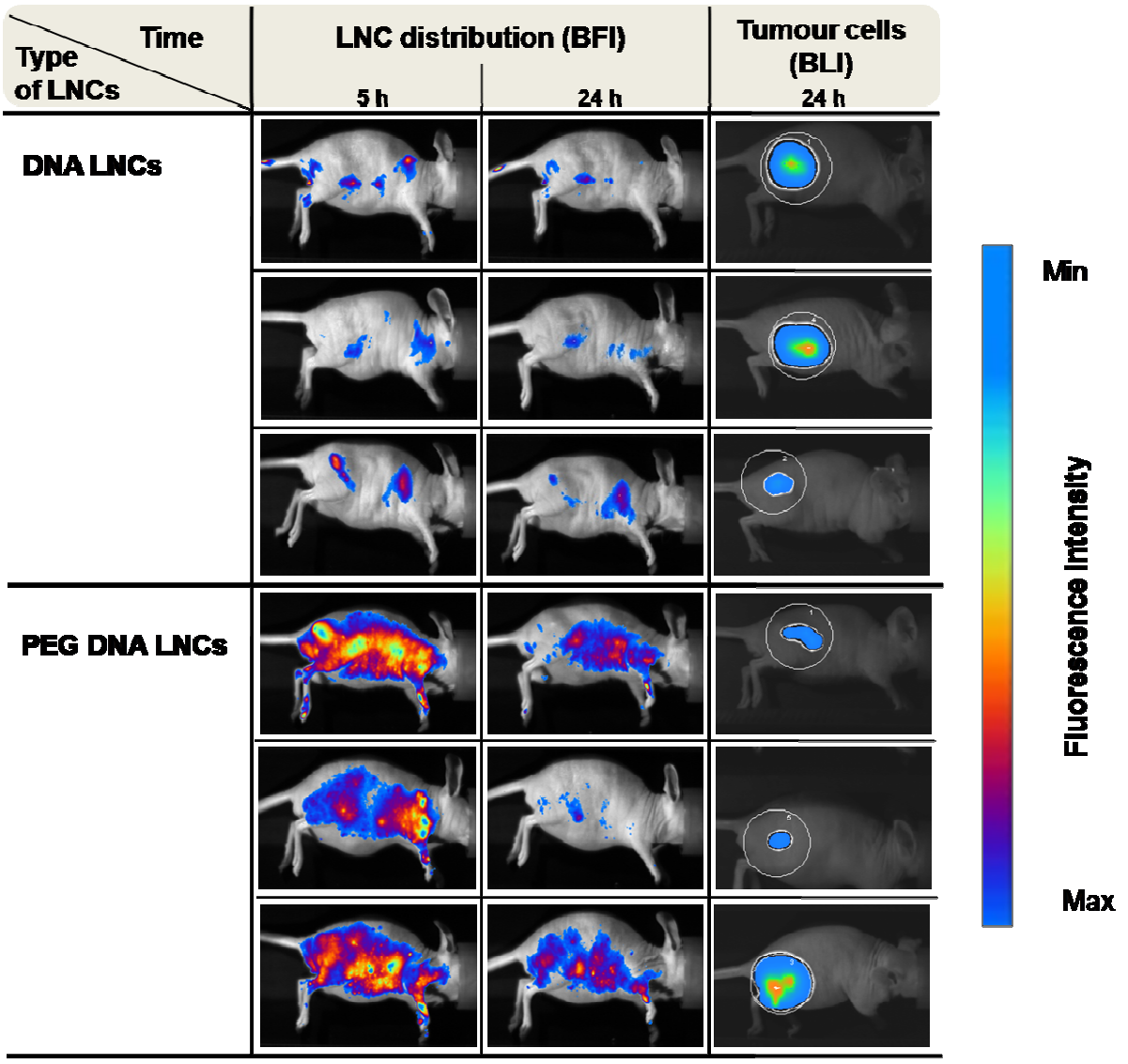

Fig. 3: BF-images at 5h and 24h after LNC injection and BL-images at 24h of 3 mice injected with DNA LNCs and PEG DNA LNCs by intravenous injection. BF-images show LNC distribution and BL-images melanoma cell localisation.

Intravenous administration of PEG DNA LNCs and subsequent treatment with ganciclovir

After these promising results of colocalisation of PEG DNA LNCs and luciferase-expressing melanoma cells, the following step of the experiment was based on ganciclovir (GCV) treatment in order to evaluate if the tumour cells were transfected with the PEG DNA LNCs and if it could influence the tumour size. The gene-suicide approach, also called gene-directed enzyme prodrug therapy (GDEPT), is based on the introduction of a gene, in our case, the gene for the herpes simplex virus encoding thymidine kinase (HSV-tk) *via* the PEG DNA

LNCs, which will sensitise the tumour cells to the subsequently-delivered GCV. To do this, HSV-tk converts the inert prodrug GCV into the active triphosphorylated GCV (GCVTP) which will act as a chain terminator after incorporation into the DNA of dividing cells (Altaner, 2008, Gutzmer and Guerry, 1998, Portsmouth *et al.*, 2007).

Nude NMRI mice, bearing subcutaneous melanoma cells, received one intravenous injection of PEG DNA LNCs and a GCV treatment twice a day for 4 days. This time period was chosen because the transfected tumour cells will inevitably die with the GCV treatment and therefore limit the time period of the therapeutic effect. Tumour establishment was followed by *in vivo* bioluminescence imaging as in the previous experiments and the PEG DNA LNCs followed via *in vivo* fluorescent imaging.

To see the treatment efficacy, *in vivo* bioluminescence imaging of luciferase-expressing melanoma cells was performed once a day during the treatment period, and 2 days after; the evolution of the luciferase-expression was quantified as photons/second (Figure 4). On Day 1, the luciferase-expression diminished slightly for all the mice. Afterwards, until Day 3, the luciferase-expression increased with time. In the group of mice treated with LNCs and GCV, the increase seems to be lower than in the control group. At Day 4, a significant difference appears between the two groups with a decrease of luciferase expression for the treated group. This difference seems to accentuate two days after the treatment period. However, considering the standard deviations certainly due to the heterogeneity of the tumour growth, another set of experiments including a large number of animals with similar tumour volumes needs to be carried out to confirm or not this therapeutic effect. Moreover, another group of control mice receiving only PEG DNA LNCs without a GCV treatment could be of interest, to evaluate the potential of a possible anti-tumour effect due to LNCs. A group receiving only GCV was realized but was not different from the control group (data not shown) confirming that GCV is only a prodrug and necessitates the presence of HSV-tk to be active.

In the literature, the gene-suicide therapy is often associated with a bystander effect. This bystander effect can either be direct on nearby cells or distant, by the induction of an immune response by natural killer cells or T-cells (Altaner, 2008). Although this bystander effect is a possibility, it is conditioned by the viability of the transfected cells. If these cells are killed too early, the bystander effect based on the transcytosis of GVC-monophosphate by passive diffusion or through gap junctions will be limited. Therefore, an important factor to take into account could be the time between the LNC administration and the GCV treatment. Here, the GCV treatment was given 8h after the LNC injection, but a GCV administration one or two

days after the LNC treatment did not show any treatment efficacy (data not shown). Another possibility to augment the treatment efficacy could be the repeated administration of PEG DNA LNCs after the gene-suicide effect.

Finally, as the passive tumour targeting by PEG LNCs was clearly demonstrated here, we plan now to test these formulations on a metastatic *luc* + tumour mouse, increasing the number of experimental and control animals. In a metastatic melanoma mouse model, a systemic administration of the treatment would be highly required and, in such conditions, PEG LNCs could represent a new promising approach.

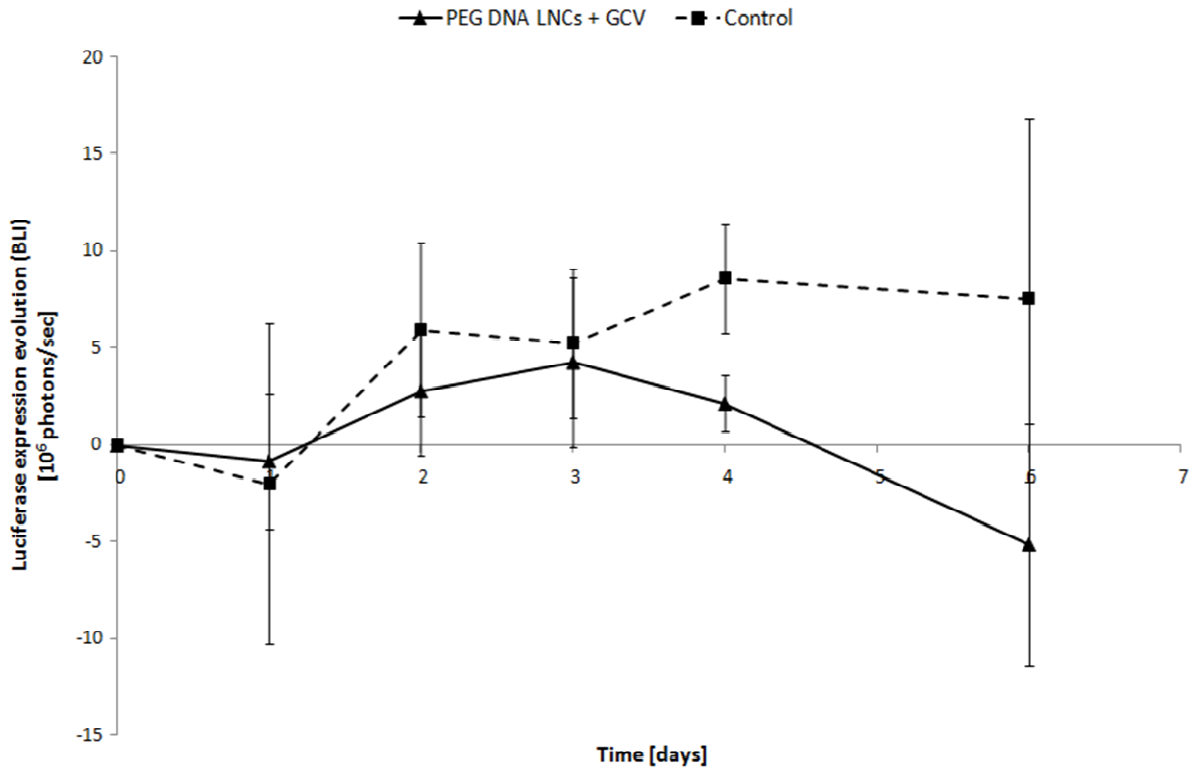

Fig. 4: Treatment efficacy of PEG DNA LNCs, encapsulating a plasmid coding for HSV-tk, in combination with GCV of melanoma bearing mice in comparison to melanoma bearing mice without LNC administration and treatment (control, n = 5). Mice were treated with one injection of PEG DNA LNCs at day 0 and afterwards twice a day for 4 days with GCV (n = 10) by intraperitoneal injection.

CONCLUSION

LNCs are promising non-viral gene delivery systems because they are well characterised, easy to formulate, adaptive to the targeted tissue and have previously proved to be efficient in term of transfection. Here, our first aim was to study the capacity of LNCs to target specifically a

melanoma tumour engrafted on a mouse model, especially when PEG motifs were incorporated into the formulation, after IV injection in order to benefit of the perturbations of the stromal micro-vascularity and the EPR effect. As a second goal, we were interested to know if tumour cells were well transfected and could be led to death whereas the PEG DNA LNCs were colocalised into the tumours.

Using *in vivo* Bioluminescence and Biofluorescence imaging systems, the images showed on the one hand, prolonged circulation time of DNA LNCs coated with long PEG chains after i.v. injection compared to non-coated DNA LNCs, and on the other hand, for the first time, colocalisation of nanocapsules and luciferase-expressing melanoma cells in mice for both types of DNA LNCs tested. These results confirmed the previous results obtained on an ectopic glioma mouse model but showed also their validity on an orthotopic melanoma mouse model.

Then, the treatment during 4 days with ganciclovir following the transfection of pHSV-tk carried out by PEG DNA LNCs showed, from day 3, an interesting decrease of photons emitted by the *luc+* tumours, reflecting probably the transfection of some cells and the action of GCV. These results are encouraging, even if further experiments have to be carried out to confirm this conclusion.

ACKNOWLEDGEMENTS

The authors would like to thank Marie Morille (Inserm U646, Angers, France) for her help and experience in the (PEG) DNA LNC formulation and the experimental setting as well as the platform SynNanoVect. This work is supported by grants from Région Pays de la Loire (CIMATH), Biogenouest, Région Bretagne, Ligue contre le cancer 29 and Canceropole Grand Ouest.

REFERENCES

Altaner, C., 2008, Prodrug cancer gene therapy, Cancer Lett, 270, (2), 191-201.

Anton, N., Gayet, P., Benoit, J. P. and Saulnier, P., 2007, Nano-emulsions and nanocapsules by the PIT method: an investigation on the role of the temperature cycling on the emulsion phase inversion, Int J Pharm, 344, (1-2), 44-52.

Chowdhury, E. H., 2009, Nuclear targeting of viral and non-viral DNA, Expert Opin Drug Deliv, 6, (7), 697-703.

Collins, S. A., Guinn, B. A., Harrison, P. T., Scallan, M. F., O'Sullivan, G. C. and Tangney, M., 2008, Viral vectors in cancer immunotherapy: which vector for which strategy?, Curr Gene Ther, 8, (2), 66-78.

de Campos, V. E., Teixeira, C. A., da Veiga, V. F., Ricci, E., Jr. and Holandino, C., 2010, L-tyrosine-loaded nanoparticles increase the antitumoral activity of direct electric current in a metastatic melanoma cell model, Int J Nanomedicine, 5, 961-971.

Garbe, C., Peris, K., Hauschild, A., Saiag, P., Middleton, M., Spatz, A., Grob, J. J., Malvehy, J., Newton-Bishop, J., Stratigos, A., Pehamberger, H. and Eggermont, A., 2010, Diagnosis and treatment of melanoma: European consensus-based interdisciplinary guideline, Eur J Cancer, 46, (2), 270-283.

Garcion, E., Lamprecht, A., Heurtault, B., Paillard, A., Aubert-Pouessel, A., Denizot, B., Menei, P. and Benoit, J. P., 2006, A new generation of anticancer, drug-loaded, colloidal vectors reverses multidrug resistance in glioma and reduces tumor progression in rats, Mol Cancer Ther, 5, (7), 1710-1722.

Goutayer, M., Dufort, S., Josserand, V., Royere, A., Heinrich, E., Vinet, F., Bibette, J., Coll, J. L. and Texier, I., 2010, Tumor targeting of functionalized lipid nanoparticles: assessment by in vivo fluorescence imaging, Eur J Pharm Biopharm, 75, (2), 137-147.

Gray-Schopfer, V., Wellbrock, C. and Marais, R., 2007, Melanoma biology and new targeted therapy, Nature, 445, (7130), 851-857.

Gutzmer, R. and Guerry, D. t., 1998, Gene therapy for melanoma in humans, Hematol Oncol Clin North Am, 12, (3), 519-538.

Hardy, J., Edinger, M., Bachmann, M. H., Negrin, R. S., Fathman, C. G. and Contag, C. H., 2001, Bioluminescence imaging of lymphocyte trafficking in vivo, Exp Hematol, 29, (12), 1353-1360.

Heurtault, B., Saulnier, P., Pech, B., Proust, J. E. and Benoit, J. P., 2002, A novel phase inversion-based process for the preparation of lipid nanocarriers, Pharm Res, 19, (6), 875-880.

Huynh, N. T., Roger, E., Lautram, N., Benoit, J. P. and Passirani, C., 2010, The rise and rise of stealth nanocarriers for cancer therapy: passive versus active targeting, Nanomedicine (Lond), 5, (9), 1415-1433.

Immonen, A., Vapalahti, M., Tyynela, K., Hurskainen, H., Sandmair, A., Vanninen, R., Langford, G., Murray, N. and Yla-Herttuala, S., 2004, AdvHSV-tk gene therapy with intravenous

ganciclovir improves survival in human malignant glioma: a randomised, controlled study, Mol Ther, 10, (5), 967-972.

Jin, S. and Ye, K., 2007, Nanoparticle-mediated drug delivery and gene therapy, Biotechnol Prog, 23, (1), 32-41.

Kang, J. H., Toita, R. and Katayama, Y., 2010, Bio and nanotechnological strategies for tumor-targeted gene therapy, Biotechnol Adv, 28, (6), 757-763.

Kreiss, P., Cameron, B., Rangara, R., Mailhe, P., Aguerre-Charriol, O., Airiau, M., Scherman, D., Crouzet, J. and Pitard, B., 1999, Plasmid DNA size does not affect the physicochemical properties of lipoplexes but modulates gene transfer efficiency, Nucleic Acids Res, 27, (19), 3792-3798.

Lin, J. Y. and Fisher, D. E., 2007, Melanocyte biology and skin pigmentation, Nature, 445, (7130), 843-850.

Maeda, H., Wu, J., Sawa, T., Matsumura, Y. and Hori, K., 2000, Tumor vascular permeability and the EPR effect in macromolecular therapeutics: a review, J Control Release, 65, (1-2), 271-284.

Maeda, H., 2001, The enhanced permeability and retention (EPR) effect in tumor vasculature: the key role of tumor-selective macromolecular drug targeting, Adv Enzyme Regul, 41, 189-207.

Moolten, F. L., 1986, Tumor chemosensitivity conferred by inserted herpes thymidine kinase genes: paradigm for a prospective cancer control strategy, Cancer Res, 46, (10), 5276-5281.

Morille, M., Passirani, C., Vonarbourg, A., Clavreul, A. and Benoit, J. P., 2008, Progress in developing cationic vectors for non-viral systemic gene therapy against cancer, Biomaterials, 29, (24-25), 3477-3496.

Morille, M., Montier, T., Legras, P., Carmoy, N., Brodin, P., Pitard, B., Benoit, J. P. and Passirani, C., 2009, Long-circulating DNA lipid nanocapsules as new vector for passive tumor targeting, Biomaterials, 31, (2), 321-329.

Morille, M., Passirani, C., Letrou-Bonneval, E., Benoit, J. P. and Pitard, B., 2009, Galactosylated DNA lipid nanocapsules for efficient hepatocyte targeting, Int J Pharm, 379, (2), 293-300.

Morille, M., Passirani, C., Dufort, S., Bastiat, G., Pitard, B., Coll, J. L. and Benoit, J. P., 2010, Tumor transfection after systemic injection of DNA lipid nanocapsules, Biomaterials, .

Portsmouth, D., Hlavaty, J. and Renner, M., 2007, Suicide genes for cancer therapy, Mol Aspects Med, 28, (1), 4-41.

Roda, A., Guardigli, M., Michelini, E. and Mirasoli, M., 2009, Bioluminescence in analytical chemistry and in vivo imaging, TrAC Trends in Analytical Chemistry, 28, (3), 307-322.

Shinoda, K. and Saito, H., 1968, The effect of temperature on the phase equilibria and the types of dispersions of the ternary system composed of water, cyclohexane, and nonionic surfactant, Journal of Colloid and Interface Science, 26, (1), 70-74.

Shinoda, K. and Saito, H., 1969, The Stability of O/W type emulsions as functions of temperature and the HLB of emulsifiers: The emulsification by PIT-method, Journal of Colloid and Interface Science, 30, (2), 258-263.

Stone, G. W., Barzee, S., Snarsky, V., Santucci, C., Tran, B., Langer, R., Zugates, G. T., Anderson, D. G. and Kornbluth, R. S., 2009, Nanoparticle-delivered multimeric soluble CD40L DNA combined with Toll-Like Receptor agonists as a treatment for melanoma, PLoS One, 4, (10), e7334.

Tawbi, H. and Nimmagadda, N., 2009, Targeted therapy in melanoma, Biologics, 3, 475-484.

Texier, I., Goutayer, M., Silva, A. D., Guyon, L., Djaker, N., Josserand, V., Neumann, E., Bibette, J. and Vinet, F., 2009, Cyanine-loaded lipid nanoparticles for improved in vivo fluorescence imaging, Journal of Biomedical Optics, 14, (5), 054005.

Viola, J. R., El-Andaloussi, S., Oprea, II and Smith, C. I., 2010, Non-viral nanovectors for gene delivery: factors that govern successful therapeutics, Expert Opin Drug Deliv, 7, (6), 721-735.

Vonarbourg, A., Saulnier, P., Passirani, C. and Benoit, J. P., 2005, Electrokinetic properties of noncharged lipid nanocapsules: influence of the dipolar distribution at the interface, Electrophoresis, 26, (11), 2066-2075.

Vonarbourg, A., Passirani, C., Saulnier, P. and Benoit, J. P., 2006, Parameters influencing the stealthiness of colloidal drug delivery systems, Biomaterials, 27, (24), 4356-4373.

Vonarbourg, A., Passirani, C., Desigaux, L., Allard, E., Saulnier, P., Lambert, O., Benoit, J. P. and Pitard, B., 2009, The encapsulation of DNA molecules within biomimetic lipid nanocapsules, Biomaterials, 30, (18), 3197-3204.

Wagner, E., Kircheis, R. and Walker, G. F., 2004, Targeted nucleic acid delivery into tumors: new avenues for cancer therapy, Biomed Pharmacother, 58, (3), 152-161.

Weiss, M. B. and Aplin, A. E., 2010, Paying "particle" attention to novel melanoma treatment strategies, J Invest Dermatol, 130, (12), 2699-2701.

Zheng, D., Li, X., Xu, H., Lu, X., Hu, Y. and Fan, W., 2009, Study on docetaxel-loaded nanoparticles with high antitumor efficacy against malignant melanoma, Acta Biochim Biophys Sin (Shanghai), 41, (7), 578-587.

Publication No 4

Treatment efficacy of DNA lipid nanocapsules and DNA multimodular systems after systemic administration in a human glioma model

David S., Montier T., Carmoy N., Clavreul A., Pitard B., Benoit JP. and Passirani C.

Gene Therapy – soumis

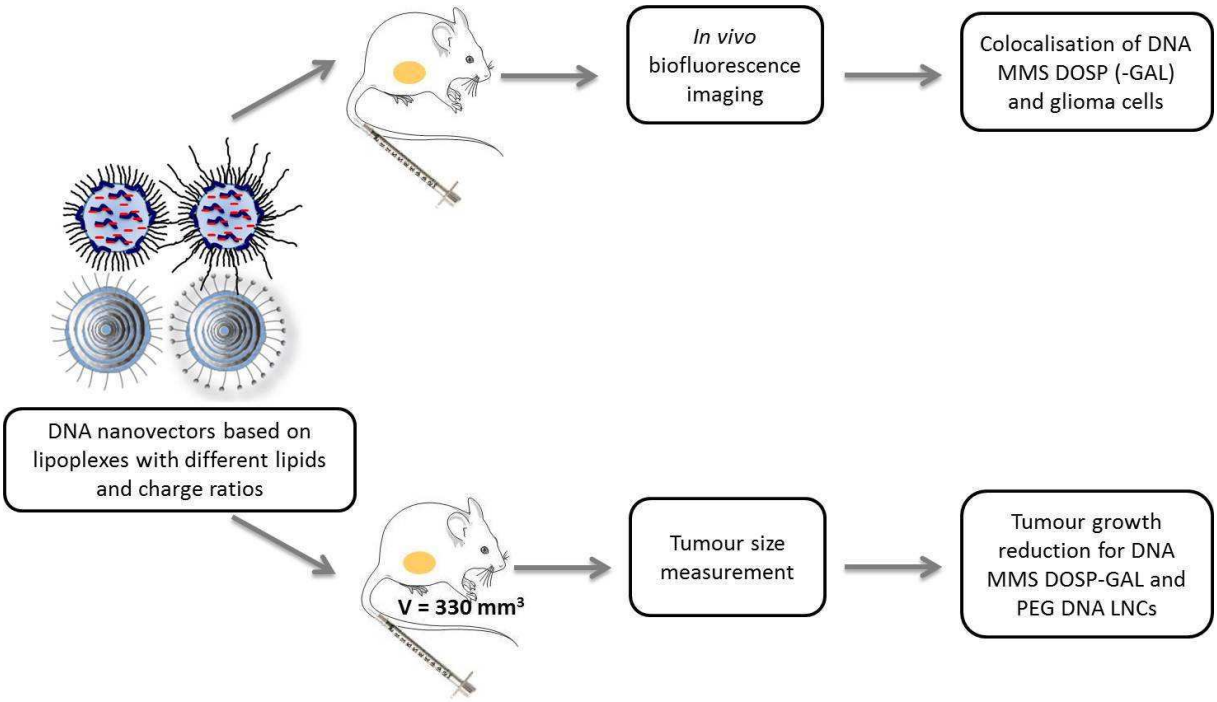

Cette dernière partie est consacrée à l'application des vecteurs ADN, caractérisés sur des souris saines en première partie de thèse, sur un modèle murin de gliome. Dans un premier temps, les profils de biodistribution des différents vecteurs sur ce modèle ont été déterminés en utilisant l'imagerie par fluorescence *in vivo*. Ensuite, les vecteurs montrant une capacité à aller dans la tumeur ont été choisis pour effectuer un traitement utilisant l'approche par gène suicide.

TREATMENT EFFICACY OF DNA LIPID NANOCAPSULES AND DNA MULTIMODULAR SYSTEMS AFTER SYSTEMIC ADMINISTRATION IN A HUMAN GLIOMA MODEL

Stephanie David[a,b,c], Tristan Montier[d,e], Nathalie Carmoy[d], Anne Clavreul[a,b,f], Bruno Pitard[c,*], Jean-Pierre Benoit[a,b] and Catherine Passirani[a,b,*]

[a]*LUNAM Université – Ingénierie de la Vectorisation Particulaire, F-49933 Angers, France*

[b]*INSERM – U646 – Université d'Angers, IBS-CHU, 4 rue Larrey, F-49933 Angers, France*

[c]*INSERM UMR915 – Université de Nantes, 8 quai Moncousu, F-44000 Nantes, France*

[d]*INSERM U613 – Université de Brest, 5 avenue du Maréchal Foch, F-29200 Brest, France*

[e]*DUMG – CHRU de Brest, avenue du Maréchal Foch, F-29200 Brest, France*

[f]*Département de Neurochirurgie – CHU d'Angers, 4 rue Larrey, F-49933 Angers, France*

*Corresponding authors:

C. Passirani:

Inserm U646, IBS-CHU, 4 rue Larrey, 49933 Angers Cedex 9, France

Tel.: +33 244 688534, Fax: +33 244 688546, E-mail: catherine.passirani@univ-angers.fr;

ABSTRACT

We previously developed different DNA nanocarriers for systemic administration. DNA lipid nanocapsules coated or not with long polyethylene (PEG) chains (PEG DNA LNCs or DNA LNCs, respectively) and different multimodular systems (MMS), containing either the cationic lipid BGTC (bis(guanidinium)-tren-cholesterol) (DNA MMS BGTC) or DOSP (dioleylamine succinyl paromomycine) (DNA MMS DOSP). The ligand galactose can be added to both types of DNA MMS for active targeting forming GAL DNA MMS BGTC or GAL DNA MMS DOSP respectively. The biodistribution profiles of these intravenously administrated systems delivering a plasmid DNA with a luciferase cassette, on an ectopic human U87MG glioma model in nude mice, were similar to those observed on healthy animals and varied in function of their composition. DNA MMS BGTC and the galactosylated DNA MMS accumulated preferentially in the liver, DNA LNCs had a brought distribution profile but were rapidly eliminated whereas DNA MMS DOSP and PEG DNA LNCs showed a prolonged circulation profile. Furthermore, PEG DNA LNCs and GAL DNA MMS DOSP showed a specific accumulation and some luciferase expression in the tumour tissue. Systemic treatment with these promising DNA nanocarriers on this glioma model using a plasmid encoding the herpes simplex virus thymidine kinase (HSV-tk) and a subsequent ganciclovir (GCV) treatment showed a tumour growth reduction compared to non-treated mice cohort. These results are in good accordance with those obtained previously with PEG DNA LNCs on a human melanoma mouse model and highlight the potential use of GAL DNA MMS DOSP and PEG DNA LNCs as future therapeutics in glioma and other cancer diseases.

Key words:

Gene therapy, GDEPT, *in vivo* biofluorescene imaging, DNA MMS DOSP GAL, PEG DNA LNCs, systemic administration

INTRODUCTION

Malignant gliomas are highly aggressive primary adult brain tumours with poor prognosis [1]. The most aggressive form is the glioblastoma multiform, characterized by its diffuse invasion of the surrounding normal tissue and its recurrence after all form of therapy [2]. The standard treatment is maximal safe surgical resection followed by radiotherapy and temozolomide chemotherapy which improves the median overall survival, up to five years in some cases [3]. However, most patients will still die of their disease and the development of new improved treatments shall be given priority.

One option is the combination of herpes simplex virus thymidine kinase (HSV-tk) with the prodrug ganciclovir (GCV), known as gene directed enzyme prodrug therapy (GDEPT) [4, 5]. This therapy was already shown to be efficient on patients with operable primary or recurrent malignant glioma. An increase in patient survival time of 71 weeks compared to 39 weeks in the control group could be attained by local HSV-tk administration after tumour resection using adenovirus [6]. The major drawbacks of viruses used as gene delivery vectors are their potential risk, associated with replication-competent viruses, immunogenicity and high cost [7-9]. For this reason non-viral delivery agents have been developed which do not present these drawbacks and present furthermore the advantages to be able to carry large inserts and to be easily modifiable for active or passive targeting [10-12].

Previously, different non-viral DNA nanocarriers were developed in our laboratories. DNA lipid nanocapsules (DNA LNCs), encapsulating DNA lipoplexes in their liquid lipid core, proved their transfection efficiency *in vitro*. PEG DNA LNCs (coated DNA LNCs with DSPE-PEG_{2000}) demonstrated their transfection efficiency *in vivo* using a luciferase coding plasmid on a tumour model (HEKβ3 in nude mice) [13-15]. DNA multimodular systems containing the cationic lipid BGTC (DNA MMS BGTC), were developed by Letrou-Bonneval et al.[16] and demonstrated a specific transfection in primary hepatocytes after a coating with galactose (GAL DNA MMS BGTC). Previously, DNA MMS based on the cationic lipid DOSP were developed and the biodistribution profiles of all these different DNA nanocarriers after systemic administration on healthy mice were analysed, revealing an accumulation in the liver for DNA MMS BGTC and galactose bearing DNA MMS and a prolonged circulation time for DNA MMS DOSP [17]. Both formulations were based on lipoplexes (complexes of DNA with a cationic lipid) and had a dual core-shell (LNCs) or core-corona structure (MMS). Our strategy was to use different DNA nanocarriers to

administer HSV-tk via systemic administration on an ectopic human U87MG glioma model in nude mice followed by a GCV treatment. In a first time, biodistribution of the systemic administrated DNA nanocarriers, encapsulating a fluorescent dye and a luciferase coding plasmid DNA, was followed via the non-invasive *in vivo* biofluorescence imaging and the luciferase expression in different organs and tumour tissue was assessed. Afterwards, DNA nanocarriers showing the best tumour targeting were chosen to administer the HSV-tk/GCV treatment in the human glioma model and to evaluate its efficiency in tumour growth reduction.

MATERIALS AND METHODS

Preparation of nanocarriers

Plasmids, lipids for liposome preparation and steric stabilisers

The pGWIZ^{TM}-luciferase DNA plasmid (Gene Therapy systems, Inc., San Diego, CA USA) was used for DNA nanocarrier characterisation, biodistribution analysis and luciferase quantification and the pORF-TK-ΔCpG DNA plasmid (InvivoGen; Toulouse, France) was used for treatment using the GDEPT. The cationic lipids DOSP (dioleylamin-succinyl paromomycin) (synthesis previously described in [18]) and BGTC (bis(guanidinium)-tris(2-aminoethyl)amine-cholesterol) (synthesis previously described in [19]) were used for DNA MMS preparation and the cationic lipid DOTAP (1.2-dioleyl-3-trimethylammoniumpropane) (Avanti® Polar Lipids Inc., Alabaster, AL, USA) for DNA LNC preparation. All lipids were combined with the neutral lipid DOPE (1.2-dioleyl-sn-glycero-3-phosphoethanolamine) (Avanti® Polar Lipids Inc., Alabaster, AL, USA). The polymer F108 (80% poly(ethylene oxide), MW 14600) was generously provided by BASF and the galactosylated form synthesised as described in [16].

Preparation of liposomes

Liposomes were composed of a cationic lipid (DOSP, BGTC or DOTAP) in addition to the neutral helper lipid DOPE in the ratio 1/1 (M/M), 3/2 (M/M) or 1/1 (M/M) respectively. The different lipids solubilised in chloroform were weighted to obtain a final concentration of 20 mM of cationic lipid charge, considering the number of lipid charges per molecule (4 for DOSP, 2 for BGTC and 1 for DOTAP). Then chloroform was evaporated under vacuum to

obtain a homogen lipid film which was hydrated with deionised water over night at 4°C. The next day liposomes were sonicated and size measurement was performed before use.

Preparation of DNA multimodular systems

To prepare multimodular systems (MMS), equal volumes of a mixture composed of the steric stabilizer (F108 or F108-gal), liposomes (BGTC/DOPE or DOSP/DOPE), and water was added to a mixture composed of plasmid DNA, NaCl and water to obtain final concentrations of 0.25g/l DNA and 0.15M NaCl, with a charge ratio (+/-) of 2 and a polymer/DNA ratio of 300 (w/w). MMS were incubated for 20 min at room temperature before use.

Preparation of (PEG) DNA LNCs

DNA LNCs were prepared as previously described [13]. Briefly, LNCs were composed of 9.9 % (w/w) lipophilic Labrafac® WL 1349 (Gatefossé S.A., Saint-Priest, France), 3.9 % (w/w) oleic Plurol® (Polyglyceryl-6 dioleate) which was kindly provided by Gatefossé S.A. (Saint-Priest, France), 1.4 % (w/w) NaCl (Prolabo, Fontenay-sous-Bois, France), 78.9 % (w/w) water (obtained from a Milli-Q-plus® system, Millipore, Paris, France) and 5.9 % (w/w) Solutol® HS-15 (BASF, Ludwigshafen, Germany). Lipoplexes containing the plasmid coding for luciferase or for HSV-tk and DOTAP/DOPE liposomes in a charge ratio (+/-) of 5 were added instead of the formulation water. For *in vivo* biofluorescence imaging, the near-infrared fluorescent dye 1,1'-dioctadecyl-3,3,3',3'-tetramethylindodicarbocyanine perchlorate (DiD, em. = 644 nm; exc. = 665 nm) (Invitrogen, Cergy-Pontoise, France) was mixed previously with Labrafac® as described in [21]. The formulation process was based on the phase inversion of a microemulsion [22]. Briefly, after mixing all the components, temperature-cycles around the phase-inversion-temperature (PIT) were performed under magnetic stirring. Afterwards, cold water (in a ratio 1:1.96) was added to dilute the microemulsion and form DNA LNCs.

DNA LNCs were then passed on PD10 Sephadex columns (Amersham Biosciences Europe, Orsay, France), ultrafiltrated with MilliporeAmicon® Ultra-15 centrifugal filter devices (Millipore, St Quentin-Yvelines, France) and the salt- and LNC-concentration were readjusted afterwards to obtain a physiologic concentration of NaCl (150mM) and the initial concentration of LNCs (152 g/l).

Half of these purified DNA LNCs were then mixed with 1,2-DiStearoyl-sn-glycero-3-PhosphoEthanolamine-N-[methoxy(polyethyleneglycol)-2000] (DSPE-mPEG$_{2000}$) (Mean Molecular Weight (MMW) = 2,805 g/mol) (Avanti Polar Lipids, Inc, Alabaster, USA), incubated for 4 h at 30 °C and vortexed every 15 minutes to obtain PEG DNA LNCs with a final polymer concentration of 10mM.

Physico-chemical characterisation of DNA nanocarriers

Coated and non-coated DNA LNCs were diluted with deionised water in a ratio of 1:100 and the different DNA MMS with 0.15M NaCl in a ratio of 4:100 before measuring their size and zeta potential with a Malvern Zetasizer® (Nano Series ZS, Malvern Instruments S.A., Worcestershire, UK) at 25 °C. All measurements were performed in triplicate and with similar conductivity values.

In vivo experiments

Ectopic human glioma model in nude mice

Six- to nine-week-old female, nude SWISS mice (Charles River, France) were housed and maintained at the University animal facility; they were processed in accordance with the Laboratory Animal Care Guidelines (NIH Publication 85-23, revised 1985) and with the agreement of the regional veterinary services (authorisation FR; 29-024).

Tumour bearing mice were prepared by injecting subcutaneously a suspension of $1x10^6$ U87MG glioblastoma-astrocytoma cells (n°HTB-14-ATCC) in 100 µl of HBBS into the right flank of athymic nude SWISS mice (6-week-old females, 20-24 g). Three weeks after tumour implantation, 150µl of DNA LNCs or PEG DNA LNCs or 200µl of DNA MMS were administered by intravenous injection into the tail vein of the mice. Animals were sacrificed 24h after intravenous injection.

In vivo biofluorescence imaging

Non-invasive biofluorescent imaging (BFI) was performed as described before [15], at 1, 3, 5, and 24 h post-injection, using the BFI system of the NightOWL II (Berthold Technologies, Germany). Briefly, the WinLight 32 software (Berthold Technologies, Germany) was used, the 590 nm excitation and 655 nm emission filters were selected and each mouse was

anaesthetised with isofluran during the acquisition (3 seconds for one fluorescent acquisition). The fluorescent signal was then overlaid on a picture of each mouse.

Luciferase quantification

Organs from the sacrificed animals were placed in tubes with PLB 1x (Passive Lysis Buffer, Promega) and shaked with the gentleMACS Dissociator. Tubes were centrifuged for 10 min at 1150 g at 4°C and the upper phase transferred in Eppendorf tubes. After another centrifugation of 10 min at 20000 g at 4°C, 25µl of the upper phase is placed, in triplicate, in a white 96 well plate and the quantification with the luciferin reagent (Promega) is performed with the MLX luminometer plate reader (Dynex, Guyancourt, France).

Treatment efficacy of DNA nanocarriers

Nude Swiss mice bearing s.c. glioma cells in the right flank were prepared as described in the previous section. Animals were weighted and tumour dimensions were measured regularly. Tumour volume was calculated using the formula $\pi/6*length^2*width$. Mice were distributed in different groups in function of their tumour volume, to obtain randomized homogen groups with a tumour volume of 330 +/- 90 mm^3 at the beginning of the treatment. Mice received one intravenous injection in the tail vein of 150µl PEG DNA LNCs or 200µl GAL DNA MMS DOSP, encapsulating a plasmid encoding the Herpes Simplex Virus thymidine kinase (HSV-tk) followed by a subsequent treatment twice a day for four days with 150µl i.p. Ganciclovir (10 mg/ml; InvivoGen, Toulouse, France), corresponding to 65 mg/kg. Control mice received no treatment, GCV alone, LNCs without DNA alone or DNA nanocarriers without GCV treatment. Mice were sacrificed at day 11 after the beginning of the treatment.

Statistical significance of various vector and treatment combinations were analysed by Student's *t* test ($n < 30$). $P < 0.05$ was considered statistically significant (two-tailed test).

RESULTS AND DISCUSSION

DNA nanocarrier presentation

In this study, six different DNA nanocarriers, previously developed in our laboratories, were used; two types of LNCs (DNA LNCs and PEG DNA LNCs) and four types of MMS using either the cationic lipid BGTC (DNA MMS BGTC, GAL DNA MMS BGTC) or DOSP

(DNA MMS DOSP, GAL DNA MMS DOSP). The physico-chemical properties of these DNA nanocarriers are presented on table 1. The recommended physico-chemical properties for an "ideal" nanocarrier administrated via systemic injection are a size between 50 and 200 nm, a neutral surface charge and the possibility to target a specific cell via active or passive targeting. In this aim, DNA LNCs were recovered by DSPE-PEG_{2000} to prolong the circulation time, necessary for passive targeting and to mask the positive surface charges due to the cationic lipid used for DNA complexation. DNA MMS had already neutral surface charges due to their composition and the ligand galactose was used for an active targeting of asialoglycoproteinreceptors on hepatocytes. However, the addition of galactose on DNA MMS BGT augmented the size above 200 nm. The physico-chemical properties of these DNA nanocarriers indicate that compromises will have to be done to obtain efficient nanocarriers.

<table>
<tr><th></th><th colspan="3">Lipoplex composition</th><th colspan="2">Surface coating</th><th colspan="2">Physico-chemical characteristics</th></tr>
<tr><th></th><th>Cationic lipid</th><th>Plasmid DNA</th><th>Charge ratio [+/-]</th><th>Polymer</th><th>Ratio polymer/DNA [w/w]</th><th>Size [nm]</th><th>Zeta potential [mV]</th></tr>
<tr><td>DNA LNC</td><td rowspan="2">DOTAP</td><td rowspan="6">pgWIZ-luciferase</td><td rowspan="2">5</td><td>-</td><td>-</td><td>114 +/- 25</td><td>27 +/- 12</td></tr>
<tr><td>PEG DNA LNC</td><td>PEG_{2000}</td><td>70</td><td>132 +/- 3</td><td>-17 +/- 3</td></tr>
<tr><td>DNA MMS BGTC</td><td rowspan="2">BGTC</td><td rowspan="4">2</td><td>F108</td><td rowspan="4">300</td><td>150 +/- 32</td><td>-3 +/- 2</td></tr>
<tr><td>GAL DNA MMS BGTC</td><td>F108-galactose</td><td>298 +/- 171</td><td>-2 +/-1</td></tr>
<tr><td>DNA MMS DOSP</td><td rowspan="2">DOSP</td><td>F108</td><td>198 +/- 57</td><td>0</td></tr>
<tr><td>GAL DNA MMS DOSP</td><td>F108-galactose</td><td>152 +/- 58</td><td>-2 +/ 0</td></tr>
</table>

Table 1: Specifications of the different DNA nanocarrier

In vivo fluorescence imaging of DNA nanocarriers

To analyse the biodistribution profiles using non-invasive *in vivo* biofluorescence imaging (BFI) a fluorescent dye, DiD, was encapsulated in the different DNA nanocarriers. Afterwards these fluorescent DNA nanocarriers were administered via systemic administration on a glioma model consisting of human U87MG cells implanted in the right flank of nude mice. As previously observed on healthy animals, the biodistribution profiles of the DNA

nanocarriers also varied in function of their lipid composition and their surface coating in this tumour model [17]. The biodistribution of DNA LNCs, showing a broad distribution 1h after administration and a rapid elimination afterwards, and PEG DNA LNCs, showing a prolonged circulation time compared to DNA LNC with a tumour accumulation for both LNC types was already reported by Morille *et al*. in the same model [20]. DNA MMS containing the cationic lipid BGTC accumulated preferentially in the liver, as indicated by a fluorescence signal persisting during the whole observation period in this organ with both types of DNA MMS BGTC. DNA MMS containing the cationic lipid DOSP had an augmented circulation time comparable with PEG DNA LNCs one demonstrated by an intense fluorescence signal in the whole body along the observation period. The addition of galactose as a ligand accentuated the accumulation in the liver for both types of DNA MMS, certainly due to the active targeting via asialoglycoprotein receptors present on hepatocytes [16, 23, 24], but also in the tumour region for the long circulating DNA MMS DOSP.

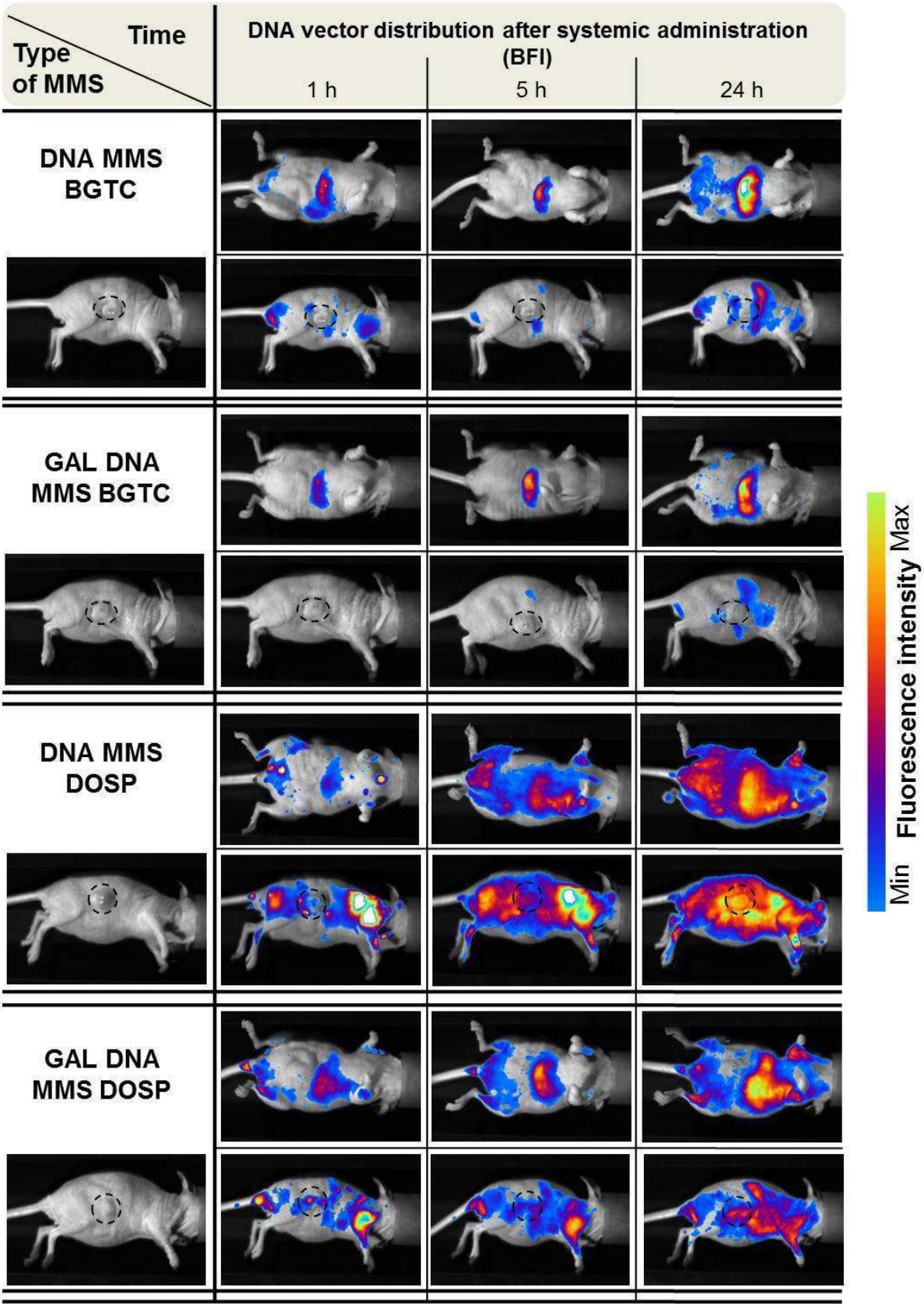

Figure 1: *In vivo* biofluorescence images of DNA MMS BGTC and DNA MMS DOSP with and without the ligand galactose at 1h, 5h and 24h after intravenous injection. One mouse per group is represented both, in the lateral and in the decubitus-dorsal view.

Quantification of luciferase expression in different organs

Twenty-four hours after administration of the six different DNA nanocarriers, encapsulating a luciferase coding plasmid DNA, animals were sacrificed and luciferase expression was quantified in different organs and tissues. In kidney, heart and lungs, no significant luciferase expression could be detected for all DNA MMS and PEG DNA LNCs and only low luciferase expression for DNA LNCs (data not shown). For DNA MMS BGTC with and without galactose, luciferase expression could neither be quantified in tumour, in liver nor in spleen. However, there is a luciferase expression following transfection with DNA MMS DOSP in presence and absence of galactose and DNA LNCs with or without surface coating with PEG_{2000} located in tumour, liver and spleen (Figure 2), compared to non-treated animals (control). GAL DNA MMS DOSP demonstrated also a luciferase expression in the tumour without any luciferase expression in liver and spleen. The presence of the ligand galactose seems to promote accumulation and transfection efficiency, as DNA MMS DOSP did not show any luciferase expression although tumour accumulation was observed via *in vivo* biofluorescence imaging. This could probably be explained as lectins, such as galactin-1 [25], a galactose-specific lectin correlating with the grade of malignancy, are highly expressed in human gliomas [26, 27]. DNA LNCs achieved low luciferase expression in the tumour, but some luciferase expression in liver and spleen. PEG DNA LNCs in return, showed lower luciferase expression in spleen and liver as DNA LNCs, but higher luciferase expression in the tumour.

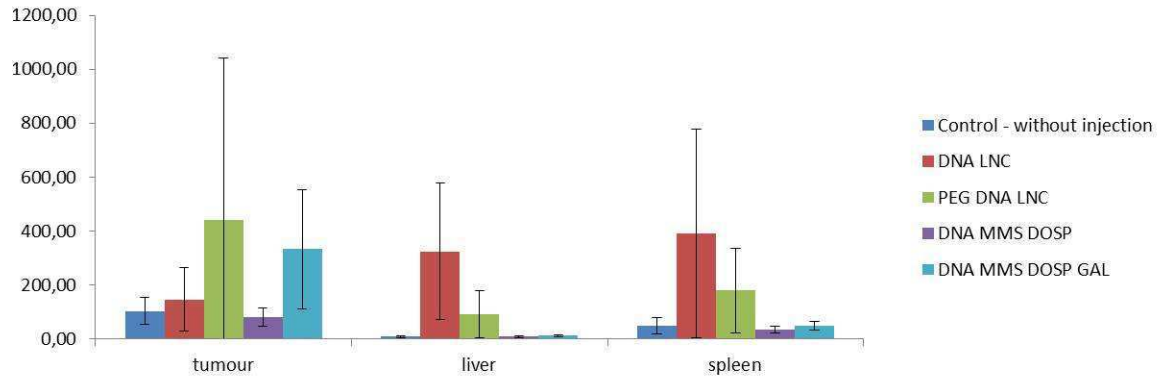

Figure 2: Quantification of luciferase expression in different organs (spleen and liver) and in the tumour 24h after intravenous injection of different DNA nanocarriers (DNA LNCs, PEG DNA LNCs, DNA MMS DOSP with and without the ligand galactose and control mice without injections, n = 8 for control mice and mice receiving DNA MMS and n = 6 for DNA LNCs and PEG DNA LNCs).

Treatment efficacy of PEG DNA LNC and GAL DNA MMS DOSP

Due to their tumour accumulation capacity, PEG DNA LNCs and GAL DNA MMS DOSP were selected and used in a GDEPT approach [4] consisting in transfection of HSV-tk in tumour cells (group TPDL and TGDMD respectively, Figure 3). This enzyme activates the prodrug ganciclovir (GCV) via phosphorylation, which in return will act as chain terminator after incorporation into the DNA of dividing (tumour) cells [4, 5]. An important bystander effect was described in the literature using this approach on glioma cells allowing the reduction of HSV-tk/GCV doses as, in certain cases, only 10% of the tumour cells have to be transfected [28-30].

Five different control groups were analysed in order to assess the efficacy of these DNA nanocarriers: (1) no treatment (CN), (2) GCV treatment alone (T), (3) PEG LNCs without DNA and without GCV treatment (PL), (4) PEG DNA LNCs without GCV treatment (PDL) and (5) GAL DNA MMS DOSP without GCV treatment (GDMD). The results obtained in our study with this approach are in good agreement with the results obtained via *in vivo* biofluorescence imaging and luciferase quantification analysis. Indeed, PEG DNA LNCs which accumulated in the tumour, had there the highest luciferase expression and were the most efficient vector using the GDEPT approach with a significant tumour growth reduction starting at day 2 ($p = 0.05$ for day 2 and 0.01 for the following days). This result is also in concordance with previous results obtained on a melanoma mouse model where treatment efficacy compared to non-treated mice was shown at day 4 after LNC administration [15]. This accumulation and expression of PEG DNA LNCs in the tumour region is certainly due to the passive targeting mechanism linked to the enhanced permeability and retention (EPR) effect, well documented in the literature [31, 32]. This EPR effect is due to the “leaky”, tortuous and heterogeneous tumour vessels with pore sizes between 100nm and almost 1 µm depending on the anatomic tumour location and tumour growth [12], which results in the enhanced retention of particles such as stealth nanocarriers. GAL DNA MMS DOSP also accumulated in the tumour tissue, but had a lower luciferase expression in this tissue compared to PEG DNA LNCs and showed therefore also a lower treatment efficacy ($p = 0.1$ for days 9, 10 and 11). Treatment of animals with GCV in absence of any DNA nanocarrier also reduced tumour growth in a non-significant manner as well as GAL DNA MMS DOSP without GCV treatment. PEG DNA LNCs without the GCV treatment in contrast reduced the

tumour growth in a comparable level to GAL DNA MMS DOSP. However, PEG LNCs without DNA and without GCV treatment did not reduce tumour growth indicating that the tumour growth reduction comes from the GCV and/or the DNA (in combination with the different nanocarriers). A cytotoxic effect of GCV alone was also observed in the literature especially at higher doses [33-35]. Seen the heterogeneous tumour growth of this glioma model, more animals in each group and an earlier treatment beginning could probably improve the difference in tumour growth between the treatment and control groups.

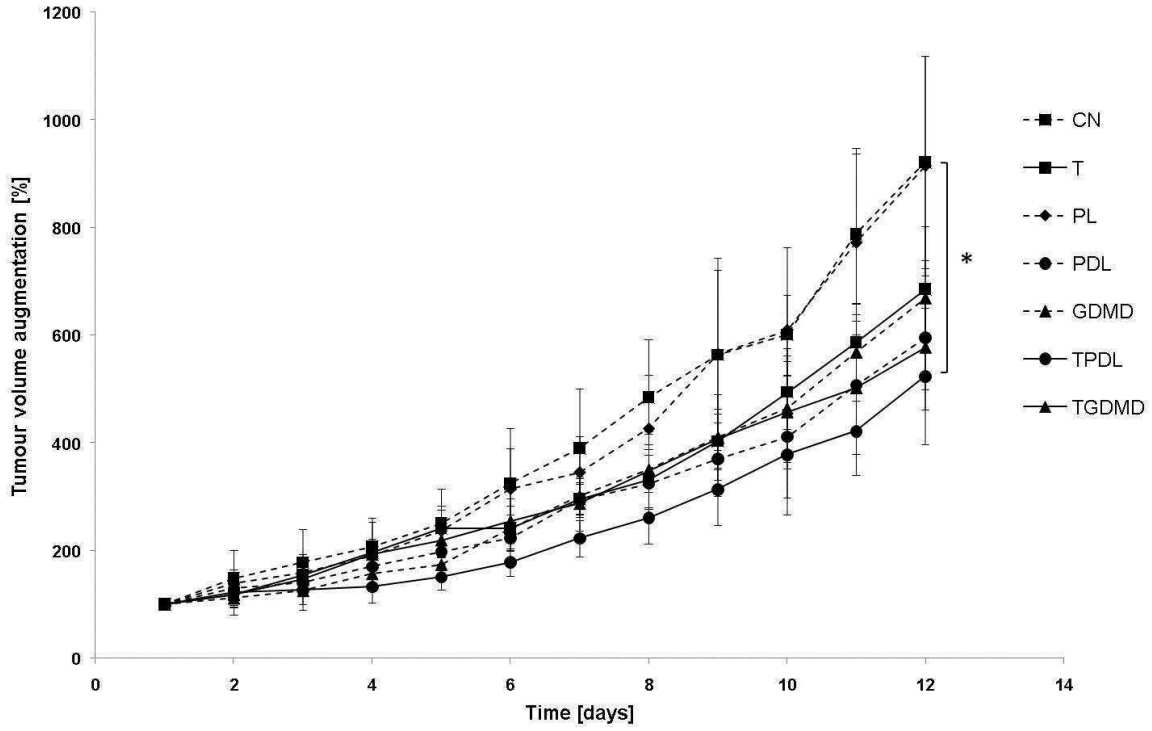

Figure 3: Treatment efficacy was determined by measuring the tumour volume once a day from the treatment day and during 11 days. It was represented in augmentation of tumor volume in % of tumor volume at day 0 (animals receiving no GCV dashed lines (n = 3), animals receiving GCV continuous lines (n = 3 for GCV treatment (T) alone and n = 6 for DNA nanocarrier administration), negative control (without injection) (CN, T) squares, GAL DNA MMS DOSP triangles (GDMD, TGDMD), PEG DNA LNCs circles (PDL, TPDL), PEG LNCs without DNA (PL) diamonds), (*significant for CN and TPDL with p = 0.01 starting at day 3).

CONCLUSION

The biodistribution, transfection and treatment efficacy of new DNA nanocarriers on an ectopic glioma mouse model after systemic administration were studied here. The results obtained in this study are showing a promising potential for PEG DNA LNCs and GAL DNA MMS DOSP as future therapeutics in glioma or other cancer diseases.

ACKNOWLEDGMENTS

The authors would like to thank Pierre Legras (SCAHU, Angers) and Pauline Resnier (Inserm U646, Angers) for their help in the design of *in vivo* experiments and their technical help. Furthermore, the authors would like to thank Mathieu Mevel (Inserm U915, Nantes) for the synthesis of the polymer F108-gal.

REFERENCES

1. **Arko, L., et al., Experimental approaches for the treatment of malignant gliomas. Pharmacol Ther, 2010. 128(1): p. 1-36.**

2. **Allard, E., C. Passirani, and J.P. Benoit, Convection-enhanced delivery of nanocarriers for the treatment of brain tumors. Biomaterials, 2009. 30(12): p. 2302-18.**

3. **Stupp, R., et al., Effects of radiotherapy with concomitant and adjuvant temozolomide versus radiotherapy alone on survival in glioblastoma in a randomised phase III study: 5-year analysis of the EORTC-NCIC trial. Lancet Oncol, 2009. 10(5): p. 459-66.**

4. **Portsmouth, D., J. Hlavaty, and M. Renner, Suicide genes for cancer therapy. Mol Aspects Med, 2007. 28(1): p. 4-41.**

5. **Altaner, C., Prodrug cancer gene therapy. Cancer Lett, 2008. 270(2): p. 191-201.**

6. **Immonen, A., et al., AdvHSV-tk gene therapy with intravenous ganciclovir improves survival in human malignant glioma: a randomised, controlled study. Mol Ther, 2004. 10(5): p. 967-72.**

7. **Chowdhury, E.H., Nuclear targeting of viral and non-viral DNA. Expert Opin Drug Deliv, 2009. 6(7): p. 697-703.**

8. **Collins, S.A., et al., Viral vectors in cancer immunotherapy: which vector for which strategy? Curr Gene Ther, 2008. 8(2): p. 66-78.**

9. **Jin, S. and K. Ye, Nanoparticle-mediated drug delivery and gene therapy. Biotechnol Prog, 2007. 23(1): p. 32-41.**

10. **Kreiss, P., et al., Plasmid DNA size does not affect the physicochemical properties of lipoplexes but modulates gene transfer efficiency. Nucleic Acids Res, 1999. 27(19): p. 3792-8.**

11. **Morille, M., et al., Progress in developing cationic vectors for non-viral systemic gene therapy against cancer. Biomaterials, 2008. 29(24-25): p. 3477-96.**

12. **Huynh, N.T., et al., The rise and rise of stealth nanocarriers for cancer therapy: passive versus active targeting. Nanomedicine (Lond), 2010. 5(9): p. 1415-33.**

13. **Vonarbourg, A., et al., The encapsulation of DNA molecules within biomimetic lipid nanocapsules. Biomaterials, 2009. 30(18): p. 3197-204.**

14. **Morille, M., et al., Tumor transfection after systemic injection of DNA lipid nanocapsules. Biomaterials, 2010.**

15. **David, S., et al., In vivo imaging of DNA lipid nanocapsules after systemic administration in a melanoma mouse model. Int J Pharm, 2011.**

16. **Letrou-Bonneval, E., et al., Galactosylated multimodular lipoplexes for specific gene transfer into primary hepatocytes. J Gene Med, 2008. 10(11): p. 1198-209.**

17. **David, S., et al., DNA nanocarriers for systemic administration - characterisation and in vivo bioimaging in healthy mice. Mol Ther, 2011.**

18. **Desigaux, L., et al., Self-assembled lamellar complexes of siRNA with lipidic aminoglycoside derivatives promote efficient siRNA delivery and interference. Proc Natl Acad Sci U S A, 2007. 104(42): p. 16534-9.**

19. **Vigneron, J.P., et al., Guanidinium-cholesterol cationic lipids: efficient vectors for the transfection of eukaryotic cells. Proc Natl Acad Sci U S A, 1996. 93(18): p. 9682-6.**

20. **Morille, M., et al., Long-circulating DNA lipid nanocapsules as new vector for passive tumor targeting. Biomaterials, 2009. 31(2): p. 321-9.**

21. **Garcion, E., et al., A new generation of anticancer, drug-loaded, colloidal vectors reverses multidrug resistance in glioma and reduces tumor progression in rats. Mol Cancer Ther, 2006. 5(7): p. 1710-22.**

22. **Heurtault, B., et al., A novel phase inversion-based process for the preparation of lipid nanocarriers. Pharm Res, 2002. 19(6): p. 875-80.**

23. **Schwartz, A.L., The hepatic asialoglycoprotein receptor. CRC Crit Rev Biochem, 1984. 16(3): p. 207-33.**

24. **Steirer, L.M., et al., The asialoglycoprotein receptor regulates levels of plasma glycoproteins terminating with sialic acid alpha2,6-galactose. J Biol Chem, 2009. 284(6): p. 3777-83.**

25. **Camby, I., et al., Galectin-1: a small protein with major functions. Glycobiology, 2006. 16(11): p. 137R-157R.**

26. **Rorive, S., et al., Galectin-1 is highly expressed in human gliomas with relevance for modulation of invasion of tumor astrocytes into the brain parenchyma. Glia, 2001. 33(3): p. 241-55.**

27. **Camby, I., et al., Galectin-1 knocking down in human U87 glioblastoma cells alters their gene expression pattern. Biochem Biophys Res Commun, 2005. 335(1): p. 27-35.**

28. **Maatta, A.M., et al., Adenovirus mediated herpes simplex virus-thymidine kinase/ganciclovir gene therapy for resectable malignant glioma. Curr Gene Ther, 2009. 9(5): p. 356-67.**

29. **Matuskova, M., et al., HSV-tk expressing mesenchymal stem cells exert bystander effect on human glioblastoma cells. Cancer Lett, 2009. 290(1): p. 58-67.**

30. **Culver, K.W., et al., In vivo gene transfer with retroviral vector-producer cells for treatment of experimental brain tumors. Science, 1992. 256(5063): p. 1550-2.**

31. **Maeda, H., et al., Tumor vascular permeability and the EPR effect in macromolecular therapeutics: a review. J Control Release, 2000. 65(1-2): p. 271-84.**

32. **Maeda, H., The enhanced permeability and retention (EPR) effect in tumor vasculature: the key role of tumor-selective macromolecular drug targeting. Adv Enzyme Regul, 2001. 41: p. 189-207.**

33. **Nanda, D., et al., Treatment of malignant gliomas with a replicating adenoviral vector expressing herpes simplex virus-thymidine kinase. Cancer Res, 2001. 61(24): p. 8743-50.**

34. Soubrane, C., et al., Direct gene transfer of a plasmid carrying the herpes simplex virus-thymidine kinase gene (HSV-TK) in transplanted murine melanoma: in vivo study. Eur J Cancer, 1996. 32A(4): p. 691-5.

35. Rosolen, A., et al., In vitro and in vivo antitumor effects of retrovirus-mediated herpes simplex thymidine kinase gene-transfer in human medulloblastoma. Gene Ther, 1998. 5(1): p. 113-20.

Discussion Générale

Administrer des siRNA ou de l'ADN plasmidique par voie systémique dans le cadre d'une thérapie génique nécessite, à quelques rares exceptions près l'utilisation de vecteurs afin d'obtenir un effet thérapeutique suffisant. Les vecteurs non-viraux utilisés dans ce but doivent franchir de multiples barrières entre le site d'administration et le site d'action avant de permettre l'action des acides nucléiques [1]. D'un point de vue des caractéristiques physico-chimiques, ces vecteurs doivent idéalement présenter:

- une petite taille,
- une charge de surface proche de la neutralité,
- un recouvrement permettant d'augmenter leur furtivité,
- un ciblage (actif ou passif) pour atteindre la cellule cible.

A partir de ces caractéristiques, l'objectif de cette thèse a été de développer de nouveaux vecteurs pour l'administration de siRNA par voie systémique au sein des deux laboratoires Inserm U646 à Angers et Inserm U915 à Nantes. En parallèle, la caractérisation des vecteurs ADN débutée lors de thèses précédentes (Arnaud Vonarbourg, 2006 et Marie Morille, 2009) a été amenée jusqu'à des premiers essais d'application thérapeutique chez l'animal, afin d'éprouver leur efficacité *in vivo*.

Les formulations siRNA

Le procédé de formulation des LNC de siRNA (LNC siRNA) est basé sur la formulation classique des nanocapsules lipidiques, développé par Heurtault *et al*. [2]. Les siRNA sont d'abord complexés avec des lipides cationiques pour être encapsulés dans les LNC. Contrairement à ce qui se passe lors de l'encapsulation d'ADN, seul l'ajout des lipoplexes en fin de formulation, dans l'eau de trempe, a permis d'aboutir à une encapsulation des siRNA.

Les avantages de ce nouveau procédé de formulation sont :

- simplicité
- rapidité
- faible énergie thermique : les lipoplexes et donc les siRNA, ne subissent pas de cycles de températures et sont ajoutés à 73°C en ayant une température proche de 0°C, évitant une dégradation potentielle

Par ailleurs, l'ajout des lipoplexes dans l'eau de trempe permet de ne pas modifier la zone d'inversion de phase et de la maintenir bien visible, ce qui donne lieu à des formulations très reproductibles, malgré un changement de manipulateur (écart-types de 1 à 2 nm tableau 3).

	Formulation 1	Formulation 2	Formulation 3	Formulation 4	Formulation 5
	BGTC/DOPE 2,5	DOPS 2	DOSP 2,5	DOSP/DOPE 2	DOSP/DOPE 2,5
Manipulateur 1	54,2	53,8	59,8	52,8	58,9
Manipulateur 2	55,3	51,6	60,4	54,3	59,7
Manipulateur 3	52,8	-	56,0	55,0	60,46
Moyenne	54,1 +/- 1,3	52,7 +/- 1,6	58,7 +/- 2,4	54,0 +/- 1,1	59,7 +/- 0,8

***Tableau 3** : Tailles des formulations réalisées par 3 manipulateurs différents*

Une analyse approfondie de cette nouvelle formulation montre que l'encapsulation des siRNA dans les LNC n'est pas complète et que cinq compartiments différents peuvent être distingués (figure 11) :

(1) des liposomes vides

(2) des lipoplexes à l'extérieur des LNC

(3) des LNC siRNA

   a. comportant des siRNA complexés au sein des lipoplexes

   b. comportant des siRNA dissociés des lipides cationiques formant initialement les lipoplexes

(4) des LNC vides

(5) des siRNA libres

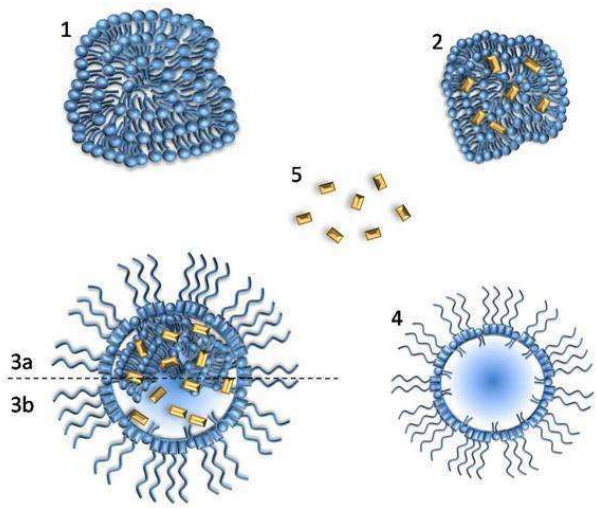

***Figure 11** : Les différents compartiments de la formulation LNC siRNA*

Différents lipides cationiques avec plusieurs rapports de charge vis-à-vis des siRNA (CR) ont été utilisés (tableau 4).

Lipide cationique	BGTC/DOPE	DOSP			DOSP/DOPE			DOTAP/DOPE	
CR [+/-]	2,5	2	2,5	5	2	2,5	5	2,5	5
Taille [nm]	55,3 +/- 0,1	51,6 +/- 0,2	60,4 +/- 1,0	52,8 +/- 0,0	53,3 +/- 0,2	59,7 +/- 0,5	61,4 +/- 0,3	184,1 +/- 28,4 53,5 +/- 6,8	124,8 +/- 0,6
PDI	0,13 +/- 0,03	0,07 +/- 0,00	0,10 +/- 0,02	0,18 +/- 0,00	0,03 +/- 0,01	0,09 +/- 0,01	0,15 +/- 0,03	0,29 +/- 0,03	0,24 +/- 0,00
Potentiel zeta [mV]	1,5 +/- 0,7	-2,4 +/- 0,7	-1,1 +/- 0,1	24,1 +/- 1,7 10,1 +/- 3,2 -3,7 +/- 4,3	-25,7 +/- 1,9	-1,5 +/- 0,4	7,8 +/- 0,9	-0,3 +/- 0,5	1,6 +/- 0,3
Taux d'encapsulation [%]	13 +/- 3	4 +/- 6	17 +/- 20	14 +/- 1	15 +/- 10	7 +/- 2	15 +/- 5	27 +/- 19	65 +/- 2

***Tableau 4** : Caractéristiques des différents LNC siRNA développés*

Comme les caractéristiques des LNC siRNA sont très proches de celles des LNC blanches, le développement d'un dosage siRNA a été une étape cruciale car cela permettait de prouver la présence de siRNA dans les LNCs. En effet, l'électrophorèse seule ne permet pas de distinguer les siRNA complexés au sein des lipoplexes en dehors des LNC et les siRNA encapsulés à l'intérieur des LNCs.

Le dosage de siRNA utilise :

- des extractions au chloroforme pour séparer les siRNA des autres composés de la formulation,
- de la soude pour dissocier les lipoplexes,
- de l'éthanol pour casser les LNC
- un dosage par spectrophotométrie UV à 260 nm pour doser les acides nucléiques.

Le taux de siRNA dans chaque fraction est ensuite calculé en utilisant les gammes étalon appropriées. Sur l'ensemble des formulations, on retrouve un taux de siRNA total entre 75 et 125%. Cette marge d'erreur est probablement due à des erreurs de manipulations, suite à l'utilisation de très petites quantités permettant d'économiser le matériel et à la faible sensibilité du spectrophotomètre.

Le dosage des siRNA a révélé des taux d'encapsulation allant jusqu'à 65% pour la formulation utilisant les lipoplexes DOTAP/DOPE au rapport de charge de 5, mais cette formulation présente une taille supérieure aux autres formulations. Cette augmentation de taille après encapsulation de lipoplexes a aussi été observée pour la formulation des LNC ADN, utilisant également ces lipides et ce CR, et pourrait être liée à la nature des lipoplexes. Le lipide DOTAP possède une seule charge positive par molécule comparé aux autres lipides

utilisés qui en possèdent 2 (BGTC) ou 4 (DOSP), donnant lieu à des lipoplexes de taille plus élevée. En effet, la taille des lipoplexes DOTAP/DOPE/siRNA au CR 5 est de 680 nm comparé à 234 nm (DOSP/DOPE/siRNA CR 5) et 344 nm (BGTC/DOPE/siRNA CR 4) (tableau 1, publication No 2). Même si un réarrangement des lipides a lieu systématiquement durant la formulation puisqu'en final les LNC siRNA ont des tailles inférieures à celles des lipoplexes, la nature et la quantité de lipide cationique ont sûrement leur influence. La structure exacte des LNC siRNA n'est pas encore connue, mais ce dosage est un premier indice permettant de localiser et de quantifier les siRNA dans la formulation.

Les formulations ADN

En parallèle, la caractérisation des vecteurs ADN développés précédemment a été poursuivie. Le tableau 5 récapitule les caractéristiques physico-chimiques des différentes formulations.

	MMS ADN BGTC	MMS ADN BGTC GAL	MMS ADN DOSP	MMS ADN DOSP GAL	LNC ADN	LNC ADN PEG
Taille [nm]	150 +/- 32	298 +/- 171	198 +/- 57	152 +/- 58	114 +/- 25	132 +/- 3
PDI	0,4	0,5	0,4	0,5	0,3	0,3
Potentiel zeta [mV]	-3 +/- 2	-2 +/- 1	0	-2 +/- 0	27 +/- 12	-17 +/- 4

Tableau 5 : *Caractéristiques des différents nanovecteurs d'ADN*

Le système MMS ADN BGTC (GAL)

Le système MMS ADN BGTC a été développé et caractérisé *in vitro* par Emilie Letrou-Bonneval *et al*. [3]. Dans ses travaux, elle montrait une accumulation spécifique des MMS ADN BGTC portant le ligand galactose dans des hépatocytes primaires *in vitro*. Cette internalisation est reliée aux récepteurs aux asialoglycoprotéines (ASGPR) exprimés par les hépatocytes et capables d'interagir avec le galactose présent à la surface des MMS ADN BGTC GAL [3-5]. Nous avons pu confirmer ces résultats *in vivo* sur des animaux sains (publication No 2) et des animaux porteurs de tumeurs (publication No 3 et 4). L'imagerie par fluorescence a révélé une accumulation spécifique des MMS ADN BGTC dans le foie qui s'accentue avec la présence de galactose à leur surface. Par contre, aucune présence de ces vecteurs dans le tissu tumoral n'a pu être détectée. Ces vecteurs, notamment en présence de

galactose, sont donc destinés à cibler spécifiquement les hépatocytes plutôt que les cellules cancéreuses (en dehors du cancer du foie). Dans cette optique, des expériences sur des souris saines utilisant ces vecteurs et un ADN plasmidique codant pour l'érythropoïétine (EPO) ont été menées (études non publiées). Le but était d'augmenter l'expression d'EPO en mettant en évidence une augmentation du taux d'hématocrite, mesuré une fois par semaine, suite à trois injections en intraveineuse une fois par semaine. Cette méthode de détection, pourtant plus sensible qu'un dosage luciférase et mesurant dans le sang indirectement l'expression de l'EPO n'a pas montré de changement du taux d'hématocrite (en moyenne 43% avant injection et durant la période d'observation). En revanche une injection intramusculaire avec un contrôle positif a induit une augmentation d'hématocrite importante de 71%, 5 semaines après la première injection.

Ces résultats amènent à se poser plusieurs questions :

- Est-ce que l'accumulation de ces systèmes dans le foie observée en imagerie par fluorescence est bien une accumulation dans les hépatocytes ou plutôt une capture par les macrophages et donc une accumulation dans des cellules Kupffer ? L'ajout de galactose pourrait éventuellement accentuer cette capture en diminuant la furtivité de ces systèmes.
- Si l'accumulation est bien dans les hépatocytes, est-ce que l'ADN plasmidique est en quantité suffisante et encore suffisamment intact pour accomplir son action ?
- L'ADN plasmidique atteint-il son site d'action, le noyau cellulaire ?

Le système MMS ADN DOSP (GAL)

Ces nouveaux vecteurs MMS ADN DOSP possèdent une taille un peu plus grande que les MMS ADN BGTC, par contre l'ajout de galactose semble diminuer leur taille qui se rapproche alors de celle des MMS ADN BGTC. Cela pourrait être du à la nature du lipide cationique, le DOSP (poids moléculaire de 1672 g/mol et 4 charges positives) qui est une molécule plus grosse que le BGTC (poids moléculaire de 716 g/mol et 2 charges positives) et forme des MMS ADN plus grand. Le galactose (poids moléculaire 180 g/mol), fixé de manière covalente au stabilisateur stérique F108 (poids moléculaire 14600 g/mol), pourrait par contre s'intercaler plus facilement entre les molécules de DOSP que celle de BGTC et, en conséquence, diminuer la taille des particules obtenues (figure 12).

Après injection par voie systémique dans des souris saines, le profil de distribution a montré un temps de circulation prolongé par rapport aux MMS ADN BGTC sans accumulation dans un organe spécifique. Cette circulation prolongée dans le sang est probablement due à la présence du F108, utilisé comme stabilisateur stérique pour les MMS ADN contenant, comme le PEG, des unités d'oxyde éthylène (80% de poly(éthylène oxyde), PEO_{127}-PP_{50}-PEO_{127} [3]). L'association de ce polymère aux lipoplexes DOSP/DOPE/ADN engendre probablement une conformation des chaînes d'oxyde d'éthylène plus intéressante qu'avec les lipoplexes BGTC/DOPE/ADN, permettant d'éviter une accumulation dans le foie (figure 12). L'ajout de galactose à la surface a entrainé une accumulation spécifique dans le foie comparable à celle obtenue avec les MMS ADN BGTC GAL et certainement liée aux interactions galactose/ASGPR [3-5].

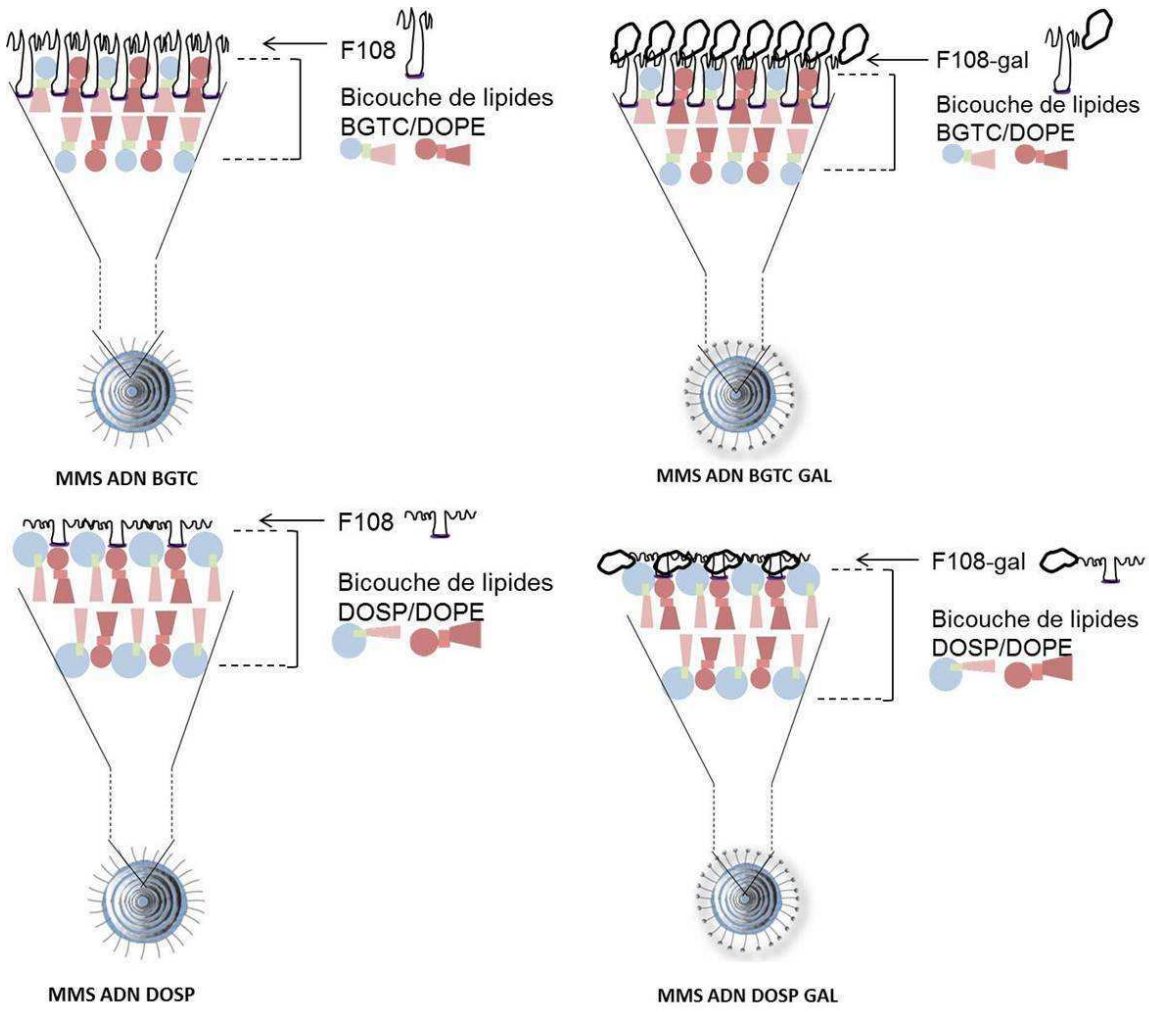

***Figure 12** : Schéma de la structure des MMS ADN BGTC GAL et MMS ADN DOSP GAL*

En présence d'une tumeur implantée en sous-cutané, le profil de biodistribution de ces vecteurs est modifié et une accumulation dans le tissu tumoral a été démontrée *in vivo* sur un modèle de gliome. Une certaine expression de luciférase dans la tumeur a également pu être détectée, mais seulement pour les systèmes portant le galactose à leur surface. Le traitement utilisant l'approche par gène suicide avec ce système MMS ADN DOSP GAL a montré une baisse de croissance tumorale intéressante, mais non-significative à partir du Jour 9 après le début du traitement. D'une part, l'effet EPR (« enhanced permeability and retention effect ») [6, 7] joue certainement un rôle pour amener les vecteurs dans le tissu tumoral, comme c'est le cas pour les MMS ADN avec et sans galactose, mais la présence de galactose à leur surface semble être importante pour obtenir une transfection. Cela peut être relié soit à une internalisation spécifique, due au galactose qui représente une source d'énergie importante et qui pourrait se fixer à des lectines comme par exemple au galectin-1 [8], surexprimé sur les cellules de gliome [9, 10], soit à leur taille, qui est plus petite en présence du galactose. Le mécanisme exact, menant à une accumulation de ce GAL MMS ADN DOSP dans la tumeur, reste encore à élucider. Pour compléter cette étude, un traitement à des temps plus précoces et des groupes avec un plus grand nombre d'animaux devraient être effectués et pourraient accentuer cette baisse de croissance tumorale. Les résultats obtenus pendant ces travaux de thèse indiquent que ces systèmes pourraient être utilisés dans le traitement de cancers, même en utilisant des injections répétées puisqu'une double injection sur souris saines n'a révélé aucune toxicité et aucune modification du profil de distribution (publication No 2).

Le système LNC ADN (PEG)

Les LNC ADN (PEG) ont déjà été caractérisées *in vitro* et *in vivo* auparavant ; par contre, la localisation exacte et la quantité d'ADN plasmidique encapsulé dans les LNC n'avaient pas encore été déterminées. Pour cette raison, le dosage développé pour quantifier et localiser les siRNA dans les formulations de LNC siRNA a été adapté pour les LNC ADN. Ce dosage a révélé un rendement d'encapsulation d'environ 23% avec quasiment la totalité d'ADN sous forme dissociée des lipides cationiques utilisés pour la formation des lipoplexes. En revanche environ 65% d'ADN plasmidique restent complexés dans des lipoplexes mais, à l'extérieur des LNC. Ces lipoplexes ne sont certainement pas totalement éliminés durant les étapes de purification ou de post-insertion de PEG, comme le révèlent les électrophorèses réalisées (figure 2a, publication no 2).

Les questions qui se posent maintenant sont :

- Le dosage de lipoplexes (libres) est-il fiable ou la soude, par exemple, est-elle capable de déstabiliser les LNC ADN pour libèrer de l'ADN plasmidique ?

Contrairement aux LNC siRNA, les LNC ADN ne contiennent pas de lipoid, ce qui rend les LNC ADN plus souples comparativement aux LNC siRNA. La soude ajoutée en quantité importante pourrait fragiliser plus facilement les LNC ADN et provoquer un relargage de l'ADN, ce qui conduirait à un taux de lipoplexes libres plus élevé qu'en réalité. Il est à noter également que le dosage des lipoplexes se fait en deux étapes. Dans la première étape, on dose d'abord les lipoplexes libres en dehors des LNC puis, dans la deuxième étape, les lipoplexes encapsulés dans les LNC. Quasiment aucun ADN complexé aux lipides cationiques n'a pu être détecté dans les dosages (tableau 1, publication No 2), ce qui pourrait également être dû au fait que tout l'ADN a déjà été libéré lors de la première étape.

- Si le dosage est fiable, est-ce que les lipoplexes ne pourraient pas s'associer d'une manière ou d'une autre aux LNC ADN empêchant leur séparation sur colonne de sépharose, ou lors de l'étape de concentration suivant la colonne ?

Cette hypothèse reste à tester.

Une administration systémique de ces LNC ADN en présence et absence de longues chaines de PEG confirment la circulation prolongée des LNC ADN PEG et l'accumulation des deux types de LNC dans les tumeurs sous-cutanées de gliome. De plus, l'accumulation dans des tumeurs de mélanome a été démontrée (publication No 3), certainement reliée à l'effet EPR [6, 7].

Un traitement utilisant l'approche par gène suicide, a montré une baisse de croissance tumorale significative à partir du jour 2 pour le modèle de gliome et du jour 4 pour le modèle de mélanome, comparativement aux animaux non-traités. Une répétition de ce traitement avec un nombre plus important d'animaux, de manière plus précoce et en débutant à un volume tumoral précis pourrait peut-être encore accentuer cet effet. Un traitement avec les LNC ADN PEG sans GCV montre également une baisse de croissance importante mais non-significative, contrairement à un traitement avec les LNC PEG sans ADN et sans GCV. Cette réduction de croissance tumorale pourrait être liée à une toxicité des lipoplexes libres. Il est à noter également que les caractéristiques physico-chimiques des 2 types de LNC ne sont pas identiques : les LNC PEG possèdent une taille d'environ 50 nm avec un potentiel zéta

légèrement négatif, les LNC ADN PEG une taille d'environ 130 nm avec un potentiel zéta de -17 mV.

Enfin, un autre moyen d'augmenter l'efficacité pourrait être de réaliser des administrations répétées. En revanche, dans le cas des LNC ADN, quelques précautions devraient être prises afin de ne pas avoir un effet inverse dû au phénomène ABC (« accelerated blood clearance phenomenon ») (Figure 13) déjà observé dans la littérature [11-13]. Ce phénomène est dû au fait que les LNC ADN PEG activent les cellules B, réactives au PEG, induisant une production d'IgM anti-PEG [14-16]. Après une deuxième injection au bout d'une semaine, le système immunitaire reconnait ces LNC ADN PEG, des cytokines sont produites et les LNC ADN PEG sont éliminées rapidement, majoritairement par les cellules de Kupffer [16-19]. De plus, comme ces vecteurs contiennent un ADN plasmidique immunogène, d'autres chemins de signalisation comme celui du « Toll-like récepteur » (TLR) 9 sont activés [18] et le fait d'utiliser des souris athymiques ne permet pas aux souris de réguler correctement ces réactions immunitaires, menant à des réactions sévères pouvant aller jusqu'à la mortalité [13, 20, 21].

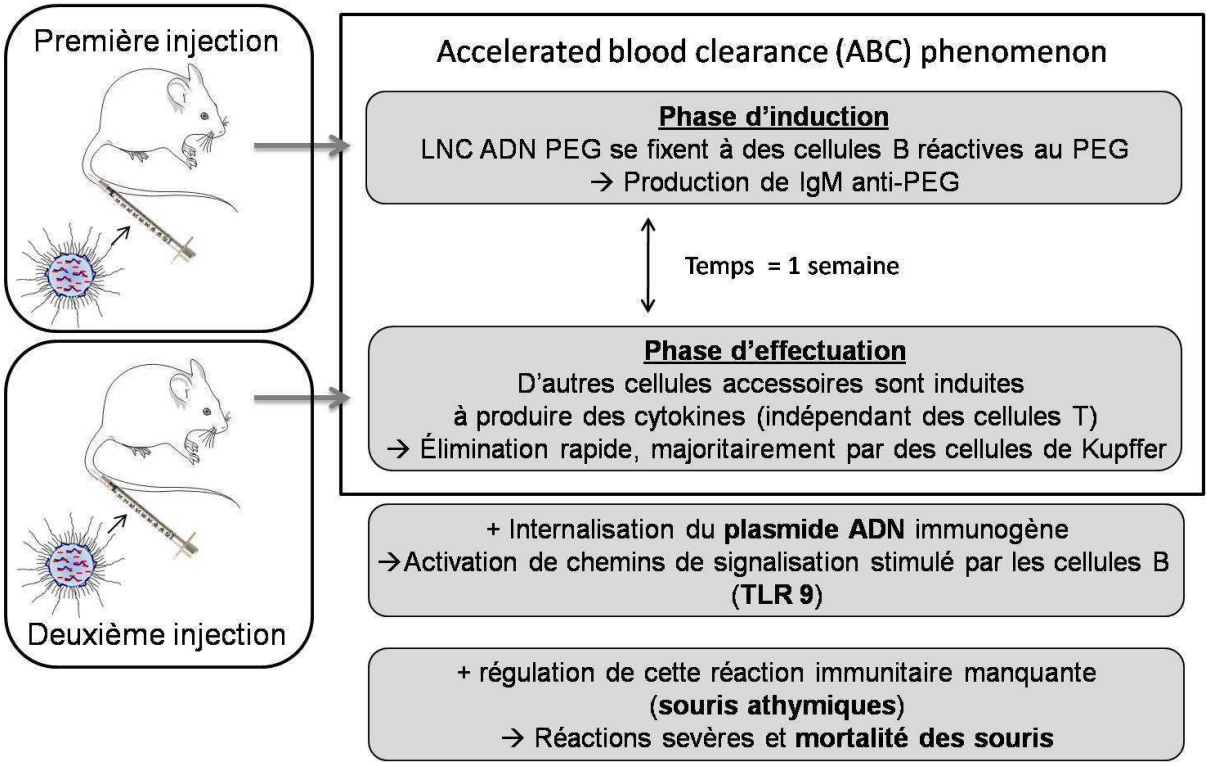

***Figure 13** : Problèmes rencontrés après une injection répétée de LNC ADN PEG*

Pour éviter ce phénomène et les réactions sévères observées, plusieurs points seront à considérer à l'avenir :

- Utiliser un autre type de PEG pour recouvrir les nanovecteurs.

Ce point est difficilement réalisable pour les LNC ADN, mais pourrait être pris en compte pour les LNC siRNA qui, a priori, risquent de montrer les mêmes effets. Dans la littérature, différents polymères (PEG-S-DMG = PEG-dimyristoylglycerol ou PVP = poly(N-vinyl-2-pyrrolidone)) ont été utilisés pour diminuer ou éviter ce phénomène ABC [12, 22].

- Changer l'intervalle de temps entre les deux injections.

Effectivement, Judge *et al*. ont déterminé une concentration maximale d'IgM anti-PEG 7 jours après la première injection qui persistait jusqu'au jour 14 et une production d'anti-IgG entre 20 et 28 jours [12, 23]. Lors de nos travaux de thèse, ce phénomène a également pu être observé, une deuxième injection 48h après la première ne montrant aucune réaction des souris et un profil de distribution similaire pour les deux injections alors qu'une injection 2 semaines après la première a induit une forte mortalité des souris.

- Utiliser un ADN plasmidique moins immunogène.

Les motifs induisant l'activation des chemins de signalisation comme TLR 9 sont les motifs CpG. Donc, l'utilisation d'un plasmide sans ces ilots CpG devrait diminuer la réaction immunitaire [13].

- Utiliser d'autres types de souris pouvant réguler ces réactions immunitaires.

Dans le cadre d'une étude sur un modèle tumoral, ce point sera également difficile à réaliser car ces souris sont utilisées pour éviter le rejet des cellules tumorales. Cependant, il est à prendre en compte étant donné que, dans la littérature, des effets beaucoup plus sévères ont été observés sur des souris athymiques ayant reçu 2 injections de liposomes contenant du PEG comparé à des souris non-athymiques. Une implication d'interleukine 10 dans la régulation de cette réponse immunitaire a été suggérée, mais le mécanisme exact de cette régulation reste à élucider [13, 20, 21].

REFERENCES

1. David, S., et al., Non-viral nanosystems for systemic siRNA delivery. Pharmacol Res, 2010. 62(2): p. 100-14.
2. Heurtault, B., et al., A novel phase inversion-based process for the preparation of lipid nanocarriers. Pharm Res, 2002. 19(6): p. 875-80.
3. Letrou-Bonneval, E., et al., Galactosylated multimodular lipoplexes for specific gene transfer into primary hepatocytes. J Gene Med, 2008. 10(11): p. 1198-209.
4. Schwartz, A.L., The hepatic asialoglycoprotein receptor. CRC Crit Rev Biochem, 1984. 16(3): p. 207-33.
5. Steirer, L.M., et al., The asialoglycoprotein receptor regulates levels of plasma glycoproteins terminating with sialic acid alpha2,6-galactose. J Biol Chem, 2009. 284(6): p. 3777-83.
6. Maeda, H., et al., Tumor vascular permeability and the EPR effect in macromolecular therapeutics: a review. J Control Release, 2000. 65(1-2): p. 271-84.
7. Maeda, H., The enhanced permeability and retention (EPR) effect in tumor vasculature: the key role of tumor-selective macromolecular drug targeting. Adv Enzyme Regul, 2001. 41: p. 189-207.
8. Camby, I., et al., Galectin-1: a small protein with major functions. Glycobiology, 2006. 16(11): p. 137R-157R.
9. Rorive, S., et al., Galectin-1 is highly expressed in human gliomas with relevance for modulation of invasion of tumor astrocytes into the brain parenchyma. Glia, 2001. 33(3): p. 241-55.
10. Camby, I., et al., Galectin-1 knocking down in human U87 glioblastoma cells alters their gene expression pattern. Biochem Biophys Res Commun, 2005. 335(1): p. 27-35.
11. Semple, S.C., et al., Immunogenicity and rapid blood clearance of liposomes containing polyethylene glycol-lipid conjugates and nucleic Acid. J Pharmacol Exp Ther, 2005. 312(3): p. 1020-6.
12. Judge, A., et al., Hypersensitivity and loss of disease site targeting caused by antibody responses to PEGylated liposomes. Mol Ther, 2006. 13(2): p. 328-37.
13. Tagami, T., et al., CpG motifs in pDNA-sequences increase anti-PEG IgM production induced by PEG-coated pDNA-lipoplexes. J Control Release, 2010. 142(2): p. 160-6.
14. Mosier, D.E. and B. Subbarao, Thymus-independent antigens: complexity of B-lymphocyte activation revealed. Immunology Today, 1982. 3(8): p. 217-222.
15. Laverman, P., et al., Factors affecting the accelerated blood clearance of polyethylene glycol-liposomes upon repeated injection. J Pharmacol Exp Ther, 2001. 298(2): p. 607-12.
16. Ishida, T., et al., Spleen plays an important role in the induction of accelerated blood clearance of PEGylated liposomes. J Control Release, 2006. 115(3): p. 243-50.

17. Jego, G., et al., Plasmacytoid dendritic cells induce plasma cell differentiation through type I interferon and interleukin 6. Immunity, 2003. 19(2): p. 225-34.

18. Peng, S.L., Signaling in B cells via Toll-like receptors. Curr Opin Immunol, 2005. 17(3): p. 230-6.

19. Poeck, H., et al., Plasmacytoid dendritic cells, antigen, and CpG-C license human B cells for plasma cell differentiation and immunoglobulin production in the absence of T-cell help. Blood, 2004. 103(8): p. 3058-64.

20. Aschenbrenner, K., et al., Selection of Foxp3+ regulatory T cells specific for self antigen expressed and presented by Aire+ medullary thymic epithelial cells. Nat Immunol, 2007. 8(4): p. 351-8.

21. Pecanha, L.M., et al., IL-10 inhibits T cell-independent but not T cell-dependent responses in vitro. J Immunol, 1993. 150(8 Pt 1): p. 3215-23.

22. Ishihara, T., et al., Evasion of the accelerated blood clearance phenomenon by coating of nanoparticles with various hydrophilic polymers. Biomacromolecules, 2010. 11(10): p. 2700-6.

23. Ishida, T., et al., Accelerated clearance of a second injection of PEGylated liposomes in mice. Int J Pharm, 2003. 255(1-2): p. 167-74.

Conclusion et Perspectives

L'objectif de cette thèse était de développer des nanovecteurs pour l'administration d'acides nucléiques par voie systémique.

En résumé cette thèse a apporté :

- ***Des nouvelles formulations LNC siRNA***

Ces nouvelles formulations LNC siRNA ont été développées avec des taux d'encapsulation et/ou des caractéristiques de vecteurs intéressants pour une administration par voie systémique. En parallèle, le dosage de siRNA a permis de déterminer la localisation des siRNA dans la formulation et le taux de siRNA présent dans les différents compartiments.
Par la suite, il faudra essayer d'augmenter l'encapsulation des siRNA dans les LNC en diminuant la proportion de lipoplexes libres, continuer leur caractérisation et tester ces nouvelles formulations *in vitro* et *in vivo*.

- ***Des informations supplémentaires sur les vecteurs ADN développés précédemment***

Le dosage développé pour caractériser les LNC siRNA a été adapté pour les LNC ADN PEG. Le taux d'encapsulation dans les LNC s'est avéré être plus faible (environ 20 – 25%) que pour les formulations siRNA. En revanche, une grande partie de l'ADN est complexée dans des lipoplexes, en dehors des LNC. Le dosage devra être perfectionné, par exemple en diminuant la quantité de soude pour élucider le fait de savoir pourquoi ces lipoplexes ne peuvent pas être éliminés, malgré la purification. Les profils de biodistribution sur des souris saines ont été déterminés pour les MMS ADN, testés auparavant uniquement *in vitro*, et pour les LNC ADN avec ou sans recouvrement de PEG, déjà testés *in vitro* et *in vivo* sur un modèle de gliome. Les profils de distribution se sont avérés différents pour chaque type de vecteur, ouvrant des possibilités d'utilisations variées. Les nanovecteurs ADN contenant le lipide cationique BGTC et/ou des ligands galactose à leur surface montrent une accumulation dans le foie. Les LNC ADN montrent une distribution sur l'ensemble de l'animal dès 1h après injection, mais sont rapidement éliminés. Par contre les nanovecteurs contenant soit le lipide cationique DOSP, soit un recouvrement de surface utilisant des longues chaines de PEG ont montré une circulation prolongée dans le sang. En revanche, l'utilisation de chaînes de DSPE-PEG_{2000} pour le recouvrement provoque une élimination rapide et une intolérance des souris après une deuxième injection. Pour la suite, il serait intéressant d'étudier précisément si, allant dans le foie, les vecteurs se dirigent vers les hépatocytes ou sont plutôt éliminés par le

système immunitaire via les cellules de Kupffer. D'autre part, l'expérience d'injection répétée des LNC ADN PEG devra être renouvelée, en utilisant dans un premier temps un ADN plasmidique CpG-free et/ou en choisissant un autre intervalle de temps entre les injections.

- ***Des premiers résultats en utilisant les nanovecteurs ADN sur des souris portant différents modèles de cancer***

L'administration systémique des nanovecteurs ADN sur des souris portant des cellules tumorales humaines en sous-cutané, montre des profils de biodistribution similaires à ceux obtenus dans les souris saines. Les nanovecteurs formulés avec le lipide cationique BGTC ne montrent pas d'accumulation dans la tumeur, contrairement aux nanovecteurs formulés avec le lipide cationique DOSP ou les LNC ADN avec ou sans recouvrement de PEG. Les LNC ADN PEG et les GAL MMS ADN DOSP donnent les taux d'expression de luciférase les plus élevés. Le traitement utilisant l'approche de gène suicide (HSV-tk/GCV) avec ces vecteurs entrainent une diminution de la croissance tumorale, comparativement aux souris non-traitées. Cette diminution de croissance tumorale pour les LNC ADN PEG est similaire entre le modèle de gliome et le modèle de mélanome. Ayant porté sur peu d'animaux avec une croissance tumorale très hétérogène, il serait intéressant de confirmer ces résultats avec un plus grand nombre d'animaux, après une injection à un volume tumoral précis et plus précoce.

Annexes

Publication en coauteur – Nature as a source of inspiration for cationic lipid synthesis

Genetica
DOI 10.1007/s10709-009-9405-8

Nature as a source of inspiration for cationic lipid synthesis

Romain Labas · Fanny Beilvert · Benoit Barteau · Stéphanie David · Raphaël Chèvre · Bruno Pitard

Received: 20 February 2009 / Accepted: 25 August 2009

Abstract Synthetic gene delivery systems represent an attractive alternative to viral vectors for DNA transfection. Cationic lipids are one of the most widely used non-viral vectors for the delivery of DNA into cultured cells and are easily synthesized, leading to a large variety of well-characterized molecules. This review discusses strategies for the design of efficient cationic lipids that overcome the critical barriers of in vitro transfection. A particular focus is placed on natural hydrophilic headgroups and lipophilic tails that have been used to synthesize biocompatible and non-toxic cationic lipids. We also present chemical features that have been investigated to enhance the transfection efficiency of cationic lipids by promoting the escape of lipoplexes from the endosomal compartment and DNA release from DNA-liposome complexes. Transfection efficiency studies using these strategies are likely to improve the understanding of the mechanism of cationic lipid-mediated gene delivery and to help the rational design of novel cationic lipids.

Keywords Cationic lipid · Design · Gene delivery · Liposome · Natural compound · Nonviral vector · Transfection

R. Labas · F. Beilvert · S. David · R. Chèvre · B. Pitard (✉)
INSERM, U915, 1 Rue Gaston Veil, 44035 Nantes, France
e-mail: bruno.pitard@univ-nantes.fr

R. Labas · F. Beilvert · S. David · R. Chèvre · B. Pitard
Université de Nantes, Faculté de Médecine, l'institut du thorax, 44000 Nantes, France

B. Barteau · B. Pitard
IN-CELL-ART, 1 place Alexis Ricordeau, 44093 Nantes, France

Abbreviations

BCAT	*O*-(2R-1,2-di-*O*-(1′Z,9′Z-octadecadienyl)-glycerol)-3-*N*-(bis-2-aminoethyl)-carbamate
BGSC	Bis-guanidinium-spermidine-cholesterol
BGTC	Bis-guanidinium-tren-cholesterol
CDAN	N^1-cholesteryloxycarbonyl-3,7-diazanonane-1,9-diamine
CHDTAEA	Cholesteryl hemidithiodiglycolyl tris(aminoethyl)amine
DCAT	*O*-(1,2-di-*O*-(9′Z-octadecenyl)-glycerol)-3-*N*-(bis-2-aminoethyl)-carbamate
DC-Chol	3β-[*N*-(*N*′, *N*′-Dimethylaminoethyl) carbamoyl]cholesterol
DLKD	*O*,*O*′-Dilauryl *N*-lysylaspartate
DMKD	*O*,*O*′-Dimyristyl *N*-lysylaspartate
DOG	Dioleylglycerol
DOGS	Dioctadecylamidoglycylspermine (Transfectam®)
DOGSDSO	1,2-Dioleoyl-*sn*-glycero-3-succinyl-2-hydroxyethyl disulfide ornithine
DOPC	1,2-Dioleoyl-*sn*-glycero-3-phosphocholine
DOPE	1,2-Dioleoyl-*sn*-glycerol-3-phosphoethanolamine
DOSN	Dioleyl succinyl ethylthioneomycin
DOSP	Dioleyl succinyl paromomycin
DOST	Dioleyl succinyl tobramycin
DOTAP	1,2-Dioleoyl-3-trimethylammoniopropane
DOTMA	*N*′-[1-(2,3-Dioleyloxy)propyl]-*N*,*N*,*N*-trimethylammonium chloride
DPPES	Di-palmitoyl phosphatidylethanolamidospermine

Published online: 11 September 2009

DS(9-yne)PE	Di(octadec-9-ynoyl)phosphatidyl ethanolamine
EDOPC	1,2-Dioleoyl-*sn*-3-ethylphosphocholine
FRET	Fluorescence resonance energy transfer
KanaCapChol	Cholesteryl caproyl kanamycin
KanaChol	3β-[6′-kanamycin-carbamoyl] cholesterol
KanaSucDODA	Dioctadecyl succinyl kanamycin
KanaSucDOLA	Dioleyl succinyl kanamycin
TGKC	3β-[6′-(1,3,3″-Triguanidino) kanamycin-carbamoyl] cholesterol
TGKSucDODA	Triguanidinium dioctadecyl succinyl kanamycin

Introduction

Gene transfer involves the delivery of nucleic acids to targeted cells and their subsequent expression. The introduction of DNA sequences that correspond to a functional gene, or interfere with the functioning of a cellular gene, is being actively investigated for the treatment of both inherited and acquired diseases (Mulligan 1993; Anderson 1998). As naked DNA alone does not promote high levels of gene expression, the success of such a strategy requires the use of efficient gene delivery vectors. Ideally, DNA delivery systems should (1) be safe, nontoxic, nonimmunogenic and well tolerated, (2) contain and protect nucleic acids in small particles, (3) interact with the cellular membrane and penetrate the target cell, (4) enable the intracellular trafficking of DNA to reach the nucleus and (5) permit biological activity by transgene expression.

Viral vectors, although very efficient, have several limitations including immunogenicity, toxicity and safety issues, in addition to large-scale production and quality-control costs. Thus, the development of non-viral alternatives has focused extensive research that has led to the emergence of two main synthetic vector categories: cationic polymers and cationic lipids. The self-assembled, nanometric complexes resulting from the electrostatic interactions between the negative phosphate groups of DNA and the positive charges of cationic lipids and cationic polymers are called lipoplexes and polyplexes, respectively (Felgner et al. 1997). Cationic lipids are amphiphilic molecules composed of a hydrophobic moiety (i.e. cholesterol, saturated or unsaturated alkyl chains) covalently linked via a spacer to a cationic headgroup. Polar hydrophilic headgroups include quaternary ammonium salts, primary, secondary and tertiary amine groups, amidinium salts and miscellaneous cationic headgroups. The linkers that connect hydrophobic and hydrophilic moieties are commonly composed of ether, ester, amide, carbamate and other labile bonds. Cationic lipids can be synthesized easily, using versatile chemical strategies that allow the modification of each constituent moiety, to produce a large variety of extensively characterized molecules. Thus, the structure–activity relationships of numerous series of cationic lipids have been investigated to elucidate the chemical requirements for efficient gene transfer (Wiethoff and Middaugh 2003; Niculescu-Duvaz et al. 2003). The polar hydrophilic headgroups enable the condensation of nucleic acids by electrostatic interactions with the negatively charged phosphate groups of the DNA, whereas the hydrophobic moieties help to maintain the self-aggregating lipid organization, such as the bilayer membrane, by co-operative intermolecular binding. The resulting lipoplexes present a heterogeneous size and supramolecular structure, depending on their composition. The physicochemical properties, on the macroscopic and the microscopic length scale, of supramolecular assemblies formed by lipoplexes are important parameters that govern transfection efficiency (Pitard 2002; Barteau et al. 2008). On the macroscopic length scale, DNA complexation and the size of lipoplexes are two essential physicochemical properties for efficient gene transfection. On the microscopic length scale, electron microscopy techniques allow the precise elucidation of the structural characteristics of the condensed structures of lipoplexes formed with various cationic lipids. Imaging of lipoplex structures by cryo-transmission electron microscopy (TEM) and small-angle X-ray scattering (SAXS) revealed that most of these cationic lipid/DNA complexes were organized as lamellar structures with DNA entrapped between the lamellae of aggregated multilamellar structures of cationic lipids.

Although the mechanism underlying cationic lipid-mediated transfection is not yet clearly established, understanding of the lipoplex characteristics involved in in vitro gene delivery has increased. In this review, we will focus on cationic lipids that have been used for in vitro gene transfection, with the particular aim to give a general overview of natural compounds that have been used as polar headgroups or hydrophobic domains for the design of cationic lipids. We will also discuss chemical features that have been evaluated to enhance the transfection efficiency of cationic lipids.

Natural lipid from plasma membrane

Since the breakthrough in lipid-mediated transfection that occurred with the development of the monocationic lipid *N*′-[1-(2,3-dioleyloxy) propyl]-*N,N,N*-trimethylammonium chloride (DOTMA) **1** (Felgner et al. 1987), the multivalent cationic lipid dioctadecylamidoglycylspermine (DOGS) **2** (Behr et al. 1989) and the cationic cholesterol derivative

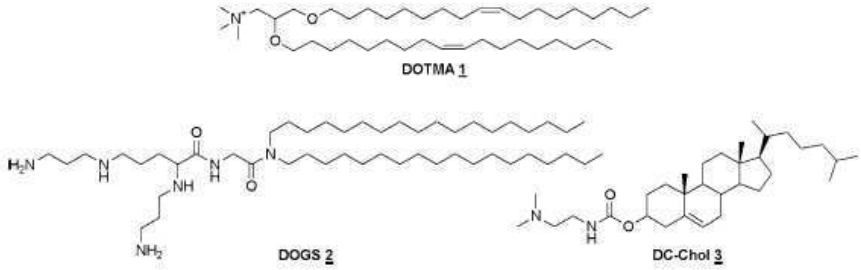

Fig. 1 Structure of cationic lipids DOTMA, DOGS and DC-Chol

3β-[*N*-(*N*′,*N*′-dimethylaminoethyl) carbamoyl] cholesterol (DC-Chol) 3 (Gao and Huang 1991), which were reported to deliver DNA efficiently into cells (Fig. 1), a large number of new synthetic cationic lipids have been characterized for their transfection efficiencies in a wide range of cell lines. Because toxicity and biocompatibility are considered to be critical factors that govern transfection efficiency, the use of natural compounds known for their safety has been actively investigated for the design of new biocompatible and non-toxic cationic lipids for DNA delivery. Table 1 summarizes the various approaches which have been followed to overcome some of the gene transfer barriers by using natural compounds. For the hydrophobic moieties of cationic lipids several natural lipids have been used including phospholipids, cholesterol and bipolar lipids from archeabacteria.

Cationic lipids derived from natural phospholipids

Phospholipids constitute major components of biological membranes and are widely used in lipoplex formulations. These natural lipids have also been converted into cationic derivatives, either by chemical modification or the synthesis of phospholipid analogues. For instance, the polycationic di-palmitoyl phosphatidylethanolamidospermine (DPPES) 4 (Behr et al. 1989) with a spermine polar headgroup and the quaternary ammonium 1,2-dioleoyl-*sn*-3-ethylphosphocholine (EDOPC) 5 (Rosenzweig et al. 2000) are two representative cationic lipids that were inspired by natural phospholipids (Fig. 2). The synthesis of analogues with chemical similarity to cell membrane phospholipids, namely phosphonate and phosphoramidate derivatives characterized by the absence of the glycerol moiety and alkyl chains directly bonded to the phosphorus atom, has also been described (representative examples 6 and 7, Fig. 2). Several structural modifications were performed including variations of the hydrophobic chain length (Le Bolc'h et al. 1995; Floch et al. 1998), the structure of the linker and of the polar head group (Lamarche et al. 2007; Mevel et al. 2007). An interesting structural modification was the substitution of the trimethylammonium polar head group by either a trimethylphosphonium or a trimethylarsonium, to decrease the toxicity of the cationic lipids (Floch et al. 2000; Guenin et al. 2000; Picquet et al. 2005). The rationale for this was based on a previous study that had used a similar strategy (Stekar et al. 1995) and on the fact that trimethylarsonium groups have been found in natural phospholipids (arsenocholine) from marine organisms (Junk et al. 1990). Thus, the replacement of a trimethylammonium polar head group by either a trimethylphosphonium or a trimethylarsonium effectively led to the development of cationic phospholipid analogues that were less toxic and showed higher transfection efficiencies up to 20-fold higher than their trimethylammonium counterparts (Montier et al. 2003).

Cationic lipids derived from cholesterol

Cholesterol is a natural compound that provides rigidity of cellular membranes and better stability of lipoplexes. Several cationic cholesterol derivatives have been synthesized, mainly using the hydroxyl group in position 3 to anchor the linker and the polar headgroup. Most of these cationic lipids are amine-containing compounds, with DNA interactions dependent on the protonation of ammonium groups. For instance, DC-Chol 3 (Fig. 1) is one of the members of the monovalent cholesterol derivatives family (Gao and Huang 1991) and cholesterylspermidine 8 (Moradpour et al. 1996) and the polyamine lipid GL67 9 (Lee et al. 1996) are multivalent cholesterol vectors for gene transfer (Fig. 2). In this category of lipids GL67 have been used to express Cystic fibrosis transmembrane conductance regulator in human clinical trials.

Cationic lipids derived from archaeal lipids

Archaea are a group of prokaryote microorganisms that were first detected in harsh environments like volcanic hot springs, but are now known to be widely distributed in nature (DeLong 1998). Their biochemistry is notably different from that of other life-forms (De Rosa et al. 1986) and archaeal membrane lipids have unique structure characteristics such as ether linkages and saturated isopranyl units (Koga and Morii 2007). The ether linkages provide a

Table 1 Summary of the various approaches which have been followed to overcome some of the gene transfer barriers by using natural compounds

Gene transfer barriers	Strategy	References
Particle formation and cellular internalization	Phospholipids	Behr et al. (1989)
		Rosenzweig et al. (2000)
		Mevel et al. (2007)
	Cholesterol derivatives	Gao and Huang (1991)
		Moradpour et al. (1996)
		Lee et al. (1996)
	Archaeal lipids	Benvegnu et al. (2005)
		Montier et al. (2008)
DNA complexation	Polyamines	Behr et al. (1989)
		Pitard et al. (1997)
		Turek et al. (2000)
	Amino acids derivatives	Byk et al. (1998)
		Heyes et al. (2002)
		Kumar et al. (2003)
		Kim et al. (2004)
		Obata et al. (2008)
	Guanidinium functions	Vigneron et al. (1996)
		Pitard et al. (2001)
	Aminoglycoside derivatives	Belmont et al. (2002)
		Sainlos et al. (2003)
		Desigaux et al. (2007)
Endosomal escape	Fusogenic lipids	Boussif et al. (2001)
		Gaucheron et al. (2001)
		Fletcher et al. (2006)
Cytoplasm delivery	Disulfide reduction	Tang and Hughes (1998, 1999)
		Byk et al. (2000)
		Wetzer et al. (2001)
		Kumar and Chaudhuri (2004)
		Bajaj et al. (2008)
Endosomal escape and cytoplasm delivery	Ortho ester functions	Zhu et al. (2000)
		By and Nantz (2004)
		Chen et al. (2007)
	Vinyl ether functions	Boomer and Thompson (1999)
		Boomer et al. (2002)
	Acylhydrazone functions	Aissaoui et al. (2004)

high chemical and enzymatic stability and the branching methyl groups improve membrane fluidity. Moreover, bipolar archaeal lipids span the membrane from one side to the other constituting a single-layer membrane with a higher degree of physical rigidity than bilayer membranes. These features have been applied to design archaeal bipolar lipid analogues for lipoplex mediated gene delivery (Benvegnu et al. 2005; Brard et al. 2007). The dicationic glycine betaine-based tetraether GRcat **10** (Fig. 3) in combination with 1,2-dioleoyl-*sn*-glycerol-3-phosphoethanolamine (DOPE), showed half of Lipofectamine transfection efficiency, while lipoplex formulations of MM18 **11** (Gilot et al. 2002) and the neutral archaeal derivative GR **12** led to in vitro transfection efficiency similar to Lipofectamine (Rethore et al. 2007). These results demonstrated that archaeal bipolar lipids can promote DNA delivery, either as helper lipids or as cationic vectors, and constitute a promising class of bio-inspired gene delivery systems (Montier et al. 2008).

Natural polar hydrophilic headgroups

The structural features of positively charged headgroups that interact with negatively charged phosphates of nucleic acids strongly impact on the transfection efficiency of cationic lipids. Therefore, the use of natural compounds including polyamine, amino acids and aminoglycoside as polar headgroups in cationic lipids has been studied to promote DNA interaction and biocompatibility.

Cationic lipids derived from natural polyamines

Spermine is a natural polyamine found in eukaryotic cells. This molecule exists in a polycationic form at physiological pH and is likely to associate with nucleic acids. The lipid DOGS **2** (Fig. 1) was the first-reported spermine derivative that led to efficient DNA delivery into cells (Behr et al. 1989). A structure–activity relationship study of geometrically differing polyamines as cationic headgroups (Fig. 4) revealed that the linear spermine derivative RPR120535 **13** displayed up to 18-fold higher transfection efficiency in HeLa cells compared with the T-shaped RPR126096 **14** or the globular and branched spermine analogues **15** and **16** (Pitard et al. 1997; Byk et al. 1998; Turek et al. 2000). This cationic lipid **13** was also found to possess a transfection efficiency similar to the commercially available Transfectam® (DOGS **2**) and Lipofectamine™ in four different cell lines (NIH3T3, 3LL mouse Lewis lung carcinoma, Caco-2 human colon carcinoma and primary rabbit smooth muscle cells). The interesting properties of this linear shaped spermine derivative **13** might result from a high steric flexibility of the polyamine linked to the lipid by one of its extremities, allowing a constructive interaction with DNA.

Amino acid-based cationic lipids

Amino acids have been described either as linkers or headgroups for the design of cationic lipids for DNA

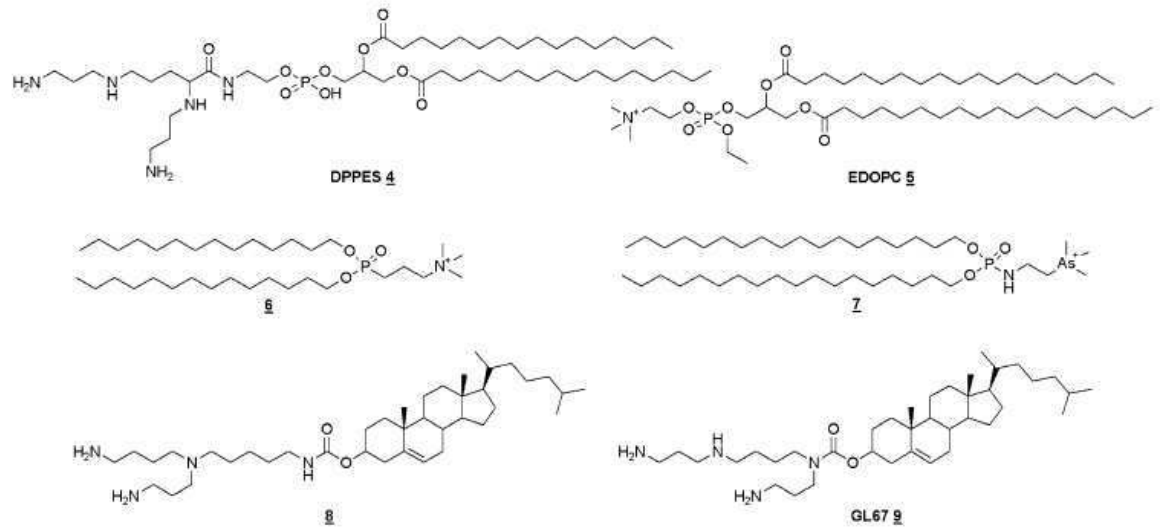

Fig. 2 Structure of cationic phospholipids and cholesterol derivatives

Fig. 3 Structure of archaeal lipid analogues and MM18

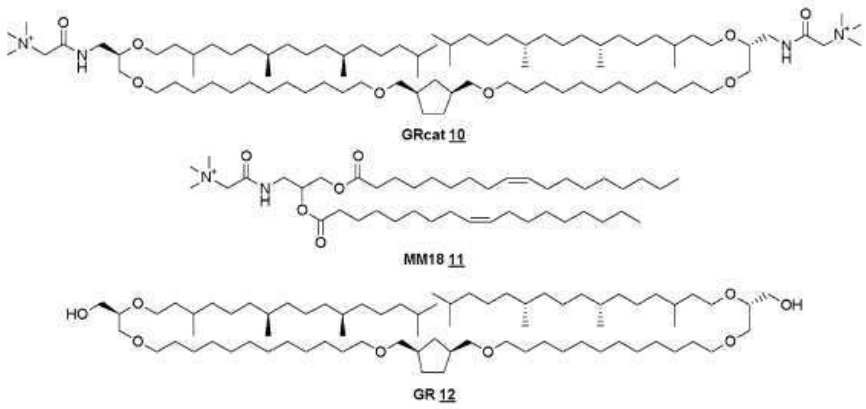

delivery. For instance, the spermine headgroup in **13** is linked to the dialkyl hydrophobic chain via a glycine (Fig. 4). The replacement of this neutral amino acid by a positively charged arginine or lysine (cationic lipids **17** and **18**, Fig. 5) increased the net positive charge of the vector and resulted in slightly decreased transfection efficiency. In contrast, the introduction of glutamic acid reduced the overall cationic charge available for DNA binding, without a loss in transfection activity (Byk et al. 1998). These results underlined the fact that increasing the net charge of the cationic headgroup is not necessarily beneficial for DNA delivery.

The introduction of a single histidine residue as a polar headgroup in cationic amphiphiles has been reported to confer endosome-disrupting characteristics that enhance gene transfer (Kumar et al. 2003). Indeed, the membrane fusion activity of the histidylated cationic lipid **20** (Fig. 5), as measured by fluorescence resonance energy transfer (FRET) experiments, was induced at pH 5.0 or 6.0, supporting the endosome-fusion property of the histidine-containing lipid **20** in the acidic environment of endosomes. The transfection efficiency of DNA complexed with lipid **20** lipoplexes compared with FuGENE^{TM}6 and DC-Chol **3** lipoplexes was similar in A549, 293T3 and HeLa cell lines and up to 100-fold higher in HepG2 cells (Kumar et al. 2003).

Novel amino acid-based cationic lipids incorporating lysine, histidine or arginine as the polar headgroup have been synthesized and tested for their transfection efficiencies (Heyes et al. 2002; Kim et al. 2004; Obata et al. 2008). The diether lipids **21** and **22**, with C_{12} alkyl chains and a lysine or an arginine headgroup (Fig. 5), were found to promote gene transfection up to tenfold higher than DC-Chol **3**/DOPE lipoplexes. The formulations containing

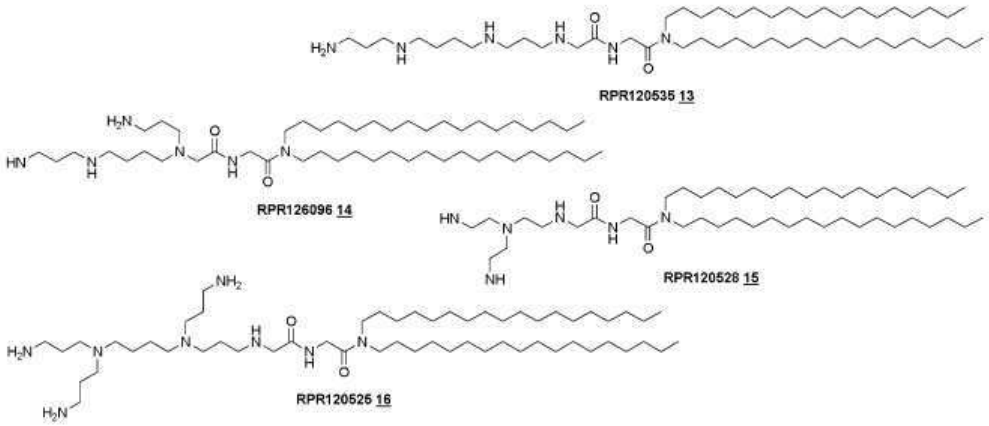

Fig. 4 Geometrically differing polyamines

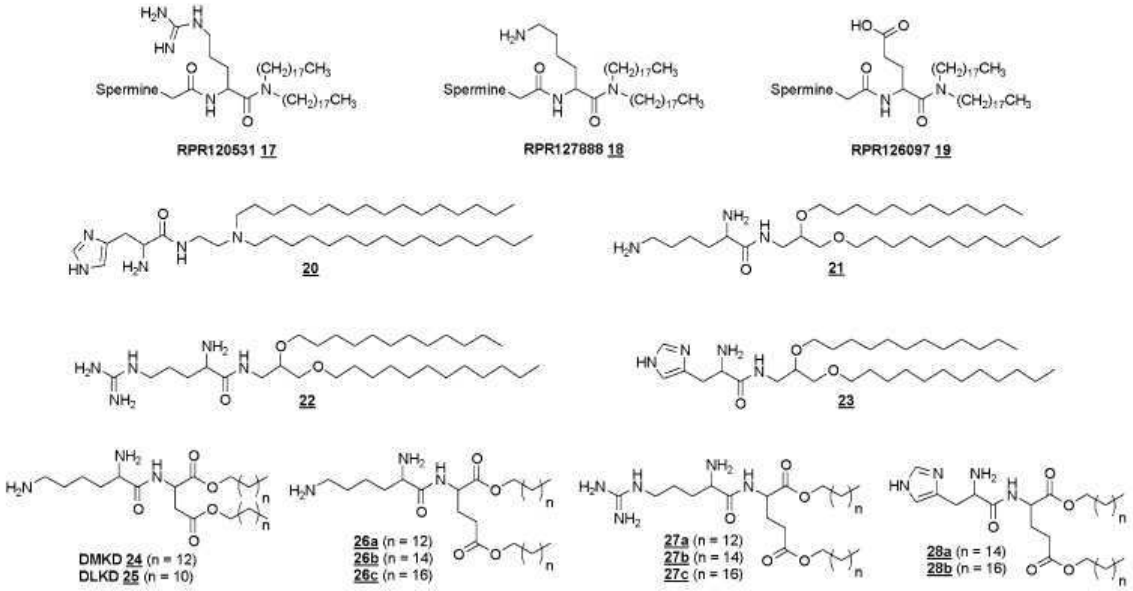

Fig. 5 Amino acid based cationic lipids

the histidinylated diether lipid **23** achieved a threefold increase in transfection efficiency compared with the control (Heyes et al. 2002). The lysine-containing cationic lipids *O,O'*-dimyristyl *N*-lysylaspartate (DMKD) **24** and *O,O'*-dilauryl *N*-lysylaspartate (DLKD) **25** with, respectively, C_{14} and C_{12} alkyl chains, were reported to be more efficient in transfecting 293 and B16BL6 cell lines than 1,2-dioleoyl-3-trimethylammoniopropane (DOTAP), contrary to the C_{16} and C_{18} derivatives (Kim et al. 2004). Moreover, the lysine- and arginine-type lipids **26a–c** and **27a–c**, having a glutamate backbone, exhibited higher gene expression efficiencies than Lipofectamine2000™, and this effect tended to increase with shorter alkyl chains. Lipoplexes containing the histidinylated lipids **28a–b** produced no detectable levels of gene expression (Obata et al. 2008).

Taken together, these observations suggest that the transfection efficiency obtained with cationic lipids containing amino acid-based headgroups is higher using lysine and arginine than with histidine, despite the endosome-disrupting characteristics of histidine. A putative explanation may be inferred from the physicochemical properties of the lipoplexes; indeed lysine and arginine derivatives **26** and **27** formed unilamellar vesicles, whereas the histidine-

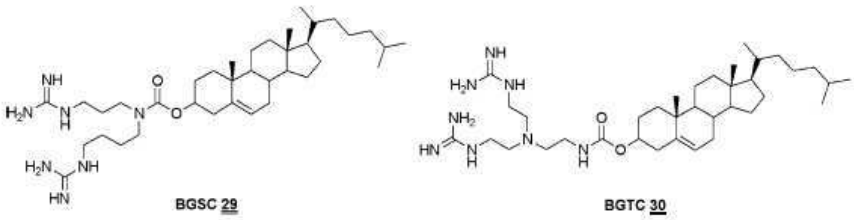

Fig. 6 Structure of bis-guanidinium-cholesterol derivatives BGSC 29 and BGTC 30

type lipid 28 formed a tube-like structure (Obata et al. 2008). In addition, gene expression seems to be enhanced by decreasing the length of the hydrophobic chain, irrespective of the linker backbone.

The strength of the electrostatic interactions between nucleic acids and cationic lipids that lead to DNA compaction mostly depends on the protonation state of ammonium groups and, consequently, relies on pH. The highly basic guanidinium function found in arginine amino acid residues remains protonated over a wide range of pHs, leading to DNA binding that is less sensitive to pH variations. Its binding to the DNA phosphate anions proceeds through a structural organization involving characteristic pairs of parallel hydrogen bonds (Cotton et al. 1973); the guanidinium group can also interact with nucleic acids via hydrogen bonds and plays a key role in DNA-binding proteins. These favorable features of the guanidinium function underlie its use as a headgroup in the development of a novel class of cationic cholesterol derivatives for DNA delivery. Bis-guanidinium-spermidine-cholesterol (BGSC) 29 and bis-guanidinium-tren-cholesterol (BGTC) 30 (Fig. 6) were the first two guanidinium-containing cationic lipids to be reported and tested for transfection (Vigneron et al. 1996). Both BGTC 30 and BGSC 29 showed higher transfection efficiencies than Lipofectin™ (DOTMA/DOPE, 1/1,w/w) in several mammalian cell lines when formulated as liposomes with DOPE. Moreover, BGTC 30 used alone as a micellar solution was found to promote efficient in vitro transfection, but to a lesser extent than its liposome formulation (Vigneron et al. 1996; Oudrhiri et al. 1997; Pitard et al. 1999, 2001). These results highlight the point that cationic lipids characterized by headgroups composed of guanidinium functions represent an attractive option for gene delivery.

Aminoglycoside-derived cationic lipids

Aminoglycoside antibiotics constitute a large family of natural polycationic compounds that are widely used for the treatment of gram-negative infections (Umezawa and Hooper 1982). Most of aminoglycosides are naturally synthesized by Actinobacteria (e.g., streptomyces) and they exhibit their antibacterial activity by selective binding to the ribosomal RNA of bacteria, which disrupts protein biosynthesis (Mingeot-Leclercq et al. 1999). Aminoglycosides are known to interact with A-form nucleic acids, especially the major groove of double-stranded RNA (Moazed and Noller 1987; Ogle et al. 2001), and their interactions with DNA have been reported to be weaker but sufficient to protect against nuclease activity. Structurally, aminoglycosides usually comprise a 2-deoxy-streptamine moiety that is monosubstituted (e.g., neamine), 4,5-disubstituted (e.g., neomycin) or 4,6 disubstituted (e.g., kanamycin) with amino sugars via a glycosidic linkage, and they carry up to six amino groups, which are mostly protonated at physiological pH (Dorman et al. 1976; Botto and Coxon 1983; Szilagyi et al. 1993). Thus, aminoglycosides provide a versatile polycationic framework that has been used for the design of novel cationic lipids for DNA delivery.

A series of kanamycin A-derived cationic lipids containing various spacers and lipophilic moieties has been synthesized (Sainlos et al. 2003) and their transfection efficiencies have been investigated (Belmont et al. 2002; Sainlos et al. 2005). The cholesterol-containing cationic lipid 3β-[6′-kanamycin-carbamoyl] cholesterol (KanaChol) 31 (Fig. 7) mediated efficient in vitro gene delivery in several mammalian cell lines, when formulated alone as micelles. The addition of DOPE into the cationic lipid formulation led to a higher transfection efficiency and decreased cytotoxicity (Belmont et al. 2002). The introduction of a spacer arm between kanamycin and cholesterol resulted in an increase in the mean molecular area and more-fluid lipidic layers that globally improved transfection efficiency; indeed cholesteryl caproyl kanamycin (KanaCapChol) 32 showed up to tenfold increased transfection activity compared with KanaChol 31 in HeLa, HEK293 and 3T3 cells (Sainlos et al. 2005). Kanamycin A-based cationic lipids with aliphatic hydrophobic moieties have also been synthesized and evaluated for DNA delivery in HeLa and 16HBE cells. Dioleyl succinyl kanamycin (KanaSucDOLA) 33 with unsaturated oleyl chains showed a higher transfection efficiency than dioctadecyl succinyl kanamycin (KanaSucDODA) 34 with saturated aliphatic chains, whether formulated with or without DOPE. A putative explanation arises from the enhancement of the layer fluidity induced by unsaturation that may give fusogenic activity to KanaSucDOLA 33 (Sainlos et al. 2005). The guanidinylated aminoglycosides 3β-[6′-(1,3,3″-triguanidino)kanamycin-carbamoyl] cholesterol (TGKC) 35 and

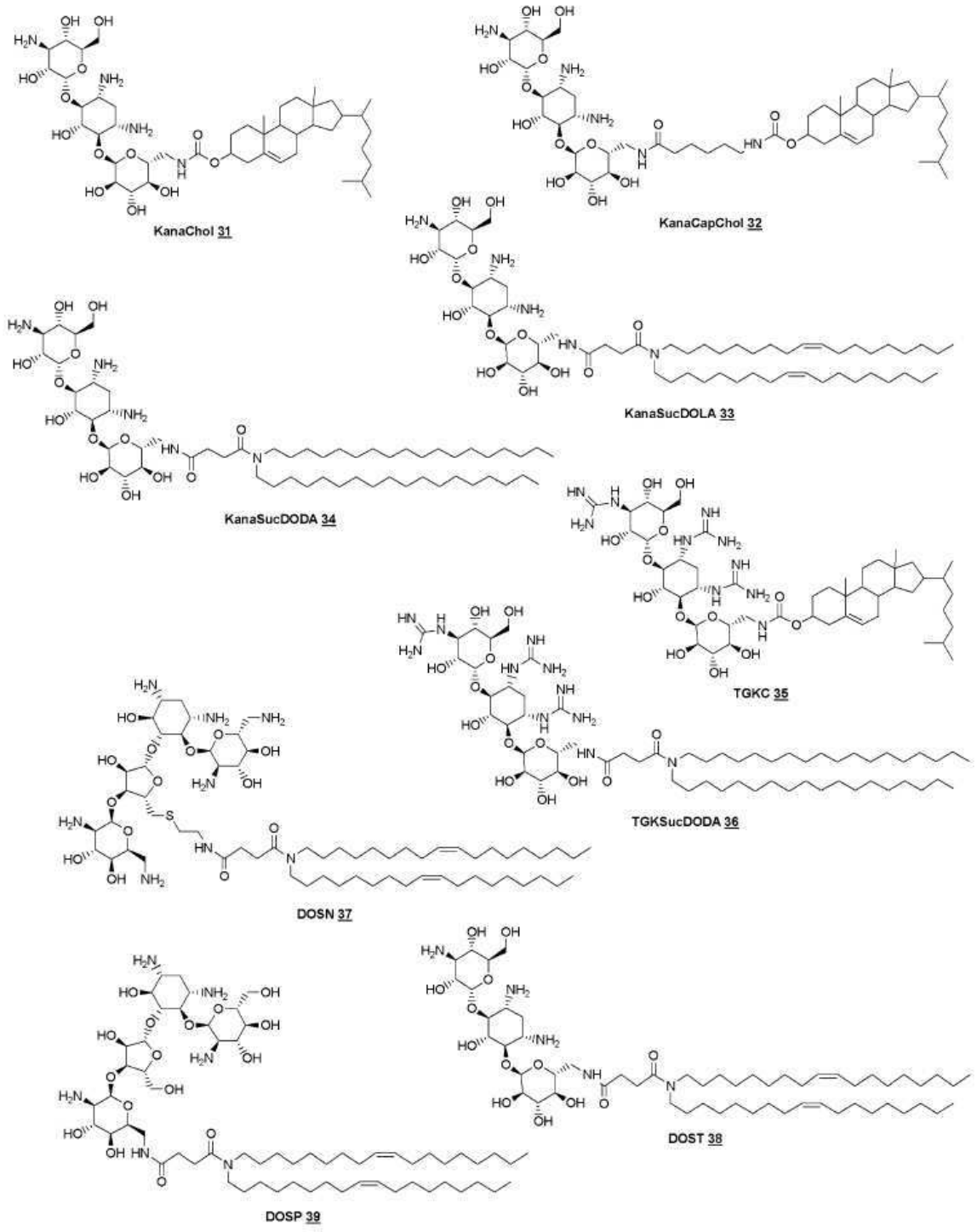

Fig. 7 Structure of aminoglycoside-based cationic lipids

triguanidinium dioctadecyl succinyl kanamycin (TGK-SucDODA) **36** were less efficient for gene delivery than their respective amino counterparts KanaChol **31** and KanaSucDODA **34**. This lower transfection activity may originate from a decreased endosomal escape of lipoplexes, caused by a lower buffering capacity of fully guanidinylated aminoglycosides (Belmont et al. 2002; Sainlos et al. 2005). It is noteworthy that aliphatic chain derivatives appeared to be more efficient than KanaChol **31**, irrespective of the formulation and the nature of the functional groups present in the aminoglycoside-based headgroup.

Aminoglycoside-based cationic aliphatic lipids for DNA transfer were also reported to promote efficient siRNA delivery and specific RNA interference into cells (Desigaux et al. 2007). Liposomes of such lipidic aminoglycoside derivatives, mixed with siRNA, exhibited various morphologies depending of the type of aminoglycoside. KanaSucDOLA **33** and dioleyl succinyl tobramycin (DOST) **38** (Fig. 7) are characterized by a 4,6-disubstituted 2-deoxystreptamine (4,6-DDS) ring and formed concentric multilamellar ("onion-like") structures consisting of a regular packing of lipid bilayers and siRNA molecules, very similar to those obtained with BGTC **30** liposomes. On the contrary, dioleyl succinyl ethylthioneomycin (DOSN) **37** and dioleyl succinyl paromomycin (DOSP) **39** containing a 4,5-disubstituted 2-deoxystreptamine (4,5-DDS) ring formed smaller lipoplexes of a much more irregular structure, composed of stacks of alternating lipid bilayers and siRNA with ordered microdomains, characterized by flat, fingerprint-like repetitions. The most active cationic lipid/siRNA complexes for gene silencing were obtained with 4,5-DDS aminoglycoside derivatives. In engineered cells expressing GFP, DOSN **37** and DOSP **39**, formulated as liposomes and complexed with GFP-targeting siRNA, effected a minimal residual GFP expression of less than 10% compared with control siRNA-transfected cells and untransfected cells. Identical results were obtained in RNA interference experiments of an endogenous gene in various human cell lines (d2GFP, HeLa and HEK293 cells) with complexes of DOSP **39** and siRNA targeting the endogenous lamin A/C expression. In transfected cells, only very low amounts of lamin A/C mRNA were detected by real-time quantitative RT-PCR, as compared with the amount detected in cells transfected with control siRNA (Desigaux et al. 2007). The evaluation of the cytotoxicity of aminoglycoside derivatives/siRNA complexes in the three different cells lines clearly showed that the viability of the transfected cells was not affected.

Altogether, these results demonstrate that aminoglycoside-based lipidic derivatives constitute a highly versatile and powerful class of cationic lipids that display a remarkably high efficiency for non-viral-mediated gene delivery and siRNA-based gene knockdown.

The contribution of organic chemistry to enhanced transfection efficiency

Escaping endosome by using fusogenic lipid strategy

Once internalized in the cell, lipoplexes must overcome several additional steps to effect efficient gene expression, and ultimately DNA molecules must be decomplexed from cationic lipids in order to be active because lipoplexes micro-injected into the nuclear compartment does not allow gene expression. As lipoplexes are generally thought to enter cells through a non-specific endocytosis mechanism (Gao and Huang 1995; Miller 1998; Aissaoui et al. 2002), their escape from the endosomal compartment is required to avoid lysosomal degradation of the DNA (El Ouahabi et al. 1997; Noguchi et al. 1998). Introduction of the natural phospholipid DOPE **40** (Fig. 8) in lipoplex formulations has been shown to provide a higher transfection efficiency in the case of many cationic lipid systems. This effect is possibly due to the fusogenic properties of DOPE that are attributed to its ability to undergo a transition from a lamellar to a hexagonal phase (Farhood et al. 1995; Hui et al. 1996). The resulting hexagonal complexes are more likely to fuse with the endosomal membrane, which may increase the subsequent disruption of this membrane and, thus, facilitate DNA release into the cytoplasm.

Several structural modifications of the helper lipid DOPE have been investigated to increase the transfection efficiency of liposome formulations. Partially fluorinated analogs of DOPE were thought to display a higher tendency to promote the transition from the lamellar to the hexagonal phase, due to their more pronounced cone-shape geometry compared to DOPE. For example, the fluorinated glycerophosphoethanolamine helper lipid [F8E11][C16]OPE **41** (Fig. 8) led to up to 90-fold higher transfection efficiency in A549 cells when formulated with the lipopolyamine pcTG90 **42** in HEPES compared to formulation containing DOPE (Boussif et al. 2001). However lipoplexes of pcTG90, DOGS or DOTAP with this fluorinated colipid formulated in 5% glucose resulted in comparable transfection efficiencies to those obtained with control DOPE lipoplexes (Gaucheron et al. 2001). Substitution of the double bond in the oleoyl fatty acid chain of DOPE with an acetylenic bond has also been investigated (Fletcher et al. 2006). The more phase-stable dialkynoyl analogue of DOPE, di(octadec-9-ynoyl) phosphatidylethanolamine (DS(9-yne)PE) **43** (Fig. 8), allowed for a reduction of the amount of the cationic lipid N^1-cholesteryloxycarbonyl-3,7-diazanonane-1,9-diamine (CDAN) **44** in lipoplex formulations with a cationic lipid/helper lipid molar ratio from 1/1 to 1/10, without apparent loss in transfection activity in Panc-1 cell line.

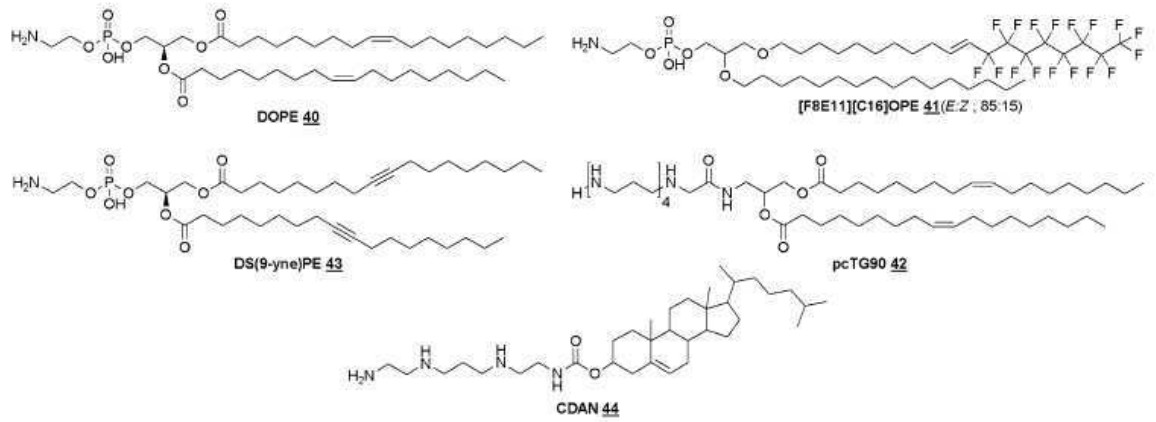

Fig. 8 Structure of helper lipids and cationic lipids pcTG90 and CDAN

Nevertheless, DOPE, 1,2-dioleoyl-*sn*-glycero-3-phosphocholine (DOPC) and cholesterol still represent the most used helper lipids in lipoplex-mediated transfection (Farhood et al. 1995; Hui et al. 1996; Pedroso de Lima et al. 2001; Zhang and Anchordoquy 2004; Majeti et al. 2005) and the development of new colipids that enhance gene delivery remains highly challenging.

Release of DNA in cytoplasm by intracellular disulfide reduction strategy

Another critical step to overcome, in order to achieve efficient transfection is the release of DNA molecules from DNA-cationic lipid lipoplexes. To ensure the intracellular collapse of the lipid-DNA complex, a rationale based on a reductive, environment-sensitive chemical function has been developed. The synthesis of disulfide bond-bearing, divalent cationic lipids that can undergo reduction by intracellular glutathione has been reported (Tang and Hughes 1998, 1999). These lipids (Fig. 9), namely cholesteryl hemidithiodiglycolyl tris(aminoethyl)amine (CHDTAEA) **45** and 1,2-dioleoyl-*sn*-glycero-3-succinyl-2-hydroxyethyl disulfide ornithine (DOGSDSO) **46**, showed, respectively, up to 7- and 50-fold higher transfection efficiencies in several cell lines compared with their non-disulfide analogues.

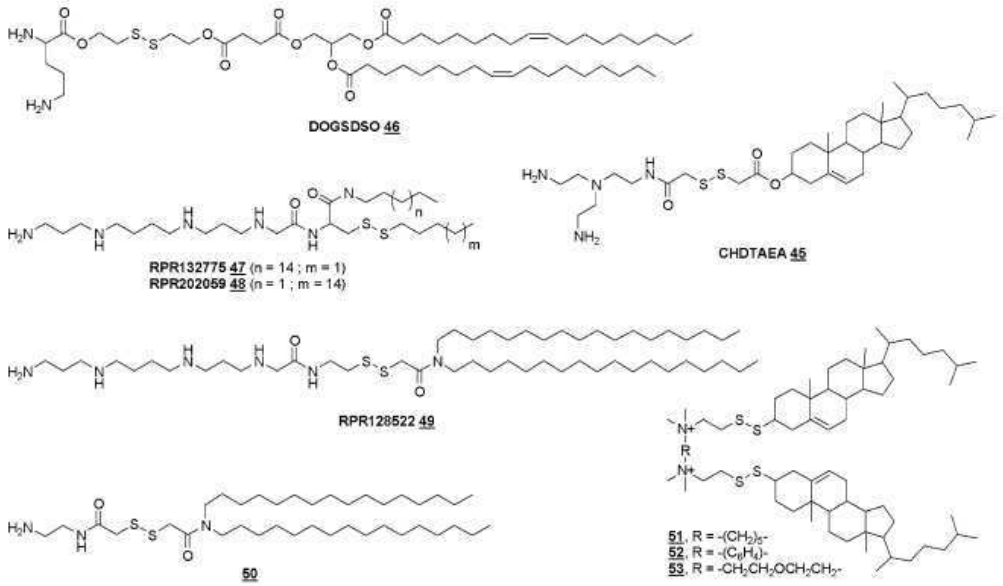

Fig. 9 Reducible cationic lipids

A structure–efficiency relationship study of reduction-sensitive lipopolyamines that contain a disulfide bond at various positions in the backbone of the lipids has also been published (Byk et al. 2000; Wetzer et al. 2001). The insertion of the disulfide bond inside one lipid chain (Fig. 9, lipids **47** and **48**) resulted in up to 1000-fold increased transfection efficiency compared with the non-disulfide lipid (Wetzer et al. 2001). In contrast, the introduction of the disulfide bond between the polyamine and the lipid (RPR128522 **49**) led to a total loss of transfection efficiency, probably due to a higher reduction kinetic, implying an early release of DNA (Byk et al. 2000). Another example of a cationic lipid that contains a disulfide bond inside the linker (Fig. 9, lipid **50**) also showed an extremely poor transfection activity compared with the non-disulfide control lipid (Kumar and Chaudhuri 2004). Electrophoric gel retardation and DNase I sensitivity experiments supported the hypothesis that the inefficient transfection activities of the disulfide bond containing lipoplexes **50** originated in part from the high degradation sensitivity of the lipoplexes by cellular DNase I. Recently, a series of thiocholesterol-derived gemini cationic lipids possessing hydrophobic flexible (Fig. 9, lipid **51**), hydrophobic rigid (lipid **52**) and hydrophilic flexible (lipid **53**) spacers were synthesized (Bajaj et al. 2008). The transfection efficiencies of the liposomal formulations were found to be dependent upon the cell line used, however the disulfide bond influence was not evaluated by comparison with the non-disulfide counterparts.

Several groups have also investigated the use of disulfide bonds to develop monomolecular particles by the dimerization of a thiol-containing, cationic detergent, entrapping only one DNA molecule per lipoplex (Blessing et al. 1998; Ouyang et al. 2000; Dauty et al. 2001; Fabio et al. 2005). The strategy relies on the ability of the cationic detergent to condense DNA into discrete particles that can consist of a single nucleic acid molecule. The particles are then "frozen" by oxidation of the thiol function that led to disulfide lipids on the template DNA (Blessing et al. 1998). The resulting small, monomolecular lipoplexes are stable in physiological conditions, have a negative zeta potential, but are not able to promote efficient transfection in cultured cells unless a large excess of detergent is present (Dauty et al. 2001) or they are mixed with a cationic vector (Ouyang et al. 2000). In these latter cases, reduction of the disulfide bond may occur inside the cell, leading to DNA release from DNA-liposome complexes. However such an effect has not yet been proven.

In conclusion, the disulfide reduction strategy is likely to promote the release of DNA from DNA-liposome complexes, leading to greater transfection activity. Nevertheless, such disulfide bond-containing cationic lipids must be designed carefully in order to avoid early lipoplex dissociation and/or degradation.

Escaping endosomes by using pH-sensitive strategy

In the cationic lipid-mediated transfection process, the endocytosis of lipoplexes is a cellular pathway characterized by a significant drop in pH. The medium of early endosomes at physiological pH, is progressively acidified to pH 6.5–6.0 in the late endosome, finally reaching pH 5.0 in the lysosome, where extensive degradation takes place (Mukherjee et al. 1997; Wiethoff and Middaugh 2003). The introduction of acid-labile groups into cationic lipids to form pH-sensitive lipoplexes represents an attractive strategy to enhance transfection efficiency because the decrease of pH in the endosome promotes the hydrolysis of the cationic lipid, leading to endosome disruption and concomitant DNA release from the lipoplex.

Ortho esters are one of the most acid-sensitive functional groups described in the literature (Cordes and Bull 1974; Deslongchamps et al. 2000) and polyortho esters have shown excellent biocompatibility for controlled drug release (Heller et al. 2002). The hydrolysis of an ortho ester starts with the rapid, acid-catalyzed cleavage of two alkoxy groups followed by the slower cleavage of the third alkoxy group that relies on the hydrolysis of an ester bond (Fig. 10).

Several ortho ester-containing cationic lipids have been synthesized and characterized for their susceptibility to undergo hydrolysis under mild acid conditions (Zhu et al. 2000; By and Nantz 2004; Chen et al. 2007). For instance, ortho ester lipid **54** (Fig. 11) underwent complete hydrolysis within 12 h after exposure to a pH 4.5 buffer solution at 38°C and its transfection efficiency in NIH 3T3 cells was up to tenfold higher than DOTAP and DC-Chol **3** (Zhu et al. 2000). A putative explanation of this improvement in transfection efficiency may lie in the detergent's behavior, induced by the hydrolysis product of **54**, a single amphiphilic alkyl chain, that is speculated to aid the escape of DNA from endosomes. The cyclic ortho ester lipid **61** (Fig. 11) also showed a significantly higher transfection efficiency than DOTAP in CV-1 and HTB-129 cells (Chen et al. 2007). In this case, two concomitant effects are thought to promptly destabilize the endosome membrane,

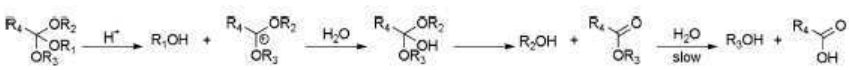

Fig. 10 General mechanism of ortho esters hydrolysis

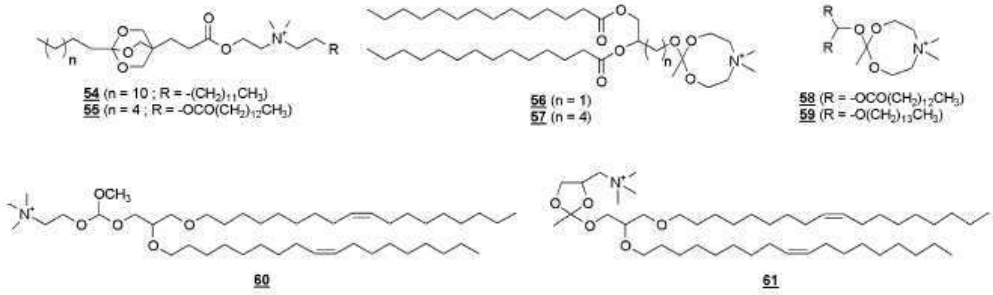

Fig. 11 Acid-labile cationic ortho esters lipids

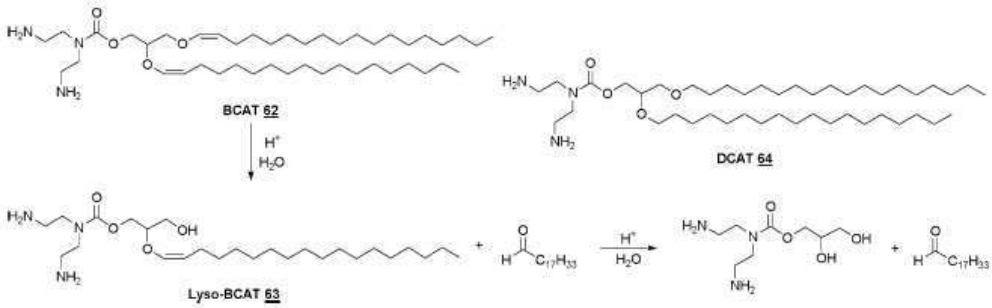

Fig. 12 Hydrolysis pathway of acid-labile lipid BCAT **62** and structure of lipid DCAT **64**

the acid-catalyzed cleavage of the cationic head groups that caused the aggregation of the lipoplexes and the generated conelike lipid dioleylglycerol (DOG) that favored the formation of the fusogenic hexagonal phase.

The use of an acid-sensitive vinyl ether linkage between the headgroup and the hydrocarbon side chains has been reported for a diplasmenyl lipid derivative (Boomer and Thompson 1999; Boomer et al. 2002). The hydrolysis pathway of the cationic lipid *O*-(2*R*-1,2-di-*O*-(1′Z,9′Z-octadecadienyl)-glycerol)-3-*N*-(bis-2-aminoethyl)-carbamate (BCAT) **62** involves the protonation of the vinyl ether *β*-carbon as the rate determining step, followed by the addition of water to the intermediate carbocation. The formed hemiacetal is then decomposed to generate a fatty aldehyde and a single chain cationic lipid fragment (Fig. 12, lyso-BCAT **63**) that undergoes hydrolysis following the same pathway (Boomer et al. 2002). Transfection experiments revealed that the acid-sensitive cationic lipid BCAT **62** exhibited luciferase expression levels five to eight times greater than the acid-insensitive control lipid *O*-(1,2-di-*O*-(9′Z-octadecenyl)-glycerol)-3-*N*-(bis-2-aminoethyl)-carbamate (DCAT) **64**, in four cells lines, without significant differences in the amount of DNA being delivered. These results strongly support the pH-sensitive strategy using vinyl ether linkage to enhance transfection efficiency.

The acid-sensitive acylhydrazone function has shown successful applications in drug delivery (Mueller et al. 1990; Kaneko et al. 1991; Kratz et al. 1997; Rodrigues et al. 1999) and has recently been applied to lipoplex-mediated gene delivery. The synthesis, characterization and transfection efficiency of a series of four cationic lipids incorporating an acylhydrazone linker between a guanidinium-based headgroup and a steroid hydrophobic moiety was reported (Aissaoui et al. 2004). The saturated steroid derivatives **65** and **66** (Fig. 13) were found to hydrolyze at a faster rate than the corresponding unsaturated lipids **67** and **68**, which contain a double bond conjugated to the C=N hydrazone double bond that provides a higher stability of the cationic lipids. Moreover, the saturated lipids **65** and **66** were unable fully to condense DNA even at high lipid/DNA charge ratios and to promote gene delivery, contrary to the unsaturated cholest-4-enone derivatives **67** and **68**. These results highlight the fact that the acid sensitivity of an acylhydrazone bond must be adjusted to promote efficient gene transfection.

The design of acid-labile cationic lipids to enhance transfection efficiency is highly versatile. The use of

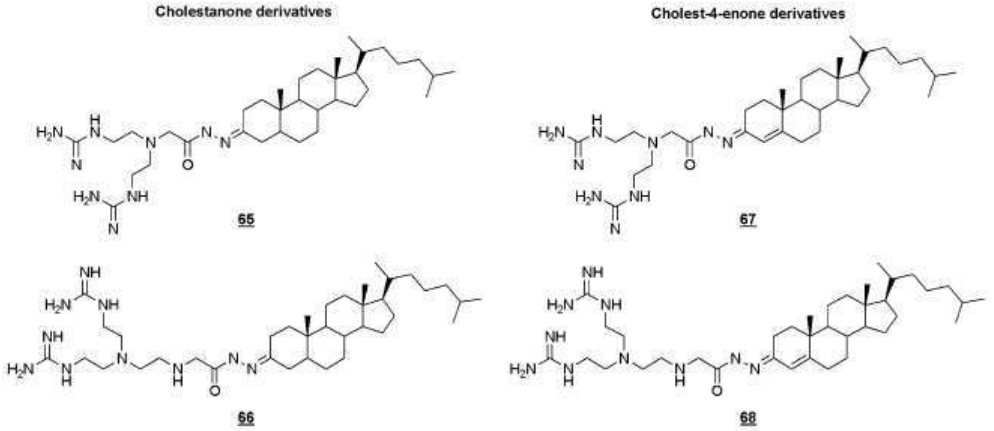

Fig. 13 Acylhydrazone containing guanidinium-based lipids

different hydrophilic headgroups, lipophilic tails and linkage configurations with acid-sensitive functional groups such as ortho esters, vinyl ethers or acylhydrazones, provides lipids with different hydrolysis kinetics and hydrolysis products of different membrane-destabilizing properties. Further development will focus on improving knowledge of structure–activity relationships and on the investigation of other sensitive functional groups.

Conclusion

Cationic lipid-mediated DNA delivery is a powerful alternative to the use of viral vectors and has prompted extensive research that has resulted in the synthesis of hundreds of molecules. Evaluation of the structure–activity relationships of numerous series of cationic lipids has allowed for the clear identification of the important parameters that govern in vitro transfection efficiency. However, despite having widely used for more than 10 years for in vitro transfection applications, the use of these molecules has not yet been translated to application in humans because of low in vivo transfection efficiencies and some toxicity issues. Therefore, there is a need to identify new cationic lipid structures. The strategies for the design of these synthetic vectors are now more rational, based on a better understanding of the critical barriers that lipoplexes must overcome, from DNA complexation to transgene expression. The synthesis of biocompatible and non-toxic cationic lipids can be achieved using natural compounds, known for their safety. Natural hydrophilic headgroups (e.g., aminoglycosides, amino acids, polyamines) and lipophilic tails derived from components of biological membranes (e.g., phospholipids, cholesterol, archaeal bipolar lipids) constitute a large pool of building blocks for the design of bio-inspired cationic lipids for gene delivery. Once cationic lipid/DNA lipoplexes are internalized in the cell, several strategies have been developed to enhance transfection efficiency by for instance, promoting the escape of lipoplexes from the endosomal compartment and the release of DNA from cationic lipid/DNA lipoplexes. The addition of fusogenic lipids into the cationic lipid formulation is thought to enhance endosomal membrane disruption, which generally leads to higher transfection efficiencies. The use of a disulfide bond, a reductive, environment-sensitive chemical function, may improve transfection efficiency, however this strategy requires the careful design of cationic lipids to avoid early lipoplex dissociation and/or DNA degradation. The versatile use of acid-sensitive functional groups in the design of cationic lipids provides synthetic vectors with different properties that are likely to promote transfection efficiency. In the future, the combination of these strategies may result in the development of sophisticated and versatile systems containing multiple components. The specific characteristics of each component will help to overcome each critical barrier encountered during transfection, such as toxicity, endosomal escape and DNA release from lipoplexes. Such multi-modular synthetic vectors will be specifically designed for particular targets and will constitute serious alternatives to viral vectors for gene therapy applications.

Acknowledgments This contribution was supported by the University of Nantes and funded by grants from the European Commission (Project SyntheGeneDelivery, No. 018716), the CNRS, the INSERM, the Ministère de l'Education Nationale, de la Recherche et de la Technologie, the "Association Française contre la Myopathie" (Evry, France), "Vaincre la Mucoviscidose" (Paris, France) and IN-CELL-ART (Nantes, France). We are also grateful to our colleagues of several years for fruitful discussions.

References

Aissaoui A, Oudrhiri N, Petit L et al (2002) Progress in gene delivery by cationic lipids: Guanidinium-cholesterol-based systems as an example. Curr Drug Targets 3:1–16

Aissaoui A, Martin B, Kan E et al (2004) Novel cationic lipids incorporating an acid-sensitive acylhydrazone linker: synthesis and transfection properties. J Med Chem 47:5210–5223

Anderson WF (1998) Human gene therapy. Nature (London) 392:25–30

Bajaj A, Kondaiah P, Bhattacharya S (2008) Effect of the nature of the spacer on gene transfer efficacies of novel thiocholesterol derived Gemini lipids in different cell lines: a structure–activity investigation. J Med Chem 51:2533–2540

Barteau B, Chevre R, Letrou-Bonneval E et al (2008) Physicochemical parameters of non-viral vectors that govern transfection efficiency. Current Gene Therapy 8:313–323

Behr JP, Demeneix B, Loeffler JP et al (1989) Efficient gene transfer into mammalian primary endocrine cells with lipopolyamine-coated DNA. Proc Natl Acad Sci USA 86:6982–6986

Belmont P, Aissaoui A, Hauchecorne M et al (2002) Aminoglycoside-derived cationic lipids as efficient vectors for gene transfection in vitro and in vivo. J Gene Med 4:517–526

Benvegnu T, Rethore G, Brard M et al (2005) Archaeosomes based on novel synthetic tetraether-type lipids for the development of oral delivery systems. Chem Commun (Camb) 553:6–5538

Blessing T, Remy JS, Behr JP (1998) Monomolecular collapse of plasmid DNA into stable virus-like particles. Proc Natl Acad Sci USA 95:1427–1431

Boomer JA, Thompson DH (1999) Synthesis of acid-labile diplasmenyl lipids for drug and gene delivery applications. Chem Phys Lipids 99:145–153

Boomer JA, Thompson DH, Sullivan SM (2002) Formation of plasmid-based transfection complexes with an acid-labile cationic lipid: characterization of in vitro and in vivo gene transfer. Pharm Res 19:1292–1301

Botto RE, Coxon B (1983) Nitrogen-15 nuclear magnetic resonance spectroscopy of neomycin B and related aminoglycosides. J Am Chem Soc 105:1021–1028

Boussif O, Gaucheron J, Boulanger C et al (2001) Enhanced in vitro and in vivo cationic lipid-mediated gene delivery with a fluorinated glycerophosphoethanolamine helper lipid. J Gene Med 3:109–114

Brard M, Laine C, Rethore G et al (2007) Synthesis of archaeal bipolar lipid analogues: a way to versatile drug/gene delivery systems. J Org Chem 72:8267–8279

By K, Nantz MH (2004) Dioxazocinium ortho esters: a class of highly pH-vulnerable amphiphiles. Angew Chem, Int Ed 43:1117–1120

Byk G, Dubertret C, Escriou V et al (1998) Synthesis, activity, and structure–activity relationship studies of novel cationic lipids for DNA transfer. J Med Chem 41:224–235

Byk G, Wetzer B, Frederic M et al (2000) Reduction-sensitive lipopolyamines as a novel nonviral gene delivery system for modulated release of DNA with improved transgene expression. J Med Chem 43:4377–4387

Chen H, Zhang H, McCallum CM et al (2007) Unsaturated cationic ortho esters for endosome permeation in gene delivery. J Med Chem 50:4269–4278

Cordes EH, Bull HG (1974) Mechanism and catalysis for hydrolysis of acetals, ketals, and ortho esters. Chem Rev 74:581–603

Cotton FA, Day VW, Hazen EE Jr et al (1973) Structure of methylguanidinium dihydrogen orthophosphate. Model compound for arginine-phosphate hydrogen bonding. J Am Chem Soc 95:4834–4840

Dauty E, Remy JS, Blessing T et al (2001) Dimerizable cationic detergents with a low Cmc condense plasmid DNA into nanometric particles and transfect cells in culture. J Am Chem Soc 123:9227–9234

De Rosa M, Gambacorta A, Gliozzi A (1986) Structure, biosynthesis, and physicochemical properties of archaebacterial lipids. Microbiol Mol Biol Rev 50:70–80

DeLong EF (1998) Everything in moderation: archaea as 'non-extremophiles'. Curr Opin Genet Dev 8:649–654

Desigaux L, Sainlos M, Lambert O et al (2007) Self-assembled lamellar complexes of SiRNA with lipidic aminoglycoside derivatives promote efficient SiRNA delivery and interference. Proc Natl Acad Sci USA 104:16534–16539

Deslongchamps P, Dory YL, Li S (2000) The relative rate of hydrolysis of a series of acyclic and six-membered cyclic acetals, ketals, orthoesters, and orthocarbonates. Tetrahedron 56:3533–3537

Dorman DE, Paschal JW, Merkel KE (1976) Nitrogen-15 nuclear magnetic resonance spectroscopy. The nebramycin aminoglycosides. J Am Chem Soc 98:6885–6888

El Ouahabi A, Thiry M, Pector V et al (1997) The role of endosome destabilizing activity in the gene transfer process mediated by cationic lipids. FEBS Lett 414:187–192

Fabio K, Di Giorgio C, Vierling P (2005) New perfluorinated polycationic dimerizable detergents for the formulation of monomolecular DNA nanoparticles and their in vitro transfection efficiency. Biochim Biophys Acta 1724:203–214

Farhood H, Serbina N, Huang L (1995) The role of dioleoyl phosphatidylethanolamine in cationic liposome mediated gene transfer. Biochim Biophys Acta, Biomembr 1235:289–295

Felgner PL, Gadek TR, Holm M et al (1987) Lipofection: a highly efficient, lipid-mediated DNA-transfection procedure. Proc Natl Acad Sci USA 84:7413–7417

Felgner PL, Barenholz Y, Behr JP et al (1997) Nomenclature for synthetic gene delivery systems. Hum Gene Ther 8:511–512

Fletcher S, Ahmad A, Perouzel E et al (2006) A dialkynoyl analogue of DOPE improves gene transfer of lower-charged, cationic lipoplexes. Org Biomol Chem 4:196–199

Floch V, Le Bolc'h G, Gable-Guillaume C et al (1998) Phosphonolipids as non-viral vectors for gene therapy. Eur J Med Chem 33:923–934

Floch V, Loisel S, Guenin E et al (2000) Cation substitution in cationic phosphonolipids: a new concept to improve transfection activity and decrease cellular toxicity. J Med Chem 43:4617–4628

Gao X, Huang L (1991) A novel cationic liposome reagent for efficient transfection of mammalian cells. Biochem Biophys Res Commun 179:280–285

Gao X, Huang L (1995) Cationic liposome-mediated gene transfer. Gene Ther 2:710–722

Gaucheron J, Boulanger C, Santaella C et al (2001) In vitro cationic lipid-mediated gene delivery with fluorinated glycerophosphoethanolamine helper lipids. Bioconj Chem 12:949–963

Gilot D, Miramon ML, Benvegnu T et al (2002) Cationic lipids derived from glycine betaine promote efficient and non-toxic gene transfection in cultured hepatocytes. J Gene Med 4:415–427

Guenin E, Herve AC, Floch V et al (2000) Cationic phosphonolipids containing quaternary phosphonium and arsonium groups for DNA transfection with good efficiency and low cellular toxicity. Angew Chem, Int Ed 39:629–631

Heller J, Barr J, Ng SY et al (2002) Poly(ortho esters): synthesis, characterization, properties and uses. Adv Drug Deliv Rev 54:1015–1039

Heyes JA, Niculescu-Duvaz D, Cooper RG et al (2002) Synthesis of novel cationic lipids: effect of structural modification on the efficiency of gene transfer. J Med Chem 45:99–114
Hui SW, Langner M, Zhao YL et al (1996) The role of helper lipids in cationic liposome-mediated gene transfer. Biophys J 71:590–599
Junk T, Pappalardo GC, Irgolic KJ (1990) Synthesis and characterization of rac-1,2-bis(Palmitoyloxy)-3-propyl[2-(trimethylarsonio)ethyl]phosphonate, an arsenic-containing phosphonolipid. Appl Organomet Chem 4:103–109
Kaneko T, Willner D, Monkovic I et al (1991) New hydrazone derivatives of adriamycin and their immunoconjugates—a correlation between acid stability and cytotoxicity. Bioconj Chem 2:133–141
Kim HS, Moon J, Kim KS et al (2004) Gene-transferring efficiencies of novel diamino cationic lipids with varied hydrocarbon chains. Bioconj Chem 15:1095–1101
Koga Y, Morii H (2007) Biosynthesis of ether-type polar lipids in archaea and evolutionary considerations. Microbiol Mol Biol Rev 71:97–120
Kratz F, Beyer U, Schumacher P et al (1997) Synthesis of new maleimide derivatives of daunorubicin and biological activity of acid labile transferrin conjugates. Bioorg Med Chem Lett 7:617–622
Kumar VV, Chaudhuri A (2004) On the disulfide-linker strategy for designing efficacious cationic transfection lipids: an unexpected transfection profile. FEBS Lett 571:205–211
Kumar VV, Pichon C, Refregiers M et al (2003) Single histidine residue in head-group region is sufficient to impart remarkable gene transfection properties to cationic lipids: evidence for histidine-mediated membrane fusion at acidic pH. Gene Ther 10:1206–1215
Lamarche F, Mevel M, Montier T et al (2007) Lipophosphoramidates as lipidic part of lipospermines for gene delivery. Bioconj Chem 18:1575–1582
Le Bolc'h G, Le Bris N, Yaouanc JJ et al (1995) Cationic phosphonolipids as non viral vectors for DNA transfection. Tetrahedron Lett 36:6681–6684
Lee ER, Marshall J, Siegel CS et al (1996) Detailed analysis of structures and formulations of cationic lipids for efficient gene transfer to the lung. Hum Gene Ther 7:1701–1717
Majeti BK, Karmali PP, Reddy BS et al (2005) In vitro gene transfer efficacies of *N*, *N*-dialkylpyrrolidinium chlorides: a structure–activity investigation. J Med Chem 48:3784–3795
Mevel M, Montier T, Lamarche F et al (2007) Dicationic lipophosphoramidates as DNA carriers. Bioconj Chem 18:1604–1611
Miller AD (1998) Cationic liposomes for gene therapy. Angew Chem Int Ed 37:1769–1785
Mingeot-Leclercq MP, Glupczynski Y, Tulkens PM (1999) Aminoglycosides: activity and resistance. Antimicrob Agents Chemother 43:727–737
Moazed D, Noller HF (1987) Interaction of antibiotics with functional sites in 16S ribosomal RNA. Nature (London) 327:389–394
Montier T, Cavalier A, Delepine P et al (2003) The use of in situ hybridization to study the transgene pathway following cellular transfection with cationic phosphonolipids. Blood Cells Mol Dis 30:112–123
Montier T, Benvegnu T, Jaffres PA et al (2008) Progress in cationic lipid-mediated gene transfection: a series of bio-inspired lipids as an example. Curr Gene Ther 8:296–312
Moradpour D, Schauer JI, Zurawski VR Jr et al (1996) Efficient gene transfer into mammalian cells with cholesteryl-spermidine. Biochem Biophys Res Commun 221:82–88
Mueller BM, Wrasidlo WA, Reisfeld RA (1990) Antibody conjugates with morpholinodoxorubicin and acid cleavable linkers. Bioconj Chem 1:325–330
Mukherjee S, Ghosh RN, Maxfield FR (1997) Endocytosis. Physiol Rev 77:759–803
Mulligan RC (1993) The basic science of gene therapy. Science (Washington, DC, 1883) 260:926–932
Niculescu-Duvaz D, Heyes J, Springer CJ (2003) Structure–activity relationship in cationic lipid mediated gene transfection. Curr Med Chem 10:1233–1261
Noguchi A, Furuno T, Kawaura C et al (1998) Membrane fusion plays an important role in gene transfection mediated by cationic liposomes. FEBS Lett 433:169–173
Obata Y, Suzuki D, Takeoka S (2008) Evaluation of cationic assemblies constructed with amino acid based lipids for plasmid DNA delivery. Bioconj Chem 19:1055–1063
Ogle JM, Brodersen DE, Clemons WM Jr et al (2001) Recognition of cognate transfer RNA by the 30S ribosomal subunit. Science 292:897–902
Oudrhiri N, Vigneron JP, Peuchmaur M et al (1997) Gene transfer by guanidinium-cholesterol cationic lipids into airway epithelial cells in vitro and in vivo. Proc Natl Acad Sci USA 94:1651–1656
Ouyang M, Remy JS, Szoka FC Jr (2000) Controlled template-assisted assembly of plasmid DNA into nanometric particles with high DNA concentration. Bioconj Chem 11:104–112
Pedroso de Lima MC, Simoes S, Pires P et al (2001) Cationic lipid-DNA complexes in gene delivery: from biophysics to biological applications. Adv Drug Deliv Rev 47:277–294
Picquet E, Le Ny K, Delepine P et al (2005) Cationic lipophosphoramidates and lipophosphoguanidines are very efficient for in vivo DNA delivery. Bioconj Chem 16:1051–1053
Pitard B (2002) Supramolecular assemblies of DNA delivery systems. Somatic Cell Mol Genet 27:5–15
Pitard B, Aguerre O, Airiau M et al (1997) Virus-sized self-assembling lamellar complexes between plasmid DNA and cationic micelles promote gene transfer. Proc Natl Acad Sci USA 94:14412–14417
Pitard B, Oudrhiri N, Vigneron JP et al (1999) Structural characteristics of supramolecular assemblies formed by guanidinium-cholesterol reagents for gene transfection. Proc Natl Acad Sci USA 96:2621–2626
Pitard B, Oudrhiri N, Lambert O et al (2001) Sterically stabilized BGTC-based lipoplexes: structural features and gene transfection into the mouse airways in vivo. J Gene Med 3:478–487
Rethore G, Montier T, Le Gall T et al (2007) Archaeosomes based on synthetic tetraether-like lipids as novel versatile gene delivery systems. Chem Commun (Camb) 205:4–2056
Rodrigues PCA, Beyer U, Schumacher P et al (1999) Acid-sensitive polyethylene glycol conjugates of doxorubicin: preparation, in vitro efficacy and intracellular distribution. Bioorg Med Chem 7:2517–2524
Rosenzweig HS, Rakhmanova VA, McIntosh TJ et al (2000) O-Alkyl dioleoylphosphatidylcholinium compounds: the effect of varying alkyl chain length on their physical properties and in vitro DNA transfection activity. Bioconj Chem 11:306–313
Sainlos M, Belmont P, Vigneron JP et al (2003) Aminoglycoside-derived cationic lipids for gene transfection: synthesis of kanamycin a derivatives. Eur J Org Chem 276:4–2774
Sainlos M, Hauchecorne M, Oudrhiri N et al (2005) Kanamycin A-derived cationic lipids as vectors for gene transfection. Chembiochem 6:1023–1033
Stekar J, Noessner G, Kutscher B et al (1995) Synthesis, antitumor activity, and tolerability of phospholipids containing nitrogen homologs. Angew Chem Int Ed 34:238–240
Szilagyi L, Pusztahelyi ZS, Jakab S et al (1993) Microscopic protonation constants in tobramycin. An NMR and pH study with the aid of partially *N*-acetylated derivatives. Carbohydr Res 247:99–109

Tang F, Hughes JA (1998) Introduction of a disulfide bond into a cationic lipid enhances transgene expression of plasmid DNA. Biochem Biophys Res Commun 242:141–145

Tang F, Hughes JA (1999) Use of dithiodiglycolic acid as a tether for cationic lipids decreases the cytotoxicity and increases transgene expression of plasmid DNA in vitro. Bioconj Chem 10:791–796

Turek J, Dubertret C, Jaslin G et al (2000) Formulations which increase the size of lipoplexes prevent serum-associated inhibition of transfection. J Gene Med 2:32–40

Umezawa H, Hooper IR (eds) (1982) Aminoglycoside antibiotics. Springer, New York

Vigneron JP, Oudrhiri N, Fauquet M et al (1996) Guanidinium-cholesterol cationic lipids: efficient vectors for the transfection of eukaryotic cells. Proc Natl Acad Sci USA 93:9682–9686

Wetzer B, Byk G, Frederic M et al (2001) Reducible cationic lipids for gene transfer. Biochem J 356:747–756

Wiethoff CM, Middaugh CR (2003) Barriers to nonviral gene delivery. J Pharm Sci 92:203–217

Zhang Y, Anchordoquy TJ (2004) The role of lipid charge density in the serum stability of cationic lipid/DNA complexes. Biochim Biophys Acta Biomembr 1663:143–157

Zhu J, Munn RJ, Nantz MH (2000) Self-cleaving ortho ester lipids: a new class of pH-vulnerable amphiphiles. J Am Chem Soc 122:2645–2646

Curriculum vitae

Stephanie DAVID

Doctorante en pharmacologie expérimentale

Date de naissance : 10/03/1981
Nationalité : allemande et française
Adresse : 2 rue Voltaire
F-49100 Angers
Téléphone : 06 81 66 32 18
Adresses de messagerie : st_da@gmx.de
Stephanie.David@univ-nantes.fr
stdavi@etud.univ-angers.fr

Expérience professionnelle	
09/2012 11/2011	**Poste ATER en pharmacie galénique, cosmétologie et industrialisation des produits de santé ; vectorisation** *UFR des Sciences Pharmaceutiques, Université de Tours* *EA 4244 « Physico-chimie des Matériaux et Biomlécules »* *(France)*

Formation	Expériences
12/2011 01/2009	**Doctorat en pharmacologie expérimentale** *Ecole doctorale Biologie – Santé Angers – Nantes (France)*	**Doctorat** Développement de nanovecteurs pour l'administration d'acides nucléiques par voie systémique *INSERM U646 « Ingénierie de la vectorisation particulaire » Angers (France)* *INSERM UMR 915 « Institut du thorax » Nantes (France)* **Monitorat** 10/2010 – 09/2011 : 64h de TP en galénique 2ième et 3ième année de pharmacie 10/2009 – 09/2010 : 96h de TP en galénique 2ième et 3ième année de pharmacie *UFR Sciences pharmaceutiques et ingénierie de la santé – Département pharmacie, Université Angers (France)*
06/2008 10/2007	**Master 2 recherche en Biologie** Signalisation et Systèmes Intégrés en Biologie *Ecole Pratique des Hautes Etudes (EPHE) Paris (France)*	**Stage de Master 2 recherche** Etude d'une protéine en solution par diffusion de la lumière en vue de sa microencapsulation *INSERM U646 « Ingénierie de la vectorisation particulaire » Angers (France)*
06/2007 11/2000	**Diplôme de Pharmacien** *Université Friedrich Alexander Erlangen Nürnberg (Allemagne)*	**Stage de fin d'études** 05/2006 – 06/2007 : Stage en officine *Adler Apotheke Erlangen(Allemagne)* 11/2005 – 04/2006 : Stage ERASMUS *INSERM U646 « Ingénierie de la vectorisation particulaire » Angers (France)*
06/2000	**Baccalauréat** *Ohm Gymnasium Erlangen (Allemagne)*	

Stephanie DAVID

Compétences
Mise au point de protocoles d'études et **réalisation** des essais en utilisant **différentes techniques** (formulation de différents vecteurs, caractérisation physico-chimique, essais *in vitro* et *in vivo*)
Compilation et interprétation des **résultats** et **recherches bibliographiques**
Rédaction de **rapports** et **présentations orales**
Encadrement d'étudiants en Master 2 (2010/2011)
Diplôme d'expérimentation animale niveau 1 (10/2010) et **autorisation d'expérimenter sur animaux vivants** (08/2011)
Enseignements
TP galénique 2ième année (dilutions, gels, emulsions, microémulsions, poudres, biochimie des protéines)
TP galénique 3ième année (TP intégrés partie contrôle des formes galéniques)
PEA biotechnologie master2 TIF Encapsulation de siRNA dans des Nanocapsules lipidiques (Encadrement des étudiants sur partie pratique du projet)
Recherche
Formulation et caractérisation de vecteurs • Formulation de nanocapsules lipidiques, systèmes multimodulaires, liposomes, lipoplexes • Encapsulation de siRNA ou de plasmides ADN • Mesures de taille, potentiel zéta, électrophorèse, dosage des acides nucléiques encapsulés par spectrophotomètre UV
Purification et extraction d'ADN • Amplification de bactéries, extraction d'ADN, • digestion plasmidique, électrophorèse, quantification par Nanodrop
Essais *in vitro* • Culture cellulaire, transfection de cellules à l'aide de nanovecteurs, dosage luciférase et protéines
Essais *in vivo* • Administration de nanovecteurs par injection i.v., suivi des vecteurs par imagerie (BLI et BFI), dosage luciférase et protéines sur organes et tissue
Publications
David S, Carmoy N, Resnier P, Denis C, Misery L, Pitard B, Benoit JP, Passirani C and Montier T. ***In vivo imaging of DNA lipid nanocapsules after systemic administration in a melanoma mouse model***. 2011, **International Journal of Pharmaceutics,** in press.
David S, Pitard B, Benoît JP, Passirani C. ***Non-viral nanosystems for systemic siRNA delivery***. **Pharmacol Res**. 2010 Aug; 62(2):100-14. Review.
Labas R, Beilvert F, Barteau B, David S, Chèvre R, Pitard B. ***Nature as a source of inspiration for cationic lipid synthesis***. **Genetica**. 2010 Feb; 138(2):153-68. Review.
Communications orales
David S., Pitard B., Benoit JP., Passirani C. ***Formulation of Nanocarriers for systemic delivery of nucleic acids*** Cinquième **Journée Thématique de l'IFR 132**. Angers, 7 mai 2010
David S., Passirani C., Benoit JP., Pitard B. ***Nanocarriers ciblés pour le transport spécifique d'acides nucléiques*** **Colloque CIMATH** Ciblage Moléculaire et Applications Thérapeutiques – **Le Croisic** 2–4 décembre 2009

Stephanie DAVID

Communications affichées	
	David S., Guillot A., Pitard B., Benoit JP., Passirani C. ***Formulation and characterization of siRNA LNC*** XXVème **Journées Scientifiques du GTRV**. Toulouse, 6-8 décembre 2010 David S., Carmoy N., Montier T., Pitard B., Benoit JP., Passirani C. ***In vivo imaging of intravenous administered DNA LNC in mice*** XXVème **Journées Scientifiques du GTRV**. Toulouse, 6-8 décembre 2010
	David S., Pitard B., Benoit JP., Passirani C. ***Formulation of Nanocarriers for systemic delivery of nucleic acids*** • XXIVème **Journées Scientifiques du GTRV**. Paris, 7-9 décembre 2009 • Quatrième **Journée de l'IFR 132.** Angers, 11 décembre 2009
Langues	
	Allemand et Français (langues maternelles), Anglais (scientifique)
Informatique	
	Certificat C2i Niveau 1 (Certificat Informatique et Internet) **Microsoft office (et Open office)** (Word, Excel, Power Point), **Internet** (Recherche bibliographique)
Loisirs	
	Sport (Gym, Natation, Ski), **Voyages, Lecture, Cinéma,**

Résumé

Deux différents types de vecteurs, les nanocapsules lipidiques (LNC) et les systèmes multimodulaires (MMS) ont été développés pour l'administration par voie systémique de deux types d'acides nucléiques, l'ADN et les petits ARN à interférence (siRNA). Ces vecteurs sont formulés à base de complexes d'acides nucléiques et de lipides cationiques (lipoplexes) qui ont été soit encapsulés au cœur des LNC, soit recouverts de stabilisateurs stériques afin de former des MMS. Une partie du travail a consisté à développer des vecteurs de siRNA et à les caractériser par des méthodes physico-chimiques. En fonction du lipide cationique utilisé, jusqu'à 65% de siRNA ont pu être encapsulés dans les LNC, en présentant des caractéristiques appropriées pour une administration par voie systémique. La seconde partie a consisté à approfondir la caractérisation des vecteurs d'ADN et à analyser leur profil de distribution en utilisant de l'imagerie par fluorescence *in vivo*. Chez la souris saine, les vecteurs d'ADN ont présenté des profils de biodistribution spécifiques à leur composition. Sur deux modèles tumoraux (gliome sous-cutané et mélanome), les vecteurs ayant un temps de circulation prolongé ont également montré une co-localisation intéressante avec les cellules tumorales. Afin de mettre en évidence l'efficacité de ces vecteurs, un plasmide codant pour la tymidine kinase du virus herpes simplex (HSV-tk) a été encapsulé et administré. Puis un traitement par le ganciclovir (GCV) basé sur l'approche par gène suicide a été effectué. Les premiers résultats sont concluants, montrant une baisse de croissance tumorale après quelques jours de traitement aussi bien dans le modèle de gliome que dans celui du mélanome. Ces résultats indiquent que ces outils sont prometteurs pour une variété d'applications en thérapie génique.

Mots clés : Thérapie génique, LNC, MMS, siRNA, ADN, imagerie par biofluorescence, HSV-tk/GCV, mélanome, gliome

Abstract

Two different types of nanocarriers, lipid nanocapsules (LNC) and multimodular systems (MMS) were developed for systemic administration of two types of nucleic acids, DNA and small interfering RNA (siRNA). These nanocarriers are based on complexes between nucleic acids and cationic lipids (lipoplexes) which were either encapsulated in LNC or coated with steric stabilizers to form MMS. One part of this work consisted in the development of siRNA nanocarriers and in their characterisation using physico-chemical methods. In function of the cationic lipid, up to 65% of siRNA could be encapsulated in LNC and presented appropriate characteristics for systemic administration. The second part consisted in the advanced characterisation of DNA nanocarriers and the analyse of their biodistribution profiles using *in vivo* biofluorescence imaging. In healthy animals, the different DNA nanocarriers presented various distribution profiles in function of their composition. On two tumour mouse models (glioma and melanoma), the DNA nanocarriers presenting a prolonged circulation time showed also colocalisation with tumour cells. To evidence their efficacy, a plasmid coding for herpes simplex virus thymidine kinase (HSV-tk) was encapsulated and administered, followed by a treatment of ganciclovir (GCV) using the gene-directed enzyme prodrug therapy. The first results are promising, and showed a tumour growth reduction after several days compared to non-treated animals. In conclusion, the results suggest that these nanocarriers could present a promising tool for various applications in gene therapy.

Keywords: Gene therapy, LNC, MMS, siRNA, DNA, *in vivo* biofluorescence imaging, HSV-tk/GCV, melanoma, glioma